Resource allocation for HARQ in mobile ad hoc networks

Xavier Leturc

université
PARIS-SACLAY

NNT : 2018SACLT008

TELECOM ParisTech

Allocation de ressources pour les HARQ dans les réseaux ad hoc mobiles

Thèse de doctorat de l'Université Paris-Saclay
préparée à Télécom ParisTech

Ecole doctorale n°580 Sciences et technologies de l'information et de la communication (STIC)
Spécialité de doctorat : Réseaux, Information et Communications

Thèse présentée et soutenue à Paris, le 07/12/2018, par

Xavier Leturc

Composition du Jury :

Luc Vandendorpe Professeur, UCL	Président
Mylène Pischella maître de conférences, CNAM	Rapporteur
David Gesbert Professeur, Eurecom	Rapporteur
E. Veronica Belmega maître de conférences, ENSEA	Examinateur
Jean-Marie Gorce Professeur, INSA-Lyon	Examinateur
Mohamad Assaad Professeur, CentraleSupélec	Examinateur
Philippe Ciblat Professeur, Télécom ParisTech	Directeur de thèse
Christophe Le Martret Expert Thales / HDR	Directeur de thèse

Thèse de doctorat

Remerciements

C'est non sans une certaine émotion que je débute la rédaction de ces remerciements, qui constituent le point final d'une aventure commencée il y a déjà 3 ans.

Mes premiers remerciements s'adressent à mes directeurs de thèse, MM. **Philippe Ciblat** et **Christophe Le Martret**. Durant ces trois années, j'ai eu l'occasion d'avoir avec eux de nombreuses discussions scientifiques enrichissantes. Je les remercie d'avoir placé leur confiance en moi, et de m'avoir laissé une grande liberté quand à l'organisation de mes travaux de recherches.

Je remercie les membres de mon jury de thèse, en commençant par M. **Luc Vandendorpe**, professeur à l'Université Catholique de Louvain, pour avoir présidé ce jury. Je remercie Mme. **Mylène Pischella**, maître de conférence au CNAM, et M. **David Gesbert**, Professeur à Eurecom, d'avoir accepté d'être rapporteurs de cette thèse. Je tiens également à remercier Mme. **E. Veronica Belmega**, maître de conférence à l'ENSEA, M. **Mohamad Assaad**, professeur à CentraleSupélec et M. **Jean-Marie Gorce**, professeur à l'INSA de Lyon, pour avoir accepté d'examiner cette thèse. D'une manière générale, je remercie sincèrement tous les membres du jury pour leur retours tant à propos du manuscrit qu'à propos de ma soutenance, qui m'ont beaucoup touché.

Je remercie M. **Jean-Luc Peron**, de Thales SIX GTS France, pour m'avoir accueilli au sein du service WFD il y a 3 ans. Je remercie bien évidemment mes collègues et amis de Thales : **Adrien, Alice, Anaël, Antonio, Arnaud, Benoit, Dorin, Elie, Florian, Hélène, Luxmiram, Marie, Olivier, Philippe, Raphaël, Romain, Serdar, Simon, Sylvain** et **Titouan**. Je remercie également les anciens stagiaires **Arthur, Eric, Lélio** et **Maxime**.

Je tiens également à remercier mes amis pour leur soutien années après années, et en particulier **Alexandre, Antoine, Charles-Damien, Guillaume, Maël, Yohan** et enfin bien évidemment **Jérôme**, ancien thésard Thales.

Je remercie **Clothilde**, récemment entrée dans ma vie, pour son soutien lors de la préparation de cette soutenance, et son intérêt pour mes activités de recherche.

Mes derniers remerciements vont à ma famille, pour leur soutien constant et sans faille durant toutes ces années d'études. Merci pour tout.

Contents

List of Acronyms

ACK	ACKnowledgment
ACMI	Accumulated Mutual Information
AO	Alternating Optimization
ARQ	Automatic Repeat reQuest
AWGN	Additive White Gaussian Noise
BER	Bit Error Rate
BF	Block Fading
BICM	Bit Interleaved Coded Modulation
BPSK	Binary Phase Shift Keying
BS	Base Station
CC	Chase Combining
CDF	Cumulative Density Function
CIR	Channel Impulse Response
COP	Convex Optimization Problem
CP	Cyclic Prefix
CRC	Cyclic Redundancy Check
CRLB	Cramer Rao Lower Bound
CSI	Channel State Information
D2D	Device-to-Device
E	Expectation
EB	Energy per Bit
EE	Energy Efficiency
EM	Expectation Maximization
FEC	Forward Error Correction
FF	Fast Fading
FH	Frequency Hopping
FLOP	Floating Point Operation
GEE	Global Energy Efficiency
GHQ	Gauss-Hermite Quadrature
GNR	Gain to Noise Ratio
GP	Geometric Program

HARQ	Hybrid ARQ
HSDPA	High Speed Downlink Packet Access
i.i.d.	independent and identically distributed
IPM	Interior Point Method
IR	Incremental Redundancy
KKT	Karush-Kuhn-Tucker
LoS	Line of Sight
LSE	Log-Sum-Exp
LTE	Long Term Evolution
M	Maximization
MAC	Medium Access Control
MANET	Mobile Ad Hoc Network
MCS	Modulation and Coding Scheme
MEE	Minimum of the links' EE
MGEE	Maximum GEE
MGO	Maximum Goodput
ML	Maximum Likelihood
MMEE	Maximum MEE
MoM	Method of Moments
MPEE	Maximum PEE
MPO	Minimum Power
MRC	Maximum Ratio Combining
MSE	Mean Square Error
MSEE	Maximum SEE
NACK	Negative ACKnowledgment
nLoS	non LoS
NMSE	Nomalized MSE
OFA	Objective Function Approximation
OFDMA	Orthogonal Frequency Division Multiple Access
OSI	Open Systems Interconnection
PA	Power Amplifier
PC	Pseudo Concave
PDF	Probability Density Function
PDU	Protocol Data Unit
PEE	Product of the links' EE
PER	Packet Error Rate
PHY	Physical
QAM	Quadrature Amplitude Modulation
QoS	Quality of Service
QPSK	Quadrature Phase Shift Keying

RA	Resource Allocation
RCPC	Rate-Compatible Punctured Convolutional
RHS	Right-Hand Side
RM	Resource Manager
RR	Rejection Rate
SC-FDMA	Single-Carrier Frequency Division Multiple Access
SCA	Successive Convex Approximation
SDU	Service Data Unit
ZF	Zero Forcing
SEE	Sum of the links' EE
SNR	Signal to Noise Ratio

General Introduction

The work presented in this Ph.D. thesis has been produced thanks to the collaboration between the "Communications et Électronique" (COMELEC) department of the Intitut Mines-Télécom / Télécom ParisTech (Paris, France) and the "Secteur Temps Réel" (STR) of Thales SIX GTS France (former Thales Communications & Security) (Gennevilliers, France), within the framework of "Convention Industrielle de Formation par la REcherche" (CIFRE). The thesis started in October 2015.

Problem statement

Unlike conventional cellular networks, ad hoc networks have no predefined infrastructure and each node can communicate with any other without Base Station (BS). This characteristic renders them especially suitable in configurations requiring fast deployment such as for instance in military communications. Ad hoc networks have received a lot of interest during the past decades, and especially Mobile Ad Hoc Network (MANET), in which all the nodes can be moving [26]. Nowadays, infrastructure-less networks such as MANETs still receive attention because they encompass Device-to-Device (D2D) communications, which are of central importance within 5G networks [105].

The performance of such multiuser wireless networks strongly depends on Resource Allocation (RA), which is the task of allocating the available physical resource to the different nodes. **This thesis main objective is to propose solutions to perform RA in multiuser MANETs, in which either the Orthogonal Frequency Division Multiple Access (OFDMA) or the Single-Carrier Frequency Division Multiple Access (SC-FDMA) is used as the multi-access technology**. The infrastructure-less nature of MANETs increases the difficulty in performing an efficient RA since there is no BS to centralize the links' instantaneous Channel State Information (CSI). To alleviate this issue, we consider that RA is performed in an assisted fashion, meaning that there is a node in the network, called the Resource Manager (RM), whose task is to perform RA. However, due to the inherent delay for each node to communicate their link's CSI to the RM, **the RM does not have access to instantaneous CSI and we assume that it has only access to statistical CSI to perform RA**.

The RA is performed by optimizing one criterion subject to Quality of Service (QoS) constraints. In wireless communications, a key objective is to maximize the equipment autonomy (i.e., the duration between complete charge and complete discharge of the battery), which can be achieved by maximizing the so-called Energy Efficiency (EE). For this reason, in this thesis, we choose to perform RA using EE-related criteria.

In our considered MANETs, the nodes do not have instantaneous CSI, and thus we further assume that they use the Hybrid ARQ (HARQ) mechanism to increase their communications reliability. HARQ is a powerful mechanism combining Forward Error Correction (FEC) and the Automatic Repeat reQuest (ARQ) retransmission mechanism, allowing to improve the transmission capability. Actually, FEC provides a correction capability while ARQ enables the system to take advantage of the time varying nature of the wireless channel. In addition, we aim to take into account the use of any realistic Modulation and Coding Scheme (MCS) in our RA algorithms such that they can be used in practical systems.

The above discussion yields the following two goals of the thesis.

1. To propose and analyse EE-based RA algorithms for MANETs taking into account the use of HARQ and practical MCS, assuming that only statistical CSI is available.
2. To estimate the channel's statistical CSI.

To detail the first aforementioned goal, we remind that the propagation channel is by nature random, and several Probability Density Function (PDF) have been proposed in the literature to describe the statistical behaviour of the sampled Channel Impulse Response (CIR) magnitude. Among them, the Rayleigh one, which is characterized only though the channel power, is popular in the literature dealing with RA with statistical CSI. However, it is known that this channel model is accurate only for communications without Line of Sight (LoS) between the transmitted and the receiver. A more general distribution overcoming this weakness is the Rician one. This channel model is characterized through both the channel power and the well known Rician K factor, which is an important indicator of the link quality. The Rician channel encompasses the conventional Rayleigh one by setting $K = 0$ and the Additive White Gaussian Noise (AWGN) channel by setting $K \to +\infty$ as special cases. Although the Rician channel is more general than the Rayleigh one, it is more rarely used in the RA since it often yields more complicated theoretical derivations. **Our first goal is thus to design EE-based RA algorithms in MANETs when only statistical CSI is available, i.e., the links' channels power and Rician K factors, and assuming that HARQ and practical MCS are used**. This goal is in the same lines as in the Ph.D dissertation [77], which addressed the RA in HARQ-based MANET with the objective of minimizing the total transmit power under the Rayleigh channel.

Let us now explain our second goal. In general in the literature, when performing RA with statistical CSI, the channel's statistics are assumed to be known. However, in practice, they have to be estimated. Since this thesis takes place in an industrial context, we aim to provide practical and implementable solutions and thus, **our second goal is to estimate the Rician K factor such that it can be used in the RA**.

Notice that we choose to organize the thesis by first addressing the estimation problem and then the RA problems since in practice, the estimation of the Rician K factor comes before the RA.

Outline and contributions

This thesis is composed of five chapters. Our original contributions are gathered in Chapters 2, 4 and 5 whereas Chapter 1 explains the context of the thesis and Chapter 3 provides an overview of the optimization framework used to solve the RA problems.

In Chapter 1, we first introduce the considered system model by describing the MANETs, the transmitter, the receiver and the channel models. We review the HARQ basics. We introduce the notion of EE, and provide numerical examples illustrating the relevancy of this metric. We also formalize the addressed EE-based RA problems as constrained optimization problems, and finally, we provide a detailed discussion regarding the two goals of the thesis.

In Chapter 2, we address the estimation of the Rician K factor with and without shadowing, when the channel samples are estimated from a training sequence and thus are noisy. In the absence of shadowing, we propose four new estimators of the Rician K factor: two deterministic and two Bayesian ones. We also derive the deterministic Cramer Rao Lower Bound (CRLB) in closed-form. In the presence of shadowing, we propose two estimation procedures: one based on the Expectation Maximization (EM), and the other one based on the Method of Moments (MoM). We perform extensive numerical simulations to show that our proposed estimators outperform existing ones from the literature.

In Chapter 3, we first provide an overview of the existing literature addressing EE-based RA problems. We then review some optimization tools that are extensively used in Chapter 4 and 5 to solve the addressed RA problems. More precisely, we present the theoretical basis and vocabulary of convex optimization, geometric programming and fractional programming. We also explain two conventional non-convex optimization procedures: the Alternating Optimization (AO) and the Successive Convex Approximation (SCA) procedures.

In Chapter 4, we solve the EE-based RA problems for Type-II HARQ under the Rayleigh channel. More precisely based on a tight approximation of the error probability available in the literature, we address four RA problems: the Sum of the links' EE (SEE) maximization, the Product of the links' EE (PEE) maximization, the Minimum of the links' EE (MEE) maximization and the Global Energy Efficiency (GEE) maximization, the GEE being the EE of the network. For the rest of this thesis, these criteria will be referred to as Maximum SEE (MSEE), Maximum PEE (MPEE), Maximum MEE (MMEE) and Maximum GEE (MGEE), respectively. We find the optimal solutions for the first three problems whereas we propose two suboptimal solutions for the MGEE problem. We analyze the solutions complexity and, since the MSEE optimal solution is computationally expensive, we propose two suboptimal less complex procedures for this problem. We provide extensive numerical results to compare these criteria with two conventional ones. We also study the impact of the HARQ retransmission mechanism on the EE.

In Chapter 5, we address the same EE-related RA problems as in Chapter 4, but now considering Type-I HARQ under the Rician channel. We first propose an approximation of the Packet Error Rate (PER) and check its accuracy through simulations. Second, we optimally solve the MSEE, MMEE and MGEE problems whereas we propose a suboptimal procedure to solve the MPEE problem. We provide guidelines to extend these results to Type-II HARQ under the Rician channel. Through numerical simulations, we illustrate the interest of taking into account the existence of a LoS during the RA process (i.e., Rician channel with Rician K factor strictly positive) instead of only taking into account the channel power (i.e., Rayleigh channel).

The thesis organization along with reading guidelines are provided in Fig. 1. Actually, reading Chapter 1 is highly recommended for all readers since it introduces notations and basic hypothesis used throughout the thesis. Chapter 2 deals with the estimation of the Rician K factor and is rather independent of the other ones in terms of both mathematical tools and addressed problem. The reader interested in RA can skip this Chapter, and directly read Chapters 3 to 5, or only Chapters 4 and 5 if he/she is familiar with the optimization framework.

Publications

The work conducted during this thesis has led to the following publications. We highlight that the material published in [C1] and [C5] is linked to results obtained during my Master internship, and thus it is not directly linked with the thesis two goals. As a consequence, it will not be developed in this document.

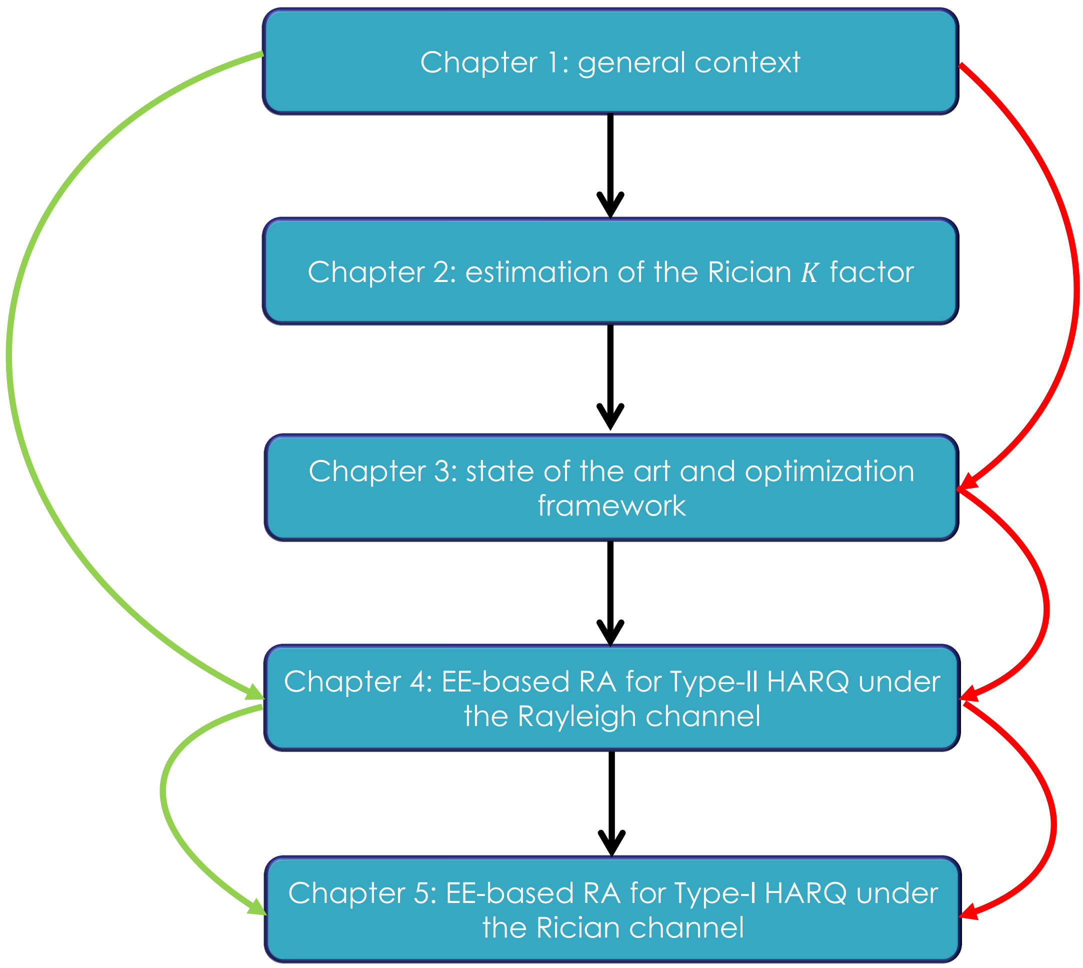

Figure 1: Thesis outline and reading guidelines. Black lines: linear reading, red lines: for reader interested only in RA who wants a reminder on the optimization framework, green lines: for reader interested only in RA who already knows the optimization framework.

Peer-reviewed Journal

J1. X. Leturc, P. Ciblat and C. J. Le Martret: "Energy-Efficient Resource Allocation for HARQ with Statistical CSI", *Submitted to IEEE Transactions on Vehicular Technology.* **Accepted for publication.**

J2. X. Leturc, P. Ciblat and C. J. Le Martret: "Energy efficient resource allocation for type-I HARQ under the Rician channel", *Submitted to IEEE Transactions on Wireless Communications.* **Under major revision.**

International Conference

C1. X. Leturc, C. J. Le Martret and P. Ciblat: "Robust Spectrum Sensing Under Noise Uncertainty", *International Conference on Military Communications and Information Systems (ICMCIS)*, Brussels (Belgium), May 2016. **Best paper award.**

C2. X. Leturc, P. Ciblat, and C.J. Le Martret: "Estimation of the Rician K-factor from noisy complex channel coefficients", *Asilomar Conference on Signals, Systems, and Computer*, Pacific Grove (USA), November 2016.

C3. X. Leturc, C. J. Le Martret and P. Ciblat: "Multi-user power and bandwidth allocation in ad hoc networks with Type-I HARQ under Rician channel with statistical CSI", *International Conference on Military Communications and Information Systems (ICMCIS)*, Oulu (Finland), May 2017. **Best paper award for young scientist.**

C4. X. Leturc, C. J. Le Martret and P. Ciblat: "Energy efficient resource allocation for HARQ with statistical CSI in multiuser ad hoc networks", *IEEE International Conference on Communications (ICC)*, Paris (France), May 2017.

C5. S. Imbert, X. Leturc and C. J. Le Martret: "On the Simulation of Correlated Mobile-to-Mobile Fading Channels for Time-Varying Velocities", *International Conference on Military Communications and Information Systems (ICMCIS)*, Warsaw (Poland), May 2018.

C6. X. Leturc, C. J. Le Martret and P. Ciblat: "Energy efficient bandwidth and power allocation for type-I HARQ under the Rician channel", *IEEE International Conference on Telecommunications (ICT)*, Saint Malo (France), June 2018.

C7. X. Leturc, P. Ciblat and C. J. Le Martret: "Maximization of the Sum of energy-Efficiency for Type-I HARQ under the Rician channel", *IEEE Signal Processing Advances in Wireless Communications (SPAWC)*, Kamalta (Greece), June 2018.

French Conference

C8. X. Leturc, C. J. Le Martret et P. Ciblat: "Minimisation de la puissance émise dans les réseaux ad hoc utilisant l'ARQ hybride de Type-I sur canal de Rice", *XXVIème Colloque GRETSI*, Juan-Les-Pins (France), September 2017.

Patents

P1. X. Leturc, C. J. Le Martret, P. Ciblat: "Procédé et dispositif pour calculer des paramètres statistiques du canal de propagation", déposé le 19/12/2017, demande de brevet no. 1701324.

Chapter 1

General Context

1.1 Introduction

Modern wireless communications often take place in a multiuser context, in which the available physical resource such as the bandwidth or transmit power are inherently limited. The performance of such systems strongly depend on the so-called RA, which consists in sharing these resource between the links in the network. Thus, performing an efficient RA is a crucial task for system designers. This thesis addresses this problem in the context of MANETs, with a special emphasize on EE.

This first Chapter presents the technical context of the thesis, and formalizes the RA problems that we address. The material and notations introduced in this Chapter serve as a basis for the rest of the thesis.

The rest of the Chapter is organized as follows. In Section 1.2, we describe the considered network model while, in Section 1.3, we give the mathematical models of the transmitter, the channel and the receiver. In Section 1.4, we review the basics of HARQ along with conventional related performance metrics. In Section 1.5, we define the notions of EE and GEE, and motivate the use of these metrics in this thesis. Section 1.6 is devoted to the formalization of RA as optimization problems. In Section 1.7, we summarize the thesis objectives. Finally, Section 1.8 concludes the Chapter.

1.2 Multiuser Context

1.2.1 System model

Unlike cellular networks, MANETs have no predefined infrastructure and each node can communicate without necessarily going through a central point such as a BS, which renders these networks highly flexible. Nowadays, this type of infrastructure-less networks receives much interest from both the scientific community and the industry since it encompasses D2D ones, which are of central importance within 5G [11, 105]. Since there is no BS, the following two solutions can be considered to perform RA:

- Performing RA in a distributed fashion, i.e., each node computes its own RA by itself, with possible message exchanges with the other nodes.
- Performing RA in an assisted fashion, i.e., there is a node in the network, called RM, whose task is to collect the links' CSI, to allocate the resources and to communicate to the links their RA.

Since assisted MANETs are of interest for Thales, we focus on this latter category in this thesis. An example of such an assisted MANET with 3 links is illustrated in Fig. 1.1. Each transmitter Txi, $i = 1, 2, 3$, transmits packets to a receiver Rxi, and the links are represented with the coloured solid lines. In this example, Tx3 is the RM and thus the receivers Rxi send their CSI to him, which is represented with the dashed lines.

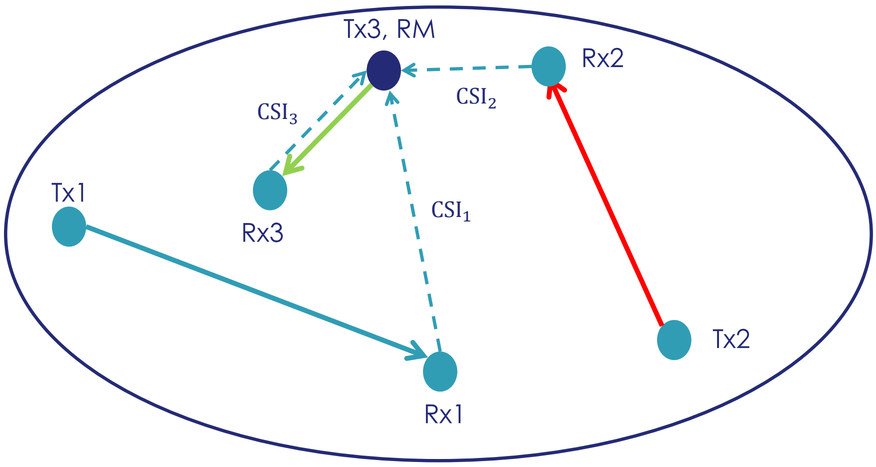

Figure 1.1: Example of a considered assisted MANET.

We consider a persistent RA, meaning that the allocation remains constant for a predefined fixed time duration T_P. During this duration, each Txi transmits several packets using the same allocation. These packets contain pilots symbols known from the Rxi, which are used to estimate the link's CIR. The estimated CIR are stored by the Rxi. Once the allocation has been used during duration T_P, each Rxi computes and transmits some CSI to the RM, which uses it to perform the new persistent RA, and sends the resulting allocation to the nodes.

From the considered system model, we see that there is a delay between the time the links send their CSI to the RM and the time the RM sends them their new allocation. This delay is due to the need to find time slots to perform the different exchanges between the nodes, and it may be larger than the channel coherence time. As a consequence, unlike in cellular systems, it is impossible to perform RA using instantaneous CIR.

For this reason, we assume that only statistical CSI is available to perform RA since the channel statistics are expected to remain constant for a time duration much longer than the channel coherence time.

1.3 Transmitter, Channel and Receiver Model

In this Section, we introduce several important hypothesis related to both the signal and the channel models, along with notations which are used throughout this thesis. In the rest of this document, $(.)^T$ stands for the transposition operator, $\mathbb{E}[.]$ denotes the mathematical expectation and $:=$ means by definition.

1.3.1 Transmit signal

Let us focus on a MANET with L active links sharing a bandwidth B, which is divided in N_c subcarriers using either the OFDMA or the SC-FDMA as the multi-access technology, without multiuser interference.

For link ℓ, the stream of transmit symbols $\{X_\ell(j)\}_{j=1}^{+\infty}$ typically corresponding to the output of a Bit-Interleaved Coded Modulator [16] is split into blocks of length n_ℓ: $\mathbf{X}_\ell(j) := [X_\ell(jn_\ell + 1), \ldots, X_\ell((j+1)n_\ell)]$ where n_ℓ is the number of subcarriers allocated to the ℓth link. The sent signal by the ℓth link during the jth OFDMA or SC-FDMA symbol writes:

$$\mathcal{S}_\ell(j) := \mathbf{C}_p \mathrm{IFFT}_{N_c}(\xi_\ell(\mathbf{Id}_{n_\ell - \mathcal{M}+1} \otimes \mathrm{FFT}_{\mathcal{D}}(\mathbf{X}_\ell(j)))), \tag{1.1}$$

where $\mathrm{FFT}_{\mathcal{D}}$ is the $\mathcal{D} \times \mathcal{D}$ Fourier transform matrix (with $\mathcal{D} = 1$ for OFDMA and $\mathcal{D} = n_\ell$ for SC-FDMA), $\otimes$ is the Kronecker product, $\mathbf{Id}_n$ is the $n \times n$ identity matrix, ξ_ℓ is a $N_c \times n_\ell$ matrix mapping the output of the Fourier transform onto the subcarriers allocated to link ℓ, IFFT_{N_c} is the $N_c \times N_c$ inverse Fourier transform matrix, and $\mathbf{C}_p$ is a matrix adding the Cyclic Prefix (CP) at the beginning of the transmitted block.

1.3.2 Channel model in the time domain

Because our RA uses statistical CSI, the underlying statistical channel model is of high importance. In this thesis, we mainly focus on the Rician channel, which is known to accurately represent the realistic statistical behaviour of wireless channel when there exists a LoS between the transmitter and the receiver [107]. This model receives today more attention in the literature due to its accuracy to model the channel in the context of millimetre wave communications [95, 110]. The Rician channel is versatile since it encompasses both the Rayleigh and the AWGN channels as special cases (detailed later). It is worth emphasizing that this channel model is rarely assumed in RA-related literature, as it will be seen in Chapter 3. This is because the performance metrics under the Rician channel often involves complicated functions, leading thus to cumbersome theoretical derivations.

We assume that each link's channel is modeled as a time-varying multipath Rician channel which is constant within the duration of an OFDMA or SC-FDMA symbol, and changes independently from symbol to symbol. Let $\mathbf{h}_\ell(j) = [h_\ell(j, 0), ..., h_\ell(j, M-1)]^T$ be the sampled CIR of link ℓ during the jth OFDMA or SC-FDMA symbol, where

M is the length of the channel. We make the common assumption of uncorrelated taps, meaning that $\mathbf{h}_\ell(j) \sim \mathcal{CN}(\mathbf{a}_\ell(j), \Sigma_\ell)$, where $\mathcal{CN}(\mathbf{a}_\ell(j), \Sigma_\ell)$ stands for the multivariate circularly-symmetric complex-valued normal distribution with covariance matrix $\Sigma_\ell := \mathrm{diag}_{M\times M}(\zeta^2_{\ell,0}, ..., \zeta^2_{\ell,M-1})$, and we assume that the first tap magnitude is Rician distributed whereas the other ones are Rayleigh distributed, i.e., $\mathbf{a}_\ell(j) := [a_\ell(j)e^{j\theta_0}, 0, \dots, 0]^T$.

Conventionally, $a_\ell(j)$ is considered as time invariant, i.e., $\forall j$, $a_\ell(j) = a_\ell$. However, because of the partial or complete blockage of the LoS component, which may occur for instance when trees or hills are located between the transmitter and the receiver, $a_\ell(j)$ might become random. This blockage phenomenon is known as **shadowing**. Actually, it is observed through measurement campaigns in [72] that the amplitude of the LoS is well modelled by a log-normal random variable in the context of shadowed land-mobile communications. Later, in [2], the authors propose to model the LoS amplitude by a Nakagami-m random variable, which is shown to produce similar results as the log-normal distribution while allowing simpler theoretical derivations. It is observed through measurements campaigns that the model from [2] is accurate for mobile-to-mobile communications in [27]. This model is also considered in several more theoretical works including [80, 108].

This shadowing phenomenon can be mathematically formalized as:

$$a_\ell(j) = c_\ell(j) a_\ell, \tag{1.2}$$

where $c_\ell(j)$ is a Nakagami-m random variable with parameters $m_{\ell,Na}$ and Ω_ℓ, whose PDF $f_{c_\ell(j)}$ is given by [89]:

$$f_{c_\ell(j)}(x) = \frac{2\left(m_{\ell,Na}\right)^{m_{\ell,Na}}}{\Gamma(m_{\ell,Na})\Omega_\ell^{m_{\ell,Na}}} x^{2m_{\ell,Na}-1} e^{-\frac{m_{\ell,Na}}{\Omega_\ell}x^2}, \tag{1.3}$$

with $\Gamma(x)$ the gamma function. For simplicity and without any loss of generality, we assume that the average shadowing power is equal to 1, i.e., $\forall \ell$, $\Omega_\ell = 1$.

In [27], the shadowing is assumed to vary independently between time slots, i.e., $\{c_\ell(j)\}_{j\in\mathbb{N}}$ are independent and identically distributed (i.i.d.) random variables. In this thesis, we consider a more general model in which $c_\ell(j)$ is constant for $N_{T_c,\ell}$ time slots, and changes independently every $N_{T_c,\ell}$ OFDMA or SC-FDMA symbols. This model encompasses the case without shadowing by setting $N_{T_c,\ell} = +\infty$ and $c_\ell(j) = 1$ $\forall j$, and the model of [27] by setting $N_{T_c,\ell} = 1$ and $N_c = 1$.

1.3.3 Received signal

At the receiver side, after removing the CP and applying the matrix FFT_{N_c}, the received signal on link ℓ on the nth subcarrier at symbol j is

$$Y_\ell(j,n) = H_\ell(j,n) X_\ell(j,n) + Z_\ell(j,n), \tag{1.4}$$

where $\mathbf{H}_\ell(j) := [H_\ell(j,0),...,H_\ell(j,N_c-1)]^T$ is the Fourier transform of $\mathbf{h}_\ell(j)$, $\mathcal{X}_\ell(j,n)$ is the nth coefficient of $\Theta_\ell(\mathbf{Id}_{n_\ell-\mathcal{M}+1} \otimes \mathrm{FFT}_{\mathcal{D}}(\mathbf{X}_\ell(j)))$, and $Z_\ell(j,n) \sim \mathcal{CN}(0, 2\sigma_n^2)$, with $2\sigma_n^2 := N_0 B/N_c$ where N_0 is the noise level in the power spectral density. The elements of $\mathbf{H}_\ell(j)$ are identically distributed random variables $H_\ell(j,n) \sim \mathcal{CN}(a_\ell(j), 2\sigma_{h,\ell}^2)$ with $2\sigma_{h,\ell}^2 := \mathrm{Tr}(\Sigma_\ell)$.

1.3.4 Fast fading

In this thesis and as in [65, 77], we assume that each modulated symbol experiences an independent channel realization. This can be achieved by either:

1. designing ξ_ℓ such that the band between the allocated sucarriers is larger than the coherence bandwidth of the channel.

2. Using a sufficiently deep interleaver.

3. Performing Frequency Hopping (FH) between consecutive OFDMA symbols.

In the rest of the thesis, this channel model is referred to as Fast Fading (FF) model.

1.3.5 Statistical CSI

With the above notations, we can define the average Gain to Noise Ratio (GNR) G_ℓ and the Rician K factor K_ℓ of the ℓth link as:

$$G_\ell := \frac{\mathbb{E}\left[|H_\ell(j,n)|^2\right]}{N_0} = \frac{\Delta_\ell}{N_0}, \tag{1.5}$$

$$K_\ell := \frac{a_\ell^2}{2\sigma_{h,\ell}^2}, \tag{1.6}$$

with $\Delta_\ell := a_\ell^2 + 2\sigma_{h,\ell}^2$.

The Rician K factor defined in (1.6) is an important indicator of the link quality. For instance, when there is no shadowing (i.e., $\forall j$, $a_\ell(j) = a_\ell$), $K_\ell = 0$ corresponds to the Rayleigh channel (worst case) whereas $K_\ell \to +\infty$ corresponds to the AWGN channel (best case). These different configurations are illustrated in Fig. 1.2. The impact of the K factor on the system performance is also illustrated in Section 1.5.

We assume that the links only communicate to the RM estimates of their average GNR and Rician K factor.

Also, since no instantaneous channel adaptation is possible, we assume that each link uses an HARQ mechanism, which is detailed in the next Section.

1.4 HARQ Basics

Let us begin this introduction to HARQ by reminding some facts about packet oriented communications.

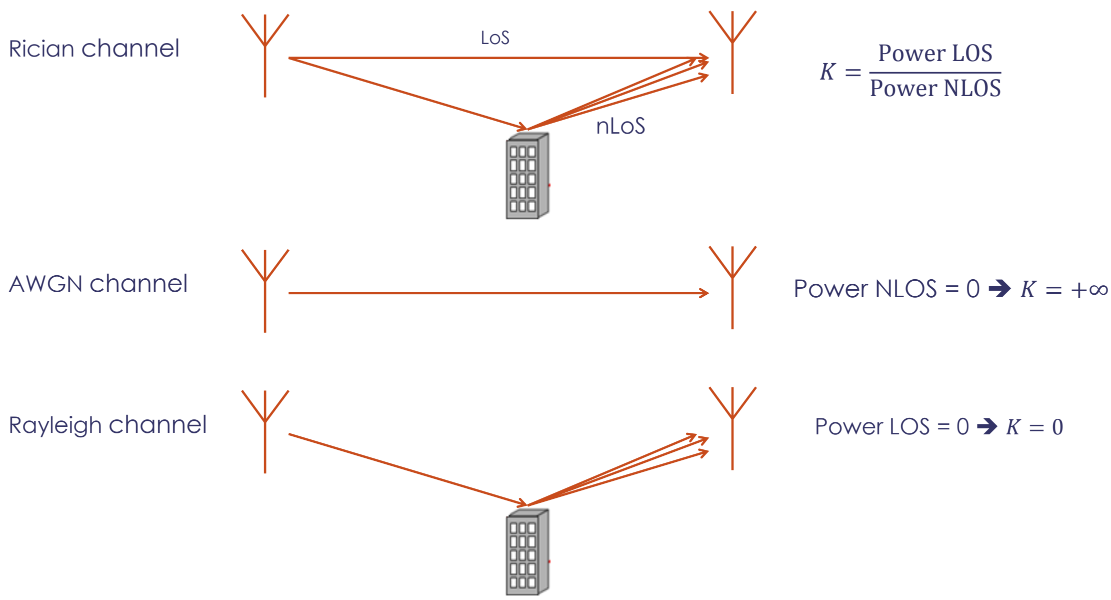

Figure 1.2: Several configurations yielding different Rician K factor.

1.4.1 Packet oriented communications systems

Nowadays, wireless communications system are often based on layer models such as the Open Systems Interconnection (OSI) model which works as follows. The incoming packet at a given layer (coming from its adjacent upper layer) is called a Service Data Unit (SDU). The layer transforms this SDU into a Protocol Data Unit (PDU), typically by adding it a header and/or a footer. Then, the PDU is passed to the adjacent lower layer, where it becomes the SDU of this layer, and so on.

In this layer model, the stream of bits is partitioned into information packets (shortened as packets in the rest of this thesis), which is the smallest piece of information that has to be transmitted.

A special case of the above discussion is the Medium Access Control (MAC) which transmits packets of information bits to the Physical (PHY) layer, whose task is to transform those bits into a signal, and to send it through the propagation medium, i.e., the channel. In wireless communications, the transmission takes place in time-varying channel yielding degradations on the signal, which have to be mitigated. To this end, in almost all practical systems, FEC codes are used. Hence, the packets can be retrieved if and only if the receiver is able to decode the codeword.

As a consequence, it appears that the PER is more adequate than Bit Error Rate (BER) to measure wireless systems' performance due to the underlying packet oriented model. Both ARQ and HARQ are mechanisms allowing to decrease the PER.

1.4.2 ARQ

The ARQ mechanism is packet oriented and works as follows: the transmitter adds Cyclic Redundancy Check (CRC) in each packet of information bits and sends them on the channel. The receiver decodes the information bits and checks for error using the CRC. If no error is detected, an ACKnowledgment (ACK) is sent, and the transmitter sends another packet. Otherwise, a Negative ACKnowledgment (NACK) is sent, and the same packet is retransmitted until either an error-free transmission occurs, or the maximum allowed number of transmissions $\mathcal{M}$ is reached. Notice that this latter case is called truncated ARQ, which is opposed to pure ARQ in which the number of transmission is theoretically infinite. The principle of ARQ is illustrated in Fig. 1.3, where KO (resp. OK) means that a packet is received in error (resp. without error).

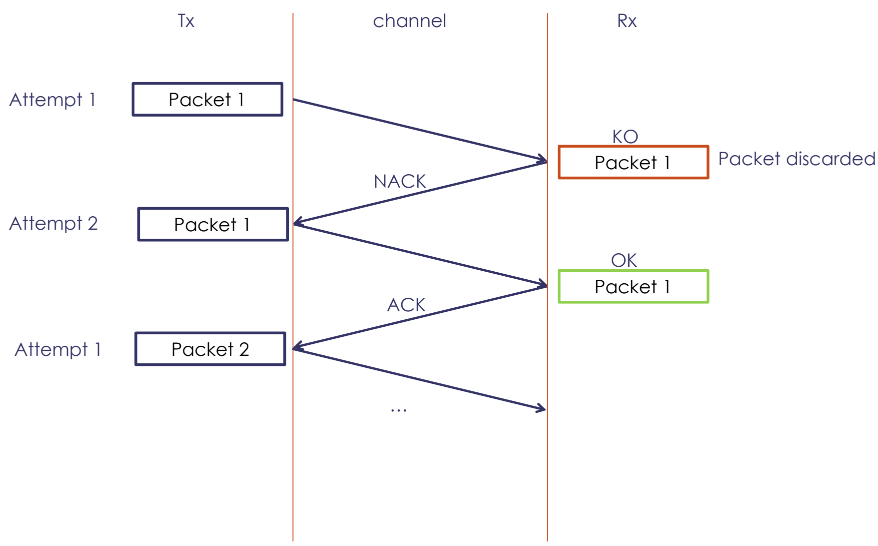

Figure 1.3: ARQ mechanism illustration.

Thus, ARQ allows to increase the reliability of a wireless communication thanks to the retransmission mechanism. However, it is known that ARQ performance significantly degrades in the case of bad channel conditions. This performance degradation can be countered through the use of HARQ.

1.4.3 Hybrid ARQ

As ARQ, the HARQ mechanism is also packet oriented and based on retransmission with the use ACK/NACK feedback. In addition, HARQ uses FEC, providing to it a correction capability to handle bad channel condition. This mechanism is nowadays used in several standards such as 4G Long Term Evolution (LTE) [97] or High Speed Downlink Packet Access (HSDPA) [42]. There exists different types of HARQ and, in this thesis, we focus on Type-I and Type-II HARQ, described hereafter.

1.4.3.1 Type-I HARQ

Type-I HARQ is the most simple HARQ scheme: after adding a CRC to the information bits, they are encoded by a FEC with rate R, and the resulting block is sent through the channel. The receiver decodes the bits and acts as in the ARQ case.

The advantage of Type-I HARQ is their straightforward implementation, making them easy to use. They have however two drawbacks: *i)* the receiver discards erroneous blocks, while they could bring information helping for the decoding of the retransmissions and *ii)* the throughput is degraded due to the use of channel coding.

1.4.3.2 Type-II HARQ

Contrarily to the simple Type-I HARQ scheme, Type-II HARQ uses all the blocks received in error to decode the information bits. There exist at least two Type-II HARQ mechanisms: Chase Combining (CC) and Incremental Redundancy (IR).

CC HARQ. In CC HARQ, the transmitter acts exactly the same way as Type-I HARQ. The difference is at the receiver side: when a block is received in error, instead of being discarded, it is kept in a buffer. Then, at the reception of the mth block ($m = 1, \ldots, \mathcal{M}$), the receiver performs the Maximum Ratio Combining (MRC) with the m available blocks. Hence, the correction capability of CC HARQ is more important than the simple Type-I HARQ scheme. The drawback of CC HARQ is, as for Type-I HARQ, the throughput degradation induced by the channel coding.

IR HARQ. The IR HARQ mechanism at both the transmitter and receiver side is different from Type-I and CC HARQ because the transmitted blocks between the several attempts to transmit one packet differ. The principle of IR HARQ is described as follows: after adding the CRC to the information bits, they are encoded by a FEC called mother code, and the coded bits are split into redundancy blocks following the rate-compatible coding principle [53]. At the receiver side, at the mth transmission ($m = 1, \ldots, \mathcal{M}$), all the received blocks are concatenated, and then decoded. In general, the throughput of IR HARQ is higher than the one of CC HARQ since it can adapt to the channel conditions by transmitting short (resp. long) packets under good (resp. bad) channel. Its drawback lies in its implementation, which is more complicated.

1.4.4 Performance metrics

There exist in the literature several metrics aiming to measure the performance of HARQ based systems and this Section provides an overview of the most common ones. It is worth noticing that giving a complete overview of HARQ metrics is out of the scope of this work, and we refer to [67] for a more comprehensive survey.

In the rest of this document, we assume that the transmitted blocks during the $\mathcal{M}$ attempts to transmit one packet have equal length $\mathcal{L}$. This assumption is always valid for Type-I and CC HARQ, and valid for several IR HARQ schemes including the nested schemes described in [43]. Let us define $q_{\ell,m}$ as the probability that the first m transmissions are all received in error on link ℓ.

1.4.4.1 Packet Error Rate

Since we consider truncated HARQ, there is a non-zero probability that a packet is dropped at the end of the $\mathcal{M}$th HARQ attempt. The PER is defined as the probability that, after the transmission of the $\mathcal{M}$th block corresponding to the same packet, a NACK is received and, as a consequence, the packet is dropped. Formally, it can be written as:

$$\mathrm{PER}_\ell := \Pr(\text{Packet discarded after the } \mathcal{M}\text{th transmission }),$$

Using the previously-introduced notations, the PER is given by:

$$\mathrm{PER}_\ell = q_{\ell,\mathcal{M}}, \tag{1.7}$$

which gives, for Type-I HARQ with no correlation between successive transmissions

$$\mathrm{PER}_\ell = (q_{\ell,1})^{\mathcal{M}}. \tag{1.8}$$

1.4.4.2 Efficiency

The efficiency e_ℓ of link ℓ is defined as the ratio between the number of successfully received information bits with the number of transmitted bits. It can be computed using the renewal theory as follows [125]:

$$e_\ell = \frac{\mathbb{E}[I_r]}{\mathbb{E}[b_r]}, \tag{1.9}$$

where I_r is a random variable representing the number of received information bits per correctly received packet and b_r is the random number of transmitted bits between two successive packets received without error. Eq. (1.9) can be computed as [77]:

$$e_\ell = \frac{1 - q_{\ell,\mathcal{M}}}{1 + \sum_{m=1}^{\mathcal{M}-1} q_{\ell,m}}. \tag{1.10}$$

When there is no correlation between successive blocks transmissions, (1.10) simplifies for Type-I HARQ as:

$$e_\ell = (1 - q_{\ell,1}). \tag{1.11}$$

Notice that (1.11) is independent of the maximum number of transmissions $\mathcal{M}$.

1.4.4.3 Goodput

A crucial figure of merit in wireless communications is the data rate. The goodput is a measure of the useful data rate, i.e., the number of information bits that can be transmitted without error per second. It is proportional to the efficiency, and for the ℓth link writes:

$$\eta_\ell := B_\ell m_\ell R_\ell e_\ell, \tag{1.12}$$

where m_ℓ is the modulation order, R_ℓ is the code rate and B_ℓ is the bandwidth used per link ℓ to communicate. This metric is now well established in the ARQ and HARQ literature to measure the useful data rate of practical systems [39]. By plugging (1.10) into (1.12) we obtain, for Type-II HARQ:

$$\eta_\ell = B_\ell m_\ell R_\ell \frac{1 - q_{\ell,\mathcal{M}}}{1 + \sum_{m=1}^{\mathcal{M}-1} q_{\ell,m}}, \tag{1.13}$$

whereas, for Type-I HARQ with no correlation between successive blocks transmissions, plugging (1.11) into (1.12) yields:

$$\eta_\ell = B_\ell m_\ell R_\ell (1 - q_{\ell,1}). \tag{1.14}$$

1.5 Energy Efficiency

In this Section, we introduce the fundamental notion of EE, which is of central importance in this thesis, and we justify the interest of considering this metric to perform RA.

1.5.1 Why considering energy efficiency?

The RA is performed by optimizing a criterion subject to QoS constraints. Two conventional objectives when designing a wireless communication system are either to maximize the data rate [84], or to minimize the power consumption [114], with maximum transmit power and/or minimum data rate constraints. For the rest of this document, the power minimization criteria will be referred to as Minimum Power (MPO) and the goodput maximization as Maximum Goodput (MGO). These two objectives are generally conflicting: indeed, increasing the data rate requires to increase the power consumption whereas minimizing the power consumption reduces the data rate. Hence, these two metrics lead to different working points of the system, depending on the system designer objective. Thus, it appears interesting to define metrics combining both power consumption and data rate in order to reach a tradeoff, which can be achieved by using the EE as defined in the next Section.

1.5.2 Energy efficiency definition

A formal definition of EE, is provided in [124], and is given as follows:

$$\mathcal{E}_\ell := \frac{\text{total amount of data delivred on link } \ell \quad \text{[bits]}}{\text{total consumed energy on link } \ell \quad \text{[joules]}}. \tag{1.15}$$

To the best of our knowledge, [124] is the first work formalizing the EE as (1.15). The authors introduce this metric in order to investigate the ARQ retransmissions impact on the energy consumption under correlated fading channels.

Since the consumed energy is equal to the product between the consumed power and the transmission time, dividing both the numerator and the denominator of (1.15) by a time unit allows us to rewrite it as follows:

$$\mathcal{E}_\ell := \frac{\eta_\ell \quad [\text{bits/s}]}{P_{O,\ell} \quad [\text{W}]}, \tag{1.16}$$

where $P_{O,\ell}$ is ℓth link power consumption.

From (1.16), we can see that the EE is defined as the ratio between the goodput and the power consumption and thus optimizing EE is expected to provide a tradeoff between these two metrics. Since [124], the EE as defined in (1.16) has been extensively studied in the literature, as it can be seen in [41, 120] and references therein.

The EE given in (1.16) is user centric since it measures the ℓth link performance. We can also define the EE of the whole network, called GEE, which is defined as the ratio between the sum of the links goodput and the sum of their power consumption and writes as:

$$\mathcal{G} := \frac{\sum_{\ell=1}^{L} \eta_\ell}{\sum_{\ell=1}^{L} P_{O,\ell}}. \tag{1.17}$$

It is worth emphasizing that a large amount of existing EE-related works consider the capacity as the measure of the data rate (i.e., η_ℓ is replaced by the Shannon capacity in (1.16) and (1.17)), see, i.e., Chapter 3, which is an upper bound of the achievable rate of real MCS. Since this thesis aims to provide algorithms for systems using practical MCS, unless otherwise stated, η_ℓ is given by (1.13) for Type-II HARQ or (1.14) for Type-I HARQ.

1.5.3 Energy consumption model

The total consumed power to send and receive one OFDMA or SC-FDMA symbol on the ℓth link is equal to the sum of the transmit power and the circuitry consumption of both the emitter and the receiver, and can be written as:

$$P_{O,\ell}(j) := \frac{1}{\kappa_\ell} \sum_{n=1}^{n_\ell} P_{T,\ell}(j,n) + P_{ctx,\ell} + P_{crx,\ell}, \tag{1.18}$$

where $\kappa_\ell \leq 1$ is the Power Amplifier (PA) efficiency, $P_{T,\ell}(j,n) := \mathbb{E}[|\mathcal{X}_\ell(j,n)|^2]$ is the transmit power on subcarrier n during the jth OFDMA (or SC-FDMA) symbol, and $P_{ctx,\ell}$ (resp. $P_{crx,\ell}$) is the per-symbol circuitry power consumption at the transmitter (resp. receiver), which are assumed to be independent of the transmit power.

1.5.4 Numerical illustration

In this Section, we numerically illustrate *i)* the interest of considering the EE as the criterion to optimize instead of the conventional ones, i.e., the MPO and the MGO, *ii)* the impact of the Rician K factor on the EE, and *iii)* the importance of taking into account practical MCS instead of capacity achieving codes during the RA process.

To do so, we focus on a single link ℓ and we assume that this link transmits on the whole bandwidth with the same power, and does not perform link adaptation (i.e., $\forall n$, $\forall j$, $P_{T,\ell}(j,n) = P_{T,\ell}$). For simplicity, in this Section, we drop the link index. The simulation setup is the following. The link distance is $\delta^{(D)} = 800$ m, we set $B = 5$ MHz, $N_0 = -170$ dBm/Hz, $\mathcal{L} = 128$. The carrier frequency is $f_c = 2400$ MHz and we set $\Delta = (4\pi f_c/c)^{-2}\delta^{(D)-3}$ where c is the speed of light in vacuum. We also set $P_{ctx} = P_{crx} = 0.05$ W and $\kappa = 0.5$.

First, let us focus on the interest of considering EE as the criterion to optimize instead of conventional ones. We consider the following three RA objectives, **O1**: minimizing the transmit power subject to minimum goodput constraint of 1 Mbits/s (MPO), **O2**: maximizing the goodput subject to maximum transmit power constraint of 35 dBm (MGO), and **O3**: maximizing the EE subject to both the minimum goodput and maximum transmit power constraints. We consider a Rayleigh FF channel (i.e., $\forall j$, $a(j) = 0$), and we consider a Type-I HARQ system using a convolutional code with generator polynomial $[171, 133]_8$ and a Quadrature Phase Shift Keying (QPSK) modulation. In Fig. 1.4, we superimpose both the goodput, given by (1.12), and the EE given by (1.16). We indicate on the figure the optimal points for each scenario **Oi**, i=1,2,3.

We can see that the optimal points of **O1** (resp. **O2**) yield an EE loss of about 65% (resp. 75%) compared with the optimal point of **O3**. An EE loss of X% means that, for a given amount of energy, X% less information bits can be transmitted. To see this, let us define $\mathcal{E}_{O_i}$ the EE achieved for a given objective **Oi**. From (1.15), $\mathcal{E}_{O_3}/\mathcal{E}_{O_i} = (b_{O_3}/E_{O_3})/(b_{O_i}/E_{O_i})$ where b_{O_i} (resp. E_{O_i}) is the number of information bits transmitted without error (resp. the energy consumption). Thus, for fixed consumed energy consumption (i.e., $E_{O_3} = E_{O_i}$), $\mathcal{E}_{O_3}/\mathcal{E}_{O_i} = b_{O_3}/b_{O_i}$. Since $\mathcal{E}_{O_3}/\mathcal{E}_{O_i} >> 1$, we infer that, for a given quantity of energy, **O3** can transmit much more information bits without error than the two conventional schemes **O1** and **O2**. We can also see that, at the optimal point of **O3**, increasing the power consumption would increase the goodput only slightly. This traduces that the EE allows us to achieve a tradeoff between these two metrics.

To further illustrate the real effectiveness of the EE criterion to achieve a better user experience than the MGO and MPO, we consider the practical example of a smartphone which has to send a sequence of messages, and evaluate for these criteria the performance achieved in terms of number of transmitted messages and battery drain. Let us consider a battery with capacity $Q_0 = 3000$ mAh, with voltage $U = 3.85$ V, which are typical values for recent smartphones. The battery drain equation as a function of time t is given by:

$$Q_\ell(t) = Q_0 - \frac{P_O t}{U}. \tag{1.19}$$

We investigate two cases: in the first one, the smartphone has to transmit 10^7 messages. In the second one, the smartphone sends messages until its battery is empty. For both

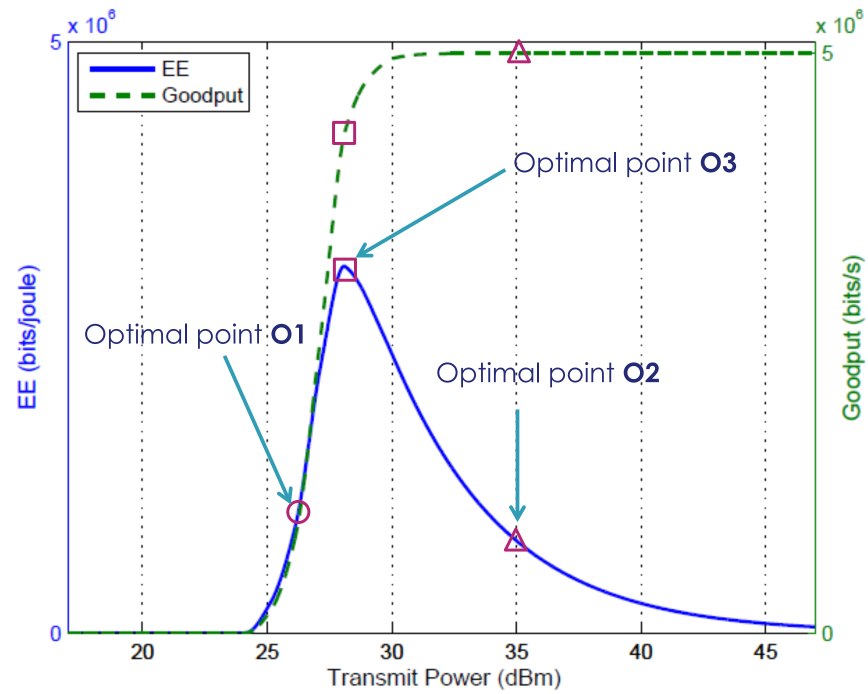

Figure 1.4: EE and goodput of Type-I HARQ scheme versus the transmit power under Rayleigh channel.

cases, we compute the following metrics: Q_r the remaining battery (in %), T_t the time to transmit the messages (in s) and N_p the number of transmitted messages, The results are reported in Table 1.1.

Table 1.1: Comparison of the EE with the conventional criteria (MPO and MGO) in terms of equipment autonomy and time to transmit information for the two cases.

Case	Criterion	Q_r	T_t (s)	N_p	η^A (Mbits/s)
10^7 sent messages	EE	96%	297	1×10^7	4.3
	MGO	85%	256	1×10^7	5
	MPO	89%	1 280	1×10^7	1
Full battery drain	EE	0%	8 327	2.8×10^8	4.3
	MGO	0%	1 800	7×10^7	5
	MPO	0%	12 180	9.5×10^7	1

In the first case, as expected, the transmit duration of the MGO is the lowest among the considered criteria since it has the highest goodput, but it has also the highest energy consumption. The EE transmit duration is slightly higher than the MGO one, but its power consumption is much lower. Regarding the MPO, its energy consumption is lower than the MGO but higher than the EE, and it has the highest transmit duration, which is explained because it has the lowest goodput.

In the second case, the EE maximization is clearly the best criterion among the considered ones since it enables to transmit more packet and to transmit for longer duration than the two other criteria. the MPO transmit more packets than the MGO, but its goodput is much less.

From the above discussion, we infer that the EE maximization enables either to transmit more packets in average than when using the MPO and the MGO at the end of the battery lifetime, or the links have higher battery levels in average for the same number of transmit messages. This clearly demonstrates the practical relevance of considering the EE when designing a RA procedure.

Now, we show the importance of taking into account both the Rician K factor and the use of practical MCS during the RA. To this end, we consider a Rician FF channel without shadowing (i.e., $\forall j$, $a(j) = a$ and $c_\ell(j) = 1$). We consider the same convolutional code as in Fig 1.4 along with both QPSK and 16-Quadrature Amplitude Modulation (QAM) modulations, and we also consider the ideal case in which the goodput η in (1.16) is replaced by the so-called ergodic capacity, defined as [107]:

$$\Theta_{erg}(P_T) := \mathbb{E}\left[\log\left(1 + P_T \frac{\Delta}{2\sigma_n^2}|H|^2\right)\right], \tag{1.20}$$

with $H \sim \mathcal{CN}(a, 2\sigma_h^2)$ with a and $2\sigma_h^2$ such that $a^2 + 2\sigma_h^2 = 1$ (i.e., the average channel power is normalized) and $a^2/(2\sigma_h^2) = K$. Eq. (1.20) is an upper bound of the achievable data rate under Rician FF channels. In Fig. 1.5, we plot the EE for the considered practical MCSs and ergodic capacity, for $K = 0$ and $K = 10$. First, concerning the impact of the Rician K factor, we can see that, for practical MCS, considering $K = 0$ when $K = 10$ or $K = 10$ when $K = 0$ yields EE losses (reported in Table 1.2), meaning that performing RA with the actual K value is of importance. Second, we clearly see the importance of taking into account practical MCS, indeed, the point maximizing the EE with capacity achieving codes yields almost zero EE for practical MCS (the EE losses are reported in Table 1.2) for both $K = 0$ and $K = 10$. As a consequence, we cannot use (1.20) to perform RA when using practical MCS.

We have hence numerically exhibited the interest of EE as compared with conventional criteria, and the importance of considering the Rician K factor and the use practical MCS during the RA.

1.6 EE-based RA as Constrained Optimization Problems

Here, we mathematically formalize the RA problems by first describing the design parameters, which are the optimization variables. Second, we present the considered constraints that we impose in the RA. Finally, we formulate the optimization problems that we solve in this thesis.

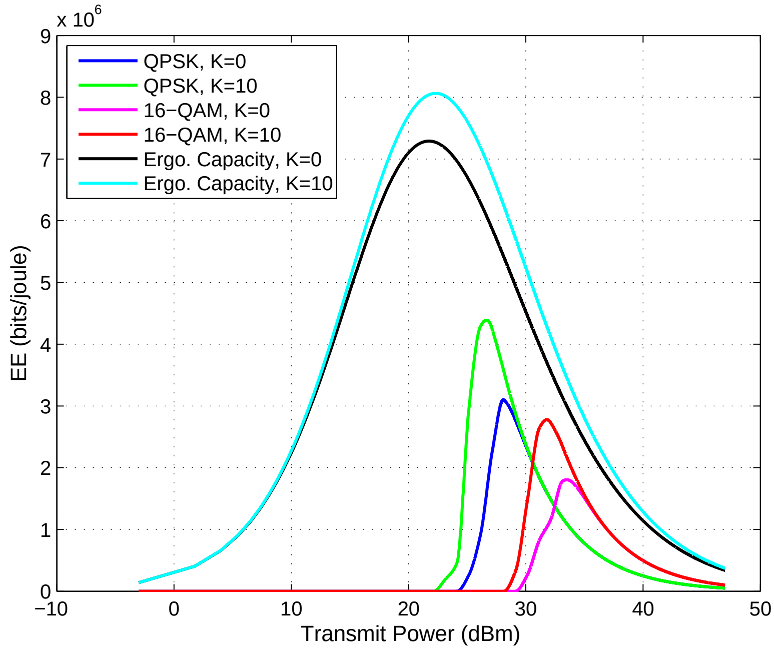

Figure 1.5: EE of Type-I HARQ scheme and ergodic capacity-based system for $K = 0$ and $K = 10$ versus the transmit power.

1.6.1 Design parameters

Our objective is to allocate to each link a transmit energy and a proportion of the bandwidth. More precisely, because the channel coefficients on each subcarrier are identically distributed and only statistical CSI is available as the RM, the same power is allocated on all the subcarriers, there is no power adaptation between OFDMA or SC-FDMA symbols (i.e., $\forall n$, $\forall j$, $P_{T,\ell}(j, n) = P_{T,\ell}$), and we allocate a proportion of the bandwidth instead of specific subcarriers. In Fig. 1.6, we represent an example of RA associated with the network in Fig. 1.1.

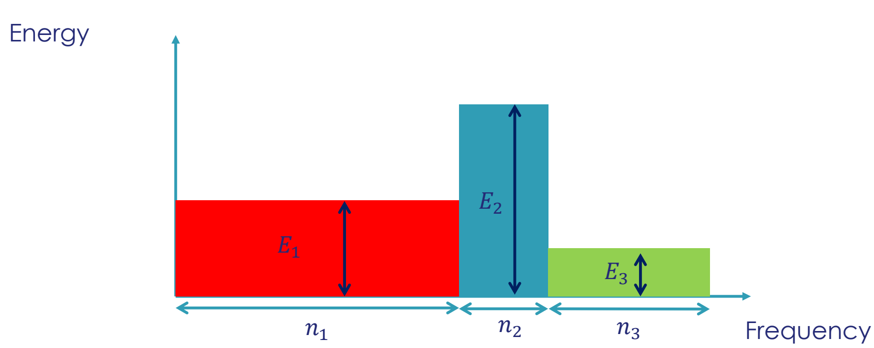

Figure 1.6: Example of a RA associated with the network in Fig. 1.1.

We can define γ_ℓ (resp. E_ℓ) as the proportion of bandwidth (resp. transmit energy)

Real scheme	Considered scheme to perform RA	EE loss
QPSK, $K = 0$	QPSK, $K = 10$	50%
	Ergodic capacity, $K = 0$	100%
QPSK, $K = 10$	QPSK, $K = 0$	20%
	Ergodic capacity, $K = 10$	99.5%
16-QAM, $K = 0$	16-QAM, $K = 10$	57%
	Ergodic capacity, $K = 0$	100%
16-QAM, $K = 10$	16-QAM, $K = 0$	22%
	Ergodic capacity, $K = 10$	100%

Table 1.2: EE loss when performing RA with communications scheme mismatch.

allocated to the ℓth link as

$$\gamma_\ell = \frac{n_\ell}{N_c}, \tag{1.21}$$

$$E_\ell := \frac{N_c}{B} P_{T,\ell}. \tag{1.22}$$

The design parameters, i.e., the resource that have to be allocated to the links, are given by $\mathbf{E} := [E_1, \dots, E_L]$ and $\boldsymbol{\gamma} := [\gamma_1, \dots, \gamma_L]$.

1.6.2 Considered constraints

Hereafter, we present the constraints that are considered in our RA problems.

Notice that, until now, $\forall \ell, m$, we have dropped the error probabilities $q_{\ell,m}$ dependency on the transmit energy E_ℓ. For the rest of this thesis, since E_ℓ is an optimization variable, we will denote this dependency by letting $q_{\ell,m}(G_\ell E_\ell)$ be a function of both G_ℓ and E_ℓ. Notice that $E_\ell G_\ell$ corresponds to the Signal to Noise Ratio (SNR) since we have

$$\mathrm{SNR}_\ell = \frac{P_{T,\ell}\Delta_\ell}{N_0 \frac{B}{N_c}} = E_\ell G_\ell. \tag{1.23}$$

Goodput constraint: a basic requirement in a communication system is to ensure a minimum data rate, providing minimum QoS guaranty. That is, in our RA problem, we want to impose a minimum value for the goodput. Since the bandwidth used per link ℓ is $B_\ell = B\gamma_\ell$, this constraint can be mathematically written as follows using (1.13):

$$B\gamma_\ell \alpha_\ell \frac{1 - q_{\ell,M}(G_\ell E_\ell)}{1 + \sum_{m=1}^{M-1} q_{\ell,m}(G_\ell E_\ell)} \geq \eta_\ell^{(1)}, \quad \forall \ell, \tag{1.24}$$

with $\alpha_\ell := m_\ell R_\ell$. Constraint (1.24) can be rewritten as:

$$\gamma_\ell \alpha_\ell \frac{1 - q_{\ell,M}(G_\ell E_\ell)}{1 + \sum_{m=1}^{M-1} q_{\ell,m}(G_\ell E_\ell)} \geq \eta_\ell^{(0)}, \quad \forall \ell, \tag{1.25}$$

with $\eta_\ell^{(0)} := \eta_\ell^{(1)}/B$. Notice that $\eta_\ell^{(0)}$ is known as the *goodput efficiency*.

For Type-I HARQ with no correlation between successive blocks transmissions, constraint (1.25) reduces to:

$$\gamma_\ell \alpha_\ell (1 - q_{\ell,1}(G_\ell E_\ell)) \geq \eta_\ell^{(0)}, \quad \forall \ell. \tag{1.26}$$

Power constraint: in order to avoid non linearity of the PA and to limit the consumption of the devices, it is natural to put a per-link maximum transmit power, which can be written as [65]:

$$\gamma_\ell E_\ell \leq P_{\max,\ell}, \quad \forall \ell. \tag{1.27}$$

Bandwidth constraint: from the definition of the bandwidth variables γ_ℓ, it is clear that the following inequality has to hold:

$$\sum_{\ell=1}^{L} \gamma_\ell \leq 1, \tag{1.28}$$

which ensures that we do not allocate more bandwidth than the total available bandwidth.

1.6.3 Problems formulation

From the considered system model and hypothesis exposed in the previous Sections, by plugging (1.13), (1.18), (1.21) and (1.22) into (1.16), the ℓth link EE can be written as

$$\mathcal{E}_\ell = \frac{\alpha_\ell (1 - q_{\ell,M}(G_\ell E_\ell))}{(1 + \sum_{m=1}^{M-1} q_{\ell,m}(G_\ell E_\ell))(\kappa_\ell^{-1} E_\ell + \gamma_\ell^{-1} E_{c,\ell})}, \tag{1.29}$$

with $E_{c,\ell} := \frac{P_{ctx,\ell} + P_{crx,\ell}}{B}$. Similarly, the GEE (1.17) writes as

$$\mathcal{G} = \frac{\sum_{\ell=1}^{L} \alpha_\ell \gamma_\ell \frac{1 - q_{\ell,M}(G_\ell E_\ell)}{1 + \sum_{m=1}^{M-1} q_{\ell,m}(G_\ell E_\ell)}}{\sum_{\ell=1}^{L} (\kappa_\ell^{-1} \gamma_\ell E_\ell + E_{c,\ell})}. \tag{1.30}$$

In this thesis, we aim to perform RA by maximizing EE under constraints. As a consequence, we wish to maximize either an aggregation of the links' individual EE (1.29), or the GEE (1.30), which writes in the following general form.

Problem 1.1. *The general EE-based RA problems write as:*

$$\begin{aligned} \max_{\mathbf{E},\gamma} \quad & \mathcal{H}(\{\mathcal{E}_\ell(E_\ell, \gamma_\ell)\}_{\ell=1,\dots,L}) \quad \text{or} \quad \mathcal{G}(\mathbf{E}, \gamma) \\ \text{s.t.} \quad & (1.25), (1.27), (1.28), \end{aligned} \tag{1.31}$$

where $\mathcal{H}$ is a function of the links' individual EE whereas $\mathcal{G}$ is the network EE. In this thesis (Chapters 3 to 5), we consider the following functions for $\mathcal{H}$:

- The sum, leading to the MSEE problem.

- The product, leading to the MPEE problem.
- The $\min_\ell$ operator, leading to MMEE problem.

On the other hand, the problem of the maximization of the GEE is called the MGEE problem. These four criteria are expected to yield different results in terms of fairness, which represents how the resource are shared among the users.

1.7 Thesis Objectives

In this Section, we give the big picture of the thesis objectives by detailing the system operation, which is represented on a time diagram in Fig. 1.7, where we focus on link 1 (each link performing the same operations). Tx1 transmits to Rx1 several OFDMA or SC-FDMA symbols using resource allocated from a previous persistent RA and, using training sequences, Rx1 estimates the CIR at different time instants. Using these CIR estimations, Rx1 estimates the channel statistics: $\hat{K}_1$, the Rician K factor estimation, and $\hat{G}_1$, the GNR estimation. Then, Rxi sends these estimated parameters to the RM. Using all the links statistics, the RM performs RA by computing $\forall \ell$, E_ℓ^* and γ_ℓ^*, the optimal values of E_ℓ and γ_ℓ, and sends these values to the links.

The thesis global objective is to propose solutions to perform RA based on statistical CSI in the context described in Fig. 1.7. In general in the literature, when performing such a RA, the channel's statistical parameters are assumed to be known. However, in practice, these parameters have to be estimated. Since this thesis is done in collaboration with Thales and is thus performed in an industrial context, we seek for practical and implementable solutions. Then, we aim to address both RA problems and the estimation of the channel statistics.

The above discussion yield the following two intermediate goals of the thesis:

1. Estimating the channel statistics using CIR estimated from a training sequence.
2. Performing RA based on channel statistical CSI.

In details, for the first goal, we aim to estimate the Rician K factor defined in (1.6) in practical configurations, i.e., when the available channel samples are estimated from a training sequence as illustrated in Fig. 1.7 and as a consequence they are noisy. This first goal is addressed in Chapter 2. For the second goal, we wish to propose algorithms based on statistical CSI with affordable complexity to solve the general RA Problem 1.1. This second goal is addressed in Chapters 3 to 5.

1.8 Conclusion

In this first Chapter, we introduced the working context of the thesis. We presented the network, the signal and the channel model. We defined the crucial notions of EE and

GEE. Finally, we formulated generals EE-based RA problems.

This Chapter serves as the basis for the rest of the thesis. In Chapter 2, we estimate the Rician K factor, defined in (1.6), whereas Chapter 3 to 5 are devoted to the solution of the RA Problem 1.1.

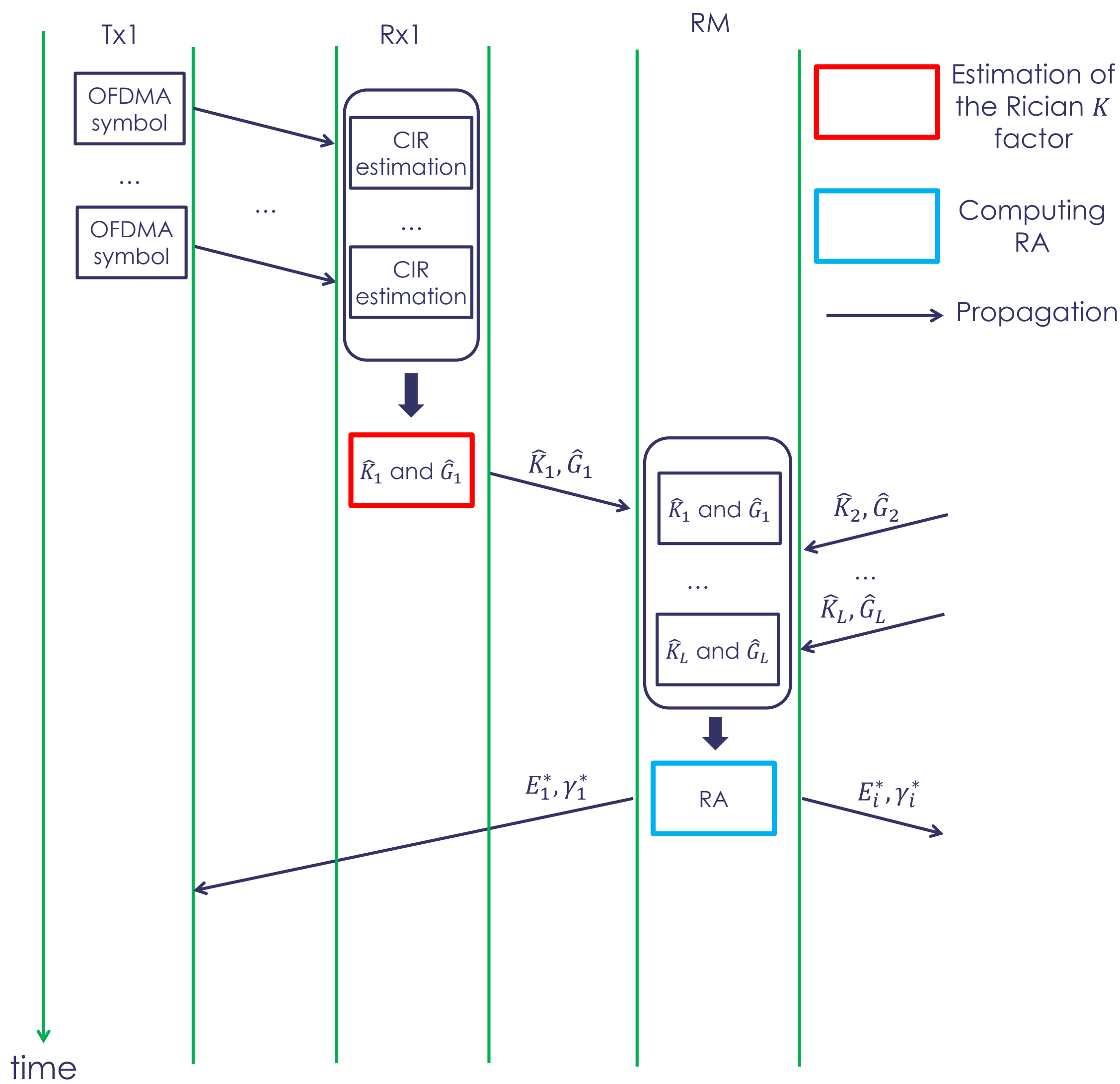

Figure 1.7: Time diagram of the operations performed by the system. The topics handled in this Thesis are represented by the red and blue boxes.

Chapter 2

Estimation of the Rician K Factor

2.1 Introduction

In this second Chapter, we address one of the goal of this thesis, which is the estimation of the Rician K factor. More precisely, we wish to estimate this parameter from imperfect (noisy) complex channels' samples. We address both cases with and without shadowing, as explained in Chapter 1.

2.1.1 State of the art

Let us review the existing works related to our estimation problems.

Existing estimators without LoS shadowing. In [1, 9, 50, 66, 79, 104, 106], different estimators using the magnitude of the complex channel coefficients are proposed and compared. The estimators developed in [5, 6, 22, 69, 92, 106] use noiseless complex channel coefficients. It is shown in [106] that using complex coefficients allows better estimation than using magnitude only. All the estimators mentioned so far consider noiseless coefficients, meaning that the channel is perfectly known. In [20] and [21], estimators based on noisy coefficients magnitude are proposed. To the best of our knowledge, the only estimators considering noisy complex channel coefficients are provided in [19], which are valid only when the channel coefficients are correlated according to the Clark's model.

Existing estimators with LoS shadowing. Only few works investigate the estimation of the Rician K factor in case of Nakagami-m shadowed LoS component [83], [47]. In [83], an estimator based on noiseless coefficients magnitude is proposed. The proposed approach is based on a MoM, and has an important drawback: the estimation of a statistical parameter of the LoS shadowing is required, and the procedure to estimate it is unclear. Recently, in [47], another estimator based on MoM is proposed. Its drawback is that it uses moments up to the order of 6 and as a consequence, it requires large sample size to produce reliable estimates. Typically, 10^5 samples are used in [47].

In addition, both [83] and [47] assume that the shadowing changes independently between consecutive channel samples. In this thesis, we assume a more general case in which the shadowing is piecewise constant (see Section 1.3.2).

The existing estimators of the Rician K factor are summarized in Table 2.1. We can see that the only estimator of the Rician K factor using noisy complex channel coefficients is [19], which requires a specific correlation among complex samples and does not take into account for LoS shadowing. Also, only two estimators address the estimation of K for shadowed LoS, and they suffer from severe drawbacks.

	Without LoS shadowing	With LoS shadowing
Noiseless magnitude	[1, 9, 50, 66, 79, 104, 106]	[47, 83]
Noisy magnitude	[20, 21]	None
Noiseless complex	[5, 6, 22, 69, 92, 106]	None
Noisy complex	[19]	None

Table 2.1: Existing estimators of the Rician K factor.

Cramer Rao Bound. The CRLB is a lower bound on the variance of any unbiased estimator [62]. The deterministic CRLB of the K factor is derived in [106] for both magnitude-based estimators and complex coefficients-based estimators in the noiseless case. The deterministic CRLB for the K factor in case of noisy coefficients magnitude is obtained numerically in [20]. The authors of [59] propose a deterministic CRLB for the complex coefficients estimation of K in the noiseless case. Finally, a stochastic CRLB is derived in [100].

From the above discussions, we see that the CRLB for the deterministic estimation of the Rician K factor without LoS shadowing using complex noisy channel coefficients is not available in the literature.

2.1.2 Contributions

The contributions of this Chapter are summarized as follows.

2.1.2.1 Without LoS shadowing

- We propose two deterministic estimators of the Rician K factor using noisy complex channel samples estimated from a training sequence. In addition, we also derive the Rejection Rate (RR) (defined in this Chapter) of these estimators.

- We design two Bayesian estimators of the Rician K factor: the mean a posteriori and the maximum a posteriori. The mean a posteriori is approximated using the Gauss-Hermite Quadrature (GHQ) whereas the maximum a posteriori is obtained by numerically finding the root of a non linear equation.

- We derive the closed-form expression of the deterministic CRLB for the estimation of the Rician K factor when using noisy complex samples to perform the estimation.

2.1.2.2 With LoS shadowing

- We propose an EM based procedure to estimate the Rician K factor with Nakagami-m shadowed LoS.

- We also derive another estimator based on MoM to initialize the EM procedure.

In both cases (i.e., with and without LoS shadowing) we perform extensive simulations to study the proposed estimators' performance, and show that they outperform the ones from the literature.

2.1.3 Chapter organization

The rest of the Chapter is organized as follows. In Section 2.2, we explain the channel estimation procedure, and we provide the system model. In Section 2.3, we address the estimation of the Rician K factor when there is no LoS shadowing, whereas, in Section 2.4, we address this estimation problem in case of Nakagami-m shadowed LoS. Finally, Section 2.5 concludes the Chapter.

2.2 Channel estimation and properties

Following the system model described in Chapter 1, we focus on a link ℓ and for simplicity, we drop the links' indices in this Chapter. Thus, the received signal on subcarrier n of the ith OFDMA or SC-FDMA symbol can be written as:

$$Y(i,n) = H(i,n)\mathcal{X}(i,n) + Z(i,n), \tag{2.1}$$

where $\mathcal{X}(i,n)$ is the ith sent symbol on subcarrier n, $Z(i,n) \sim \mathcal{CN}(0, 2\sigma_n^2)$ is a complex white Gaussian noise with zero mean and variance $2\sigma_n^2$, which is assumed to be known, and $H(i,n) \sim \mathcal{CN}(c(i)ae^{j\theta_0}, 2\sigma_h^2)$. On one hand, when there is no shadowing, $c(i) = 1\ \forall i$. On the other hand, in the case of shadowed LoS, $c(i)$ is constant during N_{T_c} OFDMA or SC-FDMA symbols, and varies independently every N_{T_c} symbols following a Nakagami-m distribution with parameters m_{Na} and $\Omega = 1$.

We assume that the channel is estimated from (2.1) using a training sequence, meaning that $\mathcal{X}(i,n)$ is known from the receiver. For instance, the channel samples $H(i,n)$ can be estimated as $\tilde{H}(i,n) = Y(i,n)/\mathcal{X}(i,n)$, yielding:

$$\tilde{H}(i,n) = H(i,n) + \hat{Z}(i,n), \tag{2.2}$$

with $\hat{Z}(i,n) \sim \mathcal{CN}(0, 2\sigma_n^2)$ is an additive complex white Gaussian noise. The number of pilots symbols per OFDMA or SC-FDMA symbol is denoted by i_f whereas the number of available OFDMA or SC-FDMA symbols is denoted by i_t. We then define the total number of available estimated channel samples as $N := i_t \times i_f$.

We assume that the frequency space between the pilots symbols within one OFDMA or SC-FDMA symbol is larger than the channel's coherence bandwidth (which can be evaluated for instance using the procedure from [44]), and thus we neglect the channel's frequency correlation. Following Chapter 1, we also neglect the channel's time correlation. The above notations are depicted in Fig. 2.1, in which the channel coherence bandwidth is two frequency bins.

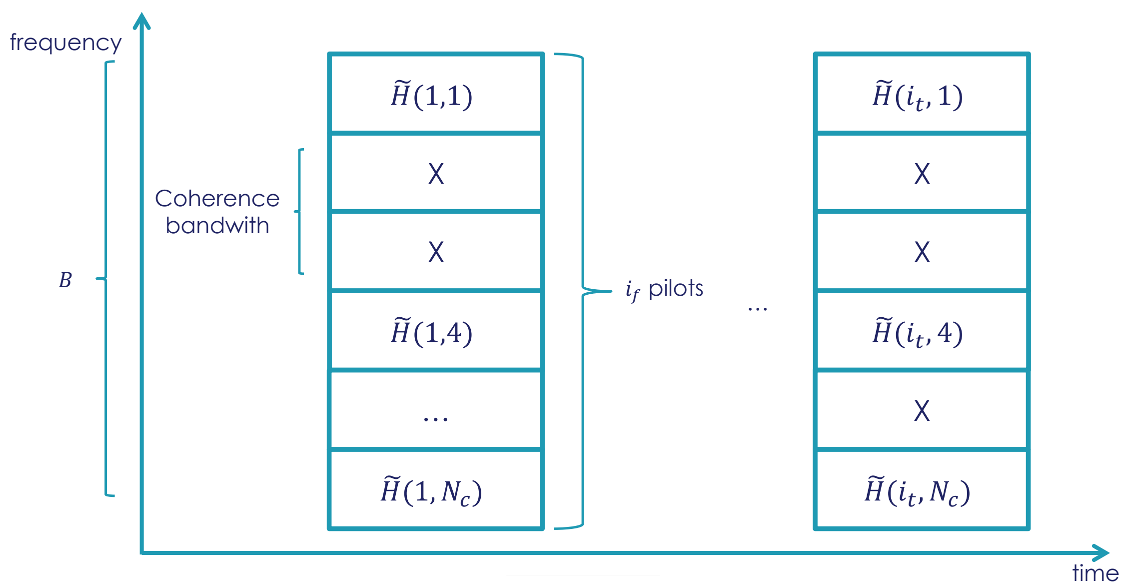

Figure 2.1: Channel estimation procedure.

For the ease of mathematical formulation, let us reshape the estimated channel samples in a matrix $\hat{\mathbf{H}}$ defined such that each column's mean is constant, and the consecutive columns' means are independent. To this end, we define $N_{m_p} := N_{T_c} i_f$ as the number of lines of $\hat{\mathbf{H}}$, and $N_{m_d} := i_t / N_{T_c}$ as its number of column (for the simplicity, we assume that N_{m_d} is integer). Notice that $N_{m_i} N_{m_d} = N$. The entries of $\hat{\mathbf{H}}$ are then given by, $\forall n$, $\forall i$:

$$\hat{H}[n,i] := \tilde{H}\left(1 + ((n-1) \bmod i_f), 1 + (i-1)N_{T_c} + \left\lfloor \frac{n-1}{i_f} \right\rfloor\right), \tag{2.3}$$

where $\lfloor x \rfloor$ is the floor function, defined as follows:

$$\lfloor x \rfloor \leq x < \lfloor x \rfloor + 1,$$

and $x \bmod y$ is the modulo operation, defined as follows:

$$x \bmod y = x - \left\lfloor \frac{x}{y} \right\rfloor y.$$

From the construction of $\hat{\mathbf{H}}$ in (2.3) and due to the considered system model, we know that the entries of $\hat{\mathbf{H}}$ are independent complex gaussian random variables, that each column has constant mean and that the columns' mean are i.i.d. random variables following a Nakagami-m distribution. Formally, we have $\hat{\mathbf{H}} = [\hat{\mathbf{H}}_1, \ldots, \hat{\mathbf{H}}_{N_{m_d}}]$, with, $\forall n \in [1, N_{m_d}]$, $\hat{\mathbf{H}}_n \sim \mathcal{CN}\left(c_n^{(c)} a e^{j\theta_0}, \mathrm{diag}_{N_{m_p} \times N_{m_p}}(2\sigma_h^2 + 2\sigma_n^2)\right)$ where $\left\{c_n^{(c)}\right\}_{n=1,\ldots,N_{m_d}}$ are i.i.d. random variables whose PDF is given by:

$$f_{c_n^{(c)}}(x) = \frac{2(m_{Na})^{m_{Na}}}{\Gamma(m_{Na})} x^{2m_{Na}-1} e^{-m_{Na}x^2}. \tag{2.4}$$

Moreover, $\forall n_1 \neq n_2$, $\mathbb{E}\left[\left(\hat{\mathbf{H}}_{n_1} - c_{n_1}^{(c)}\right)^* \left(\hat{\mathbf{H}}_{n_2} - c_{n_2}^{(c)}\right)\right] = 0$, where $(.)^*$ stands for the transpose-conjugate operator.

Our system model encompasses the case without shadowing by letting $N_{m_p} = N$, $N_{m_d} = 1$ and $c_1^{(c)} = 1$, and the case considered in [83] and [47] by setting $2\sigma_n^2 = 0$, $N_{m_p} = 1$ and $N_{m_d} = N$, i.e., the channel is perfectly known and the shadowing changes independently between consecutive channel samples.

Our objective is to estimate $K = a^2/(2\sigma_h^2)$ from the N estimated channel samples in $\hat{\mathbf{H}}$. In Table 2.2, we remind the known and unknown parameters in our system model.

Parameter	Notation	Known?
Channel's mean	a	No
Channel's variance	$2\sigma_h^2$	No
Phase of the channel's mean	θ_0	No
Rician K factor	$K = a^2/(2\sigma_h^2)$	No
Channel's average power	$\Delta = a^2 + 2\sigma_h^2$	No
Nakagami-m parameter	m_{Na}	No
Noise variance	$2\sigma_n^2$	Yes

Table 2.2: Summary of known and unknown statistical parameters in our estimation problems.

For future use, we define the following vectors of unknown parameters with and without shadowing as $\boldsymbol{\theta}^{(S)} = [a, 2\sigma_h^2, \theta_0, m_{Na}]$ and $\boldsymbol{\theta}^{(Ns)} = [a, 2\sigma_h^2, \theta_0]$, respectively.

Let us begin with the estimation of the Rician K factor in the shadowing-less case.

2.3 Estimation of K without LoS shadowing

Hereafter, we address the estimation of K without LoS shadowing. In this case, $\hat{\mathbf{H}}$ reduces to a $N \times 1$ vector, whose elements are i.i.d. complex gaussian random variables with mean $ae^{j\theta_0}$ and variance $2\sigma_h^2 + 2\sigma_n^2$. Hence, for the simplicity in this Section the ith element of $\hat{\mathbf{H}}$ is denoted by $\hat{H}[i]$ instead of $\hat{H}[i, 1]$.

First, we provide the mathematical expressions of some existing estimators from the literature. Second, we design our four proposed estimators (two deterministic and two Bayesian ones). Third, we derive the deterministic CRLB and finally, we propose numerical results to compare the proposed estimators' performance with existing ones.

2.3.1 Some existing estimators

The noiseless complex coefficients based Maximum Likelihood (ML) estimator of the Ricean K factor is derived in [22] and can be written as:

$$\hat{K}_{ML} = \frac{|\hat{a}|^2}{2\hat{\sigma}^2}, \tag{2.5}$$

with $\hat{a} = N^{-1} \sum_{i=1}^{N} \hat{H}[i]$ and $2\hat{\sigma}^2 = N^{-1} \sum_{i=1}^{N} |\hat{H}[i] - \hat{a}|^2$. It is proved in [6] that $\hat{K}_{ML}$ is biased, and the authors propose the following unbiased estimator:

$$\hat{K}_{MML} = \frac{1}{N}\left((N-2)\hat{K}_{ML} - 1\right). \tag{2.6}$$

To the best of our knowledge, $\hat{K}_{MML}$ is the best existing estimator for the Ricean K factor in term of both bias and Mean Square Error (MSE) when considering noiseless complex coefficients.

Two magnitude based estimators that consider noisy coefficients are derived in [20]. The most efficient one is given by:

$$\hat{K}_{MB} = \frac{\hat{\mu}_2(3\hat{\mu}_2\hat{\mu}_1 - 2\hat{\mu}_3 + b)}{\hat{\mu}_2(2\hat{\mu}_3 - 2\hat{\mu}_1\hat{\mu}_2) - 2\sigma_n^2(\hat{\mu}_1\hat{\mu}_2 + b)}, \tag{2.7}$$

with $\hat{\mu}_k = N^{-1} \sum_{i=1}^{N} |\hat{H}[i]|^k$ and $b = \hat{\mu}_2 \sqrt{\hat{\mu}_1^2 - \hat{\mu}_{-1}\hat{\mu}_3 + \hat{\mu}_{-1}\hat{\mu}_1\hat{\mu}_2}$.

2.3.2 Proposed estimators

Here, we derive our proposed estimators, beginning with the two deterministic ones.

2.3.2.1 Deterministic estimators

ML estimator. The invariance property of the ML estimation [62] allows us to derive the ML complex coefficients-based estimator of K in the noisy case as a straightforward extension of (2.5), yielding:

$$\hat{K}_{ML}^{n} = \frac{|\tilde{a}|^2}{2\tilde{\sigma}^2 - 2\sigma_n^2}, \tag{2.8}$$

with $\tilde{a} = N^{-1}\sum_{i=1}^{N}\hat{H}[i]$ and $2\tilde{\sigma}^2 = N^{-1}\sum_{i=1}^{N}|\hat{H}[i]-\tilde{a}|^2$. However, although the theoretical derivation of the bias of (2.8) appears to be intractable, we observe in our numerical results (Section 2.3.5) that $\hat{K}^n_{ML}$ is biased.

Corrected estimator To overcome the weakness of $\hat{K}^n_{ML}$ and inspired by the approach of [6], we study the bias of $\hat{K}_{ML}$ given by (2.5) when the samples are noisy. After some derivations provided in Appendix A.1, we obtain the following unbiased estimator of K:

$$\hat{K}^n_{Prop} = \frac{1}{N\alpha}\left((N-2)\frac{|\tilde{a}|^2}{2\tilde{\sigma}^2} - 1\right), \tag{2.9}$$

with $\alpha := \sigma_h^2/(\sigma_h^2 + \sigma_n^2)$. However, (2.9) cannot be used in practice since the value of α depends on $2\sigma_h^2$, which is unknown (i.e., Table 2.2). To tackle this problem, we derive in Appendix A.2 the following unbiased estimator of α:

$$\tilde{\alpha} := 1 + \frac{2\sigma_n^2(2-N)}{N2\tilde{\sigma}^2}. \tag{2.10}$$

We propose to replace α by $\tilde{\alpha}$ in (2.9). Although the resulting estimator of K is then biased as illustrated in Section 2.3.5, both its bias and MSE are the smallest among all the considered deterministic estimators.

Rejection rate From (2.8) and (2.9), we see that both $\hat{K}^n_{ML}$ and $\hat{K}^n_{Prop}$ might estimate negative values of K, which has no physical meaning and is thus undesirable. To characterize how often this undesirable fact happens, in [4], the authors define the RR $R_r(\hat{K})$ of a given estimator $\hat{K}$ of K as follows:

$$R_r(\hat{K}) := \Pr\left(\hat{K} < 0\right). \tag{2.11}$$

The authors compare several estimators through simulations in [4] in the noiseless case, and find out that $\hat{K}_{MML}$ has the smallest RR among the compared estimators.

In this thesis, we go further by deriving the theoretical RR of both $\hat{K}^n_{ML}$ and $\hat{K}^n_{Prop}$, which encompasses the RR of $\hat{K}_{MML}$ as a special case, i.e., by setting $2\sigma_n^2 = 0$. First, we derive the RR of $\hat{K}^n_{ML}$ in Result 2.1.

Result 2.1. *The RR of $\hat{K}^n_{ML}$ is given by:*

$$R_r(\hat{K}^n_{ML}) = \frac{\gamma_{IC}\left(N-1, N\frac{1+K}{\frac{\Delta}{2\sigma_n^2}+1+K}\right)}{\Gamma(N-1)}, \tag{2.12}$$

where $\Gamma(x)$ is the gamma function, and $\gamma_{IC}(x,y)$ is the incomplete gamma function defined as [49, Section 8.35]

$$\gamma_{IC}(\alpha, x) = \int_0^x e^{-t}t^{\alpha-1}dt. \tag{2.13}$$

Proof. Plugging (2.8) into (2.11) yields:

$$R_r(\hat{K}^n_{ML}) = \Pr\left(2\tilde{\sigma}^2 < 2\sigma_n^2\right). \tag{2.14}$$

We see from (2.14) that $R_r(\hat{K}^n_{ML})$ is given by the Cumulative Density Function (CDF) of $2\tilde{\sigma}^2$ computed in $2\sigma_n^2$. In Appendix A.1, we show that $4N\tilde{\sigma}^2/\left(2\sigma_h^2 + 2\sigma_n^2\right)$ follows a χ^2 distribution with $(2N-2)$ degrees of freedom and thus (2.12) can be readily deduced from [89], which concludes the proof. □

Also, we derive the RR of $\hat{K}^n_{Prop}$ in Result 2.2, whose proof is provided in Appendix A.3.

Result 2.2. *The RR of $\hat{K}^n_{Prop}$ is given by:*

$$\begin{aligned} R_r(\hat{K}^n_{Prop}) =& 1 + F_{2\tilde{\sigma}^2}(C_{1,Rr})\left(1 - 2F_{|\tilde{a}|^2}\left(\frac{C_{1,Rr}}{C_{2,Rr}}\right)\right) + \int_0^{C_{1,Rr}/C_{2,Rr}} f_{|\tilde{a}|^2}(x) F_{2\tilde{\sigma}^2}(C_{2,Rr}x)dx - \\ & \int_{C_{1,Rr}/C_{2,Rr}}^{\infty} f_{|\tilde{a}|^2}(x) F_{2\tilde{\sigma}^2}(C_{2,Rr}x)dx, \end{aligned} \tag{2.15}$$

with $C_{1,Rr} := 2\sigma_n^2(N-2)/N$, $C_{2,Rr} := N-2$,

$$F_{2\tilde{\sigma}^2}(x) := \frac{\gamma_{IC}\left(N-1, \frac{xN}{2\sigma_h^2+2\sigma_n^2}\right)}{\Gamma(N-1)},$$

$$f_{|\tilde{a}|^2}(x) := \frac{N}{2\sigma_h^2 + 2\sigma_n^2} e^{-\frac{xN}{2\sigma_h^2+2\sigma_n^2} - \frac{Na^2}{2\sigma_h^2+2\sigma_n^2}} I_0\left(\frac{2aN\sqrt{x}}{2\sigma_h^2 + 2\sigma_n^2}\right)$$

where $I_0(x)$ *is the zeroth order modified Bessel function, and*

$$F_{|\tilde{a}|^2}(x) := 1 - Q_1\left(a\sqrt{\frac{2N}{2\sigma_h^2 + 2\sigma_n^2}}, \sqrt{x}\frac{2aN}{2\sigma_h^2 + 2\sigma_n^2}\right),$$

where $Q_1(a, b)$ *is the Marcum function, defined as:*

$$Q_1(a, b) = \int_b^{+\infty} x e^{-\frac{x^2+a^2}{2}} I_0(ax)dx. \tag{2.16}$$

Results 2.1 and 2.2 enable us to theoretically compute the minimum number of required samples to achieve a desired RR for given K value, which might be of interest to design the length of training sequence, i.e., the value of N. The exactness of (2.12) and (2.15) are checked through numerical simulations in Section 2.3.5.

2.3.2.2 Bayesian estimators

In this Section, we design two Bayesian estimators of the Ricean K factor. Unlike in the previous Section 2.3.2.1 in which K is considered as a deterministic unknown parameter, in the Bayesian framework, K is considered as random with a given PDF, called the *prior PDF*.

Prior Density of K. As the prior PDF for K, we propose to use the log-normal distribution, which has been shown through measurement campaigns to represent the real distribution of K in different scenarios [123]. The log-normal PDF is given by:

$$f_K(K) = \frac{10}{K \log(10)\sqrt{2\pi\sigma_K^2}} e^{-\frac{(10\log_{10}(K)-a_K)^2}{2\sigma_K^2}}, \tag{2.17}$$

where σ_K^2 and a_K are the distribution's parameters, which are fixed by the system designer and thus are known.

Likelihood function of $\hat{\mathbf{H}}$. The *likelihood function* of a random variable X whose PDF depends on some parameters $\boldsymbol{\theta}$ is the PDF of X seen as a function of $\boldsymbol{\theta}$, which is given by $\mathbb{L}_X(X) = \Pr(X|\boldsymbol{\theta})$.

In this Section, we choose to work considering the unknown parameters K, Δ and θ_0 instead of $\boldsymbol{\theta}^{(Ns)}$ defined in Section 2.2 since we are able to find the closed-form expressions for the ML estimators of Δ and θ_0 (detailed latter), which simplifies the derivations of our proposed Bayesian estimators.

From the above discussion, the likelihood function $\mathbb{L}_{\hat{\mathbf{H}}}^{(Ns)}(\hat{\mathbf{H}}; K, \Delta, \theta_0)$ is the PDF of $\hat{\mathbf{H}}$ seen as a function of the unknown K, Δ and θ_0, which can be written as:

$$\mathbb{L}_{\hat{\mathbf{H}}}^{(Ns)}(\hat{\mathbf{H}}; K, \Delta, \theta_0) = \Pr(\hat{\mathbf{H}}|K, \Delta, \theta_0). \tag{2.18}$$

Since the elements of $\hat{\mathbf{H}}$ are i.i.d. complex normal random variables, (2.18) can be written as:

$$\mathbb{L}_{\hat{\mathbf{H}}}^{(Ns)}(\hat{\mathbf{H}}; K, \Delta, \theta_0) = \left(\frac{\mathcal{A}_1(K)}{\pi}\right)^N e^{-\mathcal{A}_1(K)\mathcal{A}_2(K)}, \tag{2.19}$$

with

$$\mathcal{A}_1(K) = \frac{1+K}{2\sigma_n^2(1+K)+\Delta},$$

and

$$\mathcal{A}_2(K) = \sum_{i=1}^{N} \left| \hat{H}[i] - \sqrt{\frac{K\Delta}{1+K}} e^{j\theta_0} \right|^2.$$

In what follows, Δ and θ_0 are replaced by their ML estimators, which can be obtained as a direct extension of [22] as

$$\hat{\Delta} = \arg\max_{\Delta} \mathbb{L}_{\hat{\mathbf{H}}}^{(Ns)}(\hat{\mathbf{H}}; K, \Delta, \theta_0) = \frac{1}{N}\sum_{i=1}^{N} |\hat{H}[i]|^2 - 2\sigma_n^2$$

and

$$\hat{\theta}_0 = \arg\max_{\theta_0} \mathbb{L}_{\hat{\mathbf{H}}}^{(Ns)}(\hat{\mathbf{H}}; K, \Delta, \theta_0) = \arctan\left(\frac{\sum_{i=1}^{N} \Im(\hat{H}[i])}{\sum_{i=1}^{N} \Re(\hat{H}[i])}\right),$$

where $\Re(.)$ (resp. $\Im(.)$) denotes the real (resp. imaginary) part operator. For simplicity, we denote the likelihood function (2.19) where Δ is replaced by $\hat{\Delta}$ and θ_0 by $\hat{\theta}_0$ as $\mathbb{L}_{\hat{\mathbf{H}}}^{(Ns)}(\hat{\mathbf{H}}; K) = \mathbb{L}_{\hat{\mathbf{H}}}^{(Ns)}(\hat{\mathbf{H}}; K, \hat{\Delta}, \hat{\theta}_0)$.

Mean a Posteriori. The expression of the mean a posteriori estimator of K is [62]:

$$\hat{K}_{MeanP} = \mathbb{E}_{K|\hat{\mathbf{H}}}[K], \tag{2.20}$$

where $\mathbb{E}_{x|y}[x]$ denotes the conditional expectation taken on x given y. Equation (2.20) can be written as:

$$\hat{K}_{MeanP} = \int_0^{+\infty} K f_{K|\hat{\mathbf{H}}}(K|\hat{\mathbf{H}})\mathrm{d}K, \tag{2.21}$$

where $f_{K|\hat{\mathbf{H}}}(K|\hat{\mathbf{H}})$ is the PDF of K knowing $\hat{\mathbf{H}}$. Using the Bayes rule, we can rewrite (2.21) as:

$$\hat{K}_{MeanP} = \frac{\int_0^{+\infty} K\mathbb{L}_{\hat{\mathbf{H}}}^{(Ns)}(\hat{\mathbf{H}};K) f_K(K)\mathrm{d}K}{\int_0^{+\infty} \mathbb{L}_{\hat{\mathbf{H}}}^{(Ns)}(\hat{\mathbf{H}};K) f_K(K)\mathrm{d}K}. \tag{2.22}$$

By plugging (2.17) and (2.19) into (2.22), we obtain:

$$\hat{K}_{MeanP} = \frac{\mathcal{I}_1}{\mathcal{I}_2}, \tag{2.23}$$

with

$$\mathcal{I}_i := \int_0^{+\infty} \mathcal{B}(K) K^{-i+1} e^{-\tau_1\left(\log(K)-\tau_2\right)^2}, \quad i = 1,2,$$

and

$$\mathcal{B}(K) := \left(\mathcal{A}_1(K)\right)^N e^{-\mathcal{A}_1(K)\mathcal{A}_2(K)},$$

with $\tau_1 := (10/\log(10))^2/(2\sigma_K^2)$ and $\tau_2 := a_K \log(10)/10$. To evaluate $\mathcal{I}_1$ and $\mathcal{I}_2$ in (2.23), we propose to use the GHQ [3], which allows us to perform the following integral approximation:

$$\int_{-\infty}^{+\infty} e^{-x^2} f(x)dx \approx \sum_{n=1}^{J} w_n f(x_n), \tag{2.24}$$

where J is the GHQ order and, for $n = 1,\ldots,J$, w_n (resp. x_n) are the GHQ weights (resp. absissas), which are tabulated in [3] and can be generated using the matlab code provided in [51].

To match $\mathcal{I}_i$, $i = 1,2$, with (2.24), we first perform the change of variable $u = \log(K)$, and we rewrite $\mathcal{I}_i$ as:

$$\mathcal{I}_i = \int_{-\infty}^{+\infty} \mathcal{B}\left(e^u\right) e^{-\tau_1(u-\tau_3(i))^2} e^{\tau_1(\tau_3(i))^2-\tau_1(\tau_2)^2}\mathrm{d}u, \quad i = 1,2, \tag{2.25}$$

with $\tau_3(i) := \tau_2 + (2-i)/\left(2\tau_1\right)$, $i = 1,2$. Now, performing the change of variable $w = \sqrt{\tau_1}\left(u - \tau_3(i)\right)$ yields the following expressions for $\mathcal{I}_i$:

$$\mathcal{I}_i = \frac{1}{\tau_1} e^{\tau_1(\tau_3(i))^2-\tau_1(\tau_2)^2} \int_{-\infty}^{+\infty} \mathcal{B}\left(e^{\frac{w}{\sqrt{\tau_1}}+\tau_3(i)}\right) e^{-w^2}\mathrm{d}w, \quad i = 1,2. \tag{2.26}$$

Using (2.24) to approximate (2.26), we obtain:

$$\mathcal{I}_i \approx \frac{1}{\tau_1} e^{\tau_1(\tau_3(i))^2-\tau_1(\tau_2)^2} \sum_{n=1}^{J} w_n \mathcal{B}\left(e^{\frac{x_n}{\sqrt{\tau_1}}+\tau_3(i)}\right). \tag{2.27}$$

Finally, plugging (2.27) into (2.23) yields the following simple approximate expression for $\hat{K}_{MeanP}$:

$$\hat{K}_{MeanP} = \tau_4 \frac{\sum_{n=1}^{J} w_n \mathcal{B}\left(e^{\frac{x_n}{\sqrt{\tau_1}}+\tau_3(1)}\right)}{\sum_{n=1}^{J} w_n \mathcal{B}\left(e^{\frac{x_n}{\sqrt{\tau_1}}+\tau_3(2)}\right)}, \tag{2.28}$$

with $\tau_4 := e^{\tau_2+1/(4\tau_1)}$. The impact of the GHQ order J on the estimation performance is numerically studied in Section 2.3.5. Finally, the mean a posteriori is characterized through the following property.

Property 2.1 ([62]). *When K is a random variable distributed according to (2.17), the mean a posteriori is unbiased, and minimizes the Bayesian MSE.*

Maximum a Posteriori. The maximum a posteriori estimator of K is given by:

$$\hat{K}_{MaxP} = \arg\max_{K} \left(\mathbb{L}_{\hat{\mathbf{H}}}^{(Ns)}(\hat{\mathbf{H}}; K) f_K(K)\right), \tag{2.29}$$

which is equivalent to:

$$\hat{K}_{MaxP} = \arg\max_{K} \left(\log\left(\mathbb{L}_{\hat{\mathbf{H}}}^{(Ns)}(\hat{\mathbf{H}}; K) f_K(K)\right)\right). \tag{2.30}$$

We plug (2.17) and (2.19) into (2.30), we differentiate with respect to K the resulting expression and, by setting this derivative to zero, we obtain the following relation:

$$\begin{aligned}
&-\frac{1}{\hat{K}_{MaxP}} - \frac{10}{\hat{K}_{MaxP}\sigma_K^2 \log(10)}\left(10\log_{10}\left(\hat{K}_{MaxP}\right) - a_K\right) + N.\mathcal{A}_3\left(\hat{K}_{MaxP}\right) - \\
&\mathcal{A}_4\left(\hat{K}_{MaxP}\right)\mathcal{A}_2\left(\hat{K}_{MaxP}\right) - \mathcal{A}_1\left(\hat{K}_{MaxP}\right)(\mathcal{A}_2)'\left(\hat{K}_{MaxP}\right) = 0,
\end{aligned} \tag{2.31}$$

where

$$\mathcal{A}_3(K) = \frac{\hat{\Delta}}{\left(\hat{\Delta} + 2\sigma_n^2(1+K)\right)(1+K)},$$

$$\mathcal{A}_4(K) = \frac{\hat{\Delta}}{(\hat{\Delta} + 2\sigma_n^2(1+K))^2},$$

and $(\mathcal{A}_2)'(K)$ is the first order derivative of $\mathcal{A}_2(K)$, which can be written as

$$(\mathcal{A}_2)'(K) = \frac{N\hat{\Delta}}{(1+K)^2} - \frac{\sqrt{\hat{\Delta}}}{(1+K)^{3/2}\sqrt{K}} \sum_{i=1}^{N} \Re\left(\hat{H}[i]e^{-j\hat{\theta}_0}\right).$$

$\hat{K}_{MaxP}$ can thus be obtained by finding the root of the non linear equation (2.31). This can be done using for instance the bisection or the Newton method, which are both iterative procedures.

2.3.3 Complexity of the proposed estimators

The proposed estimators complexities are summarized in Table 2.3, where N_I is the number of iterations of the chosen iterative procedure (i.e., bisection of Newton method for instance) to find the root of (2.31). We see that the Bayesian estimators are more complex than the deterministic ones, especially when the values of J or N_I are large compared with N, which is especially the case for small sample size. On the other hand, all the estimators' complexity increase only linearly with the sample size N.

Table 2.3: Complexity order of the proposed estimators.

Estimators	Deterministics	Mean a posteriori	Maximum a posteriori
Complexity	$\mathcal{O}(N)$	$\mathcal{O}(N+J)$	$\mathcal{O}(N+N_I)$

2.3.4 Deterministic Cramer Rao Lower Bound

In this Section, we derive the deterministic CRLB for the estimation of the Ricean K factor in the case of noisy complex channel coefficients. To do so, as suggested in [59], we use the joint log-likelihood function of the envelope and phase in our derivations, for which we define $r_i = |\hat{H}[i]|$ and $\phi_i = \arctan(\Im(\hat{H}_i)/\Re(\hat{H}_i))$, $i = 1, \ldots, N$. The vectors $\mathbf{r} = (r_1, ..., r_N)$ and $\boldsymbol{\phi} = (\phi_1, ..., \phi_N)$ represent the channel coefficients envelope and phase, respectively. Moreover, instead of working on the likelihood function parametrized by the parameters K, Δ and θ_0 as in (2.19), we choose to work with the log-likelihood parametrized by the parameters $\boldsymbol{\theta}^{(Ns)}$ (defined in Section 2.2) since we find the derivations simpler.

We aim to estimate K and we thus define $\mathbf{g}\left(\boldsymbol{\theta}^{(Ns)}\right) = a^2/(2\sigma_h^2)$, which is a function of the unknown parameters in $\boldsymbol{\theta}^{(Ns)}$. We know from [62, Eq. 3.30 pp. 45] that the CRLB is given by:

$$\mathrm{CRLB}(K) = \frac{\partial \mathbf{g}\left(\boldsymbol{\theta}^{Ns}\right)}{\partial \boldsymbol{\theta}^{(Ns)}} \mathbf{I}^{-1}\left(\boldsymbol{\theta}^{(Ns)}\right) \frac{\partial \mathbf{g}\left(\boldsymbol{\theta}^{(Ns)}\right)^T}{\partial \boldsymbol{\theta}^{(Ns)}}, \tag{2.32}$$

where $\mathbf{I}^{-1}\left(\boldsymbol{\theta}^{(Ns)}\right)$ is the inverse of the Fisher information matrix $\mathbf{I}\left(\boldsymbol{\theta}^{(Ns)}\right)$, whose (i, n) entry is defined as

$$\left[\mathbf{I}\left(\boldsymbol{\theta}^{(Ns)}\right)\right]_{i,n} = -\mathbb{E}\left[\frac{\partial^2 \log\left(\mathbb{L}_{\hat{\mathbf{H}}}^{(Ns)}\left(\hat{\mathbf{H}}; \boldsymbol{\theta}^{(Ns)}\right)\right)}{\partial \theta_i^{(Ns)} \partial \theta_n^{(Ns)}}\right], \tag{2.33}$$

where $\theta_i^{(Ns)}$ is the ith element of the vector $\boldsymbol{\theta}^{(Ns)}$, and $\mathbb{L}_{\hat{\mathbf{H}}}^{(Ns)}\left(\hat{\mathbf{H}}; \boldsymbol{\theta}^{(Ns)}\right)$ is the log-likelihood function of $\hat{\mathbf{H}}$ when the unknown parameters are $\boldsymbol{\theta}^{(Ns)}$, which can be written as

$$\begin{aligned}\log\left(\mathbb{L}_{\hat{\mathbf{H}}}^{(Ns)}\left(\hat{\mathbf{H}}; \boldsymbol{\theta}^{(Ns)}\right)\right) = &- N \log\left(2\pi\left(\sigma_h^2 + \sigma_n^2\right)\right) - \frac{1}{2\left(\sigma_h^2 + \sigma_n^2\right)} \sum_{i=1}^{N} (r_i)^2 - \frac{Na^2}{2\left(\sigma_h^2 + \sigma_n^2\right)} + \\ &\frac{a}{\sigma_h^2 + \sigma_n^2} \sum_{i=1}^{N} r_i \cos\left(\phi_i - \theta_0\right).\end{aligned} \tag{2.34}$$

After some derivations provided in Appendix A.4, we obtain

$$\mathbf{I}\left(\boldsymbol{\theta}^{(Ns)}\right) = \begin{bmatrix} \frac{N}{\sigma_h^2+\sigma_n^2} & 0 & 0 \\ 0 & \frac{N}{\left(2\sigma_h^2+2\sigma_n^2\right)^2} & 0 \\ 0 & 0 & \frac{Na^2}{\sigma_h^2+\sigma_n^2} \end{bmatrix}. \tag{2.35}$$

Substituting (2.35) in (2.32), we eventually obtain the following CRLB after simplification

$$\mathrm{CRLB}(K) = \frac{2K}{N}\left(1+\frac{\sigma_n^2}{\sigma_h^2}\right) + \frac{K^2}{N}\left(1+\frac{\sigma_n^2}{\sigma_h^2}\right)^2, \tag{2.36}$$

which can be rewritten in term of K and Δ as:

$$\mathrm{CRLB}(K) = \frac{2K}{N}\left(1+2(K+1)\frac{\sigma_n^2}{\Delta}\right) + \frac{K^2}{N}\left(1+2(K+1)\frac{\sigma_n^2}{\Delta}\right)^2. \tag{2.37}$$

From (2.37), we can draw the following remark concerning the asymptotic behavior of CRLB(K) as K goes to the infinity.

Remark 2.1. *The asymptotic behavior of* (2.37) *as* $K \to +\infty$ *is different in the noisy and in the noiseless cases. Indeed, in the noiseless case (i.e.,* $2\sigma_n^2 = 0$*), for* $K \to +\infty$*, we have* $\mathrm{CRLB}(K) \sim K^2/N$ *whereas, in the noisy case,* $\mathrm{CRLB}(K) \sim 4K^4\sigma_n^4/(N\Delta^2)$*. This result suggests that estimating large value of* K *is especially difficult in the noisy case.*

Intuitively, this can be explained because the denominator of K *is given by the channel variance and, in the noisy case, estimating this variance is difficult because of the noise, especially for large* K *values for which* $2\sigma_h^2$ *might be small compared with* $2\sigma_n^2$*. This remark is numerically illustrated in Fig. 2.5.*

2.3.5 Numerical Results

In this Section, the proposed estimators' performance are assessed through simulations, and compared with the one from [6] given by (2.6), and the best moment-based estimators from [20], which is (2.7). Their performance are compared in terms of bias magnitude and Nomalized MSE (NMSE), defined for a given estimator $\hat{K}$ as $\mathrm{NMSE} = \mathbb{E}\left[\left(\hat{K}-K\right)^2\right]/K^2$. Notice that, when the performance of $\hat{K}_{MML}$ are displayed, we also represent both its theoretical bias and NMSE, which can be obtained using (A.8) and (A.9) in Appendix A.1.

We set $\Delta = 1$, and the SNR is given by $\mathrm{SNR} = \Delta/(2\sigma_n^2)$. All results are averaged through $10,000$ Monte Carlo trials. The log-normal distribution parameters are $a_K = 2.5$ and $\sigma_K = 3.8$, which have been found through simulations to yield accurate estimation.

First of all, we study the impact of the GHQ order J in (2.28) on the performance of $\hat{K}_{MeanP}$. In Fig. 2.2, we set SNR = 10 dB, $N = 100$ and we plot both bias magnitude (Fig. 2.2a) and NMSE (Fig. 2.2b) of $\hat{K}_{MeanP}$ versus J for several values of K. We see that J has no real impact on the estimation performance as long as we choose $J \geq 50$ and thus in the rest of our simulations, we set $J = 50$.

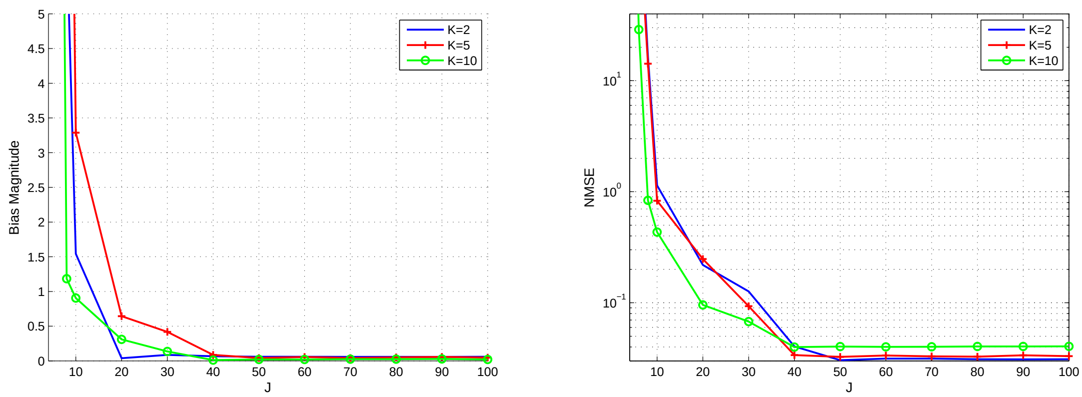

(a) Bias magnitude. (b) NMSE.

Figure 2.2: Performance of K_{MeanP} versus J for several values of K, $N = 100$, SNR = 10 dB.

In both Fig. 2.3 and 2.4, we set SNR = 10 dB, and we plot the estimators' performance versus the value of K. In Fig. 2.3, we set $N = 100$, and Fig. 2.3a and 2.3b displays the estimators' bias magnitude and NMSE, respectively. The advantage of the proposed estimators is clear since both their bias magnitude and NMSE are smaller than the one of the other considered estimators. The mean a posteriori has the smallest biais magnitude among the proposed estimators. The maximum a posteriori has a bias magnitude similar to the ML, and it has the smallest NMSE among the proposed estimators. Also, $\hat{K}^n_{Prop}$ has the smallest bias magnitude and NMSE among all the considered deterministic estimators. The NMSE of the maximum a posteriori is smaller than the CRLB, which can be explained by the prior knowledge on K introduced by the prior distribution. Moreover, its NMSE is smaller than the one of the mean a posteriori since K although this latter estimator minimizes the Bayesian NMSE. This is because K is deterministic here. We also see that the bias and the variance of $\hat{K}^n_{MML}$ obtained by simulations are in agreement with our theoretical derivations.

In Fig. 2.4, we set $N = 30$ and we plot the estimators bias magnitude in Fig. 2.4a and NMSE in Fig. 2.4b. Such small sample size is of practical interest to be able to quickly estimate the channel's statistical parameters in order to adapt the RA to the link's quality. We observe that both $\hat{K}^n_{ML}$ and $\hat{K}^n_{Prop}$ may provide unreliable estimates, especially for high values of K (i.e., $K \geq 9$). This is explained because these estimators require to estimate $2\sigma_h^2$, which is difficult when its value is close to the noise variance $2\sigma_n^2$, as explained in Remark 2.1. To illustrate how close $2\sigma_h^2$ and $2\sigma_n^2$ are, in Fig. 2.5, we plot their values versus K for SNR = 10 dB. We see that they are very close for $K \geq 9$, which corroborate our previous explanation about the performance of $\hat{K}^n_{ML}$ and $\hat{K}^n_{Prop}$ in Fig. 2.4. It can be seen that the Bayesian estimators are more robust than the deterministic ones because of the prior information provided by the prior density of K.

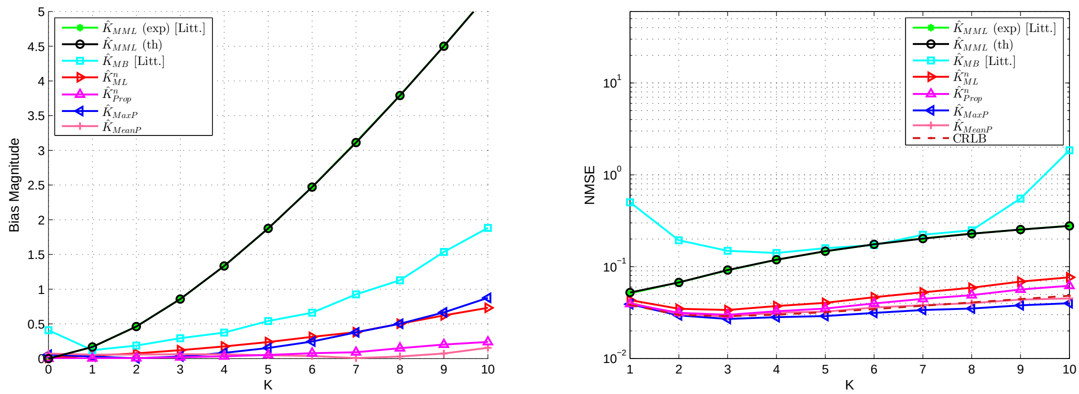

(a) Bias magnitude. (b) NMSE.

Figure 2.3: Performance of the proposed estimators versus K, SNR = 10 dB, N = 100.

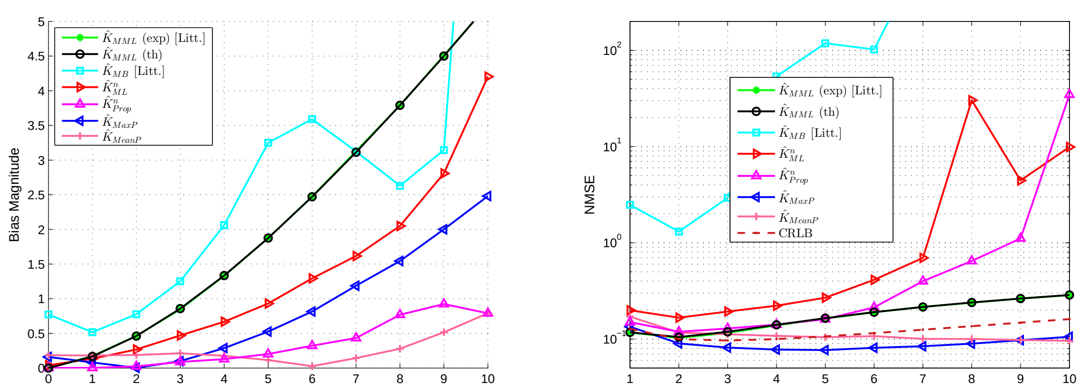

(a) Bias magnitude. (b) NMSE

Figure 2.4: Performance of the proposed estimators versus K, SNR = 10 dB, N = 30.

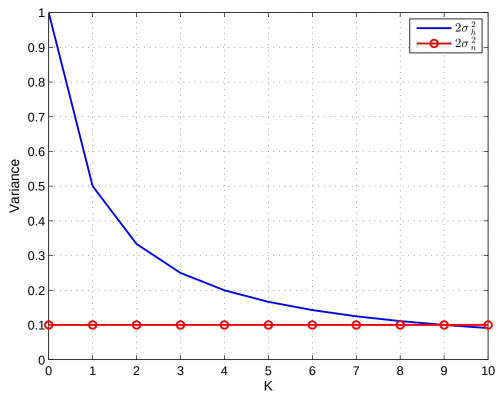

Figure 2.5: Values of $2\sigma_h^2$ and $2\sigma_n^2$ versus the value of K, SNR = 10 dB.

In Fig. 2.6, we set $K = 5$ and we plot the estimators bias and NMSE versus the SNR in Fig. 2.6a and 2.6b, respectively. We can see that the proposed deterministic estimators are unreliable for low SNR values, which is in agreement with our previous observations. Also, for very low SNR (i.e., lower than 4 dB), the mean a posteriori has lower NMSE than the maximum a posteriori. We also see that, even for high SNR, $\hat{K}^n_{ML}$ is biased whereas $\hat{K}^n_{Prop}$ is not. This is because, as SNR $\to +\infty$, $2\sigma_n^2 \to 0$ and $\hat{K}^n_{ML}$ is equivalent to (2.8), which is biased, whereas $\hat{K}^n_{Prop}$ is equivalent to (2.6), which is unbiased.

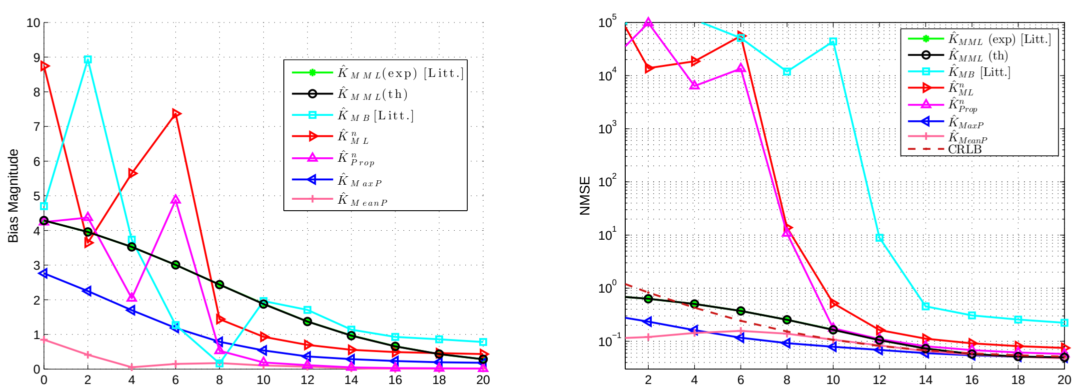

(a) Bias magnitude.

(b) NMSE

Figure 2.6: Performance of the proposed estimator versus SNR, $K = 5$, $N = 30$.

In Fig. 2.7, we set $K = 5$, SNR = 15 dB and we plot the estimators' bias magnitude in Fig 2.7a and NMSE in Fig 2.7a versus the number of samples N. Once again, we see that the Bayesian estimators are robust to small sample size, especially the mean a posteriori which has low bias magnitude even for $N = 5$.

Now, we are interested into: *i)* comparing the RR of our proposed estimators (2.8) and

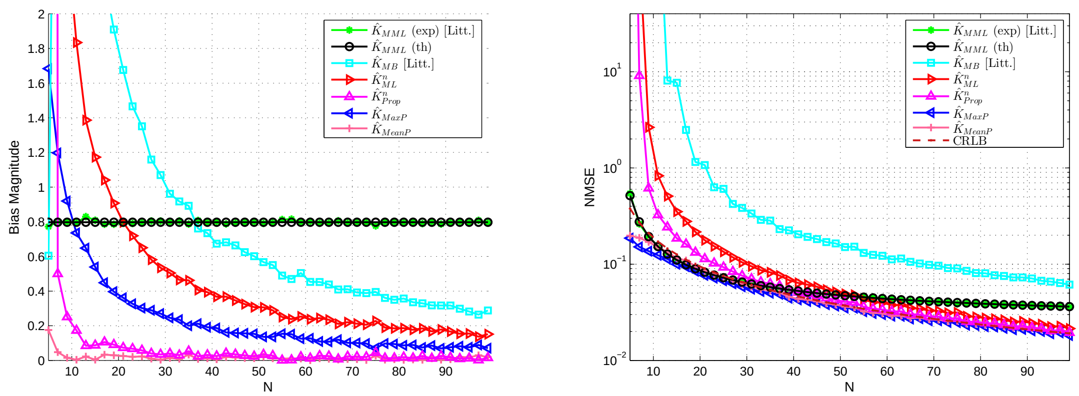

(a) Bias mangitude.

(b) NMSE.

Figure 2.7: Performance of the considered estimators versus the sample size N, SNR = 15 dB.

(2.9) with the one of (2.7), and *ii)* validating the theoretical formulas for the RR derived in Results 2.1 and 2.2. In Fig. 2.8, we set $K = 5$, SNR = 6 dB and we plot the estimators' RR versus the sample size N. Notice that the Bayesian estimators are not displayed since the use of the log-normal prior prevents from obtaining negative estimations. We see that $\hat{K}^n_{Prop}$ has a RR smaller than $\hat{K}^n_{ML}$ and $\hat{K}_{MB}$, which confirms its advantage compared with these estimators. Moreover, we see a very good agreement between the theoretical and analytical RR.

To summarize our observations, $\hat{K}^n_{Prop}$ is the most efficient deterministic estimator since it has lower bias, NMSE and RR than $\hat{K}^n_{ML}$ and $\hat{K}_{MB}$. Also, the Bayesian estimators are robust to small sample size, but they are more complex. The mean a posteriori has in general the lowest bias, whereas the maximum a posteriori has the lowest NMSE.

2.4 Estimation of K with Nakagami-m LoS shadowing

In this Section, we aim to estimate K when the LoS component is subject to Nakagami-m shadowing. In this case, we remind that, following the system model described in Section 2.2, $\hat{\mathbf{H}}$ is a $N_{m_p} \times N_{m_d}$ matrix whose entries are independent Gaussian random variables with variance $2\sigma_h^2 + 2\sigma_n^2$, whose nth column mean is $c_n^{(c)} a e^{j\theta_0}$ where $\{c_n^{(c)}\}_{n=1,\ldots,N_{m_d}}$ are i.i.d. random variables following a Nakagami-m distribution with parameters m_{Na} and $\Omega = 1$.

First, we review the two existing estimators from the literature. Second, we present the EM estimation framework. Third, we detail how we can apply EM to our problem, and fourth we propose another estimator based on the MoM to initialize the EM. Finally, we perform simulations to compare the two proposed estimators with the ones from the

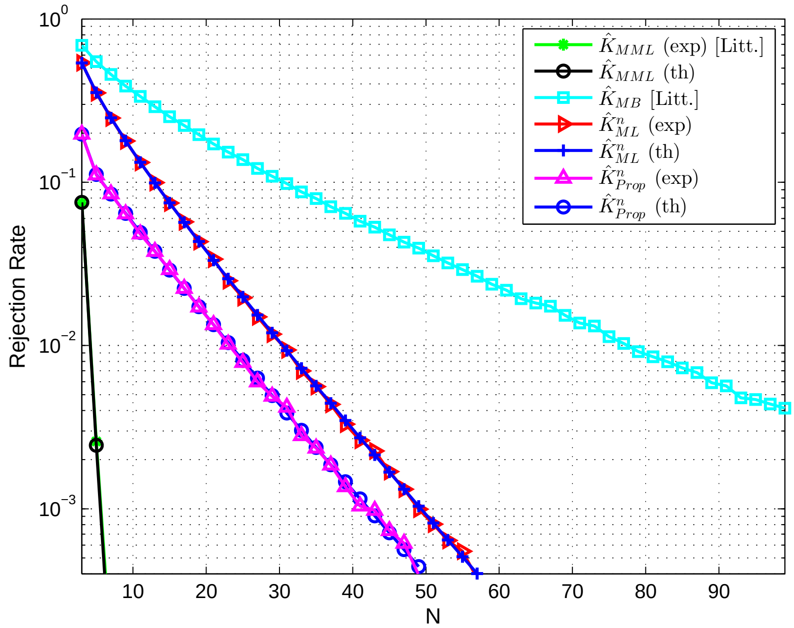

Figure 2.8: RR of the considered estimators versus the sample size.

literature.

2.4.1 Existing estimators

The two existing estimators use noiseless channel magnitudes. In [83], the authors use the MoM to propose an estimator denoted by $\hat{K}^{(S)}_{\text{WMoM}}$, which is obtained by solving the following equation:

$$\frac{\left(\hat{\mu}_1^{(S)}\right)^2}{\hat{\mu}_2^{(S)}} = \frac{\pi}{4\left(1+\hat{K}^{(S)}_{\text{WMoM}}\right)} {}_2F_1\left(-\frac{1}{2}, m_{Na}; 1; -\frac{\hat{K}^{(S)}_{\text{WMoM}}}{m_{Na}}\right), \tag{2.38}$$

where ${}_2F_1(x_1, x_2; y; z)$ is the Gauss-Hypergeometric function [3, Chapter 15], and

$$\hat{\mu}_k^{(S)} = \frac{1}{N_{m_p}N_{m_d}} \sum_{i=1}^{N_{m_p}} \sum_{n=1}^{N_{m_d}} |\hat{H}[i,n]|^k.$$

One drawback of (2.38) is that it involves the value of m_{Na} and unfortunately, in [83], it is unclear how to estimate this parameter.

Very recently, in [47], another MoM based estimator has been proposed. It requires to find the solution of a quadratic equations involving moments up to the order of 6. However, it is known that the highest the moments order, the highest the estimation variance and thus the estimator from [47] requires large sample size to provide reliable results. Since the related equation is cumbersome, it is not reported in this thesis.

2.4.2 The Expectation Maximization Procedure

We propose to estimate the Rician K factor using the EM procedure, which has been originally proposed in [30] and has widely been used in the context of channel statistical parameters estimation [14, 35, 86, 93, 118].

The EM procedure aims to find local maximum of the likelihood function iteratively. This procedure is especially interesting when analytical maximization of the log-likelihood function is intractable, but is rendered possible by fixing some parameters.

In our case, let us show that maximizing the log-likelihood function of $\hat{\mathbf{H}}$, denoted by $\log\left(\mathbb{L}^{(S)}_{\hat{\mathbf{H}}}\left(\hat{\mathbf{H}};\boldsymbol{\theta}^{(S)}\right)\right)$, is analytically intractable when the LoS is subject to Nakagami-m shadowing. To do so, we use the independence of the columns of $\hat{\mathbf{H}}$ to write

$$\log\left(\mathbb{L}^{(S)}_{\hat{\mathbf{H}}}\left(\hat{\mathbf{H}};\boldsymbol{\theta}^{(S)}\right)\right) = \sum_{n=1}^{N_{m_d}} \log\left(\mathbb{L}^{(S)}_{\hat{\mathbf{H}}_n}\left(\hat{\mathbf{H}}_n;\boldsymbol{\theta}^{(S)}\right)\right), \tag{2.39}$$

where $\mathbb{L}^{(S)}_{\hat{\mathbf{H}}_n}\left(\hat{\mathbf{H}}_n;\boldsymbol{\theta}^{(S)}\right)$ is the likelihood function of $\hat{\mathbf{H}}_n$. To derive it, we use the law of total probability as suggested in [47], which yields

$$\mathbb{L}^{(S)}_{\hat{\mathbf{H}}_n}\left(\hat{\mathbf{H}}_n;\boldsymbol{\theta}^{(S)}\right) = \int_0^{+\infty} \mathbb{L}^{(S)}_{\hat{\mathbf{H}}_n|c_n^{(c)}}\left(\hat{\mathbf{H}}_n|x;\boldsymbol{\theta}^{(S)}\right) f_{c_n^{(c)}}(x)\,dx, \tag{2.40}$$

where $\mathbb{L}^{(S)}_{\hat{\mathbf{H}}_n|c_n^{(c)}}\left(\hat{\mathbf{H}}_n|x;\boldsymbol{\theta}^{(S)}\right)$ is the PDF of $\hat{\mathbf{H}}_n$ knowing $c_n^{(c)}$, which can be written as

$$\mathbb{L}^{(S)}_{\hat{\mathbf{H}}_n|c_n^{(c)}}\left(\hat{\mathbf{H}}_n|x;\boldsymbol{\theta}^{(S)}\right) = \left(\frac{1}{\pi(2\sigma_h^2+2\sigma_n^2)}\right)^{N_{mp}} e^{-\frac{1}{2\sigma_h^2+2\sigma_n^2}\sum_{i=1}^{N_{mp}}|\hat{H}[i,n]-xae^{j\theta_0}|^2}. \tag{2.41}$$

Plugging (2.41) and (2.4) into (2.40) yields

$$\mathbb{L}^{(S)}_{\hat{\mathbf{H}}_n}\left(\hat{\mathbf{H}}_n;\boldsymbol{\theta}^{(S)}\right) = C_n^{(c)} \int_0^{+\infty} x^{2m_{Na}-1} e^{-x^2\mathcal{B}_{2,n}-x\mathcal{B}_{3,n}}\,dx, \tag{2.42}$$

with

$$C_n^{(c)} = \left(\frac{2(m_{Na})^{m_{Na}}}{\pi^{N_{mp}}(2\sigma_h^2+2\sigma_n^2)^{N_{mp}}\Gamma(m_{Na})}\right) e^{-\sum_{i=1}^{N_{mp}}\frac{|\hat{H}[i,n]|^2}{2\sigma_h^2+2\sigma_n^2}},$$

$$\mathcal{B}_{2,n} := N_{m_p}\frac{a^2}{2\sigma_h^2+2\sigma_n^2} + m_{Na}$$

and

$$\mathcal{B}_{3,n} := -\frac{a}{\sigma_h^2+\sigma_n^2}\sum_{i=1}^{N_{mp}} \Re\left(\hat{H}[i,n]e^{-j\theta_0}\right).$$

Using [49, 3.462], we obtain the following closed-form expression for (2.42):

$$\mathbb{L}^{(S)}_{\hat{\mathbf{H}}_n}\left(\hat{\mathbf{H}}_n;\boldsymbol{\theta}^{(S)}\right) = C_n^{(c)}\left(2\mathcal{B}_{2,n}\right)^{-m_{Na}}\Gamma(2m_{Na})e^{\frac{(\mathcal{B}_{3,n})^2}{8\mathcal{B}_{2,n}}} D_{-2m_{Na}}\left(\frac{\mathcal{B}_{3,n}}{\sqrt{2\mathcal{B}_{2,n}}}\right), \tag{2.43}$$

where $D_{-2m_{Na}}(x)$ is the parabolic cylinder function, whose presence in (2.43) prevents us from maximizing the log-likelihood function (2.39) analytically.

The difficulty in our estimation problem comes from the fact that the column of $\hat{\mathbf{H}}$ are random because of to the random variables $\mathbf{c} := [c_1^{(c)}, \ldots, c_{N_{m_d}}^{(c)}]$. Fixing the value of $\mathbf{c}$ would alleviate this difficulty. The EM procedure is suitable to handle this type of difficulty since it consists in considering $\mathbf{c}$ as *nuisance parameters* and averaging $\log\left(\mathbb{L}^{(S)}_{\hat{\mathbf{H}},\mathbf{c}}\left(\hat{\mathbf{H}}, \mathbf{c}; \boldsymbol{\theta}^{(S)}\right)\right)$, the complete log-likelihood function, on $\mathbf{c}$ to alleviate the influence of these nuisance parameters.

More precisely, the EM procedure alternates between the following two steps until convergence is reached.

- The Expectation (E) step.
- The Maximization (M) step.

Let us detailed these steps at given iteration t.

The E step. Suppose that the current estimation of the parameters is given by $\hat{\boldsymbol{\theta}}^{(S),(t)} = \left[\hat{a}^{(S),(t)}, 2\hat{\sigma}_h^{2,(S),(t)}, \hat{\theta}_0^{(S),(t)}, \hat{m}_{Na}^{(S),(t)}\right]$. The E step consists in computing the following expectation:

$$Q_{EM}\left(\boldsymbol{\theta}^{(S)}, \hat{\boldsymbol{\theta}}^{(S),(t)}\right) = \mathbb{E}_{\mathbf{c}|\hat{\mathbf{H}},\hat{\boldsymbol{\theta}}^{(S),(t)}}\left[\log\left(\mathbb{L}^{(S)}_{\hat{\mathbf{H}},\mathbf{c}}\left(\hat{\mathbf{H}}, \mathbf{c}; \boldsymbol{\theta}^{(S)}\right)\right)\right], \tag{2.44}$$

The M step. The M step consists in finding $\hat{\boldsymbol{\theta}}^{(S),(t+1)}$ by maximizing $Q_{EM}\left(\boldsymbol{\theta}^{(S)}, \hat{\boldsymbol{\theta}}^{(S),(t)}\right)$ defined in (2.44) w.r.t $\boldsymbol{\theta}^{(S)}$, which mathematically writes as:

$$\hat{\boldsymbol{\theta}}^{(S),(t+1)} = \arg\max_{\boldsymbol{\theta}^{(S)}}\left\{Q_{EM}\left(\boldsymbol{\theta}^{(S)}, \hat{\boldsymbol{\theta}}^{(S),(t)}\right)\right\}. \tag{2.45}$$

The EM procedure converges to a local maximum of the likelihood function (2.39) [30]. Let us now apply the EM procedure to our estimation problem, beginning with the E step.

2.4.3 The complete log-likelihood function

In this Section, we provide the closed-form expression of the complete log-likelihood function $\log\left(\mathbb{L}^{(S)}_{\hat{\mathbf{H}},\mathbf{c}}\left(\hat{\mathbf{H}}, \mathbf{c}; \boldsymbol{\theta}^{(S)}\right)\right)$. To do so, first, we decompose it as follows:

$$\log\left(\mathbb{L}^{(S)}_{\hat{\mathbf{H}},\mathbf{c}}\left(\hat{\mathbf{H}}, \mathbf{c}; \boldsymbol{\theta}^{(S)}\right)\right) = \log\left(\mathbb{L}^{(S)}_{\hat{\mathbf{H}}|\mathbf{c}}\left(\hat{\mathbf{H}}|\mathbf{c}; \boldsymbol{\theta}^{(S)}\right)\right) + \log\left(\mathbb{L}^{(S)}_{\mathbf{c}}\left(\mathbf{c}; \boldsymbol{\theta}^{(S)}\right)\right), \tag{2.46}$$

where $\mathbb{L}^{(S)}_{\mathbf{c}}\left(\mathbf{c}; \boldsymbol{\theta}^{(S)}\right)$ is the likelihood function of $\mathbf{c}$. Let us express the closed-form expression of (2.46). For fixed $\mathbf{c}$, $\log\left(\mathbb{L}^{(S)}_{\hat{\mathbf{H}}|\mathbf{c}}\left(\hat{\mathbf{H}}|\mathbf{c}; \boldsymbol{\theta}^{(S)}\right)\right)$ can be written as follows:

$$\begin{aligned}\log\left(\mathbb{L}^{(S)}_{\hat{\mathbf{H}}|\mathbf{c}}\left(\hat{\mathbf{H}}|\mathbf{c}; \boldsymbol{\theta}^{(S)}\right)\right) = &- N_{m_d}N_{m_p}\log\left(\pi\left(2\sigma_h^2 + 2\sigma_n^2\right)\right) - \\ &\frac{1}{2\sigma_h^2 + 2\sigma_n^2}\sum_{i=1}^{N_{m_p}}\sum_{n=1}^{N_{m_d}}|\hat{H}[i,n] - c_n^{(c)}ae^{j\theta_0}|^2.\end{aligned} \tag{2.47}$$

Also, the elements of $\mathbf{c}$ being i.i.d. Nakagami-m random variables, using (2.4), we obtain:

$$\begin{aligned}\log\left(\mathbb{L}_{\mathbf{c}}^{(S)}\left(\mathbf{c};\boldsymbol{\theta}^{(S)}\right)\right) =& N_{m_d}\left(m_{Na}\log\left(m_{Na}\right)+\log(2)-\log\left(\Gamma\left(m_{Na}\right)\right)\right)+\\ &(2m_{Na}-1)\sum_{n=1}^{N_{m_d}}\log\left(c_n^{(c)}\right)-m_{Na}\sum_{n=1}^{N_{m_d}}\left(c_n^{(c)}\right)^2.\end{aligned} \tag{2.48}$$

Plugging (2.47) and (2.48) into (2.46) yields the following complete log-likelihood expression:

$$\begin{aligned}\log\left(\mathbb{L}_{\hat{\mathbf{H}},\mathbf{c}}^{(S)}\left(\hat{\mathbf{H}},\mathbf{c};\boldsymbol{\theta}^{(S)}\right)\right) =& -N_{m_d}N_{m_p}\log\left(\pi\left(2\sigma_h^2+2\sigma_n^2\right)\right)-\\ &\frac{1}{2\sigma_h^2+2\sigma_n^2}\sum_{i=1}^{N_{m_p}}\sum_{n=1}^{N_{m_d}}\left(|\hat{H}[i,n]|^2-2c_n^{(c)}a\Re(\hat{H}[i,n]e^{-j\theta_0})\right)-\\ &N_{m_p}\sum_{n=1}^{N_{m_d}}\frac{\left(c_n^{(c)}\right)^2a^2}{2\sigma_h^2+2\sigma_n^2}+N_{m_d}\left(m_{Na}\log(m_{Na})+\log(2)-\log\left(\Gamma(m_{Na})\right)\right)+\\ &(2m_{Na}-1)\sum_{n=1}^{N_{m_d}}\log\left(c_n^{(c)}\right)-m_{Na}\sum_{n=1}^{N_{m_d}}\left(c_n^{(c)}\right)^2.\end{aligned} \tag{2.49}$$

2.4.4 The expectation step

To perform the E step, we plug (2.49) into (2.44), yielding:

$$\begin{aligned}Q_{EM}\left(\boldsymbol{\theta}^{(S)},\hat{\boldsymbol{\theta}}^{(S),(t)}\right) =& -N_{m_d}N_{m_p}\log\left(\pi\left(2\sigma_h^2+2\sigma_n^2\right)\right)-\\ &\frac{1}{2\sigma_h^2+2\sigma_n^2}\sum_{i=1}^{N_{m_p}}\sum_{n=1}^{N_{m_d}}\left(|\hat{H}[i,n]|^2-2\mathcal{T}_1^{(t)}(n)a\Re(\hat{H}[i,n]e^{-j\theta_0})\right)-\\ &N_{m_p}\sum_{n=1}^{N_{m_d}}\mathcal{T}_2^{(t)}(n)\frac{a^2}{2\sigma_h^2+2\sigma_n^2}+N_{m_d}\left(m_{Na}\log(m_{Na})+\log(2)-\log\left(\Gamma(m_{Na})\right)\right)+\\ &(2m_{Na}-1)\sum_{n=1}^{N_{m_d}}\mathcal{T}_3^{(t)}(n)-m_{Na}\sum_{n=1}^{N_{m_d}}\mathcal{T}_2^{(t)}(n),\end{aligned} \tag{2.50}$$

with

$$\mathcal{T}_k^{(t)}(n) := \mathbb{E}_{c_n^{(c)}|\hat{\mathbf{H}},\hat{\boldsymbol{\theta}}^{(S),(t)}}\left[\left(c_n^{(c)}\right)^k\right],\quad k=1,2, n=1,\ldots,N_{m_d}, \tag{2.51}$$

and

$$\mathcal{T}_3^{(t)}(n) := \mathbb{E}_{c_n^{(c)}|\hat{\mathbf{H}},\hat{\boldsymbol{\theta}}^{(S),(t)}}\left[\log\left(c_n^{(c)}\right)\right],\quad n=1,\ldots,N_{m_d}. \tag{2.52}$$

In what follows, we find the closed-form expressions of (2.51) and (2.52). To do so, we use the Bayes rule, which yields:

$$\mathcal{T}_k^{(t)}(n) = \frac{T_k^{(t)}(n)}{T_0^{(t)}(n)},\quad k=1,2,3, n=1,\ldots,N_{m_d}, \tag{2.53}$$

with, for $k = 0, 1, 2$:

$$T_k^{(t)}(n) = \int_0^{+\infty} \mathbb{L}^{(S)}_{\hat{\mathbf{H}}_n|c_n^{(c)}}\left(\hat{\mathbf{H}}_n|x; \hat{\boldsymbol{\theta}}^{(S),(t)}\right) f_{c_n^{(c)}}(x)\, x^k dx, \quad n = 1, \ldots, N_{m_p}, \tag{2.54}$$

and

$$T_3^{(t)}(n) = \int_0^{+\infty} \mathbb{L}^{(S)}_{\hat{\mathbf{H}}_n|c_n^{(c)}}\left(\hat{\mathbf{H}}_n|x; \hat{\boldsymbol{\theta}}^{(S),(t)}\right) f_{c_n^{(c)}}(x) \log(x)\, dx, \quad n = 1, \ldots, N_{m_p}. \tag{2.55}$$

After some derivations provided in Appendix A.5, we obtain the following closed-form expressions for (2.54) and (2.55):

$$T_k^{(t)}(n) = C_n^{(c),(t)} \left(2\mathcal{B}_{2,n}^{(t)}\right)^{-\frac{2m_{Na}+k}{2}} \Gamma(2\hat{m}_{Na}^{(S),(t)} + k) e^{\frac{\left(\mathcal{B}_{3,n}^{(t)}\right)^2}{8\mathcal{B}_{2,n}^{(t)}}} D_{-2\hat{m}_{Na}^{(S),(t)}-k}\left(\frac{\mathcal{B}_{3,n}^{(t)}}{\sqrt{2\mathcal{B}_{2,n}^{(t)}}}\right), \quad k = 0, 1, 2, \tag{2.56}$$

$$\begin{aligned} T_3^{(t)}(n) = & C_n^{(c),(t)} e^{\frac{\left(\mathcal{B}_{3,n}^{(t)}\right)^2}{8\mathcal{B}_{2,n}^{(t)}}} \Gamma\left(2\hat{m}_{Na}^{(S),(t)}\right)\left(2\mathcal{B}_{2,n}^{(t)}\right)^{-\hat{m}_{Na}^{(S),(t)}} \left(-\frac{1}{2}\log\left(2\mathcal{B}_{2,n}^{(t)}\right) D_{-2\hat{m}_{Na}^{(S),(t)}}\left(\frac{\mathcal{B}_{3,n}^{(t)}}{\sqrt{2\mathcal{B}_{2,n}^{(t)}}}\right) + \right. \\ & \left. \psi_0\left(2\hat{m}_{Na}^{(S),(t)}\right) D_{-2\hat{m}_{Na}^{(S),(t)}}\left(\frac{\mathcal{B}_{3,n}^{(t)}}{\sqrt{2\mathcal{B}_{2,n}^{(t)}}}\right) + \frac{\partial}{\partial w} D_{-2\hat{m}_{Na}^{(S),(t)}-w}\left(\frac{\mathcal{B}_{3,n}^{(t)}}{\sqrt{2\mathcal{B}_{2,n}^{(t)}}}\right)\Big|_{w=0}\right), \end{aligned} \tag{2.57}$$

where $\psi_0(x)$ is the digamma function, and with

$$C_n^{(c),(t)} = \left(\frac{2\left(\hat{m}_{Na}^{(S),(t)}\right)^{\hat{m}_{Na}^{(S),(t)}}}{\pi^{N_{mp}}\left(2\hat{\sigma}_h^{2,(S),(t)} + 2\sigma_n^2\right)^{N_{mp}} \Gamma\left(\hat{m}_{Na}^{(S),(t)}\right)}\right) e^{-\sum_{i=1}^{N_{mp}} \frac{|\hat{H}[i,n]|^2}{2\hat{\sigma}_h^{2,(S),(t)} + 2\sigma_n^2}},$$

$$\mathcal{B}_{2,n}^{(t)} := N_{m_p} \frac{\left(\hat{a}^{(S),(t)}\right)^2}{2\hat{\sigma}_h^{2,(S),(t)} + 2\sigma_n^2} + \hat{m}_{Na}^{(S),(t)},$$

and

$$\mathcal{B}_{3,n}^{(t)} := -\frac{\left(\hat{a}^{(S),(t)}\right)}{\hat{\sigma}_h^{2,(S),(t)} + \sigma_n^2} \sum_{i=1}^{N_{mp}} \Re\left(\hat{H}[i,n] e^{-j\hat{\theta}_0^{(S),(t)}}\right),$$

and where $\frac{\partial}{\partial w} D_{-2\hat{m}_{Na}^{(S),(t)}-w}\left(\frac{\mathcal{B}_{3,n}^{(t)}}{\sqrt{2\mathcal{B}_{2,n}^{(t)}}}\right)|_{w=0}$ is the derivative of $D_{-2\hat{m}_{Na}^{(S),(t)}-w}$ w.r.t. w evaluated in $w = 0$, which can be approximated according to the following equation:

$$\frac{\partial}{\partial w} D_{-2\hat{m}_{Na}^{(S),(t)}-w}(x)|_{w=0} \approx \frac{D_{-2\hat{m}_{Na}^{(S),(t)}-w+h^{(S)}}(x) - D_{-2\hat{m}_{Na}^{(S),(t)}-w-h^{(S)}}(x)}{2h^{(S)}}. \tag{2.58}$$

In our numerical results in Section 2.4.8, we set $h^{(S)} = 10^{-3}$.

2.4.5 The maximization step

During the M step, we aim to maximize (2.50) w.r.t $\boldsymbol{\theta}^{(S)}$. Then, by setting the derivative of (2.50) w.r.t the elements of $\boldsymbol{\theta}^{(S)}$ to zero, we obtain the following parameters estimators after some algebraic manipulations:

$$\hat{\theta}_0^{(S),(t+1)} = \arctan\left(\frac{\sum_{i=1}^{N_{mp}}\sum_{n=1}^{N_{m_d}}\mathcal{T}_1^{(t)}(n)\Im(\hat{H}[i,n])}{\sum_{i=1}^{N_{mp}}\sum_{n=1}^{N_{m_d}}\mathcal{T}_1^{(t)}(n)\Re(\hat{H}[i,n])}\right), \tag{2.59}$$

$$\hat{a}^{(S),(t+1)} = \frac{1}{N_{m_p}\sum_{n=1}^{N_{m_d}}\mathcal{T}_2^{(t)}(n)}\sum_{i=1}^{N_{m_p}}\sum_{n=1}^{N_{m_d}}\mathcal{T}_1^{(t)}(n)\Re\left(\hat{H}[i,n]e^{-j\hat{\theta}_0^{(S),(t+1)}}\right), \tag{2.60}$$

$$2\hat{\sigma}_h^{2,(S),(t+1)} = \frac{1}{N_{m_p}N_{m_d}}\sum_{i=1}^{N_{m_p}}\sum_{n=1}^{N_{m_d}}\left(|\hat{H}[i,n]|^2 - 2\mathcal{T}_1^{(t)}(n)\hat{a}^{(S),(t+1)}\Re\left(\hat{H}[i,n]e^{-j\hat{\theta}_0^{(S),(t+1)}}\right) + \mathcal{T}_2^{(t)}(n)\left(\hat{a}^{(S),(t+1)}\right)^2\right), \tag{2.61}$$

and

$$\hat{m}_{Na}^{(S),(t+1)} = \arg\max_{m_{Na}}\left\{N_{m_d}(m_{Na}\log(m_{Na}) - \log(\Gamma(m_{Na}))) - m_{Na}\sum_{n=1}^{N_{m_d}}\mathcal{T}_2^{(t)}(n) + (2m_{Na}-1)\sum_{n=1}^{N_{m_d}}\mathcal{T}_3^{(t)}(n)\right\}. \tag{2.62}$$

We have hence closed-form expressions for the estimators of θ_0, a and $2\sigma_h^2$ in (2.59), (2.60) and (2.61), respectively, whereas the estimator of m_{Na} is obtained by the maximization of the univariate function (2.62), which can be performed for instance using the Newton method.

2.4.6 Initialization of the EM procedure using the method of moments

The EM procedure requires to find initialization for the parameters to estimate, i.e., finding initial $\hat{\boldsymbol{\theta}}^{(S),(0)}$. It is possible to initialize these parameters randomly, however, since the EM does not guaranty global likelihood maximization, good initialization is preferable. Here, we propose to use the MoM to initialize them.

Let us first remind that $\hat{H}[i,n]$ can be expressed as follows:

$$\hat{H}[i,n] = c_n^{(c)}ae^{j\theta_0} + H_c[i,n], \tag{2.63}$$

with $H_c[i,n] \sim \mathcal{CN}(0, 2\sigma_h^2 + 2\sigma_n^2)$. From (2.63), we can compute the expectation of $\hat{H}[i,n]$ as follows:

$$\mu_1^{(S)} := \mathbb{E}\left[\hat{H}[i,n]\right] = \frac{a}{\sqrt{m_{Na}}}\left(\frac{\Gamma(m_{Na}+0.5)}{\Gamma(m_{Na})}\right)e^{j\theta_0}. \tag{2.64}$$

Second, we can infer the following two other equalities from [83]:

$$\mu_2^{(S)} := \mathbb{E}\left[|\hat{H}[i,n]|^2\right] = 2\sigma_h^2 + 2\sigma_n^2 + a^2, \tag{2.65}$$

$$\mu_4^{(S)} := \mathbb{E}\left[|\hat{H}[i,n]|^4\right] = 2\left(2\sigma_h^2 + 2\sigma_n^2\right)^2 + 4\left(2\sigma_h^2 + 2\sigma_n^2\right)a^2 + \frac{m_{Na}+1}{m_{Na}}a^4. \tag{2.66}$$

Using (2.65), we obtain

$$2\sigma_h^2 + 2\sigma_n^2 = \mu_2^{(S)} - a^2. \tag{2.67}$$

Plugging (2.67) into (2.66) yields after some algebraic manipulations:

$$m_{Na} = \frac{a^4}{\mu_4^{(S)} - 2\left(\mu_2^{(S)} - a^2\right)^2 - 4\left(\mu_2^{(S)} - a^2\right)a^2 - a^4}. \tag{2.68}$$

Plugging (2.68) into (2.64), we propose to estimate a by $\hat{a}^{(S),(0)}$ given by the solution of the following equation:

$$|\hat{\mu}_1^{(S)}|^2 = \frac{\left(\hat{a}^{(S),(0)}\right)^2}{u_S\left(\hat{a}^{(S),(0)}\right)}\left(\frac{\Gamma\left(u_S\left(\hat{a}^{(S),(0)}\right) + 0.5\right)}{\Gamma\left(u_S\left(\hat{a}^{(S),(0)}\right)\right)}\right)^2, \tag{2.69}$$

with

$$u_S(x) := \frac{x^4}{\hat{\mu}_4^{(S)} - 2\left(\hat{\mu}_2^{(S)} - x^2\right)^2 - 4\left(\hat{\mu}_2^{(S)} - x^2\right)x^2 - x^4}.$$

Then, using the above derivations, m_{Na}, $2\sigma_h^2$, and θ_0 are estimated according to the following equations:

$$\hat{m}_{Na}^{(S),(0)} = u_S\left(\hat{a}^{(S),(0)}\right), \tag{2.70}$$

$$2\hat{\sigma}_h^{2,(S),(0)} = \hat{\mu}_2^{(S)} - 2\sigma_n^2 - \left(\hat{a}^{(S),(0)}\right)^2, \tag{2.71}$$

$$\hat{\theta}_0^{(S),(0)} = \angle\left(\sqrt{\hat{m}_{Na}^{(S),(0)}}\frac{\hat{\mu}_1^{(S)}\Gamma\left(\hat{m}_{Na}^{(S),(0)}\right)}{\hat{a}^{(S),(0)}\Gamma\left(\hat{m}_{Na}^{(S),(0)} + 0.5\right)}\right), \tag{2.72}$$

where $\angle(z)$ in (2.72) is the phase of the complex number z, (2.70) is obtained from (2.68) , (2.71) from (2.67) and (2.72) from (2.64).

We also propose to estimate the Rician K factor according to the following equation:

$$\hat{K}_{MoM}^{(S)} = \frac{\left(\hat{a}^{(S),(0)}\right)^2}{2\hat{\sigma}_h^{2,(S),(0)}}. \tag{2.73}$$

2.4.7 The EM procedure algorithm

Finally, we propose the following estimator of the Rician K factor:

$$\hat{K}_{EM}^{(S)} = \frac{\left(\hat{a}^{(S),(t_{EM})}\right)^2}{2\hat{\sigma}_h^{2,(S),(t_{EM})}} \tag{2.74}$$

where t_{EM} is the number of iteration for the EM procedure to reach the convergence.

The proposed EM procedure to estimate the Rician K factor with Nakagami-m shadowed LoS is depicted in Algorithm 2.1.

Algorithm 2.1: EM procedure for estimation of the Rician K factor.

Set $\epsilon > 0$, $C = \epsilon + 1$, $t = 1$.
Initialize $\hat{a}^{(S),(0)}$, $\hat{m}_{Na}^{(S),(0)}$, $2\hat{\sigma}_h^{2,(S),(0)}$ and $\hat{\theta}_0^{(S),(0)}$ according to (2.69), (2.70), (2.71) and (2.72), respectively.
Set $\hat{\boldsymbol{\theta}}_S^{(S),(0)} = \left[\hat{a}^{(S),(0)}, 2\hat{\sigma}_h^{2,(S),(0)}, \hat{\theta}_0^{(S),(0)}, \hat{m}_{Na}^{(S),(0)}\right]$.
while $C > \epsilon$ **do**
  Compute $\hat{\theta}_0^{(S),(t)}$, $\hat{a}^{(S),(t)}$, $2\hat{\sigma}_h^{2,(S),(t)}$ and $\hat{m}_{Na}^{(S),(t)}$, and using (2.59), (2.60), (2.61) and (2.62), respectively.
  Set $\hat{\boldsymbol{\theta}}^{(S),(t)} = \left[\hat{a}^{(S),(i)}, 2\hat{\sigma}_h^{2,(S),(t)}, \hat{\theta}_0^{(S),(t)}, \hat{m}_{Na}^{(S),(t)}\right]$.
  Set $C = ||\hat{\boldsymbol{\theta}}_S^{(S),(t-1)} - \hat{\boldsymbol{\theta}}_S^{(S),(t)}||$.
  Set $t = t + 1$.
end
Set $t_{EM} = t$.
Return $K_{EM}^{(S)} = \frac{\left(\hat{a}^{(S),(t_{EM})}\right)^2}{2\hat{\sigma}_h^{2,(S),(t_{EM})}}$.

2.4.8 Numerical results

In this Section, we provide numerical to compare the proposed estimators bias magnitude and NMSE with the ones of [83] and [47], denoted by $\hat{K}_{WMoM}^{(S)}$ and $\hat{K}_{LMoM}^{(S)}$, respectively. To do so, we consider the same system model as in [83] and [47] and thus we set $N_{m_d} = N$ and $N_{m_p} = 1$, meaning that only one subcarrier is used for channel estimation and that the shadowing changes independently between consecutive OFDMA or SC-FDMA symbols. Moreover, since no noise is considered in [83] and [47], unless otherwise stated, we set $2\sigma_n^2 = 0$, i.e., the channel is perfectly known. We also compare our proposed estimators with $\hat{K}_{MML}^{n}$ given by (2.9), which does not take into account LoS shadowing. The estimators' performance are averaged through 10 000 Monte-Carlo simulations.

It is worth emphasizing that (2.38) involves m_{Na}, and it is unclear in [83] how to estimate this parameter. **Therefore, we perform our simulations of** (2.38) **considering perfect knowledge of** m_{Na}. As a consequence, the comparison is not fair since in our proposed estimators, this parameter has to be estimated, and thus (2.38) has access to more statistical information. However, it will be shown that, despite this disadvantage, our proposed estimators generally perform better than (2.38).

In Fig. 2.9, we set $m_{Na} = 5$ and $N = 100$, and we plot the estimators bias magnitude and NMSE in Figs. 2.9a and 2.9b, respectively, versus the value of K. We can see that both the proposed MoM and EM estimators perform better than the ones from [83] and [47] in terms of both bias magnitude and NMSE. Especially, we see that the estimator from [47] provides unreliable estimation since its NMSE does not even appear in the plot. This is explained because we consider $N = 100$ in our simulation and this estimator requires larger sample size. We can see that the bias of our proposed estimator is almost independent on K whereas the bias of the other considered estimators increases with K. We can also observe that, although $\hat{K}^n_{Prop}$ does not take into account the shadowing, this estimator yields the best performance among the considered estimators as long as $K < 2$. This observation is in agreement with [47] where it is observed that for low values of K, not taking into account the shadowing during the estimation does not engender important performance degradations. This is explained because for low K, the LoS component has low value and thus the shadowing has less impact. This is interesting since we can also see that the NMSE of our proposed estimators is the highest for low values of K, and thus $\hat{K}^n_{MML}$ and $\hat{K}^{(S)}_{EM}$ and $\hat{K}^{(S)}_{MoM}$ exhibit some complementarity.

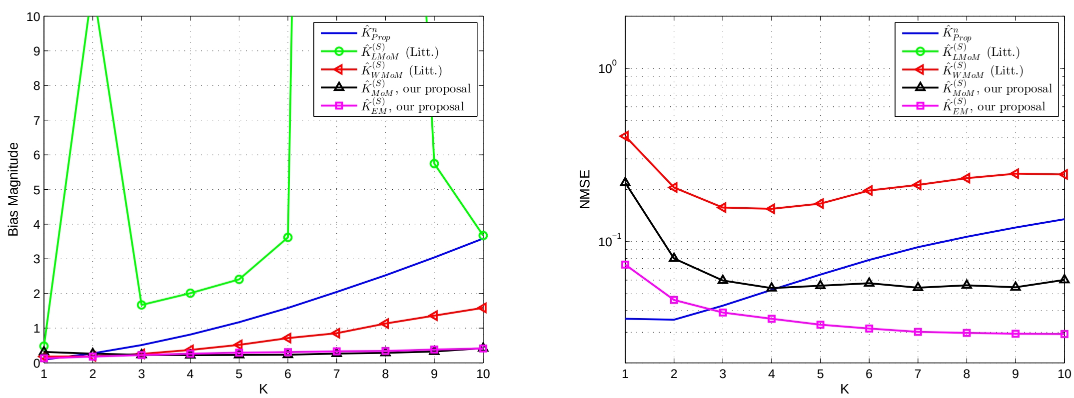

(a) Bias magnitude. (b) NMSE.

Figure 2.9: Performance of the considered estimators versus K, $2\sigma_n^2 = 0$, $m_{Na} = 5$, $N = 100$.

Now, let us study the influence of N. To do so, we set $m_{Na} = 5$ and $K = 5$. In Fig. 2.10a and 2.10b, we plot the estimators bias magnitude and NMSE, respectively, versus the value of N. We observe that the proposed estimators yield once again the best performance among the considered ones, except for $N = 50$ where $\hat{K}^n_{Prop}$ is better in terms of NMSE than $\hat{K}^{(S)}_{MoM}$. We also observe that for all the estimators except $\hat{K}^n_{MML}$ whose performance are almost independent on N, the higher the value of N, the better the performance. Especially, $\hat{K}_{LMoM}$ starts to provide reliable results when $N = 10^4$. Finally, we observe that for $N \geq 100$, $\hat{K}^{(S)}_{MoM}$ has a lower bias magnitude than $\hat{K}^{(S)}_{EM}$, which exhibits a slight bias for $N = 10^4$.

In Fig. 2.11a and 2.11b, we set $K = 5$, $N = 100$ and we plot the estimators bias magnitude and NMSE, respectively, versus the value of m_{Na}. We can draw the following observations.

- For $m_{Na} > 8$, $\hat{K}^{(S)}_{WMoM}$ provides the lowest bias magnitude among the considered estimators, but its NMSE is higher than the one of $\hat{K}^n_{Prop}$, $\hat{K}^{(S)}_{MoM}$ and $\hat{K}^{(S)}_{EM}$, regardless the value of m_{Na}.

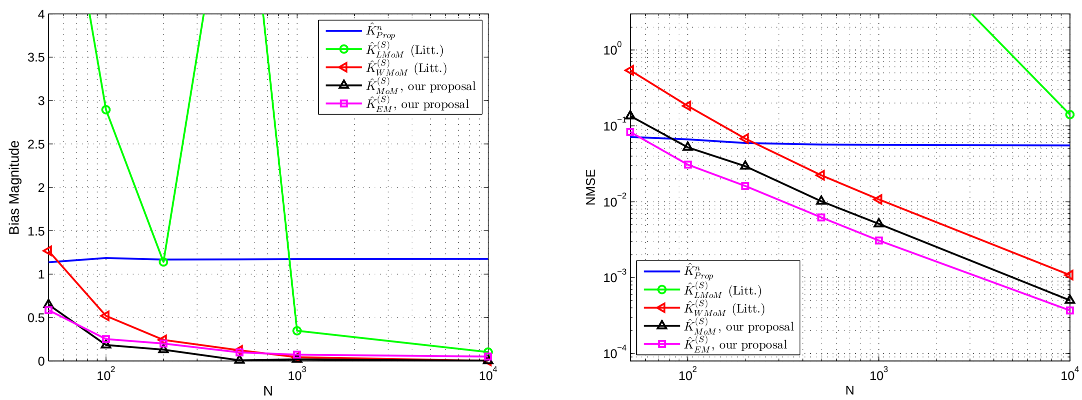

(a) Bias magnitude.

(b) NMSE.

Figure 2.10: Performance of the considered estimators versus N, $2\sigma_n^2 = 0$, $K = 5$, $m_{Na} = 5$.

- For $m_{Na} > 8$, $\hat{K}^n_{Prop}$ has the lowest NMSE among the considered estimators and, for $m_{Na} > 14$, its bias magnitude is also lower then the one of $\hat{K}^{(S)}_{MoM}$ and $\hat{K}^{(S)}_{EM}$.
- When comparing $\hat{K}^{(S)}_{MoM}$ and $\hat{K}^{(S)}_{MoM}$, $\hat{K}^{(S)}_{MoM}$ has the lowest bias whereas $\hat{K}^{(S)}_{MoM}$ has lower NMSE.

The low bias of $\hat{K}_{WMoM}$ in our first observation can be explained because this estimator has perfect knowledge of m_{Na}, however, despite this advantage, its NMSE is higher than the one of our proposed estimators.

Our second observation can be explained because, for high values of m_{Na}, the Nakagami-m distribution is tighter around its expectation and thus the random nature of the shadowing has less impact. We can also infer that it corresponds to a case in which the EM only provides local log-likelihood maximums and not global ones.

Our third observation is in agreement with Fig. 2.10, where we already observed that the bias magnitude of $\hat{K}^{(S)}_{MoM}$ is lower than the one of $\hat{K}^{(S)}_{EM}$, but its NMSE is higher.

Finally, let us now compare the estimators' performance when the samples are noisy. To this end, we set $K = 5$, $m_{Na} = 5$, $N = 100$ and, in Figs. 2.12a and 2.12b, we plot the estimators bias and NMSE, respectively, versus the SNR. We can see that $K^{(S)}_{EM}$ has the best performance among the considered estimators in terms of NMSE regardless of the SNR and that, for SNR < 14 dB, its bias magnitude is also the lowest. For SNR > 18 dB, the bias magnitude of $\hat{K}_{MoM}$ is lower than the one of $K^{(S)}_{EM}$. Thus, for low SNR, $K^{(S)}_{EM}$ is always preferable whereas for high SNR, system designers should choose between $\hat{K}_{MoM}$ which has the lowest bias and $K^{(S)}_{EM}$ which has the lowest NMSE.

To summarize our observations, our two proposed estimators outperform the existing ones from the literature in terms of both bias magnitude and NMSE. Especially, $\hat{K}^{(S)}_{EM}$ almost always provides the lowest NMSE whereas its bias magnitude is slightly higher

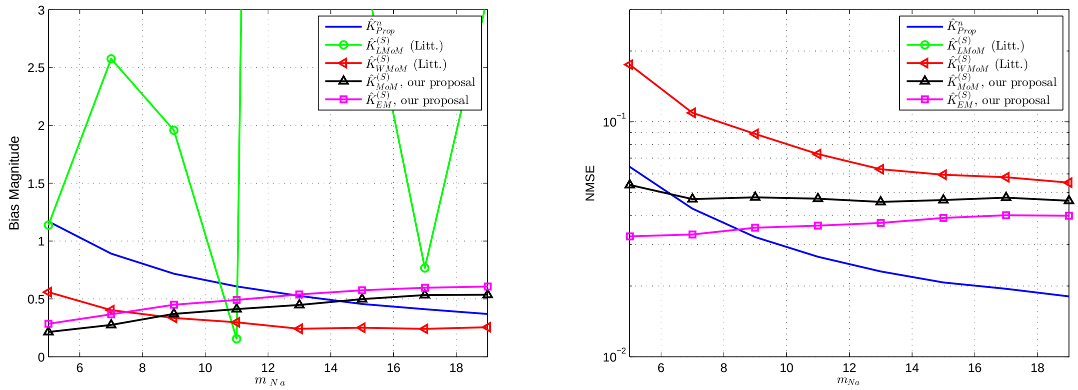

(a) Bias magnitude. (b) NMSE.

Figure 2.11: Performance of the considered estimators versus m_{Na}, $2\sigma_n^2 = 0$, $K = 5$, $N = 100$.

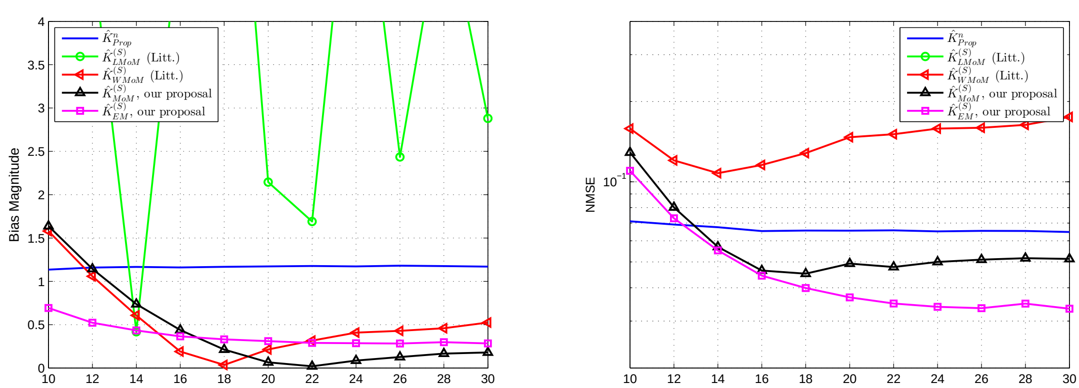

(a) Bias magnitude. (b) NMSE.

Figure 2.12: Performance of the considered estimators versus the SNR, $m_{Na} = 5$, $K = 5$, $N = 100$.

than the one of $\hat{K}^{(S)}_{MoM}$. Moreover, for high values of m_{Na} or for low values of K, $\hat{K}^{n}_{Prop}$ exhibits good performance and thus it should be of interest to design estimation procedure in which $\hat{K}^{(S)}_{Prop}$ is used in these cases, and $\hat{K}^{(S)}_{EM}$ or $\hat{K}^{(S)}_{MoM}$ are used otherwise.

2.5 Conclusion

In this Chapter, we addressed the first goal of this thesis, which is the estimation of the Rician K factor from noisy complex channel samples. We considered both the cases with and without LoS shadowing.

In the shadowing-less case, we derived four new estimators of the Rician K factor: two deterministic and two Bayesian. We also derived the deterministic CRLB in closed-form. We provided extensive numerical results and showed that our proposed estimators outperforms existing ones from the literature. We observed that the Bayesian estimators are more robust to small sample size than the deterministic ones, but they are also more complex.

In the case of Nakagami-m shadowed LoS, we proposed two estimation procedures: one based on the EM and the other one based on the MoM. We provided numerical results and showed that both the EM and the MoM estimators outperform the existing ones from the literature. We observed that the MoM-based estimator has the lowest bias, whereas the EM-based one is better in term of NMSE. We also found out that for low K value, our proposed deterministic estimator that does not take into account performs better than our two proposed shadowing-aware estimators and thus they are complementary.

Table 2.4 summarizes our proposed estimators. Part of the material presented in this Chapter has been published in [C2] and patented in [P1].

Table 2.4: Summary of our contributions on the estimation of the Rician K factor.

No LoS shadowing	Four new estimators + deterministic CRLB
Nakagami-m LoS shadowing	Two new estimators

Chapter 3

Background on Energy Efficiency Based Resource Allocation Problems

3.1 Introduction

This third Chapter introduces the second goal of this thesis, which is to propose and analyze algorithms to perform EE-based RA algorithms in MANETs when only statistical CSI is available, and when taking into account the use of HARQ and practical MCS.

We provide an overview of the existing works dealing with RA problems using EE metrics with and without HARQ. We also review the main existing optimization tools that are extensively used in Chapter 4 and 5 to solve the EE related RA Problems 1.1 introduced in Chapter 1.

The rest of the Chapter is organized as follows. In Section 3.2, we review the state of the art of existing EE-based RA schemes. Section 3.3 is dedicated to basic definitions and properties of convex optimization, geometric programming and pseudo concavity. Section 3.4 introduces tools to solve certain class of fractional programming problems. Section 3.5 is dedicated to suboptimal procedures to solve non Convex Optimization Problem (COP)s, whereas Section 3.6 concludes the Chapter, and introduces the content of Chapter 4 and 5.

3.2 Literature Review on EE based RA

3.2.1 Single user context

First, let us review the works studying the EE of HARQ in the single user context [18, 37, 45, 46, 52, 57, 63, 71, 76, 90, 94, 98, 99, 101, 111, 115]. In [18, 45, 52, 57, 63, 71, 76, 90, 94, 98, 99, 101, 111, 115], the authors consider statistical CSI at the transmitter, while in [46] imperfect CSI is assumed and in [37], perfect CSI is assumed to be available. Notice that, in [37], the authors do not explicitely consider the HARQ mechanism, but the considered metric is valid for Type-I HARQ. These works mainly address power and/or rate optimization within HARQ mechanism, typically using convex optimization.

3.2.2 Multi user context, perfect CSI at the transmitter

Second, we focus on the works dealing with the RA with EE related criteria in a multiuser context when considering perfect CSI at the transmitter side. In this category, a lot of works consider the use of capacity achieving codes [25, 32, 36, 70, 85, 109, 116, 117, 119] while practical MCS are considered in [13]. Among those works, [13, 32, 36, 70, 85, 109, 117, 119] do not consider HARQ whereas this mechanism is taken into account in [25, 116]. In details, when capacity achieving codes are considered with no HARQ, the MSEE problem is solved in [119] while the MMEE problem is solved in [70]. In [117], several heuristics are derived for the MSEE and MMEE problems. The multi-cell context is addressed in [36, 109]. In [109], the MSEE, MPEE, and MGEE problems are solved, while in [85], the MMEE problem is addressed. In [32], centralized and decentralized algorithms are proposed for the MGEE problem. In [36], a distributed algorithm is proposed to solve the MMEE problem. When capacity achieving codes are considered with HARQ and perfect CSI [25, 116], the GEE is optimized in [116] whereas several RA schemes are investigated in [25]. When practical MCS along with perfect CSI are considered without HARQ, the MGEE problem for the LTE downlink is addressed in [13]. All these works address power and/or subcarriers allocation.

3.2.3 Multi user context, statistical CSI at the transmitter

Third, we review the works addressing the RA problem with EE related objective functions when statistical CSI is available. This problem is addressed considering capacity achieving codes with no HARQ and the Rayleigh channel in [33, 121]. Practical MCS with HARQ are considered in [75] under the Rayleigh channel. In [75], the authors maximize the harmonic mean of the users' EE in a relay assisted networks when Type-I HARQ is considered.

3.2.4 Summary

Table 3.1 summarizes the existing works concerning the RA problem with EE related metrics for HARQ when considering practical MCS. We see that: *i*) the only work addressing the RA problem for HARQ based system with practical MCS and statistical CSI is [75], in which Type-I HARQ under the Rayleigh channel is considered and *ii*) no work addresses the RA problem with the objective of maximizing EE related metrics under the Rician channel when statistical CSI is available

Table 3.1: Existing works dealing with RA with EE related criteria in the multiuser context.

	Full CSI		Statistical CSI			
			Rayleigh		Rician	
	Capacity	MCS	Capacity	MCS	Capacity	MCS
No HARQ	[32, 36, 70, 85, 109, 117, 119]	[13]	[33, 121]	[75]	None	None
Type-I HARQ	[25, 116]	None	None	[75]	None	None
Type-II HARQ	[25, 116]	None	None	None	None	None

3.3 Convexity, Geometric Programming and Pseudo Convexity

This Section introduces basic definitions and properties of some conventional classes of optimization problems. All the proofs for the results presented in this Section are provided in [15, 23, 120]. First, let us review the convex optimization framework.

3.3.1 Convex optimization

3.3.1.1 Convex set

A set C is convex if, $\forall \mathbf{x}_1, \mathbf{x}_2 \in C$, $\forall \theta$ with $0 \leq \theta \leq 1$, we have:

$$\theta \mathbf{x}_1 + (1 - \theta)\mathbf{x}_2 \in C.$$

In words, C is convex if the line between any two points $\mathbf{x}_1, \mathbf{x}_2 \in C$ is in C. In Fig. 3.1, we plot an example of a convex (Fig. 3.1a) and a non-convex (Fig. 3.1b) set. In Fig. 3.1b, we also plot a red line between two points of the set that does not lie into the set, illustrating its non-convexity.

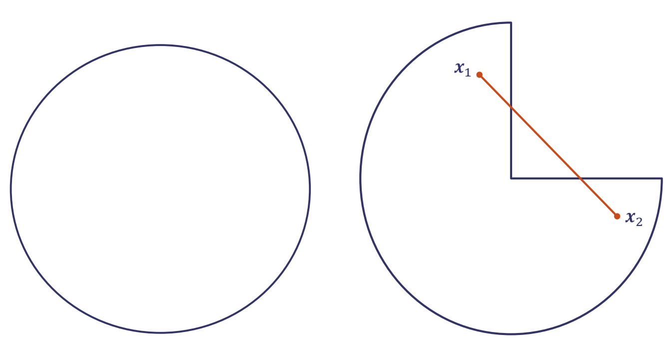

(a) Convex set. (b) non-convex set.

Figure 3.1: Illustration of convex and non-convex sets.

3.3.1.2 Convex and concave functions

Let us define $f : \mathbb{R}^n \to \mathbb{R}$. f is said to be convex if its domain $\mathbf{dom} f$ is convex, and, $\forall \mathbf{x}_1, \mathbf{x}_2 \in C$, $\forall \theta$ with $0 \leq \theta \leq 1$, the following inequality holds:

$$f(\theta \mathbf{x}_1 + (1-\theta)\mathbf{x}_2) \leq \theta f(\mathbf{x}_1) + (1-\theta) f(\mathbf{x}_2).$$

Similarly, f is said to be concave if $-f$ is convex. In Fig. 3.2, examples of univariate convex (Fig. 3.2a) and non-convex (Fig. 3.2b) functions are illustrated. In Fig. 3.2b, we plot in red a chordal of the function. This chordal is not strictly above the function, illustrating its non-convexity.

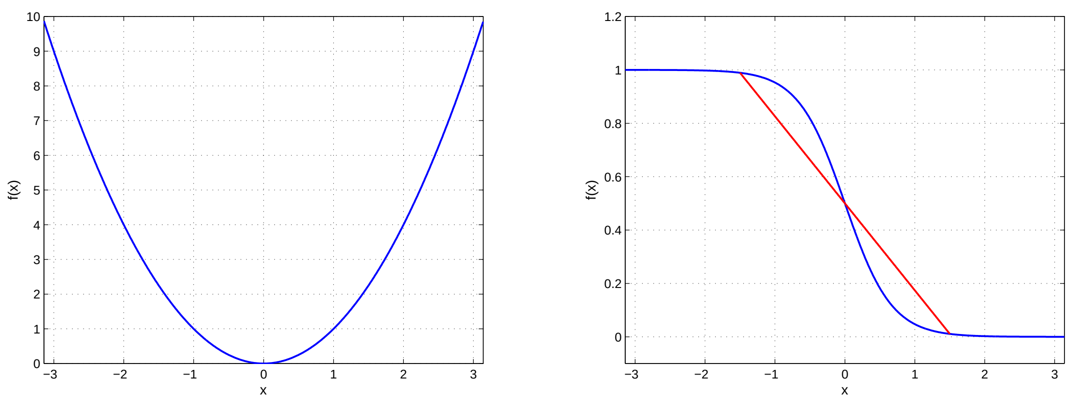

(a) Convex function. (b) non-convex function.

Figure 3.2: Illustration of convex and non-convex functions.

The following property characterizes twice differentiable convex function.

Property 3.1. *Let f be a twice differentiable function. f is convex if and only* $\mathbf{dom} f$ *is convex and if its Hessian is positive semidefinite.*

Remark 3.1. *For a twice differentiable real value function $f : \mathbb{R} \to \mathbb{R}$ with a convex domain, Property 3.1 reduces to $\forall x$, $f''(x) \geq 0$, where $f''(x)$ is the second order derivative of f.*

Hereafter, we remind some operations preserving the convexity.

Property 3.2. *Let us define $f_1, \ldots, f_i$ i convex functions, and $w_1, \ldots, w_i$ with, $\forall k \in \{1, \ldots, i\}$, $w_k \in \mathbb{R}^{+*}$. Then $\sum_{k=1}^{i} w_k f_k$ is convex.*

Property 3.3. *Let f be a convex function. Let g be the perspective of f, which is defined as:*

$$g(x,t) := tf\left(\frac{x}{t}\right).$$

Then, g is convex in (x,t).

Property 3.4. *Let us define $f : \mathbb{R}^n \to \mathbb{R}$ a convex function, $\mathbf{A} \in \mathbb{R}^{n\times m}$ and $\mathbf{b} \in \mathbb{R}^n$. Then, the function $g : \mathbb{R}^m \to \mathbb{R}$ defined as*

$$g(\mathbf{x}) = f(\mathbf{A}\mathbf{x} + \mathbf{b})$$

is convex.

3.3.1.3 Convex optimization problems

Here, we introduce the notion of constrained COPs, and the associated vocabulary. Let us consider the following general optimization problem with constraints:

Problem 3.1.

$$\min_{\mathbf{x}} \quad f_0(\mathbf{x}), \tag{3.1}$$

$$\text{s.t.} \quad f_k(\mathbf{x}) \leq 0, \quad k = 1, \ldots, i. \tag{3.2}$$

The function $f_0 : \mathbb{R}^n \to \mathbb{R}$ is called the objective function of Problem 3.1 whereas for $\forall k \in \{1, \ldots, i\}$, $f_k : \mathbb{R}^n \to \mathbb{R}$ are the inequality constraints. Notice that it is also possible to include equality constraint in Problem (3.1) as long as they are linear. Since we do not consider such constraints in our work, they are thus omitted here.

Definition 3.1. *The feasible set $\mathcal{F}$ of Problem 3.1 is defined as:*

$$\mathcal{F} := \{\mathbf{x} \in \mathbb{R}^n \text{ such that }, \forall k \in \{1, \ldots, i\}, f_k(\mathbf{x}) \leq 0\}. \tag{3.3}$$

Problem 3.1 is said to be feasible iff $\mathcal{F}$ is non empty, i.e., iff it is possible to find a point satisfying the i constraints (3.2) simultaneously. Also, Problem 3.1 is said to be a standard COP iff $f_0(x)$ is a convex function, and $\mathcal{F}$ is a convex set.

Remark 3.2. *A sufficient condition for $\mathcal{F}$ to be convex is $\forall k \in \{1, \ldots, i\}$, $f_k(\mathbf{x})$ is convex.*

Remark 3.3. *A special case of standard COP is when $\forall k \in \{0, \ldots, i\}$, $f_k(\mathbf{x})$ is linear. This type of problem is called a linear program.*

The main advantage of COPs lies in the following fundamental property.

Property 3.5. *Every local minimizer of a standard COP is a global minimizer.*

3.3.1.4 Optimality conditions

The so-called Karush-Kuhn-Tucker (KKT) conditions are necessary and sufficient to find the optimal solution of a COP. Going back to Problem 3.1 and assuming that, $\forall k \in$

$\{0, \ldots, i\}$, f_k is differentiable, the associated KKT conditions are given by:

$$\nabla f_0(\mathbf{x}^*) + \sum_{k=1}^{i} \lambda_k^* \nabla f_k(\mathbf{x}^*) = 0, \tag{3.4a}$$

$$f_k(\mathbf{x}^*) \leq 0, \quad \forall k, \tag{3.4b}$$

$$\lambda_k^* \geq 0, \quad \forall k, \tag{3.4c}$$

$$\lambda_k^* f_k(\mathbf{x}^*) = 0, \quad \forall k, \tag{3.4d}$$

where $\forall k \in \{0, \ldots, i\}$, λ_k^* is the optimal non-negative Lagrangian multiplier associated with the inequality constraint (3.2), $\nabla f_k(\mathbf{x})$ is the gradient of $f_k(\mathbf{x})$ and $\mathbf{x}^*$ is the optimal solution of Problem 3.1. The set of equalities (3.4d) are the *complementary slackness conditions*.

Solving the KKT conditions consists in finding $\lambda_1^*, \ldots, \lambda_i^*$ and $\mathbf{x}^*$ simultaneously satisfying (3.4a)-(3.4d), and allows us to find the global minimizer of a standard COP. There are two possibilities to solve these conditions.

1. The analytical methods.

2. The numerical procedures.

The analytical methods are problem-dependent and are, in general, less complex than the numerical procedures. We consider that a COP is analytically solved as long as the solution of the KKT conditions can be expressed as a function of a unique Lagrangian multiplier, as done for instance in the waterfilling [15]. However, it is not always possible to solve the KKT conditions analytically, and the numerical procedures have the merit to be problem independent.

The numerical procedures gather the Interior Point Method (IPM) and its variants (barrier or primal dual methods for instance). They are in general more complex, and use the Netwon method to numerically solve the KKT conditions [15]. There exist a number of different versions of the IPMs (barrier or primal dual methods for instance), with their own convergence rate. In [10, pp. 4], an upper bound on the IPM complexity is given by $\rho := n(n^3 + i)$.

3.3.1.5 Epigraph formulation

The epigraph formulation of Problem 3.1 consists in rewriting it equivalently as:

Problem 3.2.

$$\min_{t,\mathbf{x}} \quad t, \tag{3.5}$$

$$\text{s.t.} \quad t \leq f_0(\mathbf{x}) \tag{3.6}$$

$$f_k(\mathbf{x}) \leq 0, \quad k = 1, \ldots, i. \tag{3.7}$$

Remark 3.4. *Two optimization problems are said to be equivalent iff any optimal solution of one problem is also an optimal solution of the other one.*

Remark 3.5. *Although the number of optimization variables in Problem 3.2 is higher than in Problem 3.1, it might be easier to solve in certain cases as it will be seen in the following Chapters.*

3.3.2 Geometric programming

Geometric programming is a special case of non-convex problems that can be efficiently transformed into convex ones through a change of variables. Before defining a Geometric Program (GP), let us introduce some vocabulary.

Definition 3.2. *A monomial function is a function taking the following form:*

$$f(x_1, \ldots, x_n) = c x_1^{b_1} \ldots x_n^{b_n}, \tag{3.8}$$

with $c \in \mathbb{R}^+$ *and,* $\forall k \in \{1, \ldots, n\}$, $b_k \in \mathbb{R}$.

Definition 3.3. *A posynomial function is a function taking the following form:*

$$f(x_1, \ldots, x_n) = \sum_{k=1}^{j} c_k x_1^{b_{1,k}} \ldots x_n^{b_{n,k}}, \tag{3.9}$$

with $\forall k \in \{1, \ldots, j\}$, $c_k \in \mathbb{R}^+$ *and* $\forall p \in \{1, \ldots, n\}$, $b_{p,k} \in \mathbb{R}$.

With these two definitions, we can now define a GP as an optimization problem whose objective function and inequality constraints are posynomial. Mathematically, a GP takes the following form.

Problem 3.3.

$$\min_{\mathbf{x}} \quad P_0(\mathbf{x}), \tag{3.10}$$

$$\text{s.t.} \quad P_k(\mathbf{x}) \le 0, \quad k = 1, \ldots, i, \tag{3.11}$$

where, for $k \in \{0, \ldots, i\}$, $P_k(\mathbf{x})$ is posynomial.

In general, GPs are non-convex problems. However, the following property enables us to transform them into COPs.

Property 3.6. *The Log-Sum-Exp (LSE) function, defined as*

$$\mathcal{L}_{SE}(y_1, \ldots, y_n) := \log\left(\sum_{k=1}^{n} \exp(y_k)\right) \tag{3.12}$$

is convex.

Combining Properties 3.6 and 3.4 allows us to turn a non-convex GP into a standard COP through the following change of variables

$$y_k := \log(x_k), \quad \forall k. \tag{3.13}$$

As a consequence, GPs are a class of non COPs which can be solved with the same complexity as convex ones.

3.3.3 Pseudo concavity

In this Section, we define the notion of Pseudo Concave (PC) functions, and give a characterization of there optimum.

Definition 3.4. *Let C be a convex set, and let $f : C \to \mathbb{R}$ be a differentiable function. f is said to be PC iff, $\forall(\mathbf{x}_1, \mathbf{x}_2) \in C^2$, the following holds:*

$$f(\mathbf{x}_2) < f(\mathbf{x}_1) \implies \nabla(f(\mathbf{x}_2))^T(\mathbf{x}_1 - \mathbf{x}_2) > 0. \quad (3.14)$$

In Fig. 3.3, we represent an example of a univariate PC function along with one of its chordal, represented in red. We see that, unlike concave function, a PC function can be both above and below its chordal.

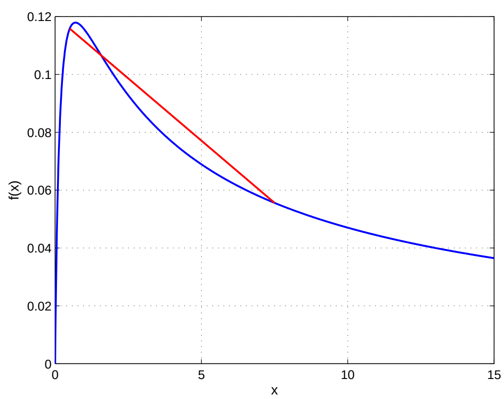

Figure 3.3: Example of a PC function with one of its chordal, represented in red.

The main advantage of PC from an optimization point of view comes from the following property.

Property 3.7. *The KKT conditions are necessary and sufficient to find the optimal solution of the maximization of a PC function over a convex set.*

3.4 Fractional Programming

In this Section, we review a class of non-COPs that are optimally solvable in polynomial time. Due to the fractional form of the EE (i.e., (1.16)), EE-based RA problems involves objective functions in the form of combinations of ratios. These type of problems are called **fractional programming problems**. In general, these problems are not convex. Fortunately, there exist in the literature several tools helping us to transform them into convex ones. In this Section, we provide an overview of these tools. The proofs of convergence and optimality for the algorithms presented in this Section are provided in [120], [28] and [61].

3.4.1 Maximization of a ratio

The general problem of the maximization of a ratio can be written:

Problem 3.4.

$$\min_{\mathbf{x}} \quad \frac{f_0(\mathbf{x})}{h_0(\mathbf{x})}, \tag{3.15}$$

$$\text{s.t.} \quad f_k(\mathbf{x}) \leq 0, \quad k = 1, \ldots, i. \tag{3.16}$$

This type of problem can be handled by the so called Dinkelbach's algorithm [34], which finds its optimal solution as long as the following hypothesis is satisfied.

Hypothesis 3.1. *In Problem 3.4, f_0 and h_0 are continuous, the feasible set is compact and h_0 is positive.*

The Dinkelbach's algorithm is used in various works dealing with RA including [13, 64, 112]. It is based on the following two steps, which are iterated until convergence to the optimal solution of Problem 3.4.

1. At iteration t, find $\mathbf{x}_t^*$, the optimal solution of the following problem:

$$\min_{\mathbf{x}} \quad f_0(\mathbf{x}) - \lambda^{(t)} h_0(\mathbf{x}), \tag{3.17}$$

$$\text{s.t.} \quad f_k(\mathbf{x}) \leq 0, \quad k = 1, \ldots, i, \tag{3.18}$$

   where $\lambda^{(t)} \geq 0$ depends on the optimal solution at iteration $(t-1)$.

2. Compute $\lambda^{(t+1)}$ using the following equation:

$$\lambda^{(t+1)} = \frac{f_0(\mathbf{x}_t^*)}{h_0(\mathbf{x}_t^*)}. \tag{3.19}$$

Notice that although the Dinkelbach's convergence Hypothesis 3.1 does not include requirements concerning the convexity or concavity of f_k and h_k, optimally solving the problem defined by (3.17)-(3.18) in step 1 is generally intractable, unless if this problem is convex, i.e., if f_0 is convex, h_0 is concave and for $k \in \{1, \ldots, i\}$, f_k is convex.

The detailed procedure to optimally solve Problem 3.4 is depicted in Algorithm 3.1.

3.4.2 Maximization of the minimum of a set of ratios

The general problem of the maximization of the minimum of a set of ratios can be written:

Problem 3.5.

$$\min_{\mathbf{x}} \quad \left\{ \max_{p \in \{1,\ldots,j\}} \frac{f_p(\mathbf{x})}{h_p(\mathbf{x})} \right\}, \tag{3.20}$$

$$\text{s.t.} \quad g_k(\mathbf{x}) \leq 0, \quad k = 1, \ldots, i. \tag{3.21}$$

Algorithm 3.1: Dinkelbach's algorithm to optimally solve Problem 3.4.

Set $\epsilon > 0$, $t = 0$ and $\lambda^{(0)} = 0$
Set $C_D = \epsilon + 1$.
while $C_D > \epsilon$ **do**
  Find $\mathbf{x}_t^*$ by optimally solving the problem defined by (3.17)-(3.18) with $\lambda^{(t)}$.
  Set $C_D = f_0(\mathbf{x}^*) - \lambda^{(t)} h_0(\mathbf{x}^*)$.
  Compute $\lambda^{(t+1)}$ using (3.19).
  Set $t = t + 1$.
end

This type of problem can be handled by the generalized Dinkelbach's algorithm [28], which finds its optimal solution as long as Hypothesis 3.1 is satisfied. This algorithm is used in different works dealing with resource allocation including [70]. The algorithm is based on the following two steps, which are iterated until convergence to the optimal solution of Problem 3.5.

1. At iteration t, find $\mathbf{x}_t^*$, the optimal solution of the following problem:

$$\min_{\mathbf{x}} \quad \max_{p\in\{1,\dots,j\}} \left\{ f_p(\mathbf{x}) - \lambda^{(t)} h_p(\mathbf{x}) \right\}, \tag{3.22}$$

$$\text{s.t.} \quad g_k(\mathbf{x}) \leq 0, \quad k = 1, \dots, i, \tag{3.23}$$

   where $\lambda^{(t)} \geq 0$ depends on the optimal solution at iteration $(t-1)$.

2. Compute $\lambda^{(t+1)}$ using the following equation:

$$\lambda^{(t+1)} = \max_{p\in\{1,\dots,j\}} \left\{ \frac{f_p(\mathbf{x}_t^*)}{h_p(\mathbf{x}_t^*)} \right\}. \tag{3.24}$$

The same comment as for the Dinkelbach's algorithm complexity holds true: the problem defined by (3.22)-(3.23) in step 1 can be solved with affordable iff it is a standard COP.

The detailed algorithm to optimally solve Problem 3.5 is given in Algorithm 3.2

Algorithm 3.2: Generalized Dinkelbach's algorithm to optimally solve Problem 3.5.

Set $\epsilon > 0$, $t = 0$ and $\lambda^{(0)} = 0$
Set $C_D = \epsilon + 1$.
while $C_D > \epsilon$ **do**
  Find $\mathbf{x}_t^*$ by optimally solving the problem defined by (3.22)-(3.23) with $\lambda^{(t)}$.
  Set $C_D = \max_{p\in\{1,\dots,j\}} \left\{ f_p(\mathbf{x}^*) - \lambda^{(t)} h_p(\mathbf{x}^*) \right\}$.
  Compute $\lambda^{(t+1)}$ using (3.24).
  Set $t = t + 1$.
end

3.4.3 Maximization of a sum ratios

The general problem of the maximization of a sum of ratios can be written as:

Problem 3.6.

$$\min_{\mathbf{x}} \quad \sum_{p=1}^{j} \frac{f_p(\mathbf{x})}{h_p(\mathbf{x})}, \tag{3.25}$$

$$\text{s.t.} \quad g_k(\mathbf{x}) \leq 0, \quad k = 1, \ldots, i. \tag{3.26}$$

This type of problem can be handled using the Jong's algorithm [61], which finds its optimal solution as long as the following hypothesis is satisfied.

Hypothesis 3.2. *In Problem 3.6, $\forall p \in \{1, \ldots, j\}$, $f_p(\mathbf{x})$ is twice continuously differentiable and convex, $h_p(\mathbf{x})$ is positive, twice continuously differentiable and concave and, $\forall k \in \{1, \ldots, i\}$, $g_k(\mathbf{x})$ is convex.*

The Jong's algorithm is used in several works dealing with RA including [12, 91, 119]. The algorithm is based on the following two steps, which are iterated until convergence to the optimal solution of Problem 3.6.

1. At iteration t, find $\mathbf{x}_t^*$, the optimal solution of the following problem:

$$\min_{\mathbf{x}} \quad \sum_{p=1}^{j} u_p^{(t)} \left(f_p(\mathbf{x}) - \beta_p^{(t)} h_p(\mathbf{x}) \right), \tag{3.27}$$

$$\text{s.t.} \quad g_k(\mathbf{x}) \leq 0, \quad k = 1, \ldots, i, \tag{3.28}$$

   where, $\forall p \in \{1, \ldots, j\}$, $u_p^{(t)} > 0$ and $\beta_p^{(t)} \geq 0$ depend on the optimal solution at iteration $(t-1)$.

2. Compute $\mathbf{u}^{(t+1)} := [u_1^{(t+1)}, \ldots, u_j^{(t+1)}]$ and $\boldsymbol{\beta}^{(t+1)} := [\beta_1^{(t+1)}, \ldots, \beta_j^{(t+1)}]$ using a modified Newton method, for which we define $\boldsymbol{\psi}(\boldsymbol{\beta}^{(t)}, \mathbf{u}^{(t)}, \mathbf{x}) := [\psi_1(\beta_1^{(t)}, u_1^{(t)}, \mathbf{x}), \ldots, \psi_{2j}(\beta_j^{(t)}, u_j^{(t)}, \mathbf{x})]$, and, $\forall p \in \{1, \ldots, j\}$:

$$\psi_p(\beta_p^{(t)}, u_p^{(t)}, \mathbf{x}) := -f_p(\mathbf{x}) + \beta_p^{(t)} h_p(\mathbf{x}), \tag{3.29}$$

$$\psi_{p+j}(\beta_p^{(t)}, u_p^{(t)}, \mathbf{x}) := -1 + u_p^{(t)} h_p(\mathbf{x}). \tag{3.30}$$

   The update equations for $\mathbf{u}^{(t+1)}$ and $\boldsymbol{\beta}^{(t+1)}$ are the following ones:

$$u_p^{(t+1)} = (1 - \epsilon^n) u_p^{(t)} + \epsilon^n \frac{1}{h_p(\mathbf{x}_t^*)}, \quad , \forall p, \tag{3.31}$$

$$\beta_p^{(t+1)} = (1 - \epsilon^n) \beta_p^{(t)} + \epsilon^n \frac{f_p(\mathbf{x}_t^*)}{h_p(\mathbf{x}_t^*)}, \quad , \forall p, \tag{3.32}$$

where $\epsilon \in (0,1)$ and $n \in \{1,2,\ldots\}$ is the largest value satisfying

$$\|\boldsymbol{\psi}(\boldsymbol{\beta}^{(t)} + \epsilon^n \mathbf{q}^{(t)}, \mathbf{u}^{(t)} + \epsilon^n \mathbf{q}^{(t)}, \mathbf{x}_t^*)\| \leq (1 - \delta\epsilon^n)\|\boldsymbol{\psi}(\boldsymbol{\beta}^{(t)}, \mathbf{u}^{(t)}, \mathbf{x}_t^*)\|,$$

with $\delta \in (0,1)$ and $\mathbf{q}^{(t)} := -[\boldsymbol{\psi}'(\boldsymbol{\beta}^{(t)}, \mathbf{u}^{(t)}, \mathbf{x}_t^*)]^{-1}\boldsymbol{\psi}(\boldsymbol{\beta}^{(t)}, \mathbf{u}^{(t)}, \mathbf{x}_t^*)$, where $\boldsymbol{\psi}'(\boldsymbol{\beta}^{(t)}, \mathbf{u}^{(t)}, \mathbf{x}_t^*)$ is the Jacobian matrix of $\boldsymbol{\psi}(\boldsymbol{\beta}^{(t)}, \mathbf{u}^{(t)}, \mathbf{x}_t^*)$.

Step 1 requires to solve a standard COP due to Hypothesis 3.2. The detailed procedure to optimally solve Problem 3.6 is given in Algorithm 3.3.

Algorithm 3.3: Jong's algorithm to optimally solve Problem 3.6.

Set $\epsilon > 0$, $t = 0$, initialize $\mathbf{u}^{(0)}$ and $\boldsymbol{\beta}^{(0)}$
Set $C_D := \epsilon + 1$.
while $C_D > \epsilon$ **do**
  Find $\mathbf{x}_t^*$ by optimally solving the problem defined by (3.27)-(3.28) with $\mathbf{u}^{(t)}$ and $\boldsymbol{\beta}^{(t)}$.
  Set $C_D := \|\boldsymbol{\psi}(\boldsymbol{\beta}^{(t)}, \mathbf{u}^{(t)}, \mathbf{x}_t^*)\|$.
  For $k = 1, \ldots, j$, compute $u_k^{(t+1)}$ and $\beta_k^{(t+1)}$ using (3.31) and (3.32), respectively.
  Set $t = t + 1$.
end

3.4.4 Summary of fractional programming tools

The algorithms enabling us to find the optimal solution of some class of fractional programming problems are summarized in Table 3.2. These algorithms are extensively used in Chapters 4 and 5.

Table 3.2: Fractional programming algorithms.

Problem's objective function	Ratio	Sum of ratios	Minimum of a set of ratios
Algorithm	Dinkelbach's	Jong's	Generalized Dinkelbach's

3.5 Other Non-Convex Optimization Procedures

When the optimization problem at hand is non-convex, i.e., when either the objective function or the feasible set is not convex, the computational complexity to find its global optimal solution is in general exponential, except fractional programs, which can be turned into COPs as it has been seen in the previous Section, and which are thus not addressed here. In this Section, we present suboptimal optimization procedures aiming to solve non-convex problems with affordable complexity.

3.5.1 Alternating optimization

Let us define the following possibly non-convex constrained problem:

Problem 3.7.

$$\min_{\mathbf{x}_1,\dots,\mathbf{x}_n} \quad f_0(\mathbf{x}_1,\dots,\mathbf{x}_n), \tag{3.33}$$

$$\text{s.t.} \quad f_k(\mathbf{x}_1,\dots,\mathbf{x}_n) \le 0, \quad k = 1,\dots,i. \tag{3.34}$$

The principle of AO, which is an iterative procedure, is to optimize alternately between the optimization variables until convergence is reached. Formally, at iteration t, there are n steps and, for a given step $p \in \{1,\dots,n\}$, we fix $(\bar{\mathbf{x}}_1^{(t)},\dots,\bar{\mathbf{x}}_{p-1}^{(t)},\bar{\mathbf{x}}_{p+1}^{(t-1)},\dots,\bar{\mathbf{x}}_n^{(t-1)})$ and we solve the following problem:

Problem 3.8.

$$\min_{\mathbf{x}_p} \quad f_0(\bar{\mathbf{x}}_1^{(t)},\dots,\bar{\mathbf{x}}_{p-1}^{(t)},\mathbf{x}_p,\bar{\mathbf{x}}_{p+1}^{(t-1)},\dots,\bar{\mathbf{x}}_n^{(t-1)}), \tag{3.35}$$

$$\text{s.t.} \quad f_k(\bar{\mathbf{x}}_1^{(t)},\dots,\bar{\mathbf{x}}_{p-1}^{(t)},\mathbf{x}_p,\bar{\mathbf{x}}_{p+1}^{(t-1)},\dots,\bar{\mathbf{x}}_n^{(t-1)}) \le 0, \quad k = 1,\dots,i. \tag{3.36}$$

AO is interesting if, $\forall p \in \{1,\dots,n\}$, finding the optimal solution of Problem 3.8 is easier than optimally solving Problem 3.7. The AO procedure to solve Problem 3.7 is depicted in Algorithm 3.4, whose convergence can be proved for instance following the proof of Theorem 1 in [81]. Notice that there is no guarantee on the optimality of the convergence point.

Algorithm 3.4: AO based procedure to solve Problem 3.7.

```
Set ε > 0, t = 1, C_AO = ε + 1.
Find (x̄_1^(0), ..., x̄_n^(0)) a feasible solution of Problem 3.7.
while C_AO > ε do
    for p = 1, ..., n do
        Find x_p^* the optimal solution of Problem 3.8 with x̄_1^(t), ..., x̄_{p-1}^(t), x̄_{p+1}^(t-1), ..., x̄_n^(t-1).
        Set x̄_p^(t) = x_p^*.
    end
    C_AO = ||[x̄_1^(t), ..., x̄_n^(t)] - [x̄_1^(t-1), ..., x̄_n^(t-1)]||.
    Set t = t + 1.
end
```

3.5.2 Successive convex approximation

The SCA procedure has been introduced in [78]. It is an iterative procedure enabling us to find KKT solutions of non COPs, which is used in various works dealing with RA, including [31, 102]. For a given iteration, it consists in approximating a non-convex problem around a feasible point by a COP we optimally solve, and to use this optimal solution as the initialization for the next iteration.

Formally, consider the following non-COP:

Problem 3.9.

$$\min_{\mathbf{x}} \quad f_0(\mathbf{x}), \tag{3.37}$$
$$\text{s.t.} \quad f_k(\mathbf{x}) \leq 0, \quad k = 1, \ldots, i, \tag{3.38}$$

where, $\forall k \in \{0, \ldots, i\}$, $f_k(\mathbf{x})$ is continuous and differentiable. At iteration t, the SCA requires to optimally solve the following optimization problem:

Problem 3.10.

$$\min_{\mathbf{x}} \quad \bar{f}_0(\mathbf{x}, \bar{\mathbf{x}}^{(t-1)}), \tag{3.39}$$
$$\text{s.t.} \quad \bar{f}_k(\mathbf{x}, \bar{\mathbf{x}}^{(t-1)}) \leq 0, \quad k = 1, \ldots, i, \tag{3.40}$$

where $\bar{\mathbf{x}}^{(t-1)}$ is the optimal solution at iteration $(t-1)$ and, $\forall k \in \{0, \ldots, i\}$, $\bar{f}_k(\mathbf{x}, \bar{\mathbf{x}}^{(t-1)})$ is the convex approximation of $f_k(\mathbf{x})$ around $\bar{\mathbf{x}}^{(t-1)}$, which is assumed to be continuous and differentiable. The SCA procedure convergence to a solution satisfying the KKT conditions of Problem 3.9 is ensured in [78] as long as Hypothesis 3.3 is satisfied. Notice that there is no guaranty regarding the global optimality of the convergence point.

Hypothesis 3.3. *In Problem 3.9 and 3.10, $\forall k \in \{0, \ldots, i\}$, $f_k(\mathbf{x})$ and $\bar{f}_k(\mathbf{x}, \mathbf{y})$ satisfy the following properties.*

- *The approximate functions are upper-bounds of the original ones, i.e., $\forall \mathbf{x}$, $\forall \mathbf{y}$, $f_k(\mathbf{x}) \leq \bar{f}_k(\mathbf{x}, \mathbf{y})$.*
- *The approximation is locally tight, i.e., $\forall \mathbf{x}$, $f_k(\mathbf{x}) = \bar{f}_k(\mathbf{x}, \mathbf{x})$.*
- *The gradient of the approximations is consistent with the gradient of the original functions, i.e., $\forall \mathbf{x}$, $\nabla f_k(\tilde{\mathbf{x}})|_{\tilde{\mathbf{x}}=\mathbf{x}} = \nabla \bar{f}_k(\tilde{\mathbf{x}}, \mathbf{x})|_{\tilde{\mathbf{x}}=\mathbf{x}}$.*

Finally, the SCA based procedure to solve Problem 3.9 is depicted in Algorithm 3.5.

3.6 Conclusion

In this Chapter, we provided a review of existing works dealing with EE-related RA problems. We also introduced the optimization framework that serves in Chapter 4 and 5 to solve Problems 1.1 described in Chapter 1.

Algorithm 3.5: SCA based procedure to solve Problem 3.9.

Set $\epsilon > 0$, $t = 0$, $C = \epsilon + 1$.

Find $\bar{\mathbf{x}}^{(0)}$ a feasible solution of Problem 3.9.

while $C > \epsilon$ **do**

  Find $\mathbf{x}^{*}$ the optimal solution of Problem 3.10.

  Compute $C = \|\mathbf{x}^{*} - \bar{\mathbf{x}}^{(t)}\|$.

  Set $\bar{\mathbf{x}}^{(t+1)} = \mathbf{x}^{*}$.

  Set $t = t + 1$.

end

Chapter 4

Resource Allocation for Type-II HARQ Under the Rayleigh Channel

4.1 Introduction

From Table 3.1 in Chapter 3, we see that the RA problem with EE-related metrics for Type-II HARQ in assisted MANETs using practical MCS under the Rayleigh channel has never been addressed in the literature. In this Chapter, we address this problem. In details, the contributions of this Chapter are the following ones.

- Considering HARQ and practical MCS, we derive optimal and computationally tractable algorithms solving the MSEE, the MPEE and the MMEE problems under per-link minimum goodput and maximum transmit power constraints. Our main technical contribution is to transform all these problems that have no special properties (like convexity) into equivalent convex ones. We also propose two suboptimal procedures to solve the MGEE problem.

- In addition, we analyze the complexity of the proposed algorithms. Since this analysis reveals that finding the optimal solution of the MSEE problem is complex, we derive two suboptimal less-complex algorithms to solve this problem.

- We show how our proposed solutions can also handle a minimum PER constraint with no additional derivations.

- We analyze the results of the proposed criteria through simulations of relevant practical scenarios. We also compare these results with two conventional criteria: the MPO from [65], and the MGO (also derived in this Chapter). Our simulations show that these two schemes actually achieve rather bad performance in EE. On the other hand, we find out that the MPEE criterion is especially relevant for MANETs.

- We also illustrate the effect of these differences on the battery drain of the same smartphone example as in Chapter 1, Section 1.5.4. The results confirm the fact that the scheme with the best PEE outperforms the conventional ones by allowing to transmit the largest amount of information bits with the least battery drain.

The rest of this Chapter is organized as follows. In Section 4.2, we present the error probability approximation used in this Chapter to solve the RA problems. In Section 4.3, we mathematically formulate the addressed RA problems whereas In Section 4.4, we present the methodology used to solve them. In Section 4.5, 4.6, 4.7 and 4.8 we solve the MSEE, MPEE, MMEE and MGEE problems, respectively. In Section 4.9, we show how our proposed framework can also handle a maximum PER constraint. In Section 4.10, we analyze the complexity of the proposed solutions. Section 4.11 is dedicated to numerical results and finally Section 4.12 concludes this Chapter.

4.2 Error Probability Approximation

We can see from (1.13), (1.29) and (1.30) in Chapter 1 that the links' goodput, the links' EE and the GEE involve the error probability $q_{\ell,m}$, which has no closed-form expressions when considering HARQ along with practical MCS. In this thesis, we overcome this issue by considering the following upper bound [96]

$$q_{\ell,m}(G_\ell E_\ell) \leq \pi_{\ell,m}(G_\ell E_\ell), \quad \forall \ell, \forall m, \tag{4.1}$$

where $\pi_{\ell,m}(G_\ell E_\ell)$ is the probability of decoding failure when p packets are available.

When OFDMA is considered along with Zero Forcing (ZF) one-tap equalizer followed by a soft decoding, as in [65], we use the following tight upper bound of $\pi_{\ell,m}(G_\ell E_\ell)$ for medium-to-high SNR.

$$\pi_{\ell,m}(G_\ell E_\ell) \leq \tilde{\pi}_{\ell,m}(G_\ell E_\ell) := \frac{g_{\ell,m}}{(G_\ell E_\ell)^{d_{\ell,m}}}, \quad \forall \ell, \forall m, \tag{4.2}$$

where $g_{\ell,m}$ and $d_{\ell,m}$ are fitting coefficients obtained through least square estimation, which depend both on the packet length and the considered MCS. Notice that these coefficients capture the effect of the frequency correlation due to multipath as well as the effect of the Bit Interleaved Coded Modulation (BICM) when the hypothesis of ideal FF channel is not fulfilled. When SC-FDMA is considered, (4.2) is still valid for ZF equalizer followed by a soft decoding with different fitting coefficients [40].

To check the accuracy of the upper bound (4.2), we consider two channel models.

1. The FF channel described in Chapter 1 corresponding to the ideal case of in which the interleaving allows each modulated symbols to act over independent frequency bins realizations

2. The Block Fading (BF) channel in which the frequency-selective channel is constant within the duration of one OFDMA symbol and varies from symbol-to-symbol. It is

simulated with $M = 10$ and $\zeta^2_{\ell,p} = \frac{\Delta_\ell}{M}, \forall p, \ell$ (i.e., uniform power delay profile), using 256 subcarriers with 20 randomly chosen subcarriers allocated to the link of interest and considering codeword of length 128 modulated symbols. As a consequence, the codeword is spanned over 7 OFDMA symbols.

In Figs. 4.1 and 4.2, we plot the error probability along with the approximation whose coefficients are reported in Table 4.1 using the same setup as in Section 4.11, versus the SNR defined in Section 1.6.2. We see that the approximation is tight for both models for medium-to-high SNR. As expected, the two schemes achieve almost the same diversity orders thanks to the BICM[1], whereas the frequency correlation of the BF model induces a performance degradation of about 1 dB. Although the results exhibited in the rest of this Chapter are obtained considering the case of ideal FF channel, it is worth emphasizing that our derivations are valid as long as fitting coefficients $g_{\ell,m}$ and $d_{\ell,m}$ are available.

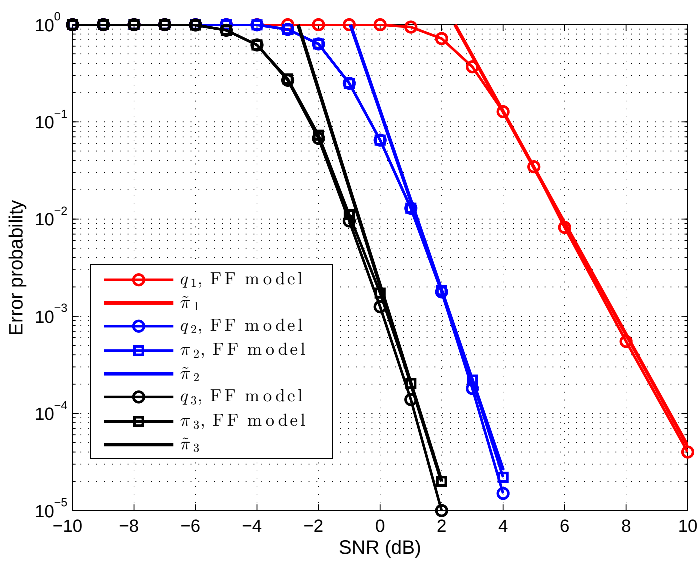

Figure 4.1: Tightness of the error probability approximation, FF model.

Table 4.1: Fitting coefficients.

	$g_{\ell,m}$, FF model	$g_{\ell,m}$, BF model	$d_{\ell,m}$, FF model	$d_{\ell,m}$, BF model
$m = 1$	25.04	29.33	5.73	5.16
$m = 2$	0.13	0.91	9.23	8.16
$m = 3$	0.0021	0.012	10.07	8.79

Thanks to (4.1) and (4.2), we can now derive the approximated expressions of the metrics of interest, replacing $q_{\ell,m}$ with its upper bound $\tilde{\pi}_{\ell,m}$, in (1.12) for the goodput,

[1]notice that the frequency correlation induces a slight diversity degradation of the BF model as compared with the ideal FF one

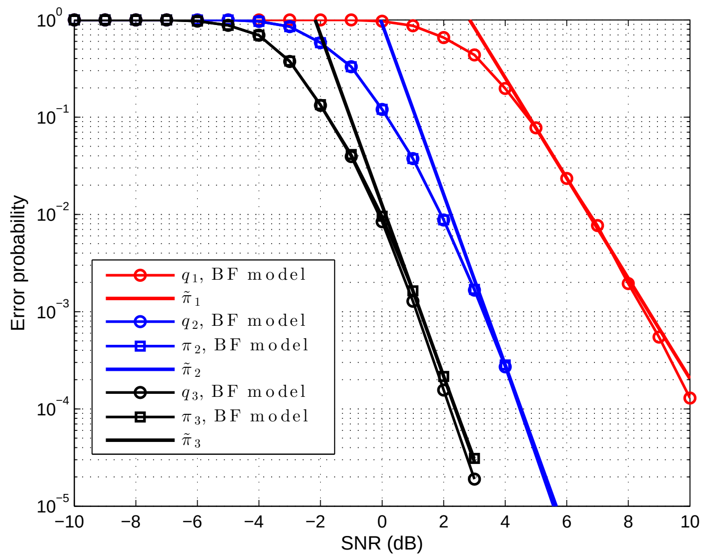

Figure 4.2: Tightness of the error probability approximation, BF model.

in (1.16) for the EE, and in (1.17) for the GEE, leading to the following approximate expressions, $\forall \ell$:

$$\tilde{\eta}_\ell(G_\ell E_\ell) := B\gamma_\ell \alpha_\ell \frac{1-\tilde{\pi}_{\ell,\mathcal{M}}(G_\ell E_\ell)}{1+\sum_{m=1}^{\mathcal{M}-1}\tilde{\pi}_{\ell,m}(G_\ell E_\ell)}, \tag{4.3}$$

$$\tilde{\mathcal{E}}_\ell(E_\ell,\gamma_\ell) := \frac{\alpha_\ell\gamma_\ell(1-\tilde{\pi}_{\ell,\mathcal{M}}(G_\ell E_\ell))}{(1+\sum_{m=1}^{\mathcal{M}-1}\tilde{\pi}_{\ell,m}(G_\ell E_\ell))(\gamma_\ell E_\ell \kappa_\ell^{-1}+E_{c,\ell})}, \tag{4.4}$$

$$\tilde{\mathcal{G}}(\mathbf{E},\gamma) := \frac{\sum_{\ell=1}^{L}\alpha_\ell\gamma_\ell\frac{1-\tilde{\pi}_{\ell,\mathcal{M}}(G_\ell E_\ell)}{1+\sum_{m=1}^{\mathcal{M}-1}\tilde{\pi}_{\ell,m}(G_\ell E_\ell)}}{\sum_{\ell=1}^{L}(\gamma_\ell E_\ell\kappa_\ell^{-1}+E_{c,\ell})}. \tag{4.5}$$

The goodput constraint (1.25) is thus approximated by:

$$\gamma_\ell\alpha_\ell\frac{1-\tilde{\pi}_{\ell,\mathcal{M}}(G_\ell E_\ell)}{1+\sum_{m=1}^{\mathcal{M}-1}\tilde{\pi}_{\ell,m}(G_\ell E_\ell)} \geq \eta_\ell^{(0)} \tag{4.6}$$

Notice that due to the upper bound of the approximation (4.1)-(4.2), if (4.6) holds then (1.25) also holds, implying that the QoS is necessarily satisfied.

In the rest of the Chapter, all our derivations are performed based on the approximations (4.3)-(4.5).

4.3 Problems Formulation

In this Section, we mathematically formulate the optimization problems we wish to solve, which are approximations of the general Problems 1.1 in Chapter 1, where the goodput, the EE and the GEE are replaced by the approximations (4.3), (4.4) and (4.5), respectively.

4.3.1 MSEE Problem

A simple way to combine the links' EE is to sum them, leading to the following MSEE problem.

Problem 4.1. *The MSEE problem for Type-II HARQ under the Rayleigh channel writes as:*

$$\begin{aligned} \max_{\mathbf{E},\gamma} \quad & \sum_{\ell=1}^{L} \frac{\tilde{D}_\ell(G_\ell E_\ell)}{\tilde{S}_\ell(G_\ell E_\ell)(\kappa_\ell^{-1} E_\ell + E_{c,\ell}\gamma_\ell^{-1})}, \\ \text{s.t.} \quad & (4.6), (1.27) \text{ and } (1.28), \end{aligned} \tag{4.7}$$

with, $\forall \ell$,

$$\tilde{D}_\ell(G_\ell E_\ell) := \alpha_\ell(1 - \tilde{\pi}_{\ell,\mathcal{M}}(G_\ell E_\ell)), \tag{4.8}$$

$$\tilde{S}_\ell(G_\ell E_\ell) := 1 + \sum_{m=1}^{\mathcal{M}-1} \tilde{\pi}_{\ell,m}(G_\ell E_\ell). \tag{4.9}$$

It is known that maximizing the sum of the individual EE of the different links may lead to unfair RA [120]. Therefore, we also investigate metrics allowing to achieve a better degree of fairness in the RA.

4.3.2 MPEE Problem

Achieving a better fairness is possible by maximizing the product of the links' EE, leading to the following MPEE problem.

Problem 4.2. *The MPEE problem for Type-II HARQ under the Rayleigh channel writes as:*

$$\begin{aligned} \max_{\mathbf{E},\gamma} \quad & \prod_{\ell=1}^{L} \frac{\tilde{D}_\ell(G_\ell E_\ell)}{\tilde{S}_\ell(G_\ell E_\ell)(\kappa_\ell^{-1} E_\ell + E_{c,\ell}\gamma_\ell^{-1})}, \\ \text{s.t.} \quad & (4.6), (1.27) \text{ and } (1.28), \end{aligned} \tag{4.10}$$

Since the function $f : x \to \log(x)$ is strictly increasing on $\mathbb{R}^{+*}$, problem 4.2 can be rewritten equivalently as follows, which is also known as the **proportional fairness** problem.

Problem 4.3. *The MPEE Problem 4.2 is equivalent to the following problem:*

$$\begin{aligned} \max_{\mathbf{E},\gamma} \quad & \sum_{\ell=1}^{L} \log\left(\frac{\tilde{D}_\ell(G_\ell E_\ell)}{\tilde{S}_\ell(G_\ell E_\ell)(\kappa_\ell^{-1} E_\ell + E_{c,\ell}\gamma_\ell^{-1})}\right), \\ \text{s.t.} \quad & (4.6), (1.27) \text{ and } (1.28), \end{aligned} \tag{4.11}$$

4.3.3 MMEE Problem

We also consider the highest degree of fairness which can be achieved by maximizing the worst link's EE. This problem is also known as the **max-min fairness** problem, and leads to the following MMEE problem.

Problem 4.4. *the MMEE problem for Type-II HARQ under the Rayleigh channel writes as:*

$$\begin{aligned} \max_{\mathbf{E},\gamma} \quad & \left(\min_{\ell\in\{1,\dots,L\}} \frac{\tilde{D}_\ell(G_\ell E_\ell)}{\tilde{S}_\ell(G_\ell E_\ell)(\kappa_\ell^{-1} E_\ell + E_{c,\ell}\gamma_\ell^{-1})} \right), \\ \text{s.t.} \quad & (4.6), (1.27) \text{ and } (1.28), \end{aligned} \tag{4.12}$$

4.3.4 MGEE Problem

Finally, we also consider the problem of maximizing the EE of the network, leading to the following MGEE problem.

Problem 4.5. *the MGEE problem for Type-II HARQ under the Rayleigh channel writes as:*

$$\begin{aligned} \max_{\mathbf{E},\gamma} \quad & \frac{\sum_{\ell=1}^{L} \gamma_\ell \frac{\tilde{D}_\ell(G_\ell E_\ell)}{S_\ell(\tilde{G}_\ell E_\ell)}}{\sum_{\ell=1}^{L} (\kappa_\ell^{-1}\gamma_\ell E_\ell + E_{c,\ell})}, \\ \text{s.t.} \quad & (4.6), (1.27) \text{ and } (1.28), \end{aligned} \tag{4.13}$$

4.3.5 Problems Feasibility

Since the feasible set in Problems 4.1 to 4.5 is identical to the one in [65], the same feasibility condition holds. This condition is not detailed in this thesis, and we only assume that the considered problems are feasible by carefully choosing $P_{\max,\ell}$ and $\eta_\ell^{(0)}$ $\forall \ell$.

4.4 Solution Methodology

As they are formulated, Problems 4.1 to 4.5 are not concave and thus, without additional efforts, they are not computationally tractable, meaning that they cannot be solved analytically or numerically with affordable complexity, i.e., in polynomial time. One of the main contribution of this Chapter is to transform these problems into equivalent simpler ones, for which standard convex optimization tools are applicable, e.g. the IPM. This Section is dedicated to the methodology used to achieve this purpose.

4.4.1 General idea

Problems 4.1 to 4.5 can be written in the general form

$$\max_{\mathbf{E},\gamma} \quad \mathcal{J}_G(\mathbf{E},\gamma), \tag{4.14}$$

$$\text{s.t.} \quad (4.6), (1.27), (1.28), \tag{4.15}$$

where $\mathcal{J}_G$ is a generic function representing the objective function of one of the considered problem.

We remark that the feasible set for Problems 4.1 to 4.5 defined by the constraints (4.6), (1.27) and (1.28) is not convex due to the non-convexity of constraint (1.27), thus preventing us from using convex optimization tools. To overcome this issue, in a first step, we rewrite these constraints in posynomial form since posynomial constraints can be transformed into convex ones through a change of variables. The posynomial form is, $\forall \ell$,

$$\eta_\ell^{(0)} \gamma_\ell^{-1} \left(1 + \sum_{m=1}^{\mathcal{M}-1} a_{\ell,m} E_\ell^{-d_{\ell,m}}\right) + \alpha_\ell a_{\ell,\mathcal{M}} E_\ell^{-d_{\ell,\mathcal{M}}} \leq \alpha_\ell, \tag{4.16}$$

$$E_\ell \gamma_\ell \leq P_{\max,\ell}, \tag{4.17}$$

$$\sum_{\ell=1}^{L} \gamma_\ell \leq 1, \tag{4.18}$$

with $a_{\ell,m} := g_{\ell,m}/G_\ell^{d_{\ell,m}} > 0$. After the change of variables (detailed in the next Section), the problem defined by (4.14)-(4.15) writes as

$$\max_{\mathbf{x},\mathbf{y}} \quad \mathcal{J}_G(\mathbf{x}, \mathbf{y}), \tag{4.19}$$

$$\text{s.t.} \quad (4.6)', (1.27)', (1.28)', \tag{4.20}$$

where $(\mathbf{x}, \mathbf{y}) := \mathcal{U}_F(\mathbf{E}, \gamma)$ with $\mathcal{U}_F$ a one-to-one mapping, and (4.6)', (1.27)' and (1.28)' are constraints (4.6), (1.27) and (1.28) after the change of variables.

In a second step, for the MSEE, MPEE and MMEE problems after the change of variables, we identify properties of the new objective functions (4.19) allowing us to optimally solve them using convex optimization procedures. Concerning the MGEE problem, we do not find such properties, leading us to work directly on Problem 4.5 before the change of variables, since its structure enables us to apply two suboptimal procedures.

4.4.2 Change of variables yielding a convex feasible set

The change of variable we apply to our problems is the one of the geometric programming [15], which writes $\mathcal{U}_F(\mathbf{E}, \gamma) = [\mathcal{U}(E_1), \ldots, \mathcal{U}(E_L), \mathcal{U}(\gamma_1), \ldots, \mathcal{U}(\gamma_L)]$ with $\mathcal{U}(u) := \log(u)$. Hence, we have, $\forall \ell$

$$x_\ell = \log(E_\ell), \tag{4.21}$$

$$y_\ell = \log(\gamma_\ell). \tag{4.22}$$

After this change of variables, constraints (4.6), (1.27) and (1.28) can be rewritten equivalently $\forall \ell$ as

$$\eta_\ell^{(0)} e^{-y_\ell} \left(1 + \sum_{m=1}^{\mathcal{M}-1} a_{\ell,m} e^{-d_{\ell,m} x_\ell}\right) + \alpha_\ell a_{\ell,\mathcal{M}} e^{-d_{\ell,\mathcal{M}} x_\ell} \leq \alpha_\ell, \tag{4.23}$$

$$e^{x_\ell + y_\ell} \leq P_{\max,\ell}, \tag{4.24}$$

$$\sum_{\ell=1}^{L} e^{y_\ell} \leq 1. \tag{4.25}$$

We can now formulate the following result concerning the feasible set of the optimization problems after the change of variables.

Result 4.1. *The set*

$$\mathcal{F}_P = \{(\mathbf{x}, \mathbf{y}) \in \mathbb{R}_+^L \times \mathbb{R}_+^L \,|\, \text{Eqs. (4.23)-(4.25) are satisfied.}\} \tag{4.26}$$

is convex.

Proof. We use the following two properties: *i*) the composition of a convex function with an affine function is convex, and *ii*) a non-negative sum of convex functions is convex [15]. We see that constraints (4.23)-(4.25) are sums of functions, which are convex since they can be expressed as the composition of the exponential function, which is convex, and affine functions. Contraints (4.23)-(4.25) are then sums of convex functions and as a result $\mathcal{F}_p$ is convex. □

We have thus converted the non convex constraints (4.6), (1.27) and (1.28) into convex ones (4.23)-(4.25) thanks to the change of variables (4.21)-(4.22). We now address the solution of Problems 4.1 to 4.5, beginning with the MSEE one.

4.5 MSEE Solution

In this Section, we provide the optimal solution of the MSEE Problem 4.1 along with two suboptimal less complex solutions.

4.5.1 Optimal solution

We obtain the optimal solution of Problem 4.1 by applying the change of variables (4.21)-(4.22), enabling us to rewrite it equivalently as:

Problem 4.6.

$$\begin{aligned} \max_{\mathbf{E},\gamma} \quad & \sum_{\ell=1}^{L} \frac{f_\ell(x_\ell)}{g_\ell(x_\ell, y_\ell)}, \\ \text{s.t.} \quad & (4.23), (4.24) \text{ and } (4.25), \end{aligned} \tag{4.27}$$

with, $\forall \ell$, $f_\ell(x_\ell) := \alpha_\ell(1-a_{\ell,\mathcal{M}} e^{-x_\ell d_{\ell,\mathcal{M}}})$ and $g_\ell(x_\ell, y_\ell) := (1+\sum_{m=1}^{\mathcal{M}-1} a_{\ell,m} e^{-x_\ell d_{\ell,m}})(\kappa_\ell^{-1} e^{x_\ell} + E_{c,\ell} e^{-y_\ell})$. Problem 4.6 is characterized in Result 4.2.

Result 4.2. *Problem 4.6 is the maximization of a sum of ratios whose numerators are concave and denominators are positive and convex, over a convex set.*

Proof. The convexity of the feasible set is given by Result 4.1. Also, the concavity of f_ℓ $\forall\ell$ can be established by computing its second order derivative whereas the positivity of g_ℓ $\forall\ell$ is straightforward and their convexity can be proved using same steps as for the proof of Result 4.1. □

Thanks to Result 4.2, we know that Problem 4.6 can be optimally solved according to the Jong's algorithm [61], by alternating between the following two steps until convergence is reached.

1. At iteration i, find the optimal solution of the problem defined by:

$$\max_{\mathbf{x},\mathbf{y}} \quad \sum_{\ell=1}^{L} u_\ell^{(i)}\left(f_\ell(x_\ell) - \beta_\ell^{(i)} g_\ell(x_\ell, y_\ell)\right), \tag{4.28a}$$

$$\text{s.t.} \quad (4.23), (4.24) \text{ and } (4.25). \tag{4.28b}$$

   where $\forall\ell$, $u_\ell^{(i)} > 0$ and $\beta_\ell^{(i)} \geq 0$ depend on the optimal solution at iteration $(i-1)$. The problem defined by (4.28a)-(4.28b) is the maximization of a concave function over a convex set (i.e., Result 4.2) and can thus be optimally solved using the IPM.

2. Compute $\forall\ell$, $u_\ell^{(i+1)}$ and $\beta_\ell^{(i+1)}$ using the modified Newton method given by (3.31) and (3.32) in Chapter 3, where $\boldsymbol{\psi}$ is given by, $\forall\ell$

$$\psi_\ell(\beta_\ell^{(i)}, u_\ell^{(i)}, x_\ell, y_\ell) := -f_\ell(x_\ell) + \beta_\ell^{(i)} g_\ell(x_\ell, y_\ell), \tag{4.29}$$

$$\psi_{\ell+L}(\beta_\ell^{(i)}, u_\ell^{(i)}, x_\ell, y_\ell) := -1 + u_\ell^{(i)} g_\ell(x_\ell, y_\ell). \tag{4.30}$$

Finally, the optimal solution of problem 4.1 is depicted in Algorithm 4.1.

Algorithm 4.1: Jong's algorithm to optimally solve the MSEE Problem 4.1.

Set $\epsilon > 0$, $i = 0$, initialize $\mathbf{u}^{(0)}$ and $\boldsymbol{\beta}^{(0)}$ using any feasible solution, for instance the MPO from [65].
Set $C_D = \epsilon + 1$.
while $C_D > \epsilon$ **do**
  Find $\mathbf{x}^*$ and $\mathbf{y}^*$, the optimal solution of the problem defined by (4.28a)-(4.28b) with $\mathbf{u}^{(i)}$ and $\boldsymbol{\beta}^{(i)}$, using the IPM.
  Set $C_D := \|\psi(\boldsymbol{\beta}^{(i)}, \mathbf{u}^{(i)}, \mathbf{x}^*, \mathbf{y}^*)\|$.
  For $\ell = 1, \ldots, L$, compute $u_\ell^{(i+1)}$ and $\beta_\ell^{(i+1)}$ using (3.31) and (3.32), respectively.
  Set $i = i + 1$.
end

4.5.2 Suboptimal solutions

Our complexity analysis (i.e., Table 4.2 in Section 4.10) reveals that finding the optimal solution of the MSEE problem is computationally demanding. For this reason, in the following, we develop two suboptimal less complex solutions: one based on AO and the other one on an approximation of the objective function, called Objective Function Approximation (OFA). In both approaches, we start from Problem 4.1 before the change of variables (4.21)-(4.22).

4.5.2.1 Alternating optimization

In our AO based approach, the optimization is performed alternately between the optimization variables $\mathbf{E}$ and γ until convergence is reached. Let us first explain the optimization w.r.t $\mathbf{E}$.

Optimization w.r.t E In a first time, γ is fixed and the optimization is performed w.r.t $\mathbf{E}$. For fixed γ, we see that Problem 4.1 is separable since there is no coupling constraints between the elements of $\mathbf{E}$, meaning that the optimization can be performed separately among the links. We thus have to solve L parallels sub problems, which write as:

Problem 4.7.

$$\max_{E_\ell} \quad \frac{\tilde{D}_\ell(G_\ell E_\ell)}{\tilde{S}_\ell(G_\ell E_\ell)(\kappa_\ell^{-1}E_\ell + F_{\ell,E})}, \tag{4.31}$$

$$\text{s.t.} \quad h_{\ell,E}(G_\ell E_\ell) \leq 0, \tag{4.32}$$

$$E_\ell - E_{\max,\ell} \leq 0, \tag{4.33}$$

with,$\forall \ell$, $h_{\ell,E}(G_\ell E_\ell) = \eta_\ell^{(0)}\gamma_\ell^{-1}\tilde{S}_\ell(G_\ell E_\ell) - \tilde{D}_\ell(G_\ell E_\ell)$, $E_{\max,\ell} = P_{\max,\ell}/\gamma_\ell$ and $F_{\ell,E} := \gamma_\ell^{-1}E_{c,\ell}$. We give a characterization of the resulting sub problems 4.7 in Result 4.3.

Result 4.3. *Problem 4.7 is the maximization of a PC function over a convex set.*

Proof. First, we prove that the feasible set defined by (4.32)-(4.33) is convex. Constraint (4.33) is linear and thus it is convex. To prove the convexity of constraint (4.32), let us prove that $\forall \ell$, $h''_{\ell,E}(G_\ell E_\ell)$, the second order derivative of $h_{\ell,E}(G_\ell E_\ell)$ w.r.t. E_ℓ, is positive:

$$h''_{\ell,E}(G_\ell E_\ell) = \eta_\ell^{(0)}\gamma_\ell^{-1}\sum_{m=1}^{\mathcal{M}-1}\frac{g_{\ell,m}d_{\ell,m}(d_{\ell,m}+1)}{G_\ell^{d_{\ell,m}}E^{d_{\ell,m}+2}} + \frac{g_{\ell,\mathcal{M}}d_{\ell,\mathcal{M}}(d_{\ell,\mathcal{M}}+1)}{G_\ell^{d_{\ell,\mathcal{M}}}E_\ell^{d_{\ell,\mathcal{M}}+2}} > 0, \quad \forall \ell. \tag{4.34}$$

Second, let us prove that the objective function (4.31) is PC. To do so, we prove that its numerator is concave and its denominator is convex and positive. We compute $\tilde{D}''_\ell(G_\ell E_\ell)$, the second order derivative of $\tilde{D}_\ell(G_\ell E_\ell)$ w.r.t. E_ℓ, as:

$$\tilde{D}''_\ell(G_\ell E_\ell) = \frac{g_{\ell,\mathcal{M}}d_{\ell,\mathcal{M}}(d_{\ell,\mathcal{M}}+1)}{G_\ell^{d_{\ell,\mathcal{M}}}E_\ell^{d_{\ell,\mathcal{M}}+2}} > 0, \quad \forall \ell, \tag{4.35}$$

proving that $\tilde{D}_\ell(G_\ell E_\ell)$ is convex. Now, let us compute the second order derivative of $\tilde{S}_\ell(G_\ell E_\ell)(\kappa_\ell^{-1}E_\ell + F_\ell)$ w.r.t. E_ℓ:

$$(\tilde{S}_\ell(G_\ell E_\ell)(\kappa_\ell^{-1}E_\ell + F_\ell))'' = \kappa_\ell^{-1}\sum_{m=1}^{\mathcal{M}-1}\frac{g_{\ell,m}}{G_\ell^{d_{\ell,m}}}(d_{\ell,m}(d_{\ell,m}+1)-2) + F_{\ell,E}\sum_{m=1}^{\mathcal{M}-1}\frac{g_{\ell,m}}{G_\ell^{d_{\ell,m}}}(d_{\ell,m}(d_{\ell,m}+1)). \tag{4.36}$$

We see from (4.36) that a sufficient condition for the second order derivative of the denominator of (4.31) to be is non-negative is, $\forall\ell$, $\forall p$, $d_{\ell,m} \geq 1$, which is the case for practical MCS. As a consequence, from (4.35) and (4.36), (4.31) is the ratio between a concave and a non-negative convex function and thus, from [120, Proposition 2.9], we can infer that it is PC, which concludes the proof. □

Hence, from [120] and Result 4.3, we know that the KKT conditions are necessary and sufficient to find the optimal solution of Problem 4.7, which is given in Theorem 4.1 whose proof is straightforward and as a consequence omitted.

Theorem 4.1. *Let $E_{\min,\ell}$ denote the unique zero of $h_{\ell,E}(G_\ell E_\ell)$ on $(g_{\ell,\mathcal{M}}^{1/d_{\ell,\mathcal{M}}}/G_\ell, E_{\max,\ell}]$, and $\mathcal{Q}_\ell$ as*

$$\mathcal{Q}_\ell(G_\ell E_\ell) = \frac{\tilde{D}_\ell(G_\ell E_\ell)}{\tilde{S}_\ell(G_\ell E_\ell)(A_\ell E_\ell + F_{\ell,E})}, \quad \forall\ell. \tag{4.37}$$

The optimal solution E_ℓ^* of problem 4.7 takes the following form:

1) If $\mathcal{Q}_\ell'(G_\ell E_{\min,\ell}) < 0$, then $E_\ell^* = E_{\min,\ell}$.

2) If $\mathcal{Q}_\ell'(G_\ell E_{\max,\ell}) > 0$, then $E_\ell^* = E_{\max,\ell}$.

3) Else, E_ℓ^* is the solution of $\mathcal{Q}_\ell'(G_\ell E_\ell^*) = 0$ in $[E_{\min,\ell}, E_{\max,\ell}]$, which is unique. This case can be easily solved using the bisection method.

Theorem 4.1 gives us an efficient method to find the optimal solution of the L sub problems. In addition, we emphasize that these L sub problems can be solved in a distributed fashion since there is no coupling constraints between the optimization variables.

Optimization w.r.t γ In the second step, $\mathbf{E}$ is fixed and the optimization is performed w.r.t γ. In this case, Problem 4.1 writes as:

Problem 4.8.

$$\max_{\gamma} \quad \sum_{\ell=1}^{L}\frac{\gamma_\ell H_\ell}{\gamma_\ell J_\ell + M_\ell} \tag{4.38}$$

$$\text{s.t.} \quad \gamma_\ell \geq \gamma_{min,\ell}, \quad \forall\ell, \tag{4.39}$$

$$\gamma_\ell \leq \gamma_{max\ell}, \quad \forall\ell, \tag{4.40}$$

$$\sum_{k=1}^{K}\gamma_\ell \leq 1, \tag{4.41}$$

with,$\forall \ell$, $\gamma_{\min,\ell} := \eta_\ell^{(0)} \tilde{S}_\ell(G_\ell E_\ell)/\tilde{D}_\ell(G_\ell E_\ell)$, $\gamma_{\max,\ell} := P_{\max,\ell}/E_\ell$, $H_\ell := \tilde{D}_\ell(G_\ell E_\ell)$, $J_\ell := \kappa_\ell^{-1} E_\ell \tilde{S}_\ell(E_\ell)$ and $M_\ell := E_{c,\ell}\tilde{S}_\ell(E_\ell)$. We give a characterization of Problem 4.8 in Result 4.4.

Result 4.4. *Problem 4.8 is the maximization of a concave function over a convex set.*

Proof. First, we remark that the constraints (4.39)-(4.41) of Problem 4.8 are all linear, and thus its feasible set is convex. Therefore, we turn our attention to the objective function (4.38). To prove its concavity, we define,$\forall \ell$,

$$f_{\ell,\gamma}(\gamma_\ell) = \frac{\gamma_\ell H_\ell}{\gamma_\ell J_\ell + M_\ell}.$$

We prove the concavity of $f_{\ell,\gamma}$ by computing its second order derivative, which is given by, $\forall \ell$,

$$f''_{\ell,\gamma}(\gamma_\ell) = -\frac{2H_\ell M_\ell J_\ell}{(J_\ell \gamma_\ell + M_\ell)^3} < 0.$$

Since the sum of concave functions is a concave function, it results that the objective function (4.38) of problem 4.8 is concave, concluding the proof. □

From Result 4.4, we know that the optimal solution of Problem 4.8 can be found by solving the KKT conditions. This optimal solution is given in theorem 4.2, whose proof is provided in appendix B.1.

Theorem 4.2. *If $\sum_{\ell=1}^{L} \gamma_{\max,\ell} \leq 1$, then the optimal solution of Problem 4.8 is given by $\forall \ell, \gamma_\ell^* = \gamma_{\max,\ell}$.*

Otherwise, let us define $\gamma_\ell^*(\lambda)$ as, $\forall \ell$

$$\gamma_\ell^*(\lambda) = \left[-\frac{M_\ell}{J_\ell} + \frac{\sqrt{H_\ell M_\ell \lambda}}{\lambda J_\ell} \right]_{\gamma_{\min,\ell}}^{\gamma_{\max,\ell}}, \tag{4.42}$$

with $[x]_a^b := \min\{b, \max\{x, a\}\}$. The optimal solution of Problem 4.8 is given by $\forall \ell$, $\gamma_\ell^* = \gamma_\ell^*(\lambda^*)$, where λ^* is the solution of $\sum_{\ell=1}^{L} \gamma_\ell^*(\lambda^*) = 1$, which is unique on $\mathbb{R}^{++}$. Moreover, λ^* lies in $[\lambda^{*-}, \lambda^{*+}]$ with $\lambda^{*-} := \min_{\ell \in \{1,\dots,L\}} (H_\ell M_\ell/(J_\ell \gamma_{\max,\ell} + M_\ell)^2)$ and $\lambda^{*+} := \max_{\ell \in \{1,\dots,L\}} (H_\ell M_\ell/(J_\ell \gamma_{\min,\ell} + M_\ell)^2)$.

Algorithm. Finally, the AO based procedure to suboptimally solve Problem 4.1 is summarized in Algorithm 4.2.

4.5.2.2 Objective function approximation

Here, we solve Problem 4.1 using our OFA approach. The difficulty to solve Problem 4.1 comes from the sum of ratios in its objective function. To alleviate this problem, we remark that the EE is defined as the inverse of the Energy per Bit (EB), defined as the energy consumed per information bit received without error. Then, we propose as a first approximation to minimize the sum of the EB instead of maximizing the SEE. The resulting optimization problem writes as:

Algorithm 4.2: AO based suboptimal solution of Problem 4.1.

Set $\epsilon > 0$, $C_A = \epsilon + 1$, $i = 0$.
Find initial feasible $\mathbf{E}^{(0)}$ and $\gamma^{(0)}$.
while $C_A > \epsilon$ **do**
 Find $\mathbf{E}^{(i+1)} := [E_1^{(i+1)}, \ldots, E_L^{(i+1)}]$ the optimal solutions of the L Problems 4.7 with $\gamma^{(i)}$ using Theorem 4.1.
 Find $\gamma^{(i+1)} := [\gamma_1^{(i+1)}, \ldots, \gamma_L^{(i+1)}]$ the optimal solution of Problem 4.8 with $\mathbf{E}^{(i+1)}$ using Theorem 4.2.
 Set $C_A = \|[\mathbf{E}^{(i)}, \gamma^{(i)}] - [\mathbf{E}^{(i+1)}, \gamma^{(i+1)}]\|$.
 Set $i = i + 1$.
end

Problem 4.9.

$$\begin{aligned} \min_{\mathbf{E},\gamma} \quad & \sum_{\ell=1}^{L} \frac{\tilde{S}_\ell(G_\ell E_\ell)(\kappa_\ell^{-1} E_\ell + E_{c,\ell}\gamma_\ell^{-1})}{\tilde{D}_\ell(E_\ell)}, \\ \text{s.t.} \quad & (4.6), (1.27) \text{ and } (1.28) \end{aligned} \tag{4.43}$$

It is worth noticing that problem 4.9 is not equivalent to Problem 4.1. Actually, one can check that minimizing the sum of the EB is equivalent to maximizing the harmonic mean of the EE. However, we expect that minimizing the sum of the EB to yield an energy efficient RA policy. Problem 4.9 is still the maximization of the sum of ratios, that is, this problem is still complex to solve. To alleviate this difficulty, we make another approximation: we consider the high SNR regime, in which we consider that $q_{\ell,\mathcal{M}} = 0$. With this approximation, Problem 4.9 can be rewritten as

Problem 4.10.

$$\begin{aligned} \min_{\mathbf{E},\gamma} \quad & \sum_{\ell=1}^{L} \frac{\tilde{S}_\ell(E_\ell)}{\alpha_\ell}(\kappa_\ell^{-1} E_\ell + E_{c,\ell}\gamma_\ell^{-1}), \\ \text{s.t.} \quad & (4.6), (1.27) \text{ and } (1.28) \end{aligned} \tag{4.44}$$

Problem 4.10 is a GP, and hence it can be efficiently solved using the IPM, as implemented for instance in [82].

4.5.3 Numerical comparison of optimal and suboptimal MSEE solutions

In this Section, we numerically compare the SEE obtained using the optimal MSEE solution (Algorithm 4.1), with the AO based procedure (Algorithm 4.2) and the OFA approach.

To do so, we consider the same setup as in Section 4.11 and, in Fig. 4.3, we plot the SEE obtained using the three considered solutions versus the maximum transmit power constraint. We can see that the optimal MSEE solution yields, as expected, the highest SEE, but we also see that the AO based solution is very close to the optimal one, especially for $P_{\max,\ell} \geq 22$ dBm, where the curves are superimposed. We can finally remark that the OFA approach yields lower SEE, but the degradation as compared with the optimal solution does not exceed 10%. On the other hand, it will be shown in Section 4.10 that these two suboptimal solutions are much less complex than the optimal one, and thus they are of interest for practical implementations.

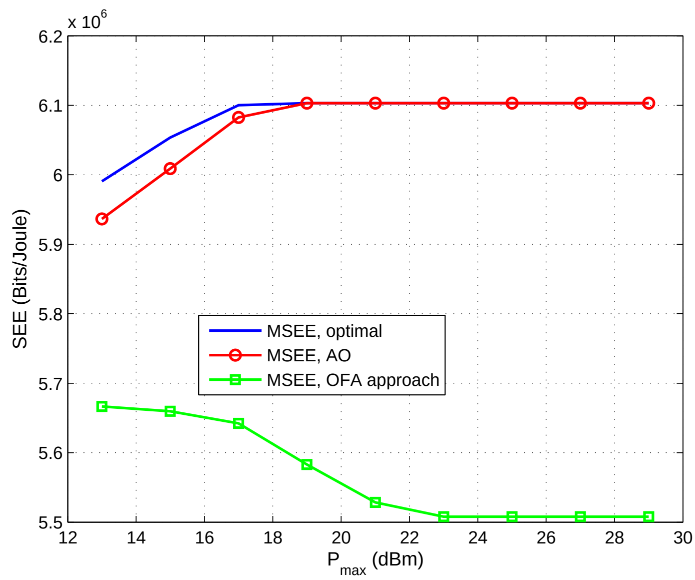

Figure 4.3: SEE of the optimal and suboptimal MSEE solutions versus $P_{\max,\ell}$.

4.6 MPEE Solution

We obtain the optimal solution of Problem 4.3 by applying the change of variables (4.21)-(4.22), enabling us to rewrite it equivalently as:

Problem 4.11.

$$\max_{\mathbf{x},\mathbf{y}} \quad \sum_{\ell=1}^{L} \left(\log\left(f_\ell(x_\ell)\right) - \log\left(g_\ell(x_\ell, y_\ell)\right)\right), \tag{4.45}$$

$$\text{s.t.} \quad (4.23), (4.24) \text{ and } (4.25). \tag{4.46}$$

In Result 4.5, we exhibit a property of Problem 4.11 allowing us to find its optimal solution.

Result 4.5. *Problem 4.11 is the maximization of a concave function over a convex set.*

Proof. The convexity of the feasible set is ensured by Result 4.1. The objective function (4.45) can be written as $\sum_{\ell=1}^{L} \mathcal{W}_\ell(x_\ell, y_\ell)$, with $\mathcal{W}_\ell(x_\ell, y_\ell) := \log(f_\ell(x_\ell)) - \log(g_\ell(x_\ell, y_\ell))$.

Let us prove that $\mathcal{W}_\ell(x_\ell, y_\ell)$ is concave. To do so, first, we remind that the logarithm of a concave function is concave [15]. As a consequence, since $f_\ell(x_\ell)$ is concave (see i.e Result 4.2), $\log(f_\ell(x_\ell))$ is concave. Second, using the convexity of the LSE function, one can prove that $\log(g_\ell(x_\ell, y_\ell))$ is convex and hence $-\log(g_\ell(x_\ell, y_\ell))$ is concave. As a consequence, $\mathcal{W}_\ell$ is concave and finally, $\sum_{\ell=1}^{L} \mathcal{W}_\ell(x_\ell, y_\ell)$ is concave, concluding the proof. □

The MPEE problem can then be optimally solved directly using the IPM, requiring no additional computation.

4.7 MMEE Solution

We obtain the optimal solution of Problem 4.4 by applying the change of variables (4.21)-(4.22), enabling us to rewrite it equivalently as:

Problem 4.12.

$$\max_{\mathbf{x},\mathbf{y}} \quad \min_{\ell \in \{1,\dots,L\}} \left\{ \frac{f_\ell(x_\ell)}{g_\ell(x_\ell, y_\ell)} \right\}, \tag{4.47}$$

$$\text{s.t.} \quad (4.23), (4.24) \text{ and } (4.25). \tag{4.48}$$

Due to Results 4.1 and 4.2, one can check that this Problem 4.12 is the maximization of the minimum of a set of ratios with concave numerators and convex denominators, over a convex set. Hence, this problem falls within the generalized fractional programming framework, and could be solved with the Generalized Dinkelbach's algorithm. However, by taking a closer look at our objective function (4.47), we are able to find a more simple procedure (not iterative) to solve this problem. To do so, we observe that each f_ℓ and g_ℓ in (4.47) are combinations of exponentials. Hence, our idea is to introduce a monomial auxiliary optimization variable and to perform the change of variable of geometric programming in this new variable to obtain a COP.

More precisely, using the epigraph formulation of Problem 4.12, we introduce the optimization variable ϕ, and the following constraint $\phi \leq \min_{\ell \in \{1,\dots,L\}} \frac{f_\ell(x_\ell)}{g_\ell(x_\ell, y_\ell)}$. Noticing that $\phi \leq \min_{\ell \in \{1,\dots,L\}} \frac{f_\ell(x_\ell)}{g_\ell(x_\ell, y_\ell)} \Leftrightarrow \phi \leq \frac{f_\ell(x_\ell)}{g_\ell(x_\ell, y_\ell)}, \forall \ell$, we can rewrite Problem 4.12 equivalently as

$$\max_{\mathbf{x},\mathbf{y},\phi} \quad \phi, \tag{4.49a}$$

$$\text{s.t.} \quad \phi g_\ell(x_\ell, y_\ell) - f_\ell(x_\ell) \leq 0, \quad \forall \ell, \tag{4.49b}$$

$$(4.23), (4.24) \text{ and } (4.25). \tag{4.49c}$$

In this new problem, the objective function (4.49a) is linear and hence concave, but the L new constraints given by (4.49b) are not convex due to the product between ϕ and g_ℓ. To render them convex, we remark that g_ℓ is a sum of exponential in x_ℓ and y_ℓ. Clearly, performing the change of variable of the geometric programming on ϕ, i.e., $z := \log(\phi)$, enables to obtain convex constraints since we exhibit a linear combination of exp–sum. After this change of variable, the problem defined by (4.49a)-(4.49c) can be rewritten as

$$\max_{\mathbf{x},\mathbf{y},z} \quad e^z, \tag{4.50a}$$

$$\text{s.t.} \quad e^z g_\ell(x_\ell, y_\ell) - f_\ell(x_\ell) \leq 0, \quad \forall \ell, \tag{4.50b}$$

$$(4.23), (4.24) \text{ and } (4.25). \tag{4.50c}$$

All the constraints defined by (4.50b)-(4.50c) are now convex. However, the objective function (4.50a) is not concave anymore. So we cannot use convex optimization tools yet. To overcome this issue, one can remark that maximizing e^z is equivalent to minimizing $1/e^z = e^{-z}$, which is convex. The resulting equivalent optimization problem writes in the following convex form

$$\min_{\mathbf{x},\mathbf{y},z} \quad e^{-z}, \tag{4.51a}$$

$$(4.50b), (4.23), (4.24) \text{ and } (4.25). \tag{4.51b}$$

The problem defined by (4.51a)-(4.51b) is the minimization of a convex function over a convex set, and then it can be optimally solved using the IPM.

4.8 MGEE Solution

Last, we address the MGEE Problem 4.5. In general, in the literature, this problem is the easiest one to tackle when there is no multiuser interference since most of the existing works consider the capacity as the measure of the useful data rate, and hence the GEE reduces to a ratio between a concave and a convex function, which can be efficiently solved using the Dinkelbach's algorithm. In our case however, the GEE problem is the most complicated one due to the consideration of the HARQ mechanism. Indeed, unlike the previously discussed problems, the numerator of the GEE is not necessarily a concave function even after the change of variables (4.21)-(4.22). Hence, to the best of our knowledge, there exists no algorithm to optimally solve this problem in polynomial time. For this reason, we propose two suboptimal solutions, one based on SCA, and the other one based on AO. We highlight that, contrary to our work to optimally solve Problem 4.1 to 4.4, we address the solution of Problem 4.5 starting from the problem before the change of variables (4.21)-(4.22) since we are able to observe specific structure of this problem. Let us first explain the SCA based solution.

4.8.1 Successive convex approximation

Following the derivations for the MSEE, MPEE and MMEE, we first searched a solution using the change of variables defined by (4.21)-(4.22) in order to render the feasible set of the problem convex and then applying the SCA procedure by approximating the objective function. We actually did not succeed to find such an approximation which has to verify certain properties to ensure the convergence of the SCA algorithm. To overcome this issue, we choose to work on the original Problem 4.5 with variables $\mathbf{E}, \boldsymbol{\gamma}$, since it allows us to use an efficient approach from the literature.

Looking at our optimization problem, we see that all the constraints and the denominator of the objective function are posynomials (i.e., (4.16)-(4.18)), but the numerator is not posynomial. This problem is closed to the framework proposed in [24], where a SCA procedure, called single condensation method for GP, is proposed to solve the problem of the minimization of a ratio of posynomials with posynomial constraints. Hence, our idea is to transform our optimization problem in order to use the approach from [24]. The first step is to transform the numerator of the objective function (4.5) into a posynomial. To do so, we introduce L new optimization variables $[z_1, \ldots, z_\ell]$ along with L new constraints $z_\ell \leq \gamma_\ell \tilde{D}_\ell(G_\ell E_\ell)/\tilde{S}_\ell(G_\ell E_\ell)$, which will be shown to be posynomials. The second step is to transform the maximization problem into a minimization one, by taking the inverse of the resulting objective function. After these two steps, Problem 4.5 can be rewritten equivalently as follows, using (4.8) and (4.9):

$$\min_{\mathbf{E},\boldsymbol{\gamma},\mathbf{z}} \quad \frac{\sum_{\ell=1}^{L}(\gamma_\ell E_\ell \kappa_\ell^{-1} + E_{c,k})}{\sum_{\ell=1}^{L} z_\ell} \tag{4.52a}$$

$$\text{s.t.} \quad z_\ell \leq \gamma_\ell \tilde{D}_\ell(G_\ell E_\ell)/\tilde{S}_\ell(G_\ell E_\ell), \quad \forall \ell, \tag{4.52b}$$

$$(4.6), (1.27) \text{ and } (1.28), \tag{4.52c}$$

with $\mathbf{z} := [z_1, \ldots, z_\ell]$. We can see that the problem defined by (4.52a)-(4.52c) is the minimization of a ratio of posynomials with posynomial constraints since constraints (4.52b) can be rewritten equivalently as follows

$$z_\ell \gamma_\ell^{-1} \left(1 + \sum_{m=1}^{\mathcal{M}-1} a_{\ell,m} E^{-d_{\ell,m}}\right) + \alpha_\ell a_{\ell,\mathcal{M}} E^{-d_{\ell,\mathcal{M}}} \leq \alpha_\ell, \quad \forall \ell, \tag{4.53}$$

which is posynomial. The solution proposed in [24] is to replace the denominator in (4.52a), at each iteration, with its best monomial lower bound in the sense of its Taylor approximation about the solution found at the previous iteration. To do so, let us first define $\mathbf{E}^{*(i)} := [E_1^{*(i)}, \ldots, E_\ell^{*(i)}]$ and $\boldsymbol{\gamma}^{*(i)} := [\gamma_1^{*(i)}, \ldots, \gamma_\ell^{*(i)}]$ the optimal solution at the end of the ith iteration of the SCA procedure. To derive the lower bound of the denominator of the ratio at the $(i+1)$th iteration, the authors of [24] take advantage of the arithmetic-geometric mean inequality to write

$$\sum_{\ell=1}^{L} z_\ell \geq \prod_{\ell=1}^{L} \left(\frac{z_\ell}{\nu_\ell^{(i)}}\right)^{\nu_\ell^{(i)}} \tag{4.54}$$

with, $\forall \ell$,

$$\nu_\ell^{(i)} := \frac{\mathcal{H}_\ell(E_\ell^{*(i)}, \gamma_\ell^{*(i)})}{\sum_{\ell=1}^{L} \mathcal{H}_\ell(E_\ell^{*(i)}, \gamma_\ell^{*(i)})}, \tag{4.55}$$

with $\mathcal{H}_\ell(E_\ell, \gamma_\ell) := \gamma_\ell \tilde{D}_\ell(G_\ell E_\ell)/\tilde{S}_\ell(G_\ell E_\ell)$. In [24], it is proven that this lower bound meets the SCA convergence hypothesis.

The problem defined by (4.52a)-(4.52c) is then approximated by replacing $\sum_{\ell=1}^{L} z_\ell$ in (4.52a) with its lower bound given in (4.54). The resulting approximated problem writes

$$\min_{\mathbf{E},\gamma,\mathbf{z}} \quad \sum_{k=1}^{K} (\gamma_\ell E_\ell \kappa_\ell^{-1} + E_{c,k}) \left(\prod_{k=1}^{K} \frac{z_\ell}{\nu_\ell^{(i)}} \right)^{-\nu_\ell^{(i)}} \tag{4.56a}$$

$$\text{s.t.} \quad (4.53), (4.6), (1.27), \text{ and } (1.28). \tag{4.56b}$$

The approximated problem defined by (4.56a)-(4.56b) is the minimization of a posynomial function (4.56a) with posynomial constraints (4.56b). Thus, it can be optimally solved by applying the change of variables of the geometric programming, i.e., (4.21)-(4.22) for $\mathbf{E}$ and γ, and $z_\ell := \log(\Phi_\ell)$, and by using the IPM on the resulting problem. Finally, the SCA procedure solving Problem 4.5 is depicted in Algorithm 4.3.

Algorithm 4.3: SCA based procedure solving the MGEE Problem 4.5.

Set $\epsilon > 0$, $i = 0$, $C = \epsilon + 1$.
Find $\mathbf{E}^{*(0)} = [E_1^{*(0)}, \dots, E_L^{*(0)}]$ and $\boldsymbol{\gamma}^{*(0)} = [\gamma_1^{*(0)}, \dots, \gamma_L^{*(0)}]$ a feasible solution or Problem 4.5.
For all ℓ, compute $\nu_\ell^{(0)}$ using (4.55).
while $C > \epsilon$ **do**
  Find $\mathbf{E}^{*(i+1)} = [E_1^{*(i+1)}, \dots, E_L^{*(i+1)}]$ and $\boldsymbol{\gamma}^{*(i+1)} = [\gamma_1^{*(i+1)}, \dots, \gamma_L^{*(i+1)}]$ the optimal solution of Problem (4.56a)-(4.56b).
  Compute $C = \|[\mathbf{E}^{*(i+1)}, \gamma^{*(i+1)}] - [\mathbf{E}^{*(i)}, \gamma^{*(i)}]\|$.
  For all ℓ, compute $\nu_\ell^{(i+1)}$ using (4.55).
  Set $i = i + 1$.
end

4.8.2 Alternating optimization

Similarly to the suboptimal AO based procedure for the MSEE problem in Section 4.5.2.1, the optimization is performed alternately with respect to the variables $\mathbf{E}$ and γ until convergence is reached. Let us first explain the optimization w.r.t. $\mathbf{E}$.

Optimization w.r.t. E when γ is fixed, Problem 4.5 writes as

$$\max_{\mathbf{E}} \quad \frac{\sum_{\ell=1}^{L} C_{\ell,E} \frac{\tilde{D}_\ell(G_\ell E_\ell)}{\tilde{S}_\ell(G_\ell E_\ell)}}{\sum_{\ell=1}^{L}(W_{\ell,E}E_\ell + E_{c,\ell})} \tag{4.57a}$$

$$\text{s.t.} \quad \frac{\tilde{D}_\ell(G_\ell E_\ell)}{\tilde{S}_\ell(G_\ell E_\ell)} \geq M_{\ell,E}, \quad \forall \ell \tag{4.57b}$$

$$E_\ell \leq E_{\max,k}, \quad \forall \ell \tag{4.57c}$$

with $C_{\ell,E} := \gamma_\ell$, $W_{\ell,E} := \gamma_\ell \kappa_\ell^{-1}$, $M_{\ell,E} := \eta_\ell^{(0)}/\gamma_\ell$ and $E_{\max,k} := P_{\max,\ell}/\gamma_\ell$.

The problem defined by (4.57a)-(4.57c) is the maximization of a ratio between two differentiable functions with positive denominator and compact feasible set and hence, it can be solved with the Dinkelbach's algorithm [120, pp. 243]. For a given iteration $(i+1)$, the Dinkelbach's algorithm requires to optimally solve the following problem:

$$\max_{\mathbf{E}} \quad \sum_{\ell=1}^{L} \left(C_{\ell,E} \frac{\tilde{D}_\ell(G_\ell E_\ell)}{\tilde{S}_\ell(G_\ell E_\ell)} - \lambda_D^{(i)}(W_{\ell,E}E_\ell + E_{c,\ell}) \right) \tag{4.58a}$$

$$\text{s.t.} \quad (4.57b), (4.57c) \tag{4.58b}$$

where $\lambda_D^{(i)} \geq 0$ depends on the optimal solution of the ith iteration. This problem defined by (4.58a)-(4.58b) is not concave due to the non concavity of the objective function (4.58a) and then we cannot apply the IPM to solve it. However, we are able to optimally solve for certain configurations, detailed later. To do so, we first remark that this problem is separable into L subproblems since there is no coupling constraints between the elements of $\mathbf{E}$. The L resulting subproblems write

$$\max_{E_\ell} \quad C_{\ell,E} \frac{\tilde{D}_\ell(E_\ell)}{\tilde{S}_\ell(E_\ell)} - \lambda_D^{(i)} W_{\ell,E} E_\ell, \quad \forall \ell, \tag{4.59a}$$

$$\text{s.t.} \quad (4.57b), (4.57c). \tag{4.59b}$$

The objective functions (4.59a) of the L subproblems are not posynomial, but using its epigraph formulation, it is possible to alleviate this issue by introducing L auxiliary optimization variables (one per subproblem) w_ℓ along with L new constraints, leading to the following L subproblems

$$\max_{E_\ell, w_\ell} \quad w_\ell \tag{4.60a}$$

$$\text{s.t.} \quad (\lambda_D^{(i)} W_{\ell,E} E_\ell + w_\ell)\tilde{S}_\ell(E_\ell) - C_{\ell,E}\tilde{D}_\ell(E_\ell) \leq 0, \quad \forall \ell \tag{4.60b}$$

$$M_{\ell,E}\tilde{S}_\ell(E_\ell) - \tilde{D}_\ell(E_\ell) \leq 0, \quad \forall \ell \tag{4.60c}$$

$$E_\ell \leq E_{\max,k}, \quad \forall \ell. \tag{4.60d}$$

Constraint (4.60c) can be rewritten in posynomial form as in (4.16), and, similarly, constraint (4.60b) can also be rewritten in posynomial form. As a consequence, the problem defined by (4.60a)-(4.60d) is the maximization of a monomial function with posynomials constraints, and it can be turned into a standard GP as follows

$$\min_{E_\ell, w_\ell} \quad w_\ell^{-1} \tag{4.61a}$$

$$\text{s.t.} \quad (4.60b), (4.60c), (4.60d). \tag{4.61b}$$

The problem defined by (4.61a)-(4.61b) is a geometric program and then it can be optimally solved performing the change of variable (4.21) on E_ℓ, by setting $\Psi_\ell := \log(w_\ell)$, and using the IPM on the resulting equivalent problem.

Notice that this approach does not work if the maximum of the subproblem defined by (4.59a)-(4.59b) is negative since it implies $w_\ell \leq 0$ and as a result, we cannot apply the change of variable $\Psi_\ell := \log(w_\ell)$. If this case occurs, it is always possible to switch the SCA based procedure using the end of the last feasible iterations of the AO based procedure for initialization.

Finally, the procedure to optimally solve the problem defined by (4.58a)-(4.58b) is given in Algorithm 4.4 whose convergence is guaranteed since it creates a non-decreasing and bounded sequence of GEE.

Algorithm 4.4: Dinkelbach's algorithm solving Problem (4.59a)-(4.59b).

Set $\epsilon > 0$, $\lambda_D^{(0)}$, $i = 0$.
Set $\lambda_D^{(i)} = \epsilon + 1$.
while $C_D > \epsilon$ **do**
- For all ℓ, find E_ℓ^* the optimal solution of Problem (4.61a)-(4.61b) with $\lambda_D^{(i)}$.
- Set $C_D := \sum_{\ell=1}^{L} \left(C_{\ell,E} \frac{\tilde{D}_\ell(G_\ell E_\ell^*)}{\tilde{S}_\ell(G_\ell E_\ell^*)} - \lambda_D^{(i)} (F_{\ell,E} E_\ell^* + E_{c,\ell}) \right)$.
- Compute $\lambda_D^{(i+1)} = \frac{\sum_{\ell=1}^{L} C_{\ell,E} \frac{\tilde{D}_\ell(G_\ell E_\ell^*)}{\tilde{S}_\ell(G_\ell E_\ell^*)}}{\sum_\ell^L (F_{\ell,E} E_\ell^* + E_{c,\ell})}$.
- Set $i = i + 1$.

end

Optimization w.r.t. γ when $\mathbf{E}$ is fixed, Problem 4.5 writes as:

$$\max_{\gamma} \quad \frac{\sum_{\ell=1}^{L} A_{\ell,\gamma} \gamma_\ell}{\sum_{\ell=1}^{L} (C_{\ell,\gamma} \gamma_\ell + E_{c,\ell})} \tag{4.62a}$$

$$\text{s.t.} \quad \gamma_\ell \geq \gamma_{\min,k} \tag{4.62b}$$

$$\gamma_\ell \leq \gamma_{\max,k} \tag{4.62c}$$

$$\sum_{k=1}^{L} \gamma_\ell \leq 1 \tag{4.62d}$$

with, $\forall \ell$, $A_{\ell,\gamma} := \tilde{D}_\ell(E_\ell)/\tilde{S}_\ell(E_\ell)$, $C_{\ell,\gamma} := E_\ell/\kappa_\ell$, and $\gamma_{\min,\ell}$ and $\gamma_{\max,\ell}$ have same definitions as in Problem 4.8.

The problem defined by (4.62a)-(4.62d) is a linear fractional programming problem, i.e., an optimization problem whose objective function (4.62a) is the ratio of two linear functions and whose constraints are all linear. Hence, it can be efficiently solved using the Charnes-Cooper transformation [17], for which we introduce the following $(L+1)$ new optimization variables

$$r_{\ell,\gamma} := \frac{\gamma_\ell}{\sum_{\ell=1}^{L}(C_{\ell,\gamma}\gamma_\ell + E_{c,\ell})}, \quad \forall \ell, \tag{4.63}$$

$$t_\gamma := \frac{1}{\sum_{\ell=1}^{L}(C_{\ell,\gamma}\gamma_\ell + E_{c,\ell})}. \tag{4.64}$$

With these new variables, we can rewrite the problem defined by (4.62a)-(4.62d) equivalently in the following linear form:

Problem 4.13.

$$\max_{\mathbf{r},t} \quad \sum_{\ell=1}^{L} A_{\ell,\gamma} r_{\ell,\gamma} \tag{4.65}$$

$$\text{s.t.} \quad r_{\ell,\gamma} \geq t_\gamma \gamma_{\min,\ell}, \quad \forall \ell, \tag{4.66}$$

$$r_{\ell,\gamma} \leq t_\gamma \gamma_{\max,\ell}, \quad \forall \ell, \tag{4.67}$$

$$\sum_{\ell=1}^{L} r_{\ell,\gamma} - t_\gamma \leq 0 \tag{4.68}$$

$$\sum_{\ell=1}^{L} C_{\ell,\gamma} r_{\ell,\gamma} + t_\gamma \sum_{\ell=1}^{L} E_{c,\ell} = 0 \tag{4.69}$$

with $\mathbf{r} := [r_{1,\gamma}, \ldots, r_{L,\gamma}]$. Problem 4.13 can be optimally solved using numerical algorithms such as the simplex method [15] or IPM. The optimal solution of the original problem (4.62a)-(4.62d) can then be deduced from (4.63)-(4.64) as follows

$$\gamma_\ell^* = \frac{r_{\ell,\gamma}^*}{t_\gamma^*}, \quad \forall \ell, \tag{4.70}$$

where, $\forall \ell$, $r_{\ell,\gamma}^*$ and t_γ^* are the optimal solution of the equivalent linear Problem 4.13.

Algorithm Finally, the AO based procedure to suboptimally solve the MGEE Problem 4.5 is depicted in Algorithm 4.5.

4.9 Adding a maximum PER constraint

Until now, we have only considered the per-link minimum goodput constraint (4.6) as a QoS constraint. Although the goodput involves the error probabilities $q_{\ell,m}$, it does not provide guarantee on the achieved PER $q_{\ell,\mathcal{M}}$ (i.e., Chapter 1), as illustrated hereafter on a simple example. Let us consider the case with $\mathcal{M} = 1$, and two energy and bandwidth

Algorithm 4.5: AO based procedure solving the MGEE Problem 4.5.

Set $\epsilon > 0$, $i = 0$, $C_D = \epsilon + 1$.
Find initial feasible $\mathbf{E}^{(0)} := [E_1^{(0)}, \ldots, E_L^{(0)}]$ and $\boldsymbol{\gamma}^{(0)} := [\gamma_1^{(0)}, \ldots, \gamma_L^{(0)}]$.
while $C_D > \epsilon$ **do**
    Find $\mathbf{E}^{(i+1)} := [E_1^{(i+1)}, \ldots, E_L^{(+1)}]$ the optimal solution of the problem defined by (4.57a)-(4.57c) with $\boldsymbol{\gamma}^{(i)}$ using Algorithm 4.4.
    Find $\boldsymbol{\gamma}^{(i+1)} := [\gamma_1^{(0)}, \ldots, \gamma_L^{(0)}]$ the optimal solution of the problem defined by (4.62a)-(4.62d) with $\mathbf{E}^{(i+1)}$ solving the linear Problem 4.13 with the IPM method and using (4.70).
    Set $C_D = \|[\mathbf{E}^{(i+1)}, \boldsymbol{\gamma}^{(i+1)}] - [\mathbf{E}^{(i)}, \boldsymbol{\gamma}^{(i)}]\|$.
    Set $i = i + 1$.
end

parameters for the ℓth link $E_{\ell,i}$ and $\gamma_{\ell,i}$, $i = 1, 2$, satisfying its minimum goodput constraint, i.e., $\alpha_\ell \gamma_{\ell,i}(1 - q_{\ell,1}(G_\ell E_{\ell,i})) \geq \eta_\ell^{(0)}$. Let us further assume that $E_{\ell,1}$ (resp. $E_{\ell,2}$) yields high (resp. low) PER value, for instance $q_{\ell,1}(G_\ell E_{\ell,1}) = 0.5$ and $q_{\ell,1}(G_\ell E_{\ell,2}) = 10^{-3}$. The same goodput can be achieved for the two set of parameters if $\gamma_{\ell,1} = 2\gamma_{\ell,2}$ since we have

$$\frac{1 - q_\ell(G_\ell E_{\ell,1})}{1 - q_\ell(G_\ell E_{\ell,2})} \approx 0.5. \tag{4.71}$$

Thus, the two set energy and bandwidth parameters yields approximately the same goodput although $E_{\ell,1}$ (resp. $E_{\ell,2}$) yields high (resp. low) PER value, simply by allocating more bandwidth when the PER is high. However, in several applications such as video, ensuring a minimum goodput constraint is not enough and forcing a maximum PER constraint is of interest [54]. For instance within LTE standard, a maximum PER of 10^{-6} must be achieved in non-conversational video [97].

Therefore, we now investigate how handling a maximum PER constraint in our solutions. This constraint which can be written as:

$$q_{\ell,\mathcal{M}}(G_\ell E_\ell) \leq q_\ell^{(t)}, \quad \forall \ell. \tag{4.72}$$

Using the approximations (4.1) and (4.2), Constraint (4.72) can be approximated as:

$$E_\ell \geq G_\ell^{-1} \left(\frac{g_{\ell,\mathcal{M}}}{q_\ell^{(t)}} \right)^{\frac{1}{d_{\ell,\mathcal{M}}}}, \quad \forall \ell. \tag{4.73}$$

Let us now rewrite Problems 4.1, 4.3 and 4.4 by adding the maximum PER constraint (4.73) in a general form similar to (4.19)-(4.20) by applying the change of variables (4.21)-(4.22):

Problem 4.14.

$$\max_{\mathbf{x},\mathbf{y}} \quad \mathcal{J}_G(\mathbf{x},\mathbf{y}), \tag{4.74}$$

$$\text{s.t.} \quad e^{-x_\ell} G_\ell^{-1}\left(\frac{g_{\ell,\mathcal{M}}}{q_\ell^{(t)}}\right)^{\frac{1}{d_{\ell,\mathcal{M}}}} \leq 1, \quad \forall \ell, \tag{4.75}$$

$$(4.23), (4.24), \text{ and } (4.25). \tag{4.76}$$

Following similar steps as for the proof of Result 4.1, we can prove the following result.

Result 4.6. *The set*

$$\mathcal{F}_{P,2} = \{(\mathbf{x},\mathbf{y}) \in \mathbb{R}_+^L \times \mathbb{R}_+^L \,|\, \text{Eqs. (4.75)-(4.76) are satisfied.}\} \tag{4.77}$$

is convex.

From Result 4.6, we can see that adding the PER constraint (4.73) does not change our solution procedures for Problems 4.1, 4.3 and 4.4 since their objective functions remains the same and thus our derivations from the previous Sections remain valid. Adding constraint (4.73) only changes the solutions computational complexity. The same observation holds for the MGEE Problem 4.5. Thus, our proposed framework can handle a maximum PER constraint with no additional derivations.

Notice that we have conducted this Section work at the end of the thesis and thus we did not include maximum PER constraints in our numerical results (except for Fig. 4.13).

4.10 Complexity Analysis

Here, we give an analysis of the proposed solutions complexity, when the PER constraint is omitted. We first remind that these solutions are iterative, and at each iteration, they all use the IPM except the MSEE AO-based suboptimal solution.

Let us define N_I as the number of times the IPM is used for a given solution. The overall complexity of the optimal solutions of the MSEE, MPEE and MMEE problems, the MSEE OFA-based solution and the MGEE SCA-based solution is given by

$$N_I \mathcal{O}(\rho)$$

with $\rho = V(V^3 + C)$, where V (resp. C) is the number of variables (resp. constraints) of the optimization problem.

Concerning the MSEE AO-based solution, the complexity is given by

$$N_{out}\mathcal{O}(N_{b,\gamma} + LN_{b,\mathbf{E}}),$$

where $N_{b,\mathbf{E}}$ (resp. $N_{b,\gamma}$) is the number of iterations of the bisection procedure aiming to solve Problem 4.7 (resp. Problem 4.8), and N_{out} is the number of times the algorithm alternates between the optimization w.r.t $\mathbf{E}$ and γ.

Concerning the MGEE AO-based solution, the complexity is given by

$$N_{out}\mathcal{O}\left(\rho_\gamma + N_I L\mathcal{O}(\rho_E)\right),$$

where $\rho_\gamma := V_\gamma(V_\gamma^3 + C_\gamma)$ where C_γ and V_γ are the number of constraints and variables of the optimization problem w.r.t $\boldsymbol{\gamma}$, respectively, and $\rho_E := V_E^3(V_E^3 + C_E)$ where C_E and V_E are the number of constraints and variables of the optimization problem w.r.t $\mathbf{E}$, respectively.

In Table 4.2, we report the values of C and V, the average values of N_I, N_{out}, $N_{b,\boldsymbol{\gamma}}$ and $N_{b,\mathbf{E}}$ for the proposed solutions, and the total number of Floating Point Operation (FLOP)s using the same setup as in Section 4.11. We see that the solutions complexity can be split into three classes. The first class includes the optimal MSEE and the SCA based MGEE solutions, which are the most complex ones because of their high number of iterations to converge (i.e., N_I is high). The second class gathers the high SNR MSEE, MPEE, MMEE and AO based MGEE solutions which are less complex. Finally, the third class is only composed of the AO based MSEE solution, which is the less complex one because we were able to find the optimal solution in quasi closed-form at each iteration, and the number of iterations to converge is low.

Finally, we see that both suboptimal MSEE solutions are much less complex than the optimal one. The AO based solution is especially of interest since it yields almost the same result as the optimal one (see Section 4.5.2.1), with much lower complexity.

Table 4.2: Problems dimensionality, number of iterations and solutions complexity.

<table>
<tr><th></th><th>V</th><th>C</th><th>N_I</th><th>N_b</th><th>N_{out}</th><th>Total FLOPs ($\mathcal{O}$)</th></tr>
<tr><td>MSEE, optimal</td><td>$2L$</td><td>$2L+1$</td><td>979.1</td><td>-</td><td>-</td><td>64 432 613</td></tr>
<tr><td rowspan="2">MSEE, AO ($\boldsymbol{\gamma}$: top, $\mathbf{E}$: bottom)</td><td>-</td><td>-</td><td>-</td><td>25.76</td><td rowspan="2">4.12</td><td rowspan="2">1,021</td></tr>
<tr><td>-</td><td>-</td><td>-</td><td>27.75</td></tr>
<tr><td>MSEE, OFA</td><td>$2L$</td><td>$2L+1$</td><td>1</td><td>-</td><td>-</td><td>65 808</td></tr>
<tr><td>MPEE</td><td>$2L$</td><td>$2L+1$</td><td>1</td><td>-</td><td>-</td><td>65 808</td></tr>
<tr><td>MMEE</td><td>$2L+1$</td><td>$3L+1$</td><td>1</td><td>-</td><td>-</td><td>83 946</td></tr>
<tr><td>MGEE, SCA</td><td>$3L$</td><td>$3L+1$</td><td>839.18</td><td>-</td><td>-</td><td>27 892 329</td></tr>
<tr><td rowspan="2">MGEE, AO ($\boldsymbol{\gamma}$: top, $\mathbf{E}$: bottom)</td><td>$L+1$</td><td>$2L+3$</td><td>1</td><td rowspan="2">-</td><td rowspan="2">3</td><td rowspan="2">20,546</td></tr>
<tr><td>1</td><td>3</td><td>3.5</td></tr>
</table>

4.11 Numerical Results

4.11.1 Setup

We use the IR-HARQ scheme based on the convolutional code with rate $R_\ell = 1/2$ described in [43, Table V], and we use a QPSK modulation. The number of links is $L = 8$ and the link distances $\delta_\ell^{(D)}$ are uniformly drawn in [50 m, 1 km]. We set $B = 5$ MHz, $N_0 = -170$ dBm/Hz and the packet length is, $\forall \ell$, $\mathcal{L}_\ell = 128$. The carrier frequency is $f_c = 2400$ MHz and we put $\Delta_\ell = (4\pi f_c/c)^{-2}\delta_\ell^{(D)-3}$. We assume that the required goodput per-link is equal for all links, and unless otherwise stated, is equal to $\eta_\ell^{(1)} = 62.5$ kbits/s. Except in Fig. 4.13, we do not consider maximum PER constraint. Also, unless otherwise stated, we put $\mathcal{M} = 3$, and we consider that $\forall \ell$, $P_{ctx,\ell} = P_{crx,\ell} = 0.4$ W and $\kappa_\ell = 0.5$. All points have been obtained by averaging through 50 random networks configurations.

4.11.2 Performance analysis

In this Section, we analyse the performance of the MSEE, MPEE,MMEE and MGEE optimal solutions. For the sake of comparison, we also display the MGO optimal solution, which is provided in Appendix B.2, and the MPO optimal solution from [65]. Notice that, for clarity, we do not plot the MSEE suboptimal solutions since we have already studied their results in Section 4.5.2.1.

In Figs. 4.4 to 4.7, we plot as the function of the maximum transmit power the SEE, PEE, MEE, and GEE obtained with the proposed solutions, the MPO, and the MGO.

The comparison between EE-related criteria with MPO and MGO shows that: *i*) the MPO gives systematically the worst performance, *ii*) the MGO gives bad MEE and PEE whereas it is comparable to SEE and GEE for low $P_{\max}$ but degrades when $P_{\max}$ increases. Both behaviors can be explained because, as observed in Chapter 1, the EE given by (4.4) is a unimodal function of E_ℓ for fixed γ, with a unique maximizer, and the E_ℓ obtained by MPO (resp. MGO) is much lower (resp. larger) than this maximizer. As a consequence, these two criteria achieve low EE values. It is worth emphasizing that the MPO is the worst due to the considered setup. Indeed, the lower the circuitry consumption, the lower the value of the EE maximizer, and thus the better the MPO and the worst the MGO. In other words, for lower values for $P_{ctx,\ell}$ and $P_{crx,\ell}$, the MPO (resp. MGO) performance would have been better (resp. worst).

The comparison between the EE-related criteria leads to the following observations: *i*) the results are in agreement with what is expected, i.e. ,maximizing a given criterion leads to the highest values with regard to this criterion. *ii*) Regarding the MGEE criterion, both SCA and AO achieve almost the same performance. Since we established that the AO has much less complexity (see Table 4.2 in Section 4.10), we recommend to use it for practical implementation. *iii*) Among all the criteria, the MPEE achieves almost the best performance for all the metrics. Moreover, since it has lowest complexity than all the other solutions (expect the AO based MSEE solution), it makes it attractive for practical implementations.

From the above observations, we provide the following recommendations for applying our algorithms to communication systems when EE is concerned. For MANETs, maximizing individual EE is of interest, and thus the MMEE is a good candidate. However, MMEE performs badly for the other criteria and thus we recommend the use of

MPEE, because of observation (*iii*) in the previous paragraph, and the fact that its performance is close to MMEE in terms of MEE.

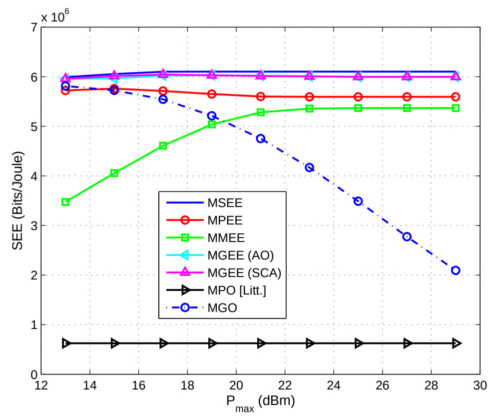

Figure 4.4: SEE of the proposed solutions versus $P_{\max,\ell}$.

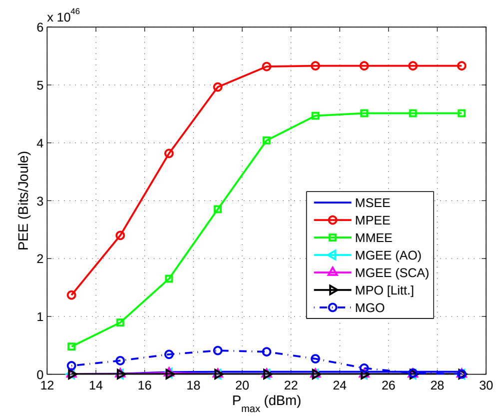

Figure 4.5: PEE of the proposed solutions versus $P_{\max,\ell}$.

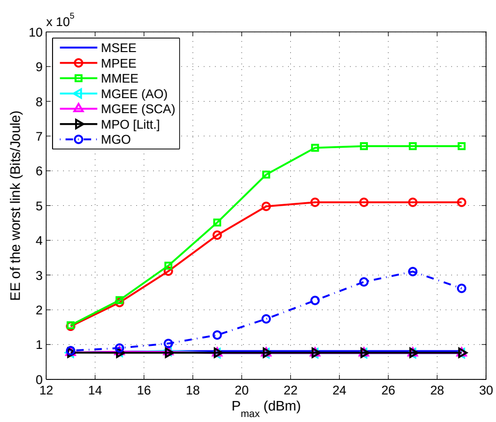

Figure 4.6: MEE of the proposed solutions versus $P_{\max,\ell}$.

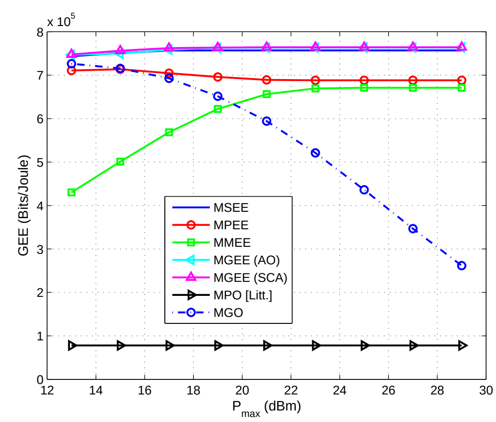

Figure 4.7: GEE of the proposed solutions versus $P_{\max,\ell}$.

4.11.3 Fairness analysis

We analyze the fairness of the proposed criterion versus the minimum required goodput and the maximum transmit power. To measure the fairness, we use the Jain's index on the links' EE $[\mathcal{E}_1, \ldots, \mathcal{E}_L]$ defined by [58]:

$$\mathcal{J}_A := \frac{\left(\sum_{\ell=1}^{L} \mathcal{E}_\ell\right)^2}{L \sum_{\ell=1}^{L} \mathcal{E}_\ell^2}. \tag{4.78}$$

It is well known that $\mathcal{J}_A \in [1/L, 1]$ for non negative $\mathcal{E}_\ell$ and the highest its value, the fairer the solution.

In Fig. 4.8, the maximum transmit power is set to 29 dBm, and we study the influence of the goodput constraint on the solutions fairness. The MMEE gives the fairest RA among the proposed algorithms, followed by the MPEE. The other EE-based criteria (MSEE and MGEE) lead to a less fair RA, especially for low required goodput because they allow to advantage only the links with good conditions. The fairness of the MSEE and MGEE increases as the minimum goodput constraint increases because it forces the algorithms to give more resource to the link with bad channel conditions, increasing their EE and as a consequence the overall fairness. The MPO is very fair because it forces all the links to achieve the same goodput (i.e., $B\eta_\ell^{(1)}$). Moreover, their power consumptions are close to each others since the transmit power is very low and then the denominator of the EE is dominated by the circuitry consumption. The MGO is very fair as well because we consider fixed MCS and high maximum transmit power. Hence, all the links achieve almost the same goodput, given by $B\alpha_\ell/L$. Moreover, the power consumption is almost equal for all the links since they all use their maximum transmit power. Hence, the links have almost equal goodput and power consumption and thus the MGO is fair.

In Fig. 4.9, we study the influence of the maximum transmit power on the solutions fairness. We observe once again that the MPO is very fair in EE but with low EE. We also see that the MMEE fairness increases with the maximum transmit power, achieving a Jain's index of one for sufficiently high value. This is because when the maximum transmit power is low, the links with bad channel conditions meet the power constraint with equality (i.e., the EE of these links cannot be increased) while the EE of the other links can be higher. The MPEE has a similar behaviour. The MSEE and MGEE lead to low fairness because the minimum required goodput is low and then these algorithms advantage only the links with good channel conditions. Finally, concerning the MGO, one can observe that for low maximum transmit power, the fairness is low for similar reasons as for the MSEE and MGEE. As the maximum transmit power increases, the fairness of the maximum goodput also increases, for the reasons already observed in Fig. 4.8.

These observations corroborate the insights of the previous section: the MPEE is of interest for MANETs since the fairness issue is of importance for this type of communications. For this reason, we only consider the MPEE in the rest of our numerical experiments.

4.11.4 Application to the smartphone case

In this Section, we extend the smartphone example of Section 1.5 to the multiuser context and illustrate the effectiveness of the MPEE criterion. We use the same numerical values for Q_0 and U as in Section 1.5, and we compute the same metrics with in addition the following ones: n_t the average number of HARQ rounds and $\bar{\gamma}$ the average used bandwidth (in %).

In the first scenario, the MPEE is the best one since it transmits all the messages within

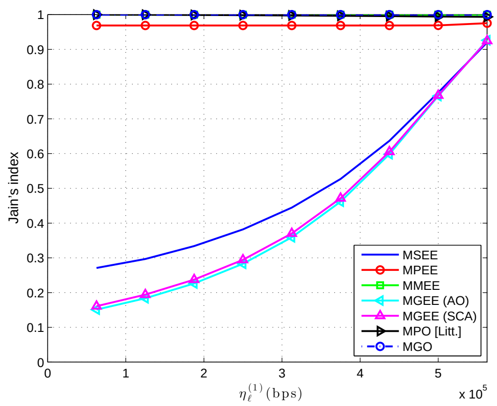

Figure 4.8: Jain's index for the links EE versus $\eta_\ell^{(1)}$.

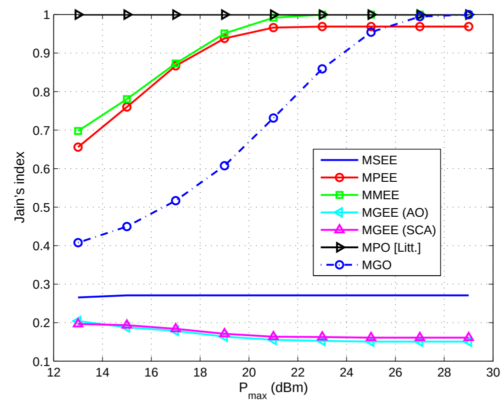

Figure 4.9: Jain's index for the links EE versus $P_{\max,\ell}$.

the shortest duration, with the least energy consumption. It is followed by the MGO which also succeeds to transmit all the messages but in a longer duration and with more energy consumption. The MPO criterion gives the worst result since the battery goes flat before succeeding to transmit all the messages. We can first see from $\bar{\gamma}$ that the MPO allocates little proportion of the bandwidth to the users which implies that the transmit duration of each message is long as observed through T_t. This actually explains the small goodput. Second, the MPO succeeds to use low transmit power taking advantage of the retransmission capability of HARQ to achieve the target goodput at the expense of the time duration. Finally the tradeoff between the (very low) transmit power and the (very large) time duration is disastrous for the energy consumed by the MPO for sending the pre-fixed number of messages.

In the second scenario, the MPEE allows to transmit more packets than the other criteria when the whole battery is used. The battery lifetime for the MPEE is also longer than for the MGO. Indeed, the average goodput is almost the same for the MPEE and the MGO, but the energy consumption is much lower for the MPEE, which gives a better tradeoff between the energy consumption and the goodput. The results for the MPO are identical to the ones for the first scenario since the baterry was already empty.

To summarize, when the RA is performed using the MPEE criterion, either the links can transmit more packets in average than when using the MPO and the MGO at the end of the battery lifetime, or the links have higher battery levels in average for the same number of transmit messages. This clearly demonstrates the practical relevance of considering the EE (and especially the MPEE) when designing a RA procedure.

Table 4.3: Comparison of the MPEE with the conventional criteria (MPO and MGO) in terms of battery lifetime and time to transmit information for both scenarios.

Scenario	Criterion	Q_r	T_t (s)	N_p	η_ℓ^A (kbits/s)	n_t	$\bar{\gamma}$ (%)
10^7 sent messages	MPEE	83%	2150	1×10^7	6150	1.02	100%
	MGO	72%	2222	1×10^7	6250	1	100%
	MPO	0%	14 271	7×10^6	63	1.2	12.2%
Full battery drain	MPEE	0%	12 937	6×10^7	6150	1.02	100%
	MGO	0%	8063	4×10^7	6250	1	100%
	MPO	0%	14 271	7×10^6	63	1.2	12.2%

4.11.5 Impact of the parameter $\mathcal{M}$

To investigate the impact of $\mathcal{M}$, we compute the PEE gains when $\mathcal{M} = 3$ compared with $\mathcal{M} = 1$, defined as:

$$100 \times \left(\frac{\text{PEE}_3}{\text{PEE}_1} - 1 \right), \tag{4.79}$$

where PEE_i stands for the optimal PEE value obtained for $\mathcal{M} = i$.

Fig. 4.10 represents this gain as a function of $P_{\max,\ell}$ for $\eta_\ell^{(1)} = 1.25$ kbits/s. Notice that the PEE obtained when $\mathcal{M} = 2$ is not displayed since it is very close to the one when $\mathcal{M} = 3$ and the curves are superimposed. This is because the throughput resulting from the RA for $\mathcal{M} = 3$ and $\mathcal{M} = 2$ are very close, and as a consequence, the EE is almost identical. Choosing between $\mathcal{M} = 2$ and $\mathcal{M} = 3$ should hence be a tradeoff between the delay and the error probability. Indeed, increasing $\mathcal{M}$ increases the delay but decreases the error probability. We observe that the gain is strictly positive and offers good improvement for low $P_{\max,\ell}$. For instance, when $P_{\max} = 0$ dBm, the gain is about 22%.

Actually, the fact that the gain is positive can be checked using the sufficient condition on the $q_{\ell,m}$s given in [96], which writes as follows:

$$\frac{q_{\ell,m+1}}{q_{\ell,m}} \leq \frac{q_{\ell,m}}{q_{\ell,m-1}}, \quad \forall m \in [1, \ldots, \mathcal{M} - 1]. \tag{4.80}$$

In Fig. 4.11 (resp. Fig. 4.12), we plot $q_{\ell,m+1}/q_{\ell,m} - q_{\ell,m}/q_{\ell,m-1}$ for $m = 1$ (resp. $m = 2$). We can see that the curves are always below 0, except for SNR = 2 dB and $m = 2$, where the value is very close to 0. This means that the sufficient condition (4.80) holds, explaining the strictly positive PEE gain observed in Fig. 4.10.

Condition (4.80) enables system designers to choose the best value of $\mathcal{M}$: for delay-tolerant application, one can choose the largest value of $\mathcal{M}$ such that (4.80) holds.

Now, let us study the PEE gains as a function of the maximum PER constraint $q_\ell^{(t)}$. To solve the MPEE Problem, we use the solution provided in Section 4.9. In Fig. 4.13, we consider same $q_\ell^{(t)}$ for all ℓ, we set $P_{\max,\ell} = 20$ dBm, and we plot the PEE gains as a function of $q_\ell^{(t)}$. We see once again a strictly positive gain when $\mathcal{M} = 3$ as compared with $\mathcal{M} = 1$,

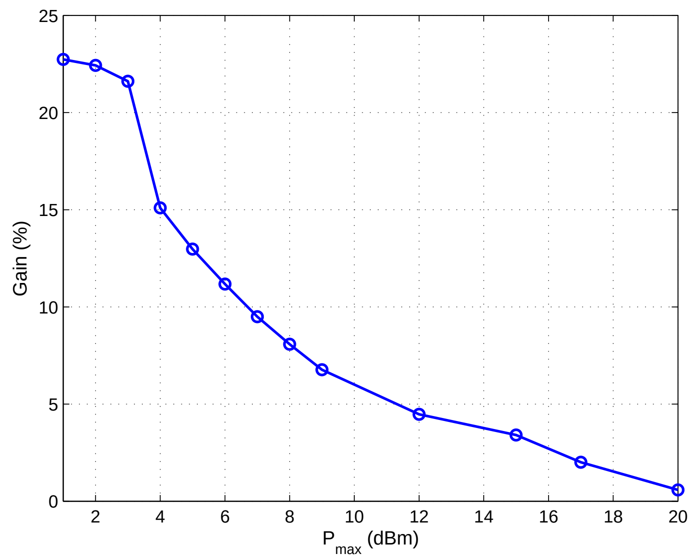

Figure 4.10: PEE gains when $\mathcal{M} = 3$ compared with $\mathcal{M} = 1$ versus $P_{\max,\ell}$.

and especially when the PER constraint is low, we see substantial gain of several hundreds of percent. These observations can be explained as follows. For the sake of explanation, we consider $\mathcal{M} = 2$ (the reasoning for $\mathcal{M} > 2$ being the same), and we plot $q_{\ell,1}$ and $q_{\ell,2}$ versus the SNR in Fig. 4.14. Let us assume that $E_\ell^{*,\bar{q}_\ell^{(t)}}$, the optimal value of E_ℓ without PER constraint, is such that $q_{\ell,1}(E_\ell^{*,\bar{q}_\ell^{(t)}} G_\ell) = 3.5 \times 10^{-1}$, yielding $q_{\ell,2}(E_\ell^{*,\bar{q}_\ell^{(t)}} G_\ell) = 2 \times 10^{-4}$ as it can be read in Fig. 4.14. Let us now impose a PER constraint $q_\ell^{(t)} = 10^{-4}$. In order to satisfy $q_{\ell,1}(G_\ell E_\ell^{*,q_\ell^{(t)}}) \leq 10^{-4}$ (if $\mathcal{M} = 1$) or $q_{\ell,2}(E_\ell^{*,q_\ell^{(t)}}) \leq 10^{-4}$ (if $\mathcal{M} = 2$), one has to increase the ℓth link transmit energy E_ℓ. We see in Fig. 4.14 that the required energy increment to reach the PER constraint is much less for $\mathcal{M} = 2$ than for $\mathcal{M} = 1$, meaning that this constraint produces a more important EE loss for the system with $\mathcal{M} = 1$ as compared with the one with $\mathcal{M} = 2$, explaining the result in Fig. 4.13.

4.11.6 Influence of an error in $P_{c,tx}$ and $P_{c,rx}$

In this Section, we illustrate the impact of a mismatch between the values of $P_{ctx,\ell}$ and $P_{crx,\ell}$ used to perform RA and their real values. To do so, we set $P_{\max,\ell} = 19$ dBm, and we solve the MPEE problem for several $P_{ctx,\ell}$ and $P_{crx,\ell}$ values, denoted by $\hat{P}_{cx}$. With the obtained optimal E_ℓ and γ_ℓ, we compute the PEE with the real value of $P_{ctx,\ell}$ and $P_{crx,\ell}$ being 0.4 W. In Fig. 4.15, we plot the PEE versus the value of $\hat{P}_{cx}$. As we can see, an error in the circuitry consumption during the RA induces a PEE loss. However, the error in the model has to be large to dramatically decreases the solutions performance. For example, an error of 0.2 W (i.e., 50%) in the circuitry consumption induces a PEE loss of approximately 1.6%. Hence, although the model is of importance, it is tolerant to small

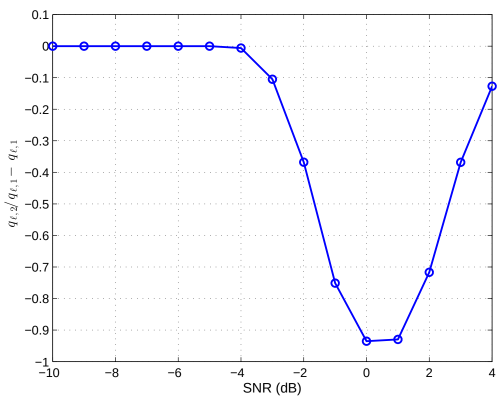

Figure 4.11: Illustration of condition (4.80) with $m = 1$.

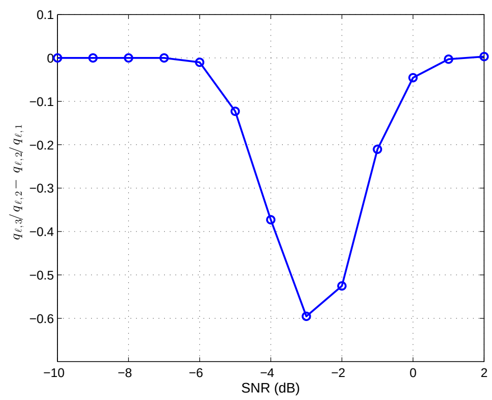

Figure 4.12: Illustration of condition (4.80) with $m = 2$.

error.

4.12 Conclusion

In this Chapter, we addressed EE-based RA problems under the Rayleigh channel in HARQ based MANETs when only statistical CSI is available and considering the use of practical MCS. More precisely, we addressed the MSEE, MPEE, MMEE and MGEE problems. For the first three, we proposed algorithms to find their optimal solutions whereas we proposed two suboptimal solutions for the MGEE one. We also proposed two suboptimal less-complex solutions for the MSEE problem. The addressed problems along with the proposed solutions and their optimality are summarized in Table 4.4. In addition, we analyzed the complexity of the procedure to find these solutions. We performed extensive simulations to analyze the relevancy of each criteria, and to compare it with conventional ones (i.e., MPO and MGO).

Problems	Solutions	Optimality
MSEE	Jong + IPM	Optimal
	AO	Suboptimal
	OFA	Suboptimal
MPEE	IPM	Optimal
MMEE	IPM	Optimal
MGEE	AO	Suboptimal
	SCA	Suboptimal

Table 4.4: Addressed problems and optimality of the proposed solution procedures.

We found out that the MPEE is especially relevant for MANETs since it allows to

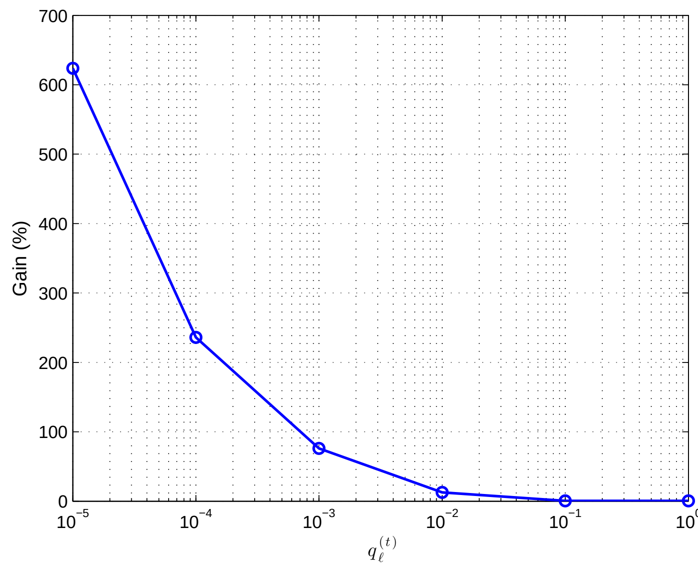

Figure 4.13: PEE gains when $\mathcal{M} = 3$ compared with $\mathcal{M} = 1$ versus $q_\ell^{(t)}$.

achieve a tradeoff between all the EE metrics, and is fair. We also observed that considering HARQ might provide very large EE gains, especially for low per-link transmit power or PER constraints.

Finally, part of the material presented in this Chapter has been published in [C4].

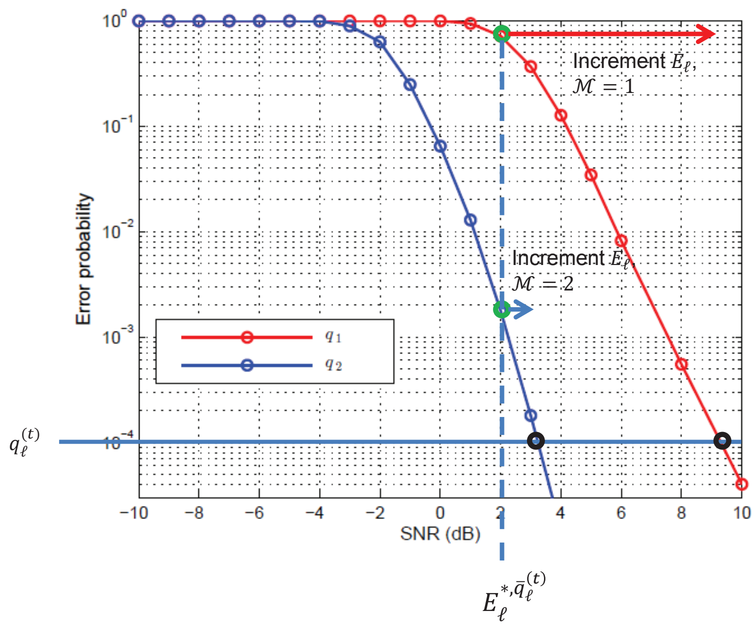

Figure 4.14: Transmit energy increment to satisfy a PER of 10^{-4} when $\mathcal{M}=1$ and $\mathcal{M}=2$.

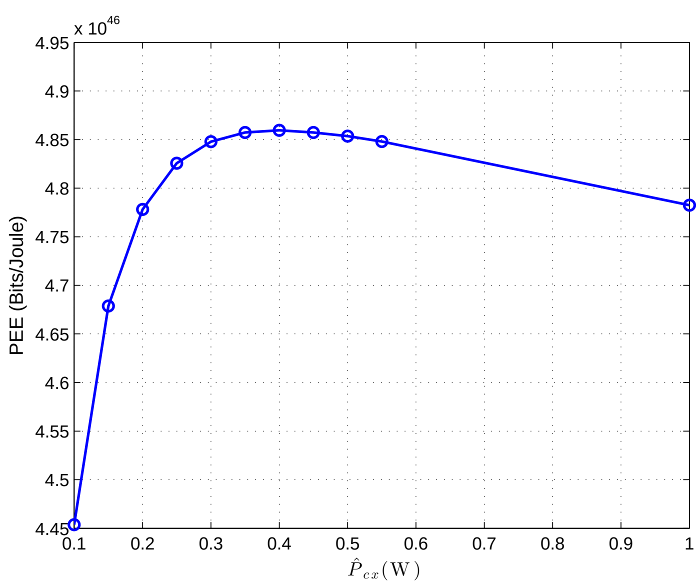

Figure 4.15: Impact of a mismatch between $\hat{P}_{cx}$ and $P_{ctx,\ell}$ and $P_{crx,\ell}$.

Chapter 5

Resource Allocation for Type-I HARQ Under the Rician Channel

5.1 Introduction

From Table 3.1 in Chapter 3, we see that the RA with EE-related metrics for Type-I HARQ in assisted MANETs using practical MCS under the Rician channel has never been addressed in the literature. In this Chapter, we address this problem when there is no shadowing (i.e., the CIR first tap's mean is time-invariant, see Chapter 1). In details, the contributions of this Chapter are the following ones.

- We provide an analytically tractable approximation of the PER under the Rician FF channel with no shadowing, and prove that this approximation is strictly convex with respect to the transmit energy.
- We optimally solve the MSEE, MGEE and MMEE problems for Type-I HARQ under the Rician FF channel. Actually, we manage to transform these problems which have no convexity properties into equivalent COPs. Our main technical contribution is to provide low-complexity algorithms finding these COPs optimal solution using the KKT conditions. We also provide an AO based suboptimal solution to the MPEE problem.
- We analyze the results of the proposed criteria through numerical simulations, and point out that substantial EE gains can be achieved by taking into account the Rician channel instead of the conventional Rayleigh ones. In other words, we exhibit the importance of taking into account the existence of a LoS during the RA instead of only considering the average channel power.
- We numerically study solutions to perform the RA for Type-II HARQ under the Rician channel. Actually, in Chapter 4 we solved RA problems for Type-II HARQ under the Rayleigh channel, whereas in this Chapter, we perform the RA for Type-I

HARQ under the Rician channel. We compare the solution from Chapter 4 and the one from this Chapter when applied on Type-II HARQ under the Rician channel. We find out that applying the Type-I HARQ Rician RA from this Chapter yields better performance than applying Type-II Rayleigh RA from Chapter 4.

The rest of this Chapter is organized as follows. In Section 5.2, we derive an approximation of the error probability under the Rician FF channel. In Section 5.3, we mathematically formulate the RA problems we wish to solve. Section 5.4 is devoted to the methodology we use to solve these problems. The problems solutions are derived in Sections 5.5, 5.6, 5.7 and 5.8. In Section 5.9, we give insights on how this Chapter's material extends to Type-II HARQ. Simulations results are given in Section 5.10 whereas Section 5.11 concludes this Chapter.

5.2 Error Probability Approximation

Our first task, as in Chapter 4, is to find an approximation of the error probability $q_{\ell,1}$, $\forall \ell$, to solve the EE-based RA problems. Unfortunately, unlike under the Rayleigh channel, we did not find such an approximation in the literature for the Rician channel. For this reason, in this Section, we develop an analytically tractable approximation of $q_{\ell,1}$ under the Rician FF channel.

To do so, we use [88], where the following two observations are drawn concerning the relation between the error probability at the output of the Viterbi decoder and the uncoded BER at the input of the decoder under the Rayleigh channel:

- This relation is almost independent of the considered modulation.
- The relation is approximately affine in the logarithmic domain.

Our proposal is to extend the approach from [88] to the Rician channel. From the two above observations, $q_{\ell,1}(G_\ell E_\ell)$ can be approximated by $\tilde{q}_{\ell,1}(G_\ell E_\ell)$ defined as:

$$\tilde{q}_{\ell,1}(G_\ell E_\ell) = (\mathrm{BER}_\ell(G_\ell E_\ell))^{a_\ell^{(T_1)}} e^{b_\ell^{(T_1)}}, \tag{5.1}$$

where $a_\ell^{(T_1)}$ and $b_\ell^{(T_1)}$ are fitting coefficients depending on the packets length $\mathcal{L}_\ell$, on the convolutional code parameters and on the Rician K factor, BER_ℓ is the ℓth link uncoded BER link under the Rician FF channel with factor K_ℓ. Notice that this type of approximation is used to perform RA in the single user context in [38], where full CSI is available at the transmitter side.

In Eq. (5.1), $\tilde{q}_{\ell,1}(G_\ell E_\ell)$ involves the ℓth link BER under the Rician fading channel, which is obtained by averaging the BER under the AWGN channel over all the possible values of the SNR. To perform this operation, we first express the ℓth link instantaneous SNR on one subcarrier as:

$$\mathrm{snr}_\ell := |H_\ell|^2 E_\ell G_\ell, \tag{5.2}$$

with $H_\ell \sim \mathcal{CN}(a_\ell, 2\sigma_{h,\ell}^2)$, where a_ℓ and $2\sigma_\ell^2$ are such that $|a_\ell|^2 + 2\sigma_{h,\ell}^2 = 1$ (i.e., normalized average channel power) and $|a_\ell|^2/(2\sigma_{h,\ell}^2) = K_\ell$. Hence, from the above discussion, the ℓth link average BER can be written as

$$\mathrm{BER}_\ell(G_\ell E_\ell) = \mathbb{E}_{\mathrm{snr}_\ell}[\mathrm{BER}_{\ell,\mathrm{AWGN}}(\mathrm{snr}_\ell)], \tag{5.3}$$

where $\mathbb{E}_{\mathrm{snr}_\ell}[.]$ is the mathematical expectation taken over the possible values of snr_ℓ, and $\mathrm{BER}_{\ell,\mathrm{AWGN}}$ is the ℓth link BER under the AWGN channel. A conventional approximation of $\mathrm{BER}_{\ell,\mathrm{AWGN}}$ is given by [48]

$$\mathrm{BER}_{\ell,\mathrm{AWGN}}(\mathrm{snr}_\ell) \approx c_\ell^{(T1)} Q\left(\sqrt{d_\ell^{(T1)}\mathrm{snr}_\ell}\right), \tag{5.4}$$

where $c_\ell^{(T1)}$ and $d_\ell^{(T1)}$ are modulation-dependent parameters whose values can be found in Table 6.1 in [48], and $Q(.)$ is the Q-function. Calculating the exact value of the expectation in (5.3) appears to be difficult since it involves numerical integrations due to the presence of the Q-function, and for this reason, we propose to approximate it by a combination of exponentials as suggested for example in [73] or [74]:

$$Q(x) \approx \sum_{i=1}^{i_{max}} \delta_i^{(T1)} e^{-\theta_i^{(T1)} x^2}, \tag{5.5}$$

where, $\forall i$, $\delta_i^{(T1)}$ and $\theta_i^{(T1)}$ are fitting coefficients and i_{max} is the number of exponentials in the sum. The larger the value of i_{max}, the better the approximation. In this thesis, we use the coefficients proposed in [74], where $i_{max} = 4$. The expectation in (5.3) can thus be approximated as

$$\mathrm{BER}_\ell(G_\ell E_\ell) \approx c_\ell^{(T1)} \sum_{i=1}^{4} \delta_i^{(T1)} \mathbb{E}_{\mathrm{snr}_\ell}[e^{-\theta_i^{(T1)} d_\ell^{(T1)} \mathrm{snr}_\ell}]. \tag{5.6}$$

The expectation in (5.6) is exactly the moment generating function of the distribution of snr_ℓ evaluated in $-\theta_i^{(T_1)} d_\ell^{(T_1)}$. One can prove that $\mathrm{snr}_\ell/(G_\ell E_\ell \sigma_{h,\ell}^2)$ follows a noncentral chi-square distribution with 2 degrees of freedom and noncentrality parameter $|a_\ell|^2/\sigma_{h,\ell}^2$, yielding [89]:

$$\mathrm{BER}_\ell(G_\ell E_\ell) \approx c_\ell^{(T1)} \sum_{i=1}^{4} \delta_i^{(T1)} \frac{e^{-\frac{|a_\ell|^2 G_\ell E_\ell \theta_i^{(T1)} d_\ell^{(T1)}}{1+2\sigma_{h,\ell}^2 G_\ell E_\ell \theta_i^{(T1)} d_\ell^{(T1)}}}}{1 + 2\sigma_{h,\ell}^2 G_\ell E_\ell \theta_i^{(T1)} d_\ell^{(T1)}}. \tag{5.7}$$

Thus, the error probability $q_{\ell,1}(G_\ell E_\ell)$ can be approximated by plugging (5.7) into (5.1), yielding, $\forall \ell$:

$$\tilde{q}_{\ell,1}(G_\ell E_\ell) = \left(c_\ell^{(T1)} \sum_{i=1}^{4} \delta_i^{(T1)} \frac{e^{-\frac{|a_\ell|^2 G_\ell E_\ell \theta_i^{(T1)} d_\ell^{(T1)}}{1+2\sigma_{h,\ell}^2 G_\ell E_\ell \theta_i^{(T1)} d_\ell^{(T1)}}}}{1 + 2\sigma_{h,\ell}^2 G_\ell E_\ell \theta_i^{(T1)} d_\ell^{(T1)}}\right)^{a_\ell^{(T1)}} e^{b_\ell^{(T1)}}. \tag{5.8}$$

The accuracy of the approximation (5.8) is numerically checked in Fig. 5.1 (resp. 5.2) where we plot both $q_{\ell,1}$ and $\tilde{q}_{\ell,1}$ versus the SNR for Binary Phase Shift Keying (BPSK) (resp. QPSK) modulation using the same setup a in Section 5.10. The fitting coefficients are obtained through curve fitting are provided in Table 5.1. We can observe that the approximation is quiet accurate, and therefore can be used to predict $q_{\ell,1}(G_\ell E_\ell)$ with an analytically tractable expression.

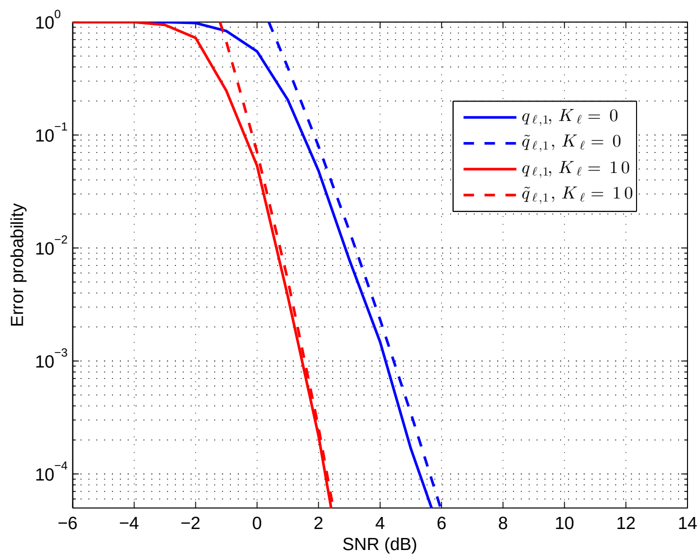

Figure 5.1: Tightness of the approximation of the error probability $\tilde{q}_{\ell,1}$ under the FF Rician channel, BPSK modulation.

K_ℓ	0	10
$a_\ell^{(T_1)}$	9.73	9.39
$b_\ell^{(T_1)}$	18.57	19.37

Table 5.1: Fitting coefficients for the approximation (5.8).

Approximating $q_{\ell,1}(x)$ by $\tilde{q}_{\ell,1}(x)$, the per-link minimum goodput constraint for Type-I HARQ (1.26) can be approximated as:

$$\alpha_\ell \gamma_\ell (1 - \tilde{q}_{\ell,1}(G_\ell E_\ell)) \geq \eta_\ell^{(0)}, \quad \forall \ell. \tag{5.9}$$

Moreover, the approximation (5.8) is characterized in Lemma 5.1.

Lemma 5.1. *The approximation $\tilde{q}_{\ell,1}(x)$ given by (5.8) is strictly convex.*

Proof. First, let us prove the strict convexity of each term in the sum in (5.8). To do so, let us prove that $f_c^n(x) := \exp(-a_c^n x/(1 + 2b_c^n x))/(1 + 2b_c^n x)$, where a_c^n and b_c^n are non-negative

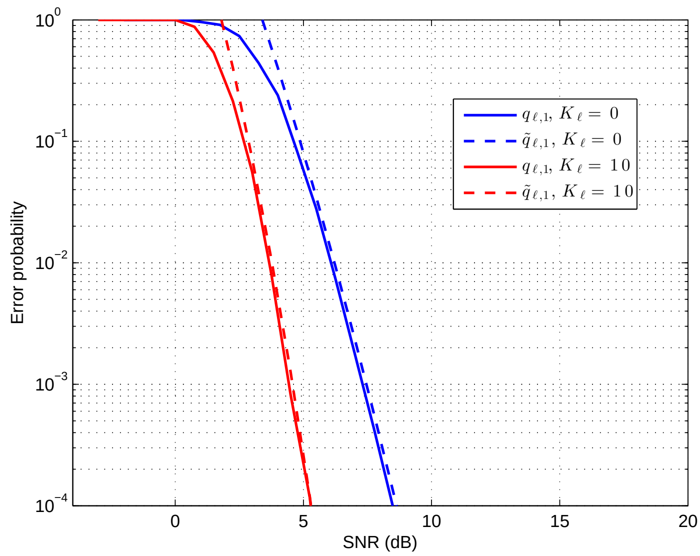

Figure 5.2: Tightness of the approximation of the error probability $\tilde{q}_{\ell,1}$ under the FF Rician channel, QPSK modulation.

constants, is strictly log-convex by computing the second order derivative of $\log(f_c^n(x))$:

$$\log(f_c^n(x))'' = \frac{4a_c^n b_c^n}{(1+2b_c^n x)^3} + \frac{4(b_c^n)^2}{(1+2b_c^n x)^2} > 0. \tag{5.10}$$

Therefore, $f_c^n(x)$ is strictly log-convex and as a consequence it is stricly convex [15]. It follows that $\tilde{q}_{\ell,1}$ is strictly convex since it can be expressed as $(g_c^n(x))^{u_c^n}$ where $g_c^n(x)$ is a non-negative linear combination of convex function, and $u_c^n \geq 1$. $\square$

With Lemma 5.1 at hand, we now address the solution of the RA problems, beginning with their mathematical formulations.

5.3 Problem Formulation

In this Section, we mathematically formulate the optimization problems we wish to solve, which are based on the same criteria as in Chapter 4, the difference being the following ones:

- In this Chapter, we consider Type-I HARQ under the Rician channel, yielding different performance closed-form expressions (see Chapter 1) and error probability approximation from in Chapter 4.
- In this Chapter, unlike in Chapter 4, we do not take into account the per-link maximum transmit power constraint (1.27) for technical reason. Actually, not considering (1.27) enables us to derive the analytical optimal solutions for the MSEE, MMEE

and MGEE problems. Although we cannot control the maximum transmit power anymore, since the optimized metrics are EE-related, the energy consumption of the proposed criteria is finite (i.e., it does not go to the infinity as for instance the MGO criterion with no transmit power constraint). Notice that relaxing this constraint in Chapter 4 would not have alleviated the solutions complexity since the main difficulty lies in the combination mechanism of packets received in error in Type-II HARQ.

5.3.1 MSEE Problem

First, we address the MSEE problem under the Rician channel, which is a natural aggregation of the links' EE.

Problem 5.1. *The MSEE problem for Type-I HARQ under the Rician channel can be written as:*

$$\begin{aligned} \max_{\mathbf{E},\gamma} \quad & \sum_{\ell=1}^{L} \frac{\alpha_\ell(1-\tilde{q}_{\ell,1}(G_\ell E_\ell))}{\kappa_\ell^{-1} E_\ell + E_{c,\ell}\gamma_\ell^{-1}}, \\ \text{s.t.} \quad & (5.9) \text{ and } (1.28). \end{aligned} \tag{5.11}$$

5.3.2 MPEE Problem

Second, we address the MPEE problem under the Rician channel, which was shown in Chapter 4 to be especially relevant for MANETs.

Problem 5.2. *The MPEE problem for Type-I HARQ under the Rician channel can be written as:*

$$\begin{aligned} \max_{\mathbf{E},\gamma} \quad & \prod_{\ell=1}^{L} \frac{\alpha_\ell(1-\tilde{q}_{\ell,1}(G_\ell E_\ell))}{\kappa_\ell^{-1} E_\ell + E_{c,\ell}\gamma_\ell^{-1}}, \\ \text{s.t.} \quad & (5.9) \text{ and } (1.28). \end{aligned} \tag{5.12}$$

5.3.3 MMEE Problem

Third, we address the MMEE problem under the Rician channel, which yields the highest fairness.

Problem 5.3. *the MMEE problem for Type-I HARQ under the Rician channel can be written as:*

$$\begin{aligned} \max_{\mathbf{E},\gamma} \quad & \left(\min_{\ell\in\{1,\dots,L\}} \frac{\alpha_\ell(1-\tilde{q}_{\ell,1}(G_\ell E_\ell))}{\kappa_\ell^{-1} E_\ell + E_{c,\ell}\gamma_\ell^{-1}} \right), \\ \text{s.t.} \quad & (5.9) \text{ and } (1.28). \end{aligned} \tag{5.13}$$

5.3.4 MGEE Problem

Finally, we address the MGEE problem under the Rician channel, which is of interest when network EE is at stake.

Problem 5.4. *the MGEE problem for Type-I HARQ under the Rician channel can be written as:*

$$\max_{\mathbf{E},\gamma} \quad \frac{\sum_{\ell=1}^{L} \alpha_\ell \gamma_\ell (1 - \tilde{q}_{\ell,1}(G_\ell E_\ell))}{\sum_{\ell=1}^{L} (\kappa_\ell^{-1} \gamma_\ell E_\ell + E_{c,\ell})}, \tag{5.14}$$
$$\text{s.t.} \quad (5.9) \text{ and } (1.28).$$

5.4 Solution Methodology

5.4.1 General idea

As they are stated, Problems 5.1-5.4 have no special properties like convexity and thus, without additional efforts, they cannot be directly solved with affordable complexity. To overcome this issue, we first propose a change of variables, enabling us to convert three of them (Problems 5.1, 5.3 and 5.4) into equivalents COPs using the fractional programming framework. It is worth emphasizing that, unlike in Chapter 4, the error probability approximation under the Rician FF channel (5.8) is not posynomial. As a consequence, the change of variables of geometric programming (4.21)-(4.22) does not render our problems convex, and thus we have to find another change of variables. Second, using the KKT conditions, we propose low-complexity algorithms finding the optimal solutions of these equivalents COPs.

5.4.2 Change of variable enabling us to apply convex optimization tools

The change of variables we propose to apply convex optimization tools to Problems 5.1-5.4 is the following one: $(\gamma, \mathbf{E}) \mapsto (\gamma, \mathbf{Q})$, with $\mathbf{Q} := [Q_1, \ldots, Q_L]$, and

$$Q_\ell := \gamma_\ell E_\ell, \quad \forall \ell. \tag{5.15}$$

Using (5.15), constraint (5.9) can be rewritten equivalently as:

$$\alpha_\ell \gamma_\ell \left(1 - \tilde{q}_{\ell,1}\left(G_\ell \frac{Q_\ell}{\gamma_\ell}\right)\right) \geq \eta_\ell^{(0)}, \quad \forall \ell. \tag{5.16}$$

Moreover, using the change of variables (5.15), Problems 5.1-5.4 can be rewritten equivalently as follows.

Problem 5.5. *The MSEE Problem 5.1 can be equivalently rewritten as:*

$$\max_{\mathbf{Q},\gamma} \quad \sum_{\ell=1}^{L} \frac{\alpha_\ell \gamma_\ell (1 - \tilde{q}_{\ell,1}(G_\ell Q_\ell / \gamma_\ell))}{\kappa_\ell^{-1} Q_\ell + E_{c,\ell}}, \tag{5.17}$$
$$\text{s.t.} \quad (5.16) \text{ and } (1.28),$$

Problem 5.6. *The MPEE Problem 5.2 can be equivalently rewritten as:*

$$\begin{aligned} \max_{\mathbf{Q},\gamma} \quad & \prod_{\ell=1}^{L} \frac{\alpha_\ell \gamma_\ell (1 - \tilde{q}_{\ell,1}(G_\ell Q_\ell / \gamma_\ell))}{\kappa_\ell^{-1} E_\ell + E_{c,\ell} \gamma_\ell^{-1}}, \\ \text{s.t.} \quad & (5.16) \text{ and } (1.28), \end{aligned} \tag{5.18}$$

Problem 5.7. *The MMEE Problem 5.3 can be equivalently rewritten as:*

$$\begin{aligned} \max_{\mathbf{Q},\gamma} \quad & \left(\min_{\ell \in \{1,\dots,L\}} \frac{\alpha_\ell \gamma_\ell (1 - \tilde{q}_{\ell,1}(G_\ell Q_\ell / \gamma_\ell))}{\kappa_\ell^{-1} E_\ell + E_{c,\ell} \gamma_\ell^{-1}} \right), \\ \text{s.t.} \quad & (5.16) \text{ and } (1.28), \end{aligned} \tag{5.19}$$

Problem 5.8. *The MGEE Problem 5.4 can be equivalently rewritten as:*

$$\begin{aligned} \max_{\mathbf{Q},\gamma} \quad & \frac{\sum_{\ell=1}^{L} \alpha_\ell \gamma_\ell (1 - \tilde{q}_{\ell,1}(G_\ell Q_\ell / \gamma_\ell))}{\sum_{\ell=1}^{L} (\kappa_\ell^{-1} \gamma_\ell E_\ell + E_{c,\ell})}, \\ \text{s.t.} \quad & (5.16) \text{ and } (1.28), \end{aligned} \tag{5.20}$$

Remark 5.1. *We did not apply the change of variables (5.15) in Chapter 4 since applying it on Problems 4.1 to 4.5 prevents us from finding their optimal solution since the EE expression for Type-II HARQ has a more complicated denominator preventing us from finding a convex property, whereas we were able to find it using the change of variables of geometric programming (4.21)-(4.22).*

Problems 5.5, 5.7 and 5.8 are characterized in Lemma 5.2.

Lemma 5.2. *The numerators of the objective functions of Problems 5.5, 5.7 and 5.8 are concave, their denominators are convex and the feasible set defined by (5.16) and (1.28) is convex.*

Proof. First, let us prove that the feasible set defined by constraints (1.28) and (5.16) is convex. Constraint (1.28) is linear and as a consequence it is convex. Moreover, $\gamma_\ell(1 - \tilde{q}_{\ell,1}(G_\ell Q_\ell/\gamma_\ell))$ is the so called perspective [15] of the concave function $1 - \tilde{q}_{\ell,1}(G_\ell E_\ell)$ (i.e., Lemma 5.1) and thus it is concave, meaning that constraint (5.16) is convex.

Second, let us focus on the objective functions of Problems 5.5, 5.7 and 5.8. We remark that there denominators are linear and thus they are convex. The numerators of the objective functions of Problems 5.5 and 5.7 are given by $\alpha_\ell \gamma_\ell (1 - \tilde{q}_{\ell,1}(G_\ell Q_\ell/\gamma_\ell))$ and hence they are concave as the perspective of concave functions. For Problem 5.8, the numerator is given by $\sum_{\ell=1}^{L} \alpha_\ell(\gamma_\ell(1-\tilde{q}_{\ell,1}(G_\ell Q_\ell/\gamma_\ell)))$ and thus it is concave as a positive sum of concave functions, concluding the proof. □

According to Lemma 5.2, we know that Problems 5.5, 5.7 and 5.8 (and thus Problems 5.1, 5.3 and 5.4 since they are equivalent) can be optimally solved iteratively: Problem 5.5 can be solved using the Jong's algorithm [61], Problem 5.7 using the Generalized Dinkelbach's algorithm [28] and Problem 5.8 using the Dinkelbach's algorithm [34]. At each iteration, these three algorithms require to solve a COP. The main technical contribution of this Chapter is to provide these COPs optimal solutions using the so-called KKT conditions [15].

For these three COPs, we solve the KKT solution as follows: we first express the optimal solution as a function of a single parameter, and second we find the optimal value of this parameter.

Concerning the MPEE Problem 5.6, we do not find specific properties such as Lemma 5.2. Therefore, we propose a suboptimal AO based solution, working on the original Problem 5.2 before the change of variable.

5.5 MSEE Solution

Due to Lemma 5.2, we know that the MSEE Problem 5.5 can be solved using the Jong's algorithm [61]. This iterative algorithm requires to solve the following COP at iteration i:

Problem 5.9.

$$\begin{aligned} \max_{\mathbf{Q},\gamma} \quad & \sum_{\ell=1}^{L} u_\ell^{(i)}(\alpha_\ell\gamma_\ell(1-\tilde{q}_{\ell,1}(G_\ell Q_\ell/\gamma_\ell)) - \beta_\ell^{(i)}\kappa_\ell^{-1}Q_\ell), \\ \text{s.t.} \quad & (5.16) \text{ and } (1.28), \end{aligned} \tag{5.21}$$

where, $\forall\ell$, $u_\ell^{(i)} > 0$ and $\beta_\ell^{(i)} \geq 0$ depend on the optimal solution at iteration $(i-1)$.

Due to the concavity of Problem 5.9 (i.e., Lemma 5.2), we know that the KKT conditions are necessary and sufficient to find its optimal solution [15]. Defining $\boldsymbol{\delta} := [\delta_1, \ldots, \delta_L]$ and λ as the Lagrangian multipliers associated with constraints (5.16) and (1.28), respectively, the KKT conditions of Problem 5.9 write:

$$\alpha_\ell G_\ell \tilde{q}'_{\ell,1}(G_\ell Q_\ell/\gamma_\ell)(u_\ell^{(i)} + \delta_\ell) + u_\ell^{(i)}\beta_\ell^{(i)}\kappa_\ell^{-1} = 0, \quad \forall\ell, \tag{5.22}$$

$$\alpha_\ell h_{\ell,M}^{(T_1)}(G_\ell Q_\ell/\gamma_\ell)(u_\ell^{(i)} + \delta_\ell) + \lambda = 0, \quad \forall\ell, \tag{5.23}$$

with $h_{\ell,M}^{(T_1)}(x) := -1 + \tilde{q}_{\ell,1}(x) - x\tilde{q}'_{\ell,1}(x)$. In addition, the following complementary slackness conditions hold at the optimum:

$$\delta_\ell(\eta_\ell^{(0)} - \alpha_\ell\gamma_\ell(1-\tilde{q}_{\ell,1}(G_\ell Q_\ell/\gamma_\ell))) = 0, \quad \forall\ell, \tag{5.24}$$

$$\lambda\left(\sum_{\ell=1}^{L}\gamma_\ell - 1\right) = 0. \tag{5.25}$$

To solve the optimality conditions (5.22)-(5.25), in a first time we consider the value of λ as fixed and we find the optimal solution as a function of this multiplier. In a second time, we search for the optimal value of this multiplier.

5.5.1 Solution for fixed λ

From (5.22), we obtain the following L relations:

$$u_\ell^{(i)} + \delta_\ell = \frac{-u_\ell^{(i)}\beta_\ell^{(i)}\kappa_\ell^{-1}}{\alpha_\ell G_\ell \tilde{q}'_{\ell,1}(x_\ell^*(\lambda))}, \quad \forall \ell, \tag{5.26}$$

with, $\forall \ell$, $x_\ell^*(\lambda) := G_\ell Q_\ell^*(\lambda)/\gamma_\ell^*(\lambda)$, where $Q_\ell^*(\lambda)$ (resp. $\gamma_\ell^*(\lambda)$) is the optimal Q_ℓ (resp. γ_ℓ) for given λ. Then, by plugging (5.26) into (5.23), we get

$$f_{\ell,M}^{(T_1)}(x_\ell^*(\lambda)) = \frac{\lambda}{u_\ell^{(i)}\beta_\ell^{(i)}\kappa_\ell^{-1}}, \quad \forall \ell, \tag{5.27}$$

with $f_{\ell,M}^{(T_1)}(x) := h_{\ell,M}^{(T_1)}(x)/(G_\ell \tilde{q}'_{\ell,1}(x))$. We prove that, $\forall \ell$, $f_{\ell,M}^{(T_1)}(x)$ is strictly increasing by computing its derivative, which is given by:

$$f_{\ell,M}^{(T_1)\prime}(x) = \frac{\tilde{q}''_{\ell,1}(x)(1-\tilde{q}_{\ell,1}(x))}{G_\ell \tilde{q}'_{\ell,1}(x)^2} > 0. \tag{5.28}$$

The strict monotonicity of $f_{\ell,M}^{(T_1)}(x)$ allows us to obtain $x_\ell^*(\lambda)$ using (5.27) as:

$$x_\ell^*(\lambda) = f_{\ell,M}^{(T_1)-1}\left(\frac{\lambda}{u_\ell^{(i)}\beta_\ell^{(i)}\kappa_\ell^{-1}}\right), \quad \forall \ell, \tag{5.29}$$

where $f_{\ell,M}^{(T_1)-1}(x)$ is the inverse of $f_{\ell,M}^{(T_1)}(x)$ with respect to the composition. We can then plug this optimal value (5.29) into Problem 5.9 , which can be rewritten as:

Problem 5.10.

$$\max_{\gamma} \quad \sum_{\ell=1}^{L} \mathcal{K}_\ell(\lambda)\gamma_\ell, \tag{5.30}$$

$$\text{s.t.} \quad \gamma_\ell \geq \gamma_{\min,\ell}(\lambda), \quad \forall \ell, \tag{5.31}$$

$$(1.28). \tag{5.32}$$

with, $\forall \ell$, $\mathcal{K}_\ell(\lambda) := \alpha_\ell u_\ell^{(i)}(1-\tilde{q}_{\ell,1}(x_\ell^*(\lambda))) - u_\ell^{(i)}\beta_\ell^{(i)}\kappa_\ell^{-1}x_\ell^*(\lambda)G_\ell^{-1}$ and $\gamma_{\min,\ell}(\lambda) := \eta_\ell^{(0)}/(\alpha_\ell(1-\tilde{q}_{\ell,1}(x_\ell^*(\lambda))))$. Problem 5.10 is a linear program depending only on the optimization variables $\boldsymbol{\gamma}$. In addition, since there is only one coupling constraint (1.28), its optimal solution is obtained according to Theorem 5.3.

Theorem 5.3. *The optimal solution of Problem 5.10 is given according to the following two cases.*

1. *If, $\forall \ell$, $\mathcal{K}_\ell(\lambda) < 0$: $\forall \ell$, $\gamma_\ell^*(\lambda)$, the optimal value of $\gamma_\ell(\lambda)$, is given by $\gamma_\ell^*(\lambda) = \gamma_{\min,\ell}(\lambda)$.*
2. *If, $\exists \ell$, such that $\mathcal{K}_\ell(\lambda) \geq 0$: let $\ell_{M,\mathcal{K}}$ be such that, $\forall \ell$, $\mathcal{K}_{\ell_{M,\mathcal{K}}}(\lambda) \geq \mathcal{K}_\ell(\lambda)$. Then, $\forall \ell \neq \ell_{M,\mathcal{K}}$, $\gamma_\ell^*(\lambda) = \gamma_{\min,\ell}(\lambda)$ and $\gamma_{\ell_{M,\mathcal{K}}}^*(\lambda) = 1 - \sum_{\ell \neq \ell_{M,\mathcal{K}}} \gamma_{\min,\ell}(\lambda)$.*

So far, we have exhibited the optimal solution of Problem 5.9 as a function of the single Lagrangian multiplier λ. Let us now turn our attention to finding the optimal value of this multiplier.

5.5.2 Search for the optimal λ

To find λ^*, the optimal value of λ, we discuss the following two possibilities: either there exists ℓ such that $\delta_\ell = 0$, or $\forall \ell$, $\delta_\ell > 0$.

Case 1: $\exists \ell$ such that $\delta_\ell = 0$. In Lemma 5.4, whose proof is provided in Appendix C.1, we exhibit λ^*.

Lemma 5.4. *If there is at least one link ℓ_1 with $\delta_{\ell_1} = 0$, then we have*

$$\lambda^* = -\arg\min_{\ell} \left\{ \alpha_\ell u_\ell h^{(T_1)}_{\ell,M}(x^*_{\ell,\delta_\ell=0}) \right\}, \tag{5.33}$$

with $\forall \ell$, $x^*_{\ell,\delta_\ell=0} := \tilde{q}'^{-1}_{\ell,1}(-\beta^{(i)}_\ell \kappa^{-1}_\ell / (\alpha_\ell G_\ell))$.

Thanks to Lemma 5.4, we can optimally solve Problem 5.9 by solving Problem 5.10 with low complexity using Theorem 5.3. Moreover, Lemma 5.4 enables us to check whether $\exists \ell$ such that $\delta_\ell = 0$ by computing λ^* and plugging it into Problem 5.10. If the resulting problem is feasible, then we know that $\exists \ell$ such that $\delta_\ell = 0$.

Case 2: $\forall \ell, \delta_\ell > 0$. In this case, $\gamma^*_\ell(\lambda)$ can be obtained more easily using (5.24), which gives us

$$\gamma^*_\ell(\lambda) = \frac{\eta^{(0)}_\ell}{\alpha_\ell(1 - \tilde{q}_{\ell,1}(x^*_\ell(\lambda)))}, \quad \forall \ell, \tag{5.34}$$

where $x^*_\ell(\lambda)$ is given by (5.29). Since $f^{(T_1)}_{\ell,M}(x)$ is strictly increasing (i.e., (5.28)), $f^{(T_1)-1}_{\ell,M}(x)$ is also strictly increasing and as a consequence $x^*_\ell(\lambda)$ is also increasing (i.e., (5.29)), implying that $\gamma^*_\ell(\lambda)$ is strictly decreasing due to (5.34). To find λ^*, we use the complementary slackness condition (5.25). To this end, we define the following function representing the sum of the optimal bandwidth parameters:

$$\tilde{\Gamma}_M(\lambda) := \sum_{\ell=1}^{L} \gamma^*_\ell(\lambda). \tag{5.35}$$

Since $\gamma^*_\ell(\lambda)$ is strictly decreasing, there are two possibilities: either $\tilde{\Gamma}_M(0) \leq 1$ and in this case $\lambda^* = 0$, or λ^* is such that $\tilde{\Gamma}_M(\lambda^*) = 1$. Thus, λ^* can be found by a one dimensional linesearch method.

5.5.3 Solution

Finally, the optimal solution of Problem 5.5 is depicted in Algorithm 5.1. for which we define $\boldsymbol{\psi}^{(T_1)}(\boldsymbol{\beta}^{(i)}, \mathbf{u}^{(i)}, \boldsymbol{\gamma}, \mathbf{Q}) := [\psi^{(T_1)}_1(\beta^{(i)}_1, u^{(i)}_1, \gamma_1, Q_1), \ldots, \psi^{(T_1)}_{2L}(\beta^{(i)}_L, u^{(i)}_L, \gamma_L, Q_L)]$, with $\boldsymbol{\beta}^{(i)} := [\beta^{(i)}_1, \ldots, \beta^{(i)}_L]$ and $\mathbf{u}^{(i)} := [u^{(i)}_1, \ldots, u^{(i)}_L]$ and, for $\ell = 1, \ldots, L$:

$$\psi^{(T_1)}_\ell(\beta^{(i)}_\ell, u^{(i)}_\ell, \gamma_\ell, Q_\ell) := -\alpha_\ell \gamma_\ell (1 - \tilde{q}_{\ell,1}(G_\ell Q_\ell / \gamma_\ell)) + \beta^{(i)}_\ell (\kappa^{-1}_\ell Q_\ell + E_{c,\ell}), \tag{5.36}$$

$$\psi^{(T_1)}_{\ell+L}(\beta^{(i)}_\ell, u^{(i)}_\ell, \gamma_\ell, Q_\ell) := -1 + u^{(i)}_\ell (\kappa^{-1}_\ell Q_\ell + E_{c,\ell}). \tag{5.37}$$

Algorithm 5.1: Optimal solution of Problem 5.5.

Set $\epsilon > 0$, $i = 0$, $C_D = \epsilon + 1$.

Initialize $\boldsymbol{\beta}^{(0)} = [\beta_0, \ldots, \beta_L]$ and $\mathbf{u}^{(0)} = [u_0, \ldots, u_L]$ with any feasible solution as for instance the MPO solution.

while $C_D > \epsilon$ **do**

Set $\lambda^* = -\min_\ell \left\{\alpha_\ell u_\ell h_{\ell,M}^{(T_1)}(x^*_{\ell,\delta_\ell=0})\right\}$, where $\forall \ell$, $x^*_{\ell,\delta_\ell=0}$ is computed as in Lemma 5.4

if Problem 5.10 is feasible with λ^* **then**

Find $(\mathbf{Q}^*, \boldsymbol{\gamma}^*)$, Problem 5.9 optimal solution by solving Problem 5.10 using Theorem 5.3 with $\boldsymbol{\beta}^{(i)}$ and $\mathbf{u}^{(i)}$.

else

Find $(\mathbf{Q}^*, \boldsymbol{\gamma}^*)$ using a linesearch method with $\boldsymbol{\beta}^{(i)}$ and $\mathbf{u}^{(i)}$ (case 2 in Section 5.5.2).

Set $C_D = \|\boldsymbol{\psi}^{(T_1)}(\boldsymbol{\beta}^{(i)}, \mathbf{u}^{(i)}, \boldsymbol{\gamma}^*, \mathbf{Q}^*)\|$.

For $\ell = 1, \ldots, L$, compute $u_\ell^{(i+1)}$ and $\beta_\ell^{(i+1)}$ using (3.31) and (3.32), respectively.

Set $\boldsymbol{\beta}^{(i+1)} = [\beta_1^{(i+1)}, \ldots, \beta_L^{(i+1)}]$ and $\mathbf{u}^{(i+1)} = [u_1^{(i+1)}, \ldots, u_L^{(i+1)}]$.

Set $i = i + 1$.

end

5.6 MPEE Solution

Unlike for the MSEE, MMEE and MGEE problems, we are not able to find specific properties such as Lemma 5.2 enabling us to transform either Problem 5.2 or 5.6 into COPs. As a consequence, we propose suboptimal AO based solution, in which we optimize alternately between $\mathbf{E}$ and $\boldsymbol{\gamma}$ until convergence is reached. We apply this procedure on the original Problem 5.2 before the change of variables (5.15). Let us begin with the optimization w.r.t $\mathbf{E}$.

Optimization w.r.t E In a first time, $\boldsymbol{\gamma}$ is fixed and the optimization is performed w.r.t $\mathbf{E}$. For fixed $\boldsymbol{\gamma}$, we see that Problem 5.6 is separable since there is no coupling constraints between the elements of $\mathbf{E}$, meaning that the optimization can be performed separately among the links. We thus have to solve L parallels sub problems, which write as:

Problem 5.11.

$$\max_{E_\ell} \quad \frac{\alpha_\ell(1-\tilde{q}_{\ell,1}(G_\ell E_\ell))}{\kappa_\ell^{-1}E_\ell + F_{\ell,E}}, \tag{5.38}$$

$$\text{s.t.} \quad h_{\ell,E}^{(T_1)}(G_\ell E_\ell) \leq 0, \tag{5.39}$$

with $h_{\ell,E}^{(T_1)}(G_\ell E_\ell) := \eta_\ell^{(0)}\gamma_\ell^{-1}\alpha_\ell^{-1} + \tilde{q}_{\ell,1}(G_\ell E_\ell) - 1$ and $F_{\ell,E}$ is defined in Section 4.5.2.1. Problem 5.11 is characterized in Result 5.1, whose proof is identical to the one of Result 4.3.

Result 5.1. *Problem 5.11 is the maximization of a PC function over a convex set.*

Thus, according to [120], the optimal solution of Problems 5.11 can be obtained using the KKT conditions, and is given in Theorem 5.5, whose proof is straightforward and thus omitted.

Theorem 5.5. *Let $E_{\min,\ell}$ denote the unique zero of $h^{(T_1)}_{\ell,E}(G_\ell E_\ell)$ on $(0, +\infty]$, and $Q_{\ell,M}$ be defined as*

$$Q_{\ell,M}(G_\ell E_\ell) = \frac{\alpha_\ell(1 - \tilde{q}_{\ell,1}(G_\ell E_\ell))}{\kappa_\ell^{-1} E_\ell + F_{\ell,E}}, \quad \forall \ell. \tag{5.40}$$

The optimal solution E^*_ℓ of Problem 5.11 takes the following form:
1) If $Q'_{\ell,M}(G_\ell E_{\min,\ell}) < 0$, then $E^*_\ell = E_{\min,\ell}$.
2) Else, E^*_ℓ is the solution of $Q'_{\ell,M}(G_\ell E^*_\ell) = 0$ in $[E_{\min,\ell}, +\infty]$, which is unique.

Optimization w.r.t γ In the second step, **E** is fixed and the optimization is performed w.r.t γ. In this case, Problem 5.6 can be written as:

Problem 5.12.

$$\max_{\gamma} \quad \prod_{\ell=1}^{L} \frac{H^{(T_1)}_\ell}{J^{(T_1)}_{\ell,\gamma} + E_{c,\ell}\gamma_\ell^{-1}}, \tag{5.41}$$

$$\text{s.t.} \quad \gamma_\ell^{-1}\gamma^{(T_1)}_{\min,\ell} \leq 1, \quad \forall \ell, \tag{5.42}$$

$$(1.28). \tag{5.43}$$

with,$\forall \ell$, $H^{(T_1)}_\ell := \alpha_\ell(1 - \tilde{q}_{\ell,1}(G_\ell E_\ell))$, $J^{(T_1)}_\ell := \kappa_\ell^{-1} E_\ell$, and $\gamma^{(T_1)}_{\min,\ell} := \eta^{(0)}_\ell / (\alpha_\ell(1 - \tilde{q}_{\ell,1}(G_\ell E_\ell)))$. Problem 5.12 be can rewritten as a geometric program as follows:

Problem 5.13.

$$\min_{\gamma} \quad \prod_{\ell=1}^{L} \left(\frac{J^{(T_1)}_\ell}{H^{(T_1)}_\ell} + \frac{E_{c,\ell}}{H^{(T_1)}_\ell}\gamma_\ell^{-1} \right), \tag{5.44}$$

$$\text{s.t.} \quad (5.42) \text{ and } (1.28). \tag{5.45}$$

$$\tag{5.46}$$

Since both the objective function (5.44) and constraints (5.46) of Problem 5.13 are posynomials, it falls within the GP framework, and can be optimally solved with the IPM [82].

AO based algorithm to solve Problem 5.2 The AO based procedure to suboptimally solve Problem 5.2 is depicted in Algorithm 5.2, whose convergence can be proved using the same argument as for the convergence proof of Algorithm 4.2.

Algorithm 5.2: AO based suboptimal solution of Problem 5.6.

Set $\epsilon > 0, C_A = \epsilon + 1, i = 0$.
Find $\mathbf{E}^{(0)} = [E_1^{(0)}, \ldots, E_L^{(0)}]$ and $\boldsymbol{\gamma}^{(0)} = [\gamma_1^{(0)}, \ldots, \gamma_L^{(0)}]$, with any feasible solution as for instance the MPO solution.
while $C_A > \epsilon$ **do**
  Find $\mathbf{E}^{(i+1)} = [E_1, \ldots, E_L^*]$, the optimal solution of the L Problems 5.11 with $\boldsymbol{\gamma}^{(i)}$ using Theorem 5.5.
  Find $\boldsymbol{\gamma}^{(i+1)} = [\gamma_1^{(i+1)}, \ldots, \gamma_L^{(i+1)}]$, the optimal solution of Problem 5.13 with $\mathbf{E}^{(i+1)}$ using the IPM.
  Set $C_A = \|[\mathbf{E}^{(i)}, \boldsymbol{\gamma}^{(i)}] - [\mathbf{E}^{(i+1)}, \boldsymbol{\gamma}^{(i+1)}]\|$.
  Set $i = i + 1$.
end

5.7 MMEE Solution

Due to Lemma 5.2, we know that the MMEE Problem 5.7 can be solved using the so-called generalized Dinkelach's algorithm [28]. This iterative algorithm requires to solve the following COP at iteration i:

Problem 5.14.

$$\max_{\mathbf{Q},\boldsymbol{\gamma}} \quad \min_{\ell} \left\{ \alpha_\ell \gamma_\ell (1 - \tilde{q}_{\ell,1}(G_\ell Q_\ell / \gamma_\ell)) - \psi_{GD}^{(i)} (\kappa_\ell^{-1} Q_\ell + E_{c,\ell}) \right\}, \tag{5.47}$$

$$\text{s.t.} \quad (5.16), (1.28), \tag{5.48}$$

where $\psi_{GD}^{(i)} \geq 0$ depends on the optimal solution at iteration $(i-1)$. We solve this problem using its epigraph formulation [15], i.e., we introduce an auxiliary optimization variable t along with the following L new constraints:

$$t \leq \alpha_\ell \gamma_\ell (1 - \tilde{q}_{\ell,1}(G_\ell Q_\ell / \gamma_\ell)) - \psi_{GD}^{(i)} (\kappa_\ell^{-1} Q_\ell + E_{c,\ell}), \quad \forall \ell, \tag{5.49}$$

allowing us to rewrite Problem 5.14 equivalently as follows:

Problem 5.15.

$$\max_{\mathbf{Q},\boldsymbol{\gamma},t} \quad t, \tag{5.50}$$

$$\text{s.t.} \quad (5.49), (5.16) \text{ and } (1.28). \tag{5.51}$$

Problem 5.15 is the maximization of a concave function over a convex set (i.e., Lemma 5.2). Defining $\boldsymbol{\omega} := [\omega_1, \ldots, \omega_L]$ as the Lagrangian multipliers associated with constraints (5.49) and using the same notations as in Section 5.5 for the multipliers associated with constraints (5.16) and (1.28), the KKT conditions of Problem 5.15 are given by

$$\sum_{\ell=1}^{L} \omega_\ell - 1 = 0, \tag{5.52}$$

$$\alpha_\ell G_\ell \tilde{q}'_{\ell,1}(G_\ell Q_\ell/\gamma_\ell)(\omega_\ell+\delta_\ell)+\omega_\ell \psi_{GD}^{(i)}\kappa_\ell^{-1}=0, \quad \forall \ell, \tag{5.53}$$

$$\alpha_\ell h_{\ell,M}^{(T_1)}(G_\ell Q_\ell/\gamma_\ell)(\omega_\ell+\delta_\ell)+\lambda=0, \quad \forall \ell. \tag{5.54}$$

In addition, the following complementary slackness conditions hold at the optimum:

$$\omega_\ell(t-\alpha_\ell\gamma_\ell(1-\tilde{q}_{\ell,1}(G_\ell Q_\ell/\gamma_\ell))+\psi_{GD}^{(i)}(\kappa_\ell^{-1}Q_\ell+E_{c,\ell}))=0, \quad \forall \ell, \tag{5.55}$$

$$\delta_\ell(\eta_\ell^{(0)}-\alpha_\ell\gamma_\ell(1-\tilde{q}_{\ell,1}(G_\ell Q_\ell/\gamma_\ell)))=0, \quad \forall \ell, \tag{5.56}$$

$$\lambda\left(\sum_{\ell=1}^{L}\gamma_\ell-1\right)=0. \tag{5.57}$$

We observe an important difference between the KKT conditions related to Problem 5.15 as compared with the ones related to Problem 5.9: $\forall \ell$, the optimality condition (5.54) involves three distinct Lagrangian multipliers, λ, ω_ℓ and δ_ℓ, preventing us from expressing the optimal solution of Problem 5.15 as a function of a single multiplier. Fortunately, in the following lemma whose proof is provided in Appendix C.2, we are able to prove that constraints (1.28) and (5.49) hold with equality.

Lemma 5.6. *At the optimum of Problem 5.15, $\lambda > 0$ and, $\forall \ell$, $\omega_\ell > 0$.*

Since $\lambda > 0$, the KKT conditions (5.53) and (5.54) can be rewritten as follows:

$$\alpha_\ell G_\ell \tilde{q}'_{\ell,1}(G_\ell Q_\ell/\gamma_\ell)(\tilde{\omega}_\ell+\tilde{\delta}_\ell)+\tilde{\omega}_\ell \psi_{GD}^{(i)}\kappa_\ell^{-1}=0, \quad \forall \ell, \tag{5.58}$$

$$\alpha_\ell h_{\ell,M}^{(T_1)}(G_\ell Q_\ell/\gamma_\ell)(\tilde{\omega}_\ell+\tilde{\delta}_\ell)+1=0, \quad \forall \ell, \tag{5.59}$$

with, $\forall \ell$, $\tilde{\omega}_\ell := \omega_\ell/\lambda$ and $\tilde{\delta}_\ell := \delta_\ell/\lambda$.

Thanks to Lemma 5.6, we can use tools from the multilevel waterfilling theory [87] to find the optimal solution of Problem 5.15. The idea is to express the parameters $x_\ell := G_\ell Q_\ell/\gamma_\ell$ (which are equal to $G_\ell E_\ell$) and γ_ℓ as functions of the single parameter t using (5.55). The condition (5.57) is then used to obtain the optimal value of t, enabling us to find the optimal values of γ_ℓ and x_ℓ, and as a consequence the optimal Q_ℓ and then E_ℓ.

Let us define $\tilde{\boldsymbol{\omega}} := [\tilde{\omega}_1, \ldots, \tilde{\omega}_L]$. We also define I_t (resp. $\bar{I}_t$) as the set of links with $\tilde{\delta}_\ell = 0$ (resp. $\tilde{\delta}_\ell > 0$). In the following, we first consider $\tilde{\boldsymbol{\omega}}$ and t as fixed, and we find the optimal values of x_ℓ and γ_ℓ for the links in I_t and $\bar{I}_t$ as a function of t, as well as a characterization of these two sets.

5.7.1 Solution for fixed $\tilde{\omega}$ and t

Case 1: $\ell \in I_t$. From (5.58), we obtain $x^*_{\ell,1}$, the optimal value of x_ℓ, as follows:

$$x^*_{\ell,1}=\tilde{q}'^{-1}_{\ell,1}\left(\frac{-\psi^{(i)}\kappa_\ell^{-1}}{\alpha_\ell G_\ell}\right). \tag{5.60}$$

Using Lemma 5.6 and (5.55), we obtain $\gamma^*_{\ell,1}(t)$, the optimal value of γ_ℓ, depending only on t as:

$$\gamma^*_{\ell,1}(t) = \frac{t + \psi^{(i)}_{GD} E_{c,\ell}}{\alpha_\ell(1 - \tilde{q}_{\ell,1}(x^*_{\ell,1})) - \psi^{(i)}_{GD} \kappa_\ell^{-1} G_\ell^{-1} x^*_{\ell,1}}. \tag{5.61}$$

Lemma 5.7, whose proof is provided in Appendix C.3, enables us to check whether ℓ belongs to I_t or not.

Lemma 5.7. *A link ℓ is in I_t iff the following inequality holds:*

$$t \geq t^T_\ell, \tag{5.62}$$

with $t^T_\ell := -\psi^{(i)}_{GD} E_{c,\ell} + \eta^{(0)}_\ell (1 - (\psi^{(i)}_{GD} \kappa_\ell^{-1} G_\ell^{-1} x^*_{\ell,1})/(\alpha_\ell(1 - \tilde{q}_{\ell,1}(x^*_{\ell,1}))))$.

Case 2: $\ell \in \bar{I}_t$. Optimal solution as a function of $\tilde{\omega}_\ell$ Similarly to the derivations related to Problem 5.9, using (5.58) and (5.59) we obtain $x^*_{\ell,2}(\tilde{\omega}_\ell)$, the optimal x_ℓ, as follows:

$$x^*_{\ell,2}(\tilde{\omega}_\ell) := f^{(T_1)-1}_{\ell,M}\left(\frac{1}{\tilde{\omega}_\ell \psi^{(i)}_{GD} \kappa_\ell^{-1}}\right). \tag{5.63}$$

Since $\tilde{\delta}_\ell > 0$, we obtain from (5.56) $\gamma^*_{\ell,2}(\tilde{\omega}_\ell)$, the optimal γ_ℓ, depending only on $\tilde{\omega}_\ell$ as:

$$\gamma^*_{\ell,2}(\tilde{\omega}_\ell) = \frac{\eta^{(0)}_\ell}{\alpha_\ell(1 - \tilde{q}_{\ell,1}(x^*_{\ell,2}(\tilde{\omega}_\ell)))}. \tag{5.64}$$

We have managed to obtain the optimal values of x_ℓ and γ_ℓ for fixed $\tilde{\boldsymbol{\omega}}$ and t. Now, we turn our attention to exhibit a relation between $\tilde{\omega}_\ell$ and t in order to express $x^*_{\ell,2}(\tilde{\omega}_\ell)$ and $\gamma^*_{\ell,2}(\tilde{\omega}_\ell)$ as function of t.

Relation between $\tilde{\omega}_\ell$ and t. Using Lemma 5.6, we obtain the following L relations by plugging (5.63) and (5.64) into (5.55):

$$t = \mathcal{M}^{(T_1)}_{\ell,M}(\tilde{\omega}_\ell), \quad \forall \ell, \tag{5.65}$$

with $\omega \mapsto \mathcal{M}^{(T_1)}_{\ell,M}(\omega) := \eta^{(0)}_\ell - \psi^{(i)}(\kappa_\ell^{-1} \alpha_\ell^{-1} x^*_{\ell,2}(\omega)/(1 - \tilde{q}_{\ell,1}(x^*_{\ell,2}(\omega))) + E_{c,\ell})$. To express $\tilde{\omega}_\ell$ as a function of t, we use Lemma 5.8, whose proof is provided in Appendix C.4.

Lemma 5.8. *$\forall \ell$, the function $\mathcal{M}^{(T_1)}_{\ell,M}$ is continuous and strictly increasing, and thus $\mathcal{M}^{(T_1)-1}_{\ell,M}$ exists and is strictly increasing.*

Using Lemma 5.8 in conjunction with (5.65) yields

$$\tilde{\omega}_\ell = \mathcal{M}^{(T_1)-1}_{\ell,M}(t), \quad \forall \ell, \tag{5.66}$$

and then we can obtain $\gamma^*_{\ell,2}$ as a function of t by plugging (5.66) into (5.64). As a consequence, $\gamma^*_{\ell,2}(\mathcal{M}^{(T_1)-1}_{\ell,M}(t))$, shortened to $\gamma^*_{\ell,2}(t)$ by abuse of notation, is given by:

$$\gamma^*_{\ell,2}(t) = \frac{\eta^{(0)}_\ell}{\alpha_\ell(1 - \tilde{q}_{\ell,1}(x^*_{\ell,2}(\mathcal{M}^{(T_1)-1}_{\ell,M}(t))))}. \tag{5.67}$$

For a given t, we have succeeded to find a necessary and sufficient condition given in Lemma 5.7 to check whether a node belongs to I_t or $\bar{I}_t$, and we have found the optimal parameters in both cases. Now we search for the optimal value of t.

5.7.2 Search for the optimal t

To find t^*, the optimal value of t, we use the complementary slackness condition (5.57). Let us define the following function representing the sum of the bandwidth parameters for given value of t

$$\tilde{\Gamma}_{GD}(t) := \sum_{\ell \in I_t} \gamma^*_{\ell,1}(t) + \sum_{\ell \in \bar{I}_t} \gamma^*_{\ell,2}(t). \tag{5.68}$$

Due to (5.57), t^* is such that $\tilde{\Gamma}(t^*) = 1$. In the following lemma whose proof is provided in Appendix C.5, we prove that such a t^* always exists, and can be found through a linesearch.

Lemma 5.9. *The function $\tilde{\Gamma}_{GD}(t)$ is continuous, strictly decreasing, and there exists t^* such that $\tilde{\Gamma}_{GD}(t^*) = 1$.*

The optimal solution of Problem 5.15 can be found by solving $\tilde{\Gamma}(t^*) = 1$, which always has a solution. Then, the optimal values $x^*_{\ell,i}(t^*)$ and $\gamma^*_{\ell,i}(t^*)$, $i \in \{1, 2\}$, are computed, and we deduce the optimal $Q^*_\ell(t^*)$.

Algorithm 5.3: Optimal solution of the MMEE Problem 5.7.

Set $\epsilon > 0$, $\psi^{(0)}_{GD} = 0$, $i = 0$, $t^* = \epsilon + 1$.
while $t^* > \epsilon$ **do**
  Compute t^*, $\mathbf{Q}^*$ and $\boldsymbol{\gamma}^*$ by solving Problem 5.15 with $\psi^{(i)}_{GD}$.
  Update $\psi^{(i+1)}_{GD} = \min_{\ell \in \{1,\ldots,L\}} \{\mathcal{E}_\ell(Q^*_\ell/\gamma^*_\ell, \gamma^*_\ell)\}$.
  $i = i + 1$.
end

5.8 MGEE Solution

Due to Lemma 5.2, we know that the MGEE Problem 5.8 can be solved using the Dinkelbach's algorithm [34]. This iterative algorithm requires to solve the following COP at iteration i:

Problem 5.16.

$$\max_{\mathbf{Q},\gamma} \quad \sum_{\ell=1}^{L}(\alpha_\ell\gamma_\ell(1-\tilde{q}_{\ell,1}(G_\ell Q_\ell/\gamma_\ell)) - \nu^{(i)}\kappa_\ell^{-1}Q_\ell), \tag{5.69}$$
$$\text{s.t.} \quad (5.16) \text{ and } (1.28),$$

where $\nu^{(i)} \geq 0$ depends on the optimal solution at iteration $(i-1)$. Using the same notations for the Lagrangian multipliers as for the MSEE Problem 5.5 (i.e., Section 5.5), the KKT conditions of Problem 5.16 write as follows:

$$\alpha_\ell G_\ell \tilde{q}'_{\ell,1}(G_\ell Q_\ell/\gamma_\ell)(1+\delta_\ell) + \nu^{(i)}\kappa_\ell^{-1} = 0, \quad \forall \ell, \tag{5.70}$$

$$\alpha_\ell h_{\ell,M}^{(T_1)}(G_\ell Q_\ell/\gamma_\ell)(1+\delta_\ell) + \lambda = 0, \quad \forall \ell, \tag{5.71}$$

and the complementary slackness conditions are given by

$$\delta_\ell(\eta_\ell^{(0)} - \alpha_\ell\gamma_\ell(1-\tilde{q}_{\ell,1}(G_\ell Q_\ell/\gamma_\ell))) = 0, \quad \forall \ell, \tag{5.72}$$

$$\lambda\left(\sum_{\ell=1}^{L}\gamma_\ell - 1\right) = 0. \tag{5.73}$$

We observe that, if $\forall \ell$ we set $u_\ell^{(i)} = 1$ and $\beta_\ell^{(i)} = \nu^{(i)}$, then the optimality conditions of the MSEE problem, i.e., (5.22)-(5.25) are the same as the ones of the MGEE problem, i.e., (5.70)-(5.73). Hence, we can apply the same procedure to solve Problem 5.16 as the one of 5.9. Algorithm 5.4 depicts the optimal solution of Problem 5.8.

Algorithm 5.4: Optimal solution of the MGEE Problem 5.8.

Set $\epsilon > 0$, $i = 0$, $C_D = \epsilon + 1$.
Set $\nu^{(0)} = 0$.
while $C_D > \epsilon$ **do**
  Set $\lambda^* = -\min_\ell\left\{\alpha_\ell u_\ell h_{\ell,M}^{(T_1)}(x^*_{\ell,\delta_\ell=0})\right\}$, where $\forall \ell$, $x^*_{\ell,\delta_\ell=0}$ is computed as in Lemma 5.4
  if Problem 5.10 is feasible with λ^* **then**
    Find $(\mathbf{Q}^*, \gamma^*)$, Problem 5.9 optimal solution by solving Problem 5.10 using Theorem 5.3 with $\nu^{(i)}$.
  else
    Find $(\mathbf{Q}^*, \gamma^*)$ using a linesearch method with $\nu^{(i)}$ (case 2 in Section 5.5.2)
  Set $C_D = \sum_{\ell=1}^{L}\left(\alpha_\ell\gamma_\ell^*(1-\tilde{q}_{\ell,1}(G_\ell Q_\ell^*/\gamma_\ell^*)) - \nu^{(i)}(\kappa_\ell^{-1}Q_\ell^* + E_{c,\ell})\right)$.
  Set $\nu^{(i+1)} = \mathcal{G}\left(\frac{\mathbf{Q}^*}{\gamma^*}, \gamma^*\right)$.
  Set $i = i + 1$.
end

5.9 Extension to Type-II HARQ

In this Section, we study how to extend the work done for Type-I HARQ under the Rician channel, and for Type-II HARQ under the Rayleigh channel to Type-II HARQ under the Rician channel. Indeed, we did not succeed to identify neither specific properties nor change of variables enabling us to find the optimal solution for the considered RA problems for Type-II HARQ under the Rician channel and thus we seek for suboptimal procedures based on solutions from this Chapter (Type-I HARQ under the Rician channel, this RA will be referred in the sequel as RAIRi) and Chapter 4 (Type-II HARQ under the Rayleigh channel, this RA will be referred in the sequel as RAIIRa). In Table 5.2, we remind the existing solutions performing EE-based RA for Type-I and Type-II HARQ under Rayleigh and Rician channel, where RAIRa is the RA performed for Type-I HARQ under the Rayleigh channel.

Table 5.2: Existing EE-based RA algorithms for HARQ with practical MCS and statistical CSI in the multiuser context.

	Rayleigh channel	Rician channel
Type-I HARQ	[75], Chapter 4 (RAIRa)	This Chapter (RAIRi)
Type-II HARQ	Chapter 4 (RAIIRa)	None

To investigate the extension of Table 5.2 solutions to Type-II HARQ under the Rician channel, we consider the following two possibilities:

1. Applying the resources found by Type-II HARQ Rayleigh RA (i.e., RAIIRa from Chapter 4) to Type-II HARQ system under the Rician channel, leading to what we call here a **channel model mismatch**. The result from this mismatch will be referred to as RAIIRa-IIRi in the sequel.

2. Applying the resources found by Type-I HARQ Rician RA (i.e., RAIRi from this Chapter) to Type-II HARQ system under the Rician channel, leading to what we call here an **HARQ type mismatch**. The result from this mismatch will be referred to as RAIRi-IIRi in the sequel.

In Fig. 5.3, we illustrate the two considered mismatches. For the two above possibilities, we consider a given GNR defined in (1.5), meaning that the ℓth link channel has the same average power $\Delta_\ell = a_\ell^2 + 2\sigma_{h,\ell}^2$. The two approaches differ in the values of a_ℓ and $2\sigma_{h,\ell}^2$ during RA. In the channel model mismatch approach, RA is performed by assuming that $K_\ell = 0$ and thus $a_\ell = 0$ and $\Delta_\ell = 2\sigma_{h,\ell}^2$, whereas in the HARQ type mismatch approach, RA is performed by taking into account the Rician K factor and as a consequence a_ℓ.

Notice that since in this Chapter we do not consider per-link maximum transmit power constraint, we also neglect this constraint when applying the solutions from Chapter 4.

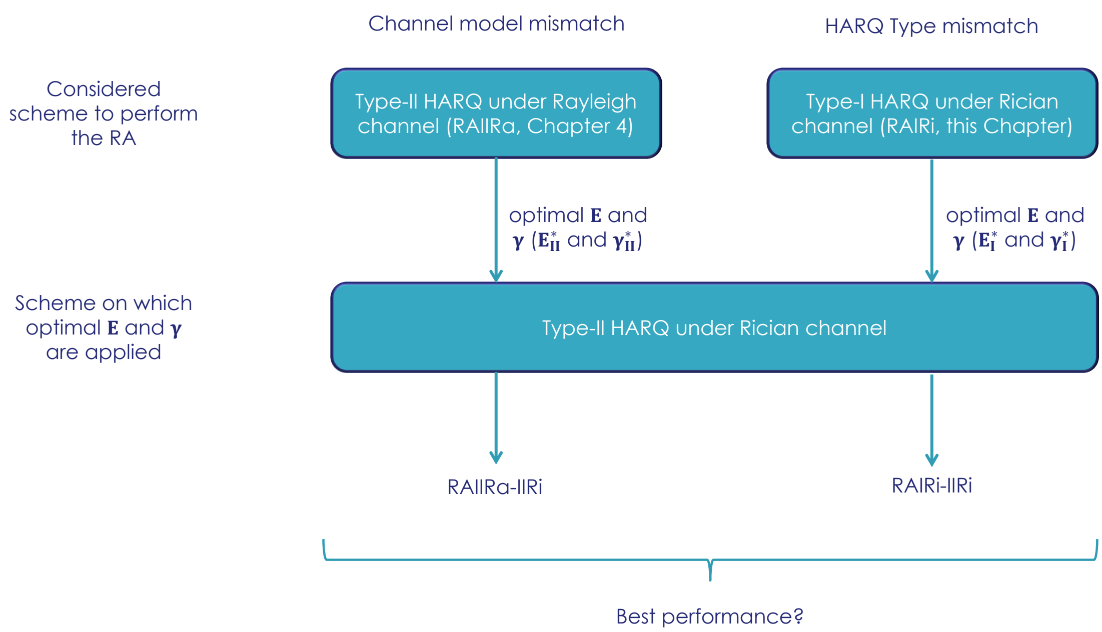

Figure 5.3: The two possible extensions of previous solutions to handle Type-II HARQ under the Rician channel.

To determine the less detrimental mismatch among the two considered ones, we simulate a CC HARQ scheme with $\mathcal{M} = 3$ under the Rician FF channel using the same setup as in Section 5.10. The Rician channel is such that, $\forall \ell$, $K_\ell = 10$. We focus on the MSEE criterion since we are able to optimally solve this problem for both Type-II HARQ under the Rayleigh channel and Type-I HARQ under the Rician channel.

In Fig. 5.4, we plot RAIIRa-IIRi and RAIRi-IIRi versus $\eta_\ell^{(1)}$. We observe that RAIRi-IIRi yields much higher SEE than RAIIRa-IIRi, whatever the value of $\eta_\ell^{(1)}$. Thus, **we advocate an HARQ type mismatch approach rather than a channel model mismatch approach to perform suboptimal Type-II RA under the Rician channel**. It is worth to emphasize that this conclusion only applies to the considered setup (i.e., with neither maximum PER nor maximum transmit power constraints) and thus this subject should deserve more investigations. The material presented in this Section provides a framework to perform such investigations.

5.10 Numerical results

In this Section, the results of the proposed algorithms are numerically studied and compared with the MPO from [77].

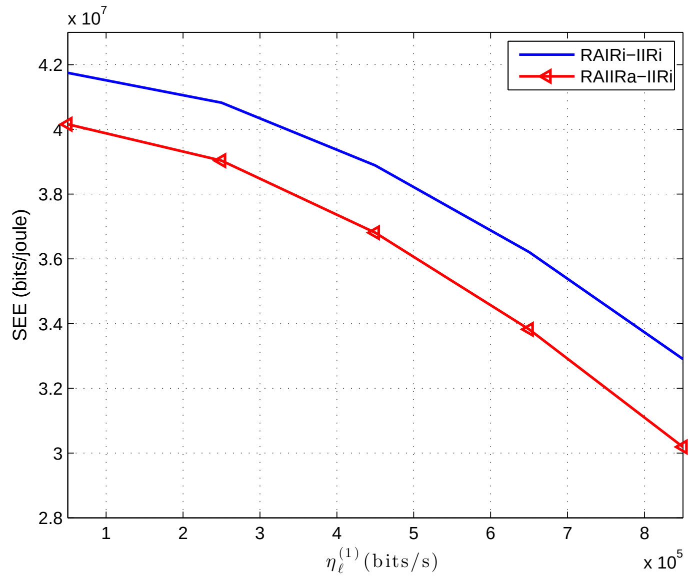

Figure 5.4: RAIIRa-IIRi and RAIRi-IIRi versus $\eta_\ell^{(1)}$.

5.10.1 Setup

We use a convolutional code with rate 1/2 with generator polynomial $[171, 133]_8$, and we use the QPSK modulation, i.e., $m_\ell = 2$. The number of link is $L = 5$ and the link distances $\delta_\ell^{(D)}$ are uniformly drawn in [50 m, 1 km]. We consider that all the links have identical K factor value, and that the minimum goodput constraint is equal for all the links. Unless otherwise stated, we simulate both a Rician channel in which $\forall \ell$, $K_\ell = 10$ and a Rayleigh channel in which $\forall \ell$, $K_\ell = 0$. We set $B = 5$ MHz, $N_0 = -170$ dBm/Hz and $\mathcal{L}_\ell = 128$. The carrier frequency is $f_c = 2\,400$ MHz and we put $\Delta_\ell = (4\pi f_c/c)^{-2}\delta_\ell^{(D)-3}$. We assume that the minimum goodput constraint is equal for all links. We put $\forall \ell$, $P_{ctx,\ell} = P_{crx,\ell} = 0.05$ W and $\kappa_\ell = 0.5$. The results are obtained by averaging through 50 random networks configurations.

5.10.2 Performance analysis

In Figs. 5.5-5.8, we plot the SEE, PEE, MEE and GEE obtained with the proposed criteria and with the MPO versus $\eta_\ell^{(1)}$. We perform the optimal RA according to the links channel distribution: Rayleigh RA under Rayleigh channel and Rician RA under Rician channel. As expected, the maximization of a given criterion yields the highest value for this criterion. The proposed criteria yield higher EE than the MPO, especially for low goodput constraint. In addition, due to the LoS component, the performance under the Rician channel are much higher than those obtained under the Rayleigh channel. This is interesting since considering the Rician channel does not induce additional complexity as compared with considering the conventional Rayleigh channel for the problems

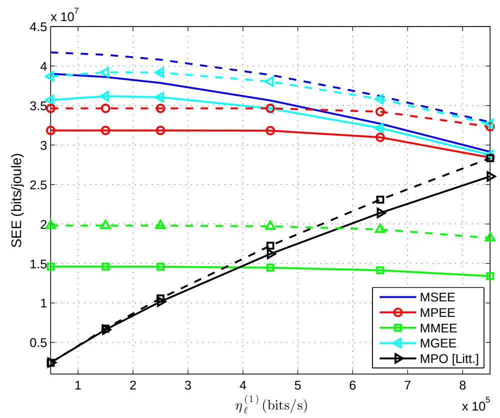

Figure 5.5: SEE obtained for the considered criteria versus $\eta_\ell^{(1)}$, solid lines: Rayleigh channel, dashed lines: Rician channel.

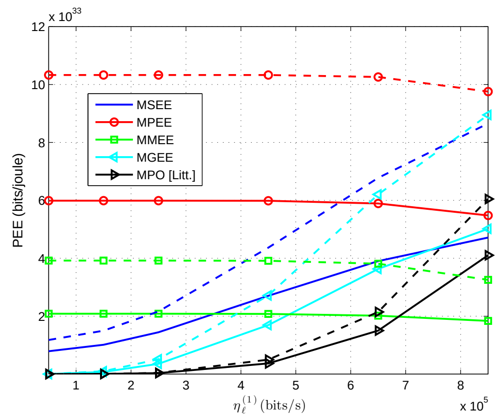

Figure 5.6: PEE obtained for the considered criteria versus $\eta_\ell^{(1)}$, solid lines: Rayleigh channel, dashed lines: Rician channel.

addressed in this Chapter. We can also make the following additional observations.

1. When maximizing a given criterion, increasing the goodput constraint decreases this criterion performance.

2. In Figs. 5.6 and 5.8, we see that increasing $\eta_\ell^{(1)}$ increases the MEE and PEE of both MSEE and MGEE criteria.

3. Increasing the goodput constraint also increases the EE performance of the MPO.

The first observation is explained because increasing $\eta_\ell^{(1)}$ reduces the feasible set of the optimization problems and thus there is less degrees of freedom for the solutions, which degrades the criteria performance.

The second observation is explained because both MSEE and MGEE are unfair criteria, and thus they advantage only the links with good channel quality (see Chapter 4). Increasing $\eta_\ell^{(1)}$ forces these criteria to give more resource to links' with poor quality and since both the PEE and MEE relies on the performance of the links' with poor channel condition, increasing $\eta_\ell^{(1)}$ increases the MSEE and MGEE performance on PEE and MEE.

Finally, the third observation explanation is the following one. The MPO yields low EE since it gives few resource to the link, i.e., Chapters 1 and 4. Increasing $\eta_\ell^{(1)}$ forces the MPO to give more resource to the links', thus increasing their EE.

5.10.3 Channel model mismatch

In this section, we consider the same cases as in Section 5.9, and we investigate the impact of a channel model mismatch on all the criteria. To do so, let us define the gains of the

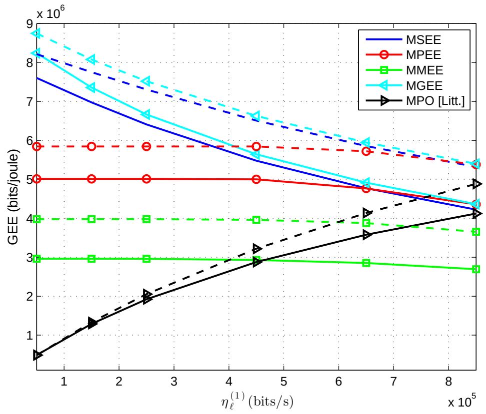

Figure 5.7: GEE obtained for the considered criteria versus $\eta_\ell^{(1)}$, solid lines: Rayleigh channel, dashed lines: Rician channel.

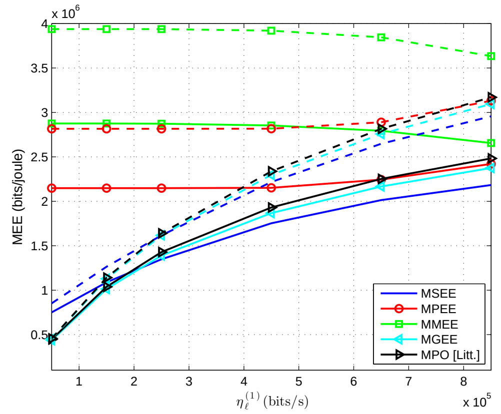

Figure 5.8: MEE obtained for the considered criteria versus $\eta_\ell^{(1)}$, solid lines: Rayleigh channel, dashed lines: Rician channel.

Rician allocation over the Rayleigh one as follows:

$$100 \times \frac{(\mathcal{Z}_G(\mathbf{E}_{\mathrm{I}}^{*,Ri}, \gamma_{\mathrm{I}}^{*,Ri}) - \mathcal{Z}_G(\mathbf{E}_{\mathrm{I}}^{*,Ra}, \gamma_{\mathrm{I}}^{*,Ra}))}{\mathcal{Z}_G(\mathbf{E}_{\mathrm{I}}^{*,Ri}, \gamma_{\mathrm{I}}^{*,Ri})}, \tag{5.74}$$

where $\mathcal{Z}_G(\mathbf{E}, \gamma)$ stands for either the SEE, PEE, MEE or GEE computed for Type-I HARQ under the Rician channel, $\mathbf{E}_{\mathrm{I}}^{*,Ri}$ and $\gamma_{\mathrm{I}}^{*,Ri}$ are the optimal transmit energy and bandwidth parameters obtained using RAIRi, and $\mathbf{E}_{\mathrm{I}}^{*,Ra}$ and $\gamma_{\mathrm{I}}^{*,Ra}$ are the optimal transmit energy and bandwidth parameters obtained using RAIRa.

In Fig. 5.9, we plot the EE gains for the different criteria versus the minimum goodput constraint. We observe that substantial EE gains can be achieved when considering the Rician K factor during the RA process. Especially, we observe that the Rician channel enables for very large PEE (up to more than 55%) and MEE (up to more than 35%) gains, which can be explained as follows. These two metrics highly depends on the worst link's EE. As a consequence, since the EE is higher under the Rician channel than under the Rayleigh one (i.e., Chapter 1), the Rician channel enables us to improve these worst link's EE, improving thus the MPEE and MMEE performance.

In Fig. 5.10, we set $\eta_\ell^{(1)} = 6.5 \times 10^5$ bps, and we plot the criteria gains versus the number of Rician links in the network. We see that the gain is a strictly increasing nearly-linear function of the number of Rician links for all the considered criteria, confirming thus once again that the Rician K factor should be included during the RA process.

5.11 Conclusion

In this Chapter, we first proposed an analytically tractable approximation of the error probability under the Rician FF channel, and second we addressed EE-based RA problems

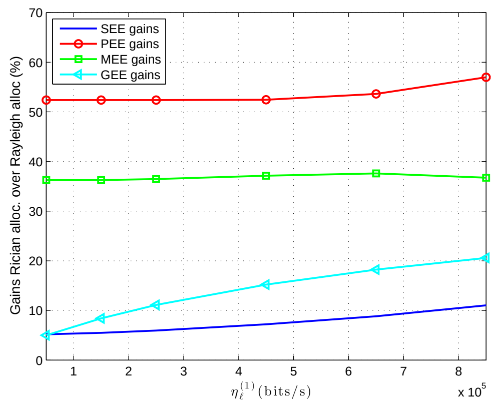

Figure 5.9: Gains between the Rician and the Rayleigh allocations under the Rician channel, versus $\eta_\ell^{(1)}$.

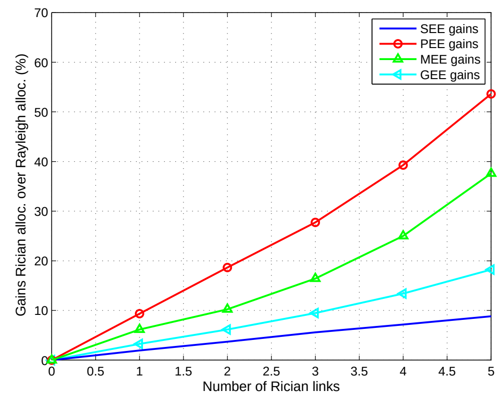

Figure 5.10: Gains between the Rician and the Rayleigh allocations under the Rician channel, versus the number of Rician links.

under the Rician channel in HARQ based MANETs when only statistical CSI is available and considering the use of practical MCS. More precisely, we optimally solved the MSEE, MMEE and MGEE problems whereas we proposed a suboptimal AO based solution for the MPEE one. Table 5.3 summarizes the addressed problems along with the proposed solutions optimality.

Problem	Solutions optimality
MSEE	Optimal
MPEE	Sub-optimal
MMEE	Optimal
MGEE	Optimal

Table 5.3: Addressed problems and optimality of proposed algorithms.

We performed extensive simulations to show that substantial EE gains can be achieved by taking into account the Rician K factor during the RA process instead of only considering the pathloss.

In addition, we also studied how to extentend this work to perform EE-based RA for Type-II HARQ under the Rician channel. We found out that an HARQ type mismatch (i.e., performing the RA considering Type-I HARQ under the Rician channel) produces better SEE performance than a channel model mismatch (i.e., performing the RA considering Type-II HARQ under the Rayleigh channel).

Finally, part of the material presented in this Chapter has been published in [C3], [C6] and [C7]. It is worth noticing that, in [C7], we considered another MSEE problem formulation, yielding completely different derivations to solve the KKT conditions.

Conclusions and Perspectives

The main objective of this thesis was to propose and analyze RA schemes for MANETs assuming that only statistical CSI is available to perform the RA at the RM. This objective was decomposed into the following two intermediate goals:

1. To estimate the channel's statistical CSI, i.e., the Rician K factor with and without shadowing.

2. To propose and analyze new EE-based RA algorithms for MANETs taking into account the use of HARQ and practical MCS, and assuming that only statistical CSI is available.

In Chapter 1, we introduced the technical context of the thesis. We described the considered MANETs along with the signal and the channel models. We provided an introduction to the basics of HARQ. We introduced the EE and formalized EE-based RA problems as constrained optimization ones. Finally, we detailed the two goals of the thesis.

In Chapter 2, we addressed the Rician K factor estimation when the available channel samples are estimated from a training sequence and as a consequence are noisy. We considered both the cases with and without LoS shadowing. In the absence of shadowing, we proposed two deterministic estimators. We also proposed two Bayesian estimators, the mean a posteriori which is approximated using the GHQ, and the maximum a posteriori, which is obtained by solving a non-linear equation. We derived the CRLB in closed-form. We showed that our proposed estimators outperform existing ones from the literature, and we found out that the Bayesian estimators are more robust to small sample size, but they are also more complex. In the presence of shadowing, we proposed two estimation procedures, one based on the EM principle, and the other one based on the MoM. We performed extensive simulations to show the superiority of our proposed estimators as compared with existing ones from the literature. We observed that the MoM-based estimator provides the lowest bias, whereas the EM-based one is better in term of NMSE. We also found that, in certain cases, not considering the shadowing during the estimation might be preferable, and thus we recommend to use shadowing-aware and shadowing-unaware estimators complementarily.

In Chapter 3, we first provided a state of the art of existing works addressing EE-based RA problems. Second, we reviewed the optimization framework that serves as a basis to solve the EE-based RA problems: we provided an overview of convex optimization, fractional programming and geometric programing. Finally, we explained two non-convex optimization procedures.

In Chapter 4, we provided the optimal solutions for the the MSEE, MPEE and MMEE problems under the Rayleigh channel for Type-II HARQ, along with two suboptimal solutions for the MGEE problems. We also provided two suboptimal solutions for the MSEE problems, and showed by simulation that they achieve almost the same performance as the optimal one with much less complexity. We compared the solutions in terms of performance, fairness and complexity and we found out that the MPEE criterion is especially relevant for MANETs. We illustrated the practical relevancy of this criterion on a smartphone example by comparing it to conventional criteria. Through this example, we showed that, as compared with the conventional criteria, *i)* for a given energy, the MPEE can transmit more information packets and *ii)* when transmitting a given number of packets, the MPEE energy consumption is lower. We also provided guidelines regarding the choice of the number of transmissions for the HARQ mechanism.

In Chapter 5, we provided the optimal solutions of MSEE, MMEE and MGEE problems under the Rician channel for Type-I HARQ, along with a suboptimal solution for the MPEE problem. We studied how to extend this work to Type-II HARQ under the Rician channel, and we found out that an HARQ type mismatch is preferable to a channel model mismatch, i.e., when performing a Type-II HARQ under the Rician channel, the RA for Type-I HARQ under the Rician channel provides better result than the one for Type-II HARQ under the Rayleigh channel. Finally, we provided numerical results to exhibit the interest of taking into account the existence of a LoS when performing the RA rather than only considering the channel power. In other words, we showed that incorporating the knowledge of the Rician K factor during the RA enables substantial EE gains.

Our contributions related to the estimation of the Rician K factor (i.e., Chapter 2) are summarized in Table 5.4, whereas our contributions related to RA (i.e., Chapters 4 and 5) are summarized in Table 5.5.

No LoS shadowing	Four new estimators + deterministic CRLB
Nakagami-m LoS shadowing	Two new estimators

Table 5.4: Summary of the thesis contributions on the estimation of the Rician K factor.

	Type-I HARQ, Rician channel	Type-II HARQ, Rayleigh channel
MSEE	Optimal	Optimal + 2 suboptimals
MPEE	Suboptimal	Optimal
MMEE	Optimal	Optimal
MSEE	Optimal	2 suboptimals

Table 5.5: Summary of the thesis contributions on the EE-based RA problems.

Perspectives

The following issues should deserve to be addressed in future works.

System design

All our algorithms have been proposed and validated assuming ideal fully interleaved fading channel. Moreover, the RA algorithms assumed perfect knowledge of the channel's statistics. Therefore, it should be of high practical interest to study *i)* the impact of both frequency and time correlation on the estimation and the RA performance and *ii)* using channel's statistics estimated using our estimators from Chapter 2 in the RA algorithms.

Estimation of the Rician K factor

1. In practical communications, the Rician K factor is likely to be time-varying, for instance if the transmitter moves from a place with LoS to another place with no LoS, the Rician K factor is likely to decrease suddenly. Thus, being able to track the Rician K factor time-variation should be of great interest, in order to constantly adapt the RA. We have conducted some preliminary works regarding this perspective (not presented in this document) which have been patented in [P1], where we proposed to use a sliding window in conjunction with tools from change detection theory [8].

2. In Chapter 2, the noise variance $2\sigma_n^2$ is considered as known. However, in practice, this variance has to be estimated and it is thus of interest to study solutions to perform this estimation.

Resource allocation

1. The algorithms developed in Chapters 4 and 5 require either the use of the IPM, or several numerical functions inversion, which might be too complex for embedded systems. Some recent works have proposed the use of neural networks to alleviate the RA complexity [29, 68, 122], and it should be of interest to study how to apply this framework to our algorithms.

2. Our proposed solutions are centralized and a perspective for the future should be to study solutions to perform the RA in a distributed fashion.

3. We performed RA assuming that only statistical CSI is available at the RM. Incorporating more knowledge regarding the channel would increase the algorithms performance, for instance, it is shown in [56, 103] that using Accumulated Mutual Information (ACMI) for power or rate adaptation between HARQ transmissions yields substantial gains as compared with persistent RA. However, using this type of CSI requires more exchanges of information between the nodes and thus, an interesting perspective is to study the tradeoff between the achievable performance gains and the additional exchange requirements.

Appendix A

Appendix related to Chapter 2

A.1 Derivations leading to (2.9)

Here, we present the derivations yielding the unbiased estimator $\hat{K}^n_{Prop}$ in (2.9). To find an unbiased estimator of K in the noisy case, we study the bias of $\hat{K}_{ML}$ from (2.5) when the channel coefficients are noisy. We rewrite (2.5) when the channel coefficients are replaced by their noisy estimation:

$$\hat{K}_{ML} = \frac{|\tilde{a}|^2}{2\tilde{\sigma}^2}. \tag{A.1}$$

We observe that $\tilde{a}$ is a complex Gaussian random variable with mean $ae^{j\theta_0}$ and variance $\lambda = N^{-1}(2\sigma_h^2 + 2\sigma_n^2)$. Therefore, $X = 2|\tilde{a}|^2/\lambda$ follows a noncentral χ^2 distribution with two degrees of freedom and noncentrality parameter $\omega = 2a^2/\lambda$. Also, we can prove that $Y = 4\tilde{\sigma}^2/\lambda$ follows a central χ^2 distribution with degrees of freedom $2N-2$. Moreover, using the Cochran's theorem [55], we know that X and Y are independent.

Following similar lines as [7], we define

$$\hat{K}' = \frac{X/2}{Y/(2N-2)}. \tag{A.2}$$

Since $\hat{K}'$ is the ratio of a noncentral χ^2 distributed random variable with a central χ^2 distributed random variable, which are independent and both normalized by their respective degrees of freedom, $\hat{K}'$ has a noncentral F distribution with degrees of freedom 2 and $2N-2$ and noncentrality parameter ω. Its mathematical expectation can be found in [60] and is given by:

$$\mathbb{E}\left[\hat{K}'\right] = \frac{(2N-2)(2+\omega)}{2(2N-4)}. \tag{A.3}$$

Since $\hat{K}_{ML} = (N-1)^{-1}\hat{K}'$, the expectation of $\hat{K}_{ML}$ can be deduced as

$$\mathbb{E}\left[\hat{K}_{ML}\right] = \frac{1+\frac{\omega}{2}}{N-2}. \tag{A.4}$$

Observing that

$$\frac{\omega}{2} = N\frac{\sigma_h^2}{\sigma_h^2+\sigma_n^2}K \tag{A.5}$$

leads to

$$\mathbb{E}[\hat{K}_{ML}] = \frac{1 + KN\alpha}{N-2}, \tag{A.6}$$

where $\alpha = \sigma_h^2/(\sigma_h^2 + \sigma_n^2)$.

The bias of $\hat{K}_{ML}$ in case of noisy coefficients is obtained from (A.6) and is expressed as $\mathbb{E}[\hat{K}_{ML} - K] = (N-2)^{-1}(1 + K(N\alpha - N + 2))$. Using this expression, we deduce the following unbiased estimator of K:

$$\hat{K}^n_{Prop} = \frac{1}{N\alpha}\left((N-2)\frac{|\tilde{\mu}|^2}{2\tilde{\sigma}^2} - 1\right). \tag{A.7}$$

Notice that, as a byproduct of the previous derivations, we can derive the variance of $\hat{K}_{ML}$ in case of noisy channel coefficients, which is given by $Var[\hat{K}_{ML}] = (2N-4)^{-1}(N-3)^{-1}((2N-4)^{-1}(\omega+2)^2 + 2\omega + 2)$. Moreover, we can also derive both the bias and the variance of $\hat{K}_{MML}$ when the coefficients are noisy, which are given by

$$\mathbb{E}[\hat{K}_{MML} - K] = K(\alpha - 1), \tag{A.8}$$

$$Var[\hat{K}_{MML}] = N^{-2}(N-2)^2 Var[\hat{K}_{ML}]. \tag{A.9}$$

A.2 Derivations leading to (2.10)

In this appendix, we present the derivations yielding the unbiased estimation of α (2.10). In (2.9), α has to be estimated, and a natural estimator of α is $\tilde{\alpha} = (\tilde{\sigma}^2 - \sigma_n^2)/\tilde{\sigma}^2$. Let us study the bias of $\tilde{\alpha}$. To do so, we write

$$\mathbb{E}[\tilde{\alpha}] = 1 - \sigma_n^2 \mathbb{E}\left[\frac{1}{\tilde{\sigma}^2}\right]. \tag{A.10}$$

From Appendix A.1, we know that $4\tilde{\sigma}^2/\lambda$ follows a χ^2 distribution with degrees of freedom $2N-2$. Then, $\lambda/(4\tilde{\sigma}^2)$ follows an inverse chi-square distribution with degrees of freedom $2N-2$, and its expectation is given by [113]:

$$\mathbb{E}[\tilde{\alpha}] = 1 - \frac{N\sigma_n^2}{(N-2)(\sigma_n^2 + \sigma_h^2)}. \tag{A.11}$$

We thus derive an unbiased estimator of α as:

$$\tilde{\alpha} = 1 + \frac{(2-N)2\sigma_n^2}{2N\tilde{\sigma}^2}. \tag{A.12}$$

A.3 Proof of Result 2.2

In this Appendix, we derive the RR of $\hat{K}^n_{Prop}$. Replacing α by $\tilde{\alpha}$ in (2.9) and plugging the resulting expression into (2.11) yields after straightforward algebraic manipulations:

$$R_r\left(\hat{K}^n_{Prop}\right) = \Pr\left(\left(\tilde{\alpha} < 0 \cap (N-2)\frac{|\tilde{a}|^2}{2\tilde{\sigma}^2} - 1 > 0\right) \cup \left(\tilde{\alpha} > 0 \cap (N-2)\frac{|\tilde{a}|^2}{2\tilde{\sigma}^2} - 1 < 0\right)\right), \tag{A.13}$$

which can be rewritten as:

$$R_r\left(\hat{K}^n_{Prop}\right) = A_{Rr} + B_{Rr}, \tag{A.14}$$

with $A_{Rr} := \Pr\left(\tilde{\alpha} < 0 \cap (N-2)\frac{|\tilde{a}|^2}{2\tilde{\sigma}^2} - 1 > 0\right)$ and $B_{Rr} := \Pr\left(\tilde{\alpha} > 0 \cap (N-2)\frac{|\tilde{a}|^2}{2\tilde{\sigma}^2} - 1 < 0\right)$. First, let us focus on computing A_{Rr}. Plugging (2.10) into A_{Rr} yields after some algebraic manipulations:

$$A_{Rr} = \Pr\left(2\tilde{\sigma}^2 < C_{1,Rr} \cap 2\tilde{\sigma}^2 < C_{2,Rr}|\tilde{a}|^2\right), \tag{A.15}$$

Using the independence of $|\tilde{a}|^2$ and $2\tilde{\sigma}^2$ (see Appendix A.1), (A.15) can be rewritten as:

$$A = \int_{x=0}^{+\infty}\int_{y=0}^{\min\{C_{1,Rr},C_{2,Rr}x\}} f_{|\tilde{a}|^2}(x) f_{2\tilde{\sigma}^2}(y) dx dy, \tag{A.16}$$

with $f_{|\tilde{a}|^2}(x)$ (resp. $f_{2\tilde{\sigma}^2}(y)$) the PDF of $|\tilde{a}|^2$ (resp. $2\tilde{\sigma}^2$). From Appendix A.1, we know that $2|\tilde{a}|^2/\lambda$ has a noncentral χ^2 distribution with two degrees of freedom and noncentrality parameter $\omega = 2|a|^2/\lambda$, and that $4\tilde{\sigma}^2/\lambda$ follows a central χ^2 distribution with $2N-2$ degrees of freedom. Thus we know from [89] that:

$$f_{|\tilde{a}|^2}(x) = \frac{1}{\lambda} e^{-\frac{x}{\lambda}-\frac{\omega}{2}} I_0\left(\sqrt{\frac{2x\omega}{\lambda}}\right), \tag{A.17}$$

$$f_{2\tilde{\sigma}^2}(y) = \frac{1}{\lambda}\frac{1}{\Gamma(N-1)}\left(\frac{x}{\lambda}\right)^{N-2} e^{-\frac{x}{\lambda}}. \tag{A.18}$$

The integrals in (A.16) can be separated as follows:

$$A_{Rr} = \int_{x=0}^{C_{1,Rr}/C_{2,Rr}} f_{|\tilde{a}|^2}(x) \int_{y=0}^{C_{2,Rr}x} f_{2\tilde{\sigma}^2}(y) dx dy + \int_{x=C_{1,Rr}/C_{2,Rr}}^{+\infty} f_{|\tilde{a}|^2}(x) \int_{y=0}^{C_{1,Rr}} f_{2\tilde{\sigma}^2}(y) dx dy \tag{A.19}$$

yielding

$$A_{Rr} = \int_{x=0}^{C_{1,Rr}/C_{2,Rr}} f_{|\tilde{a}|^2}(x) F_{2\tilde{\sigma}^2}(C_{2,Rr}x) dx + F_{2\tilde{\sigma}^2}(C_{1,Rr}) \int_{x=C_{1,Rr}/C_{2,Rr}}^{+\infty} f_{|\tilde{a}|^2}(x) dx, \tag{A.20}$$

with $F_{2\tilde{\sigma}^2}(y)$ the CDF of $2\tilde{\sigma}^2$, which writes as [89]:

$$F_{2\tilde{\sigma}^2}(y) = \frac{\gamma_{IC}\left(N-1, \frac{y}{\lambda}\right)}{\Gamma(N-1)}. \tag{A.21}$$

By performing similar algebraic manipulations, B_{Rr} in (A.14) can be obtained as:

$$B_{Rr} = (1 - F_{2\tilde{\sigma}^2}(C_{1,Rr})) \int_{x=0}^{C_{1,Rr}/C_{2,Rr}} f_{|\tilde{a}|^2}(x) dx + \int_{x=C_{1,Rr}/C_{2,Rr}}^{+\infty} f_{|\tilde{a}|^2}(x)(1 - F_{2\tilde{\sigma}^2}(C_{2,Rr}x)) dx. \tag{A.22}$$

Plugging (A.20) and (A.22) into (A.14) yields:

$$\begin{aligned} R_r\left(\hat{K}^n_{Prop}\right) =& 1 + F_{2\tilde{\sigma}^2}(C_{1,Rr})\left(\int_{C_{1,Rr}/C_{2,Rr}}^{+\infty} f_{|\tilde{a}|^2}(x) dx - \int_0^{C_{1,Rr}/C_{2,Rr}} f_{|\tilde{a}|^2}(x) dx\right) - \\ & \int_{C_{1,Rr}/C_{2,Rr}}^{+\infty} f_{|\tilde{a}|^2}(x) F_{2\tilde{\sigma}^2}(C_{2,Rr}x) dx + \int_0^{C_{1,Rr}/C_{2,Rr}} f_{|\tilde{a}|^2}(x) F_{2\tilde{\sigma}^2}(C_{2,Rr}x) dx. \end{aligned} \tag{A.23}$$

Also, $F_{|\tilde{a}|^2}(x) := \int_0^x f_{|\tilde{a}|^2}(u)du$ is the CDF of $|\tilde{a}|^2$, which is given by [89]

$$F_{|\tilde{a}|^2}(x) = 1 - Q_1\left(\sqrt{\omega}, \sqrt{\frac{2x}{\lambda}}\right), \tag{A.24}$$

concluding the proof.

A.4 Derivations leading to (2.35)

In this Appendix, we derive the Fisher information matrix (2.35). To this end, we compute the derivative involved in (2.33):

$$\frac{\partial^2 \log\left(\mathbb{L}_{\hat{\mathbf{H}}}^{(Ns)}\left(\hat{\mathbf{H}};\boldsymbol{\theta}^{(Ns)}\right)\right)}{\partial\left(2\sigma_h^2\right)^2} = \frac{1}{\left(2\sigma_h^2+2\sigma_n^2\right)^3}\left(N\left(2\sigma_h^2+2\sigma_n^2\right) - 2A_{CRLB} - 2Na^2 + 4aB_{CRLB}\right), \tag{A.25}$$

$$\frac{\partial^2 \log\left(\mathbb{L}_{\hat{\mathbf{H}}}^{(Ns)}\left(\hat{\mathbf{H}};\boldsymbol{\theta}^{(Ns)}\right)\right)}{\partial(a)^2} = -\frac{N}{\sigma_h^2+\sigma_n^2}, \tag{A.26}$$

$$\frac{\partial^2 \log\left(\mathbb{L}_{\hat{\mathbf{H}}}^{(Ns)}\left(\hat{\mathbf{H}};\boldsymbol{\theta}^{(Ns)}\right)\right)}{\partial(\theta_0)^2} = -\frac{a}{\sigma_h^2+\sigma_n^2}B_{CRLB}, \tag{A.27}$$

$$\frac{\partial^2 \log\left(\mathbb{L}_{\hat{\mathbf{H}}}^{(Ns)}\left(\hat{\mathbf{H}};\boldsymbol{\theta}^{(Ns)}\right)\right)}{\partial a\partial 2\sigma_h^2} = \frac{1}{2\left(\sigma_h^2+\sigma_n^2\right)^2}\left(Na - B_{CRLB}\right), \tag{A.28}$$

$$\frac{\partial^2 \log\left(\mathbb{L}_{\hat{\mathbf{H}}}^{(Ns)}\left(\hat{\mathbf{H}};\boldsymbol{\theta}^{(Ns)}\right)\right)}{\partial a\partial\theta_0} = \frac{1}{\sigma_h^2+\sigma_n^2}C_{CRLB}, \tag{A.29}$$

$$\frac{\partial^2 \log\left(\mathbb{L}_{\hat{\mathbf{H}}}^{(Ns)}\left(\hat{\mathbf{H}};\boldsymbol{\theta}^{(Ns)}\right)\right)}{\partial 2\sigma_h^2\partial\theta_0} = -\frac{a}{2\left(\sigma_h^2+\sigma_n^2\right)^2}C_{CRLB}, \tag{A.30}$$

with $A_{CRLB} := \sum_{i=1}^N (r_i)^2$, $B_{CRLB} := \sum_{i=1}^N r_i \cos\left(\phi_i - \theta_0\right)$ and $C_{CRLB} := \sum_{i=1}^N r_i \sin\left(\phi_i - \theta_0\right)$.

Using $\mathbb{E}\left[A_{CRLB}\right] = N\left(a^2 + 2\sigma_h^2 + 2\sigma_n^2\right)$, $\mathbb{E}\left[B_{CRLB}\right] = Na$ and $\mathbb{E}\left[C_{CRLB}\right] = 0$ into (A.25)-(A.30) yields (2.35).

A.5 Derivations leading to (2.56) and (2.57)

In this Appendix, we compute the closed form expressions of $T_k(n)$, $k = 0,\ldots,3$, $n = 1,\ldots,N$.

First, let us focus on $T_k(n), k = 0,1,2$. Plugging (2.41) and (2.4) into (2.54) yields, for $n = 1,\ldots,N$

$$T_k(n) = C_n^{(c),(t)} \int_0^{+\infty} x^{2\hat{m}_{Na}^{(S),(t)}-1+k} e^{-x^2\mathcal{B}_{2,n}^{(t)} - x\mathcal{B}_{3,n}^{(t)}} dx. \tag{A.31}$$

The integral in (A.31) can be computed using [49, 3.462] which yields (2.56).

Now, let us compute $T_3(n)$. To do so, we use the following relationship [93]:

$$\int_0^{+\infty} \log(x) g(x) dx = \frac{\partial}{\partial w} \int_0^{+\infty} x^w g(x) dx|_{w=0}. \tag{A.32}$$

Plugging (2.41) and (2.4) into (2.55) and using (A.32), we obtain for $n = 1, \dots, N$

$$T_3(n) = C_n^{(c),(t)} \frac{\partial}{\partial w} \left(\int_0^{+\infty} x^{2\hat{m}_{Na}^{(S),(t)} - 1 + w} e^{-x^2 \mathcal{B}_{2,n}^{(t)} - x\mathcal{B}_{3,n}^{(t)}} dx \right)|_{w=0}. \tag{A.33}$$

Using once again [49, 3.462], we can compute (A.33) as follows:

$$T_3(n) = C_n^{(c),(t)} e^{\frac{\left(\mathcal{B}_{3,n}^{(t)}\right)^2}{8\mathcal{B}_{2,n}^{(t)}}} \frac{\partial}{\partial w} \left(\left(2\mathcal{B}_{2,n}^{(t)}\right)^{-\frac{2\hat{m}_{Na}^{(S),(t)} + w}{2}} \Gamma\left(2\hat{m}_{Na}^{(S),(t)} + w\right) D_{-2\hat{m}_{Na}^{(S),(t)} - w} \left(\frac{\mathcal{B}_{3,n}^{(t)}}{\sqrt{2\mathcal{B}_{2,n}^{(t)}}} \right) \right)|_{w=0}. \tag{A.34}$$

Finally, (2.57) is obtained by computing the derivative in (A.34).

Appendix B

Appendix related to Chapter 4

B.1 Proof of Theorem 4.2

Here, we optimally solve Problem 4.8. To do so, let us define $\boldsymbol{\delta} = [\delta_1, ..., \delta_L]$, $\boldsymbol{\mu} = [\mu_1, ..., \mu_L]$ and λ as the non-negative Lagrangian multipliers associated with constraints (4.39), (4.40) and (4.41), respectively. The KKT conditions of Problem 4.8 write:

$$\frac{H_\ell M_\ell}{(J_\ell \gamma_\ell + M_\ell)^2} - \delta_\ell + \mu_\ell - \lambda = 0, \quad \forall \ell. \tag{B.1}$$

Moreover, the following complementary slackness conditions hold at the optimum:

$$\mu_\ell(\gamma_\ell - \gamma_{\min,\ell}) = 0, \quad \forall \ell, \tag{B.2}$$

$$\delta_\ell(\gamma_\ell - \gamma_{\max,\ell}) = 0, \quad \forall \ell, \tag{B.3}$$

$$\lambda(\sum_{\ell=1}^{L} \gamma_\ell - 1) = 0. \tag{B.4}$$

To solve the optimality conditions (B.1)-(B.4), we proceed in two steps: first, we solve them for fixed value of λ, and second we find the optimal value of λ.

Step 1: solution for fixed λ Here, we discuss the possible values of δ_ℓ and μ_ℓ in order to exhibit the solution of (B.1)-(B.4) as a function of λ.

Case 1): $\delta_\ell > 0, \mu_\ell > 0$: the complementary slackness conditions (B.2) and (B.3) gives us $\gamma_\ell^* = \gamma_{\min,\ell} = \gamma_{\max,\ell}$, meaning that γ_ℓ can take only one value. Let $I_{\bar{\mu},\bar{\delta}} \subseteq \{1, \cdots, L\}$ denote the set of links for which $\delta_\ell > 0, \mu_\ell > 0$.

Case 2) $\delta_\ell > 0, \mu_\ell = 0$: the complementary slackness condition (B.3) gives us $\gamma_\ell^* = \gamma_{\max,\ell}$, whereas the KKT condition (B.1) yields

$$\lambda < \frac{H_\ell M_\ell}{(J_\ell \gamma_{\max,\ell} + M_\ell)^2}. \tag{B.5}$$

Let $I_{\mu,\bar{\delta}} \subseteq \{1, \cdots, L\}$ denote the set of links for which $\delta_\ell > 0, \mu_\ell = 0$.

Case 3) $\delta_\ell = 0, \mu_\ell > 0$: according to (B.2), we have $\gamma_\ell^* = \gamma_{\min,\ell}$ and similarly to the previous case, (B.1) gives us the following inequality

$$\lambda > \frac{H_\ell M_\ell}{(J_\ell \gamma_{\min,\ell} + M_\ell)^2}. \tag{B.6}$$

Let $I_{\bar{\mu},\delta} \subseteq \{1, \cdots, L\}$ denote the set of links for which $\delta_\ell = 0, \mu_\ell > 0$.

Case 4) $\delta_\ell = 0, \mu_\ell = 0$: in this case, we have from (B.1)

$$\frac{F_\ell J_\ell}{(H_\ell \gamma_\ell + J_\ell)^2} = \lambda. \tag{B.7}$$

We can see that γ_ℓ is the solution of a quadratic equation, which can be obtained as

$$\gamma_\ell^* = -\frac{M_\ell}{J_\ell} + \frac{\sqrt{H_\ell M_\ell \lambda}}{\lambda J_\ell}. \tag{B.8}$$

Let $I_{\mu,\delta} \subseteq \{1, \cdots, L\}$ denote the set of links for which $\delta_\ell = 0, \mu_\ell = 0$.

The solutions of cases 1 to 4 can be written in the following compact form

$$\gamma_\ell^* = \left[-\frac{M_\ell}{J_\ell} + \frac{\sqrt{H_\ell M_\ell \lambda}}{\lambda J_\ell} \right]_{\gamma_{\min,\ell}}^{\gamma_{\max,\ell}}. \tag{B.9}$$

We have expressed the optimal solution of Problem 4.8 as a function of the unique multiplier λ. Now, we focus on finding the optimal value of this Lagrangian multiplier.

Step 2: search for optimal λ To find the optimal value of λ, we use the complementary slackness condition (B.4). In details, we form the sum of the optimal value of the bandwidth sharing factors

$$\Gamma(\Lambda) = \sum_{\ell \in I_{\bar{\mu},\bar{\delta}}} \gamma_{\min,k} + \sum_{\ell \in I_{\mu,\bar{\delta}}} \gamma_{\max,\ell} + \sum_{\ell \in I_{\bar{\mu},\delta}} \gamma_{\min,\ell} + \sum_{\ell \in I_{\mu,\delta}} \left(-\frac{M_\ell}{J_\ell} + \frac{\sqrt{H_\ell M_\ell \lambda}}{\lambda J_\ell} \right). \tag{B.10}$$

We have the following property concerning Γ.

Proposition B.1. *Γ is a continuous non increasing function of Λ.*

Proof. To prove Proposition B.1, we first define $\forall \ell \in \{1, L\}$, $\Lambda_\ell = H_\ell M_\ell / (J_\ell \gamma_{\max,\ell} + M_\ell)^{-2}$ and $\forall \ell \in \{L+1, 2L\}$, $\Lambda_\ell = H_\ell M_\ell / (J_\ell \gamma_{\min,\ell} + M_\ell)^{-2}$. Moreover, we define ℓ'_m as a one-to-one mapping from $\{1, 2L\}$ in itself such that $\Lambda_{\ell'_1} \leq \ldots \leq \Lambda_{\ell'_{2L}}$. First of all, we see that $\Gamma(\Lambda)$ is continuous on every open set $(\Lambda_{\ell' i}, \Lambda_{\ell'_{i+1}})$ since the three first term of the Right-Hand Side (RHS) of (B.10) are constants, and the function $F_{T,\ell}$ defined for all ℓ as

$$F_{T,\ell}(x) = -\frac{M_\ell}{J_\ell} + \frac{\sqrt{H_\ell M_\ell}}{\sqrt{x} J_\ell} \tag{B.11}$$

is continuous on $\mathbb{R}^{+*}$. Moreover, it can be proved that F_ℓ is strictly decreasing on $\mathbb{R}^{+*}$, which implies that Γ is also decreasing on $(\Lambda_{\ell' i}, \Lambda_{\ell'_{i+1}})$. Finally, one can check that, $\forall i$, Γ is continuous in $\Lambda_{\ell'_i}$, concluding the proof. ◻

We have the following two possibilities for the optimal solution of Problem 4.8.

Either $\sum_{\ell=1}^{L}\gamma_{\max,\ell} \le 1$. Since the objective function of Problem 4.8 is increasing in γ, the optimal solution is $\forall k \in \{1,\cdots,L\}, \gamma_\ell^* = \gamma_{\max,\ell}$.

Or $\sum_{\ell=1}^{L}\gamma_{\max,\ell} > 1$. In this case, the optimal value of λ is strictly positive, and thus λ has to be increased such that $\Gamma(\lambda) = 1$. Therefore, the optimal solution of Problem 4.8 is given in this case by $\forall \ell \in \{1,\cdots,L\}, \gamma_\ell^* = \left[-M_\ell/J_\ell + \sqrt{H_\ell M_\ell \lambda^*}/(\lambda^* J_\ell)\right]_{\gamma_{\min,\ell}}^{\gamma_{\max,\ell}}$ where λ^* is the unique solution of $\Gamma(\lambda^*) = 1$ on $\mathbb{R}^{+*}$.

Finally, from (B.5), one can see that $\Gamma(\Lambda)$ is constant as long as $\Lambda \ge \max_\ell(\frac{H_\ell M_\ell}{(J_\ell \gamma_{\min,k}+M_\ell)^2})$. Therefore, we can deduce that λ^* is upper bounded as follows

$$\lambda^* \le \max_{\ell\in\{1,\cdots,L\}} \left(\frac{H_\ell M_\ell}{(J_\ell \gamma_{\min,\ell} + M_\ell)^2}\right). \tag{B.12}$$

Similarly, we can obtain the following lower-bound for the optimal λ:

$$\lambda^* \ge \min_{\ell\in\{1,\cdots,L\}} \left(\frac{H_\ell M_\ell}{(J_\ell \gamma_{\max,\ell} + M_\ell)^2}\right). \tag{B.13}$$

Eq. (B.12) and (B.13) facilitate the search of λ^*, which can be performed with the bisection method.

B.2 Optimal solution of the maximum goodput problem

In this Appendix, we find the optimal solution of the MGO problem, which writes as:

Problem B.1.

$$\begin{aligned} \max_{\mathbf{E},\gamma} \quad & \sum_{\ell=1}^{L} \frac{\tilde{D}_\ell(G_\ell E_\ell)}{\gamma_\ell^{-1}\tilde{S}_\ell(G_\ell E_\ell)}, \\ \text{s.t.} \quad & (4.6), (1.27) \text{ and } (1.28). \end{aligned} \tag{B.14}$$

Applying the change of variables (4.21)-(4.22) to Problem B.1 enables us to rewrite it equivalently as:

Problem B.2.

$$\max_{\mathbf{E},\gamma} \quad \sum_{\ell=1}^{L} \frac{f_\ell(x_\ell)}{e^{-y_\ell}(1 + \sum_{p=1}^{M-1} a_{\ell,p} e^{-x_\ell d_{\ell,p}})}, \tag{B.15}$$

$$\text{s.t.} \quad (4.23), (4.24) \text{ and } (4.25). \tag{B.16}$$

Following same steps as for the proof of Result 4.2, one can check that Problem B.2 is the maximization of a sum of ratios whose numerators are concave and denominators are convex over a convex set. Hence, similarly to the MSEE problem, the Jong's algorithm allows us to optimally solve it.

Appendix C

Appendix related to Chapter 5

C.1 Proof of Lemma 5.4

First due to (5.23), we are only interested in solutions yielding non-positive values for $h^{(T_1)}_{\ell,M}(x)$. If there exists at least one link ℓ_1 with $\delta_{\ell_1} = 0$, we obtain the optimal value of x_{ℓ_1} using (5.22) as:

$$x^*_{\ell_1} = x^*_{\ell_1,\delta_{\ell_1}=0} = \tilde{q}'^{-1}_{\ell_1}\left(\frac{-\beta^{(i)}_{\ell_1}\kappa^{-1}_{\ell_1}}{\alpha_{\ell_1}G_{\ell_1}}\right). \tag{C.1}$$

By plugging (C.1) into (5.23), we obtain the optimal value of λ as:

$$\lambda^* = -\alpha_{\ell_1}u^{(i)}_{\ell_1}h^{(T_1)}_{\ell_1,M}(x^*_{\ell_1,\delta_{\ell_1}=0}) \geq 0. \tag{C.2}$$

Hence, we prove that $\ell_1 \in \arg\min_\ell\{\alpha_\ell u^{(i)}_\ell h^{(T_1)}_{\ell,M}(x_{\ell,\delta_\ell=0})\}$. To do so, we proceed by contradiction: we assume that $\exists \ell_2$ such that $\alpha_{\ell_2}u^{(i)}_{\ell_2}h^{(T_1)}_{\ell_2,M}(x^*_{\ell_2,\delta_{\ell_2}=0}) < \alpha_{\ell_1}u^{(i)}_{\ell_1}h^{(T_1)}_{\ell_1,M}(x^*_{\ell_1,\delta_{\ell_1}=0})$, and we prove that the KKT condition (5.23) cannot hold for ℓ_2. This condition writes as follows:

$$\alpha_{\ell_2}u^{(i)}_{\ell_2}h^{(T_1)}_{\ell_2,M}(x^*_{\ell_2})(u^{(i)}_{\ell_2} + \delta_{\ell_2}) - \alpha_{\ell_1}u^{(i)}_{\ell_1}h^{(T_1)}_{\ell_1,M}(x^*_{\ell_1,\delta_{\ell_1}=0}) = 0. \tag{C.3}$$

To prove that (C.3) cannot hold, we upper bound it by a term stricly lower than 0. To this end, we use the following proposition.

Lemma C.1. *$\forall \ell$, the following inequality holds:*

$$h^{(T_1)}_{\ell,M}(x^*_\ell) \leq h^{(T_1)}_{\ell,M}(x^*_{\ell,\delta_{\ell=0}}). \tag{C.4}$$

Proof. First, let us study the monotonicity of $h^{(T_1)}_{\ell,M}(x)$ by computing its first order derivative:

$$h^{(T_1)'}_{\ell,M}(x) = -x\tilde{q}''_{\ell,1}(x). \tag{C.5}$$

Due to the strict convexity of $\tilde{q}_{\ell,1}$, it results from (C.5) that $h^{(T_1)}_{\ell,M}(x)$ is strictly decreasing.

Second, let us compare x^*_ℓ with $x^*_{\ell,\delta_{\ell=0}}$. From (5.22), we have

$$x^*_\ell = \tilde{q}'^{-1}_{\ell,1}\left(\frac{-u^{(i)}_\ell \beta^{(i)}_\ell \kappa^{-1}_\ell}{\alpha_\ell G_\ell(u^{(i)}_\ell + \delta_\ell)}\right). \tag{C.6}$$

Since $\tilde{q}'^{-1}_{\ell,1}$ is strictly increasing, the following inequality holds

$$x^*_\ell \geq x^*_{\ell,\delta_\ell=0}. \tag{C.7}$$

Finally, the proof is completed using (C.5). □

Using Proposition C.1 we can upper bound (C.3) as follows

$$\begin{aligned} &\alpha_{\ell_2} u^{(i)}_{\ell_2} h^{(T_1)}_{\ell_2,M}(x^*_{\ell_2})(u^{(i)}_{\ell_2} + \delta_{\ell_2}) - \alpha_{\ell_1} u^{(i)}_{\ell_1} h^{(T_1)}_{\ell_1,M}(x^*_{\ell_1,\delta_{\ell_1}=0}) \leq \\ &\alpha_{\ell_2} u^{(i)}_{\ell_2} h^{(T_1)}_{\ell_2,M}(x^*_{\ell_2,\delta_{\ell_2}=0})(u^{(i)}_{\ell_2} + \delta_{\ell_2}) - \alpha_{\ell_1} u^{(i)}_{\ell_1} h^{(T_1)}_{\ell_1,M}(x^*_{\ell_1,\delta_{\ell_1}=0}). \end{aligned} \tag{C.8}$$

Since by hypothesis, $\alpha_{\ell_2} u_{\ell_2} h^{(T_1)}_{\ell_2,M}(x^*_{\ell_2,\delta_{\ell_2}=0}) < \alpha_{\ell_1} u_{\ell_1} h^{(T_1)}_{\ell_1,M}(x^*_{\ell_1,\delta_{\ell_1}=0})$, $\alpha_{\ell_1} u_{\ell_1} h^{(T_1)}_{\ell_1,M}(x^*_{\ell_1,\delta_{\ell_1}=0}) = -\lambda^* \leq 0$ and $\delta_{\ell_2} \geq 0$, we obtain from (C.8)

$$\alpha_{\ell_2} u^{(i)}_{\ell_2} h^{(T_1)}_{\ell_2,M}(x^*_{\ell_2})(u^{(i)}_{\ell_2} + \delta_{\ell_2}) - \alpha_{\ell_1} u^{(i)}_{\ell_1} h^{(T_1)}_{\ell_1,M}(x^*_{\ell_1,\delta_{\ell_1}=0}) < 0. \tag{C.9}$$

Due to (C.9), the KKT condition (5.23) cannot hold for link ℓ_2 yielding a contradiction and thus concluding the proof.

C.2 Proof of Lemma 5.6

First, let us prove that $\lambda > 0$. We need the following intermediate result, whose proof is provided in [28].

Proposition C.1. *[28, Proposition 2] At any iteration i, the optimal t for Problem 5.15 is such that $t \geq 0$.*

The rest of the proof of Lemma 5.6 is by contradiction: we assume that $\lambda = 0$, and we prove that it yields a strictly negative value for t, which contradicts Proposition C.1. To do so, we remark from (5.52) that $\sum_{\ell=1}^{L} \omega_\ell = 1$, meaning that $\exists \ell$ such that $\omega_\ell > 0$. Let us focus on this link. We consider the following two possible cases: either $\delta_\ell = 0$ or $\delta_\ell > 0$.

Case 1: $\delta_\ell = 0$. Using (5.53) and (5.54), we obtain:

$$\alpha_\ell(\tilde{q}_{\ell,1}(x_\ell) - 1) + \frac{x_\ell \kappa^{-1}_\ell \psi^{(i)}_{GD}}{G_\ell} = 0, \tag{C.10}$$

with $x_\ell := G_\ell Q_\ell / \gamma_\ell$. In addition, since $\omega_\ell > 0$, plugging (C.10) into (5.55) yields

$$t = \gamma_\ell \left(\alpha_\ell(1 - \tilde{q}_{\ell,1}(x_\ell)) - \frac{x_\ell \psi^{(i)}_{GD} \kappa^{-1}_\ell}{G_\ell}\right) - \psi^{(i)}_{GD} E_{c,\ell} = -\psi^{(i)}_{GD} E_{c,\ell} < 0. \tag{C.11}$$

Case 2: $\delta_\ell > 0$. The condition (5.53) gives us:

$$\alpha_\ell(-1 + \tilde{q}_{\ell,1}(x_\ell) - x_\ell \tilde{q}'_{\ell,1}(x_\ell)) = 0. \tag{C.12}$$

Since $\delta_\ell > 0$, we obtain:

$$\gamma_\ell = \frac{\eta_\ell^{(0)}}{\alpha_\ell(1 - \tilde{q}_{\ell,1}(x_\ell))}. \tag{C.13}$$

By plugging (C.12) and (C.13) into (5.55), we obtain

$$t = \eta_\ell^{(0)}\left(1 + \frac{\psi_{GD}^{(i)}\kappa_\ell^{-1}}{\alpha_\ell G_\ell \tilde{q}'_{\ell,1}(x_\ell)}\right) - \psi_{GD}^{(i)} E_{c,\ell}. \tag{C.14}$$

To upper bound (C.14), we use (5.54) which gives us

$$\frac{\psi_{GD}^{(i)}\kappa_\ell^{-1}}{\alpha_\ell G_\ell \tilde{q}'_{\ell,1}(x_\ell)} < -1. \tag{C.15}$$

Using (C.15) into (C.14) yields $t < 0$.

Gathering case 1 and case 2 together, we obtain that $\lambda = 0$ yields $t < 0$, contradicting Proposition C.1. Hence, we deduce that $\lambda > 0$.

Now, let us prove that, $\forall \ell$, $\omega_\ell > 0$. Assume that there exists ℓ such that $\omega_\ell = 0$. We can see from (5.53) that $\delta_\ell = 0$. However, plugging $\omega_\ell = 0$ and $\delta_\ell = 0$ into (5.54) implies $\lambda = 0$, which contradicts $\lambda > 0$. Hence, $\forall \ell$, $\omega_\ell > 0$ which concludes the proof.

C.3 Proof of Lemma 5.7

First, assume that a link ℓ belongs to I_t. Its optimal values for x_ℓ and γ_ℓ are given by (5.60) and (5.61), respectively. Moreover, link ℓ has to satisfy its goodput constraint (5.16). By plugging (5.60) and (5.61) into (5.16), the direct part of Lemma 5.7 is proved.

Second, we prove the converse part of Lemma 5.7 by contradiction: assuming that there exists a link ℓ such that inequality (5.62) holds and which is not in I_t, we prove that the optimality condition (5.56) cannot hold. Let us define $x^*_{\ell,2}(\delta_\ell)$ (resp. $\gamma^*_{\ell,2}(\delta_\ell, t)$) the optimal value of x_ℓ (resp. γ_ℓ) for fixed ω_ℓ and t. Notice that $x^*_{\ell,2}(0)$ (resp. $\gamma_{\ell,2}(0, t)$) coincides with $x^*_{\ell,1}$ (resp. $\gamma^*_{\ell,1}(t)$). With these notations, (5.62) can be rewritten as follows:

$$\eta_\ell^{(0)} \leq \alpha_\ell \gamma^*_{\ell,2}(0, t)(1 - \tilde{q}_{\ell,1}(x^*_{\ell,2}(0))). \tag{C.16}$$

Since $\delta_\ell > 0$, (5.56) yields:

$$\eta_\ell^{(0)} = \alpha_\ell \gamma^*_{\ell,2}(\delta_\ell, t)(1 - \tilde{q}_{\ell,1}(x^*_{\ell,2}(\delta_\ell))). \tag{C.17}$$

To show the contradiction, we prove that (C.17) cannot hold using the following proposition.

Proposition C.2. *For all $\delta_\ell > 0$ and $\forall \ell$, the following inequalities hold:*

$$x^*_{\ell,2}(\delta_\ell) > x^*_{\ell,2}(0) \tag{C.18}$$

$$\gamma^*_{\ell,2}(\delta_\ell, t) > \gamma^*_{\ell,2}(0, t) \tag{C.19}$$

Proof. We start by proving (C.18). Using (5.59), we obtain

$$x^*_{\ell,2}(\delta_\ell) = \tilde{q}'^{-1}_{\ell,1}\left(\frac{-\omega_\ell \psi^{(i)}_{GD}\kappa^{-1}_\ell}{\alpha_\ell G_\ell(\omega_\ell + \delta_\ell)}\right). \tag{C.20}$$

Since $\tilde{q}'^{-1}_{\ell,1}$ is continuous, differentiable with non zero derivative and strictly increasing, $x^*_{\ell,2}(\delta_\ell)$ is a continuous, differentiable and strictly increasing function of δ_ℓ, which proves (C.18).

Now, let us focus on $\gamma^*_{\ell,2}(\delta_\ell, t)$. Using Lemma 5.6, we can obtain:

$$\gamma^*_{\ell,2}(\delta_\ell, t) = \frac{t + \psi^{(i)}_{GD}E_{c,\ell}}{p^{(T_1)}_\ell(\delta_\ell)}, \tag{C.21}$$

with $p^{(T_1)}_\ell(\delta_\ell) := \alpha_\ell(1 - \tilde{q}_{\ell,1}(x^*_{\ell,2}(\delta_\ell)) - \psi^{(i)}_{GD}\kappa^{-1}_\ell G^{-1}_\ell x^*_{\ell,2}(\delta_\ell)$. To prove (C.19), let us prove that $p^{(T_1)}_\ell(\delta_\ell)$ is strictly decreasing by computing its derivative:

$$p^{(T_1)'}_\ell(\delta_\ell) = -x^{*'}_{\ell,2}(\delta_\ell)\mathcal{V}_\ell(\delta_\ell), \tag{C.22}$$

with $x^{*'}_{\ell,2}(\delta_\ell) > 0$ the derivative of $x^*_{\ell,2}(\delta_\ell)$ with respect to δ_ℓ, and $\mathcal{V}_\ell(\delta_\ell) := (\alpha_\ell \tilde{q}'_{\ell,1}(x^*_{\ell,2}(\delta_\ell)) + \psi^{(i)}_{GD}\kappa^{-1}_\ell G^{-1}_\ell)$. Using (C.20), we can see that $\mathcal{V}_\ell(0) = 0$, meaning that $p'_\ell(0) = 0$. In addition, we can prove that $\mathcal{V}_\ell(\delta_\ell)$ is strictly increasing by computing its derivative, meaning that, for all $\delta_\ell > 0$, $\mathcal{V}_\ell(\delta_\ell) > 0$ which, together with (C.22) concludes the proof. □

Using Proposition C.2, we hence have, for all $\delta_\ell > 0$:

$$\alpha_\ell \gamma^*_{\ell,2}(\delta_\ell, t)(1 - \tilde{q}_{\ell,1}(x^*_{\ell,2}(\delta_\ell))) > \alpha_\ell \gamma^*_{\ell,2}(0, t)(1 - \tilde{q}_{\ell,1}(x^*_{\ell,2}(0))) \geq \eta^{(0)}_\ell, \tag{C.23}$$

which contradicts (C.17) and concludes the proof.

C.4 Proof of Lemma 5.8

To prove Lemma 5.8, it is sufficient to prove that, $\forall \ell$, $\mathcal{F}^{(T_1)}_{\ell,M}(\omega_\ell) := x^*_{\ell,2}(\omega_\ell)/(1 - \tilde{q}_{\ell,1}(x^*_{\ell,2}(\omega_\ell)))$ is strictly decreasing. Let us compute the derivative of $\mathcal{F}^{(T_1)}_\ell(\omega_\ell)$:

$$\mathcal{F}^{(T_1)'}_{\ell,M}(\omega_\ell) = -\frac{x^{*'}_{\ell,2}(\omega_\ell)h^{(T_1)}_{\ell,M}(x^*_{\ell,2}(\omega_\ell))}{(1 - \tilde{q}_{\ell,1}(x^*_{\ell,2}(\omega_\ell)))^2}, \tag{C.24}$$

with $x^{*'}_{\ell,2}(\omega_\ell) = -1/(\omega^2_\ell \psi^{(i)}_{GD}\kappa^{-1}_\ell)(f^{(T_1)-1}_{\ell,M})'(\omega^{-1}_\ell \kappa_\ell/\psi^{(i)}_{GD}) < 0$. Moreover, due to (5.59), we are only interested in the values of $x^*_{\ell,2}(\omega_\ell)$ such that $h^{(T_1)}_{\ell,M}(\omega_\ell) < 0$. As a consequence, $\mathcal{F}^{(T_1)}_{\ell,M}(\omega_\ell)$ is strictly decreasing and it follows that $\mathcal{M}^{(T_1)}_{\ell,M}(\omega_\ell)$ is strictly increasing, which concludes the proof.

C.5 proof of Lemma 5.9

Let us define k'_m a one-to-one mapping from $\{1, \cdots, L\}$ in itself such that $t^T_{k'_1} \leq \cdots \leq t^T_{k'_L}$ where $t^T_{k'_i}$ is defined in (5.62). To prove Theorem 5.9, we first observe that the first term in the RHS of $\tilde{\Gamma}_{GD}(t)$ is continuous and strictly increasing on every open set $(t^T_{k'_i}, t^T_{k'_{i+1}})$. Second, let us prove that the second term is also strictly increasing. To this end, we remind that $\gamma^*_{\ell,2}(t)$ is expressed as

$$\gamma^*_{\ell,2}(t) = \frac{\eta^{(0)}_\ell}{\alpha_\ell(1 - \tilde{q}_{\ell,1}(x^*_{\ell,2}(\mathcal{M}^{(T_1)-1}_{\ell,M}(t))))}. \tag{C.25}$$

Since $\mathcal{M}^{(T_1)-1}_{\ell,M}(t)$ is strictly increasing and $x^*_{\ell,2}(\tilde{\omega}_\ell)$ is strictly decreasing, we infer that $1 - \tilde{q}_{\ell,1}(x^*_{\ell,2}(\mathcal{M}^{(T_1)-1}_{\ell,M}(t)))$ is decreasing and as a consequence $\gamma^*_{\ell,2}(t)$ is strictly increasing. Third, it can be checked that $\tilde{\Gamma}_{GD}(t)$ is continuous in every $t^T_{k'_i}$ by checking that $\lim_{t \nearrow t^T_{k'_i}} \tilde{\Gamma}_{GD}(t) = \lim_{t \searrow t^T_{k'_i}} \tilde{\Gamma}_{GD}(t)$.

Finally, by letting $\tilde{t}$ be sufficiently small, one can show that $\gamma^*_{\ell,2}(t)$ goes to $\eta^{(0)}_\ell / \alpha_\ell$, and we have $\sum_{\ell=1}^L \eta^{(0)}_\ell / \alpha_\ell \leq 1$ (otherwise the problem would be infeasible). Moreover, when t is sufficiently large, it is clear that $\tilde{\Gamma}_{GD}(t) > 1$. Hence, there exists t^* such that $\tilde{\Gamma}_{GD}(t^*) = 1$, which concludes the proof.

Bibliography

[1] A. Abdi, C. Tepedelenlioglu, M. Kaveh, and G. Giannakis, "On the estimation of the K parameter for the rice fading distribution," **IEEE Communications Letters**, vol. 5, no. 3, pp. 92–94, Mar. 2001. Cited pages 27 and 28

[2] A. Abdi, W. C. Lau, M. S. Alouini, and M. Kaveh, "A new simple model for land mobile satellite channels: first- and second-order statistics," **IEEE Transactions on Wireless Communications**, vol. 2, no. 3, pp. 519–528, May 2003. Cited page 10

[3] M. Abramowitz and I. A. Stegun, **Handbook of mathematical functions, with formulas, graphs, and mathematical tables**, 20th ed., ser. Applied Mathematics. National Bureau of Standards, Jun. 1972, vol. 55. Cited pages 36 and 44

[4] M. I. Andries, P. Besnier, and C. Lemoine, "Rician channels in a RC: statistical uncertainty of K estimations versus K fluctuations due to unstirred paths," in **Proceedings of the 5th European Conference on Antennas and Propagation (EUCAP)**, Apr. 2011, pp. 1758–1762. Cited page 33

[5] G. Azemi, B. Senadji, and B. Boashash, "Ricean K-factor estimation in mobile communication systems," **IEEE Communications Letters**, vol. 8, no. 10, pp. 617–619, Oct. 2004. Cited pages 27 and 28

[6] K. Baddour and T. Willink, "Improved estimation of the ricean K-factor from I/Q fading channel samples," **IEEE Transactions on Wireless Communications**, vol. 7, no. 12, pp. 5051–5057, Dec. 2008. Cited pages 27, 28, 32, 33, and 39

[7] ——, "Improved estimation of the ricean K factor from I/Q samples," in **IEEE Vehicular Technology Conference (VTC) Fall**, 2007, pp. 1228–1232. Cited page 135

[8] M. Basseville, I. V. Nikiforov **et al.**, **Detection of abrupt changes: theory and application**, vol. 104. Cited page 133

[9] N. C. Beaulieu and Y. Chen, "Map estimation of the ricean K factor," **Canadian Journal of Electrical and Computer Engineering**, vol. 38, no. 2, pp. 130–131, Spring 2015. Cited pages 27 and 28

[10] A. Ben-Tal and A. Nemirovski, **Lectures on modern convex optimization: analysis, algorithms, and engineering applications**. Siam, 2001, vol. 2. Cited page 62

[11] F. Boccardi, R. W. Heath, A. Lozano, T. L. Marzetta, and P. Popovski, "Five disruptive technology directions for 5G," **IEEE Communications Magazine**, vol. 52, no. 2, pp. 74–80, Feb. 2014. Cited page 7

[12] E. Boshkovska, D. W. K. Ng, N. Zlatanov, and R. Schober, "Practical non-linear energy harvesting model and resource allocation for SWIPT systems," **IEEE Communications Letters**, vol. 19, no. 12, pp. 2082–2085, Dec. 2015. Cited page 67

[13] B. Bossy, P. Kryszkiewicz, and H. Bogucka, "Optimization of energy efficiency in the downlink LTE transmission," in **IEEE International Conference on Communications (ICC)**, May 2017. Cited pages 58, 59, and 65

[14] N. Bouhlel and A. Dziri, "Maximum likelihood parameter estimation of nakagami-gamma shadowed fading channels," **IEEE Communications Letters**, vol. 19, no. 4, pp. 685–688, Apr. 2015. Cited page 45

[15] S. Boyd and L. Vandenberghe, **Convex optimization**. Cambridge university press, 2004. Cited pages 59, 62, 79, 80, 87, 93, 111, 114, 115, and 120

[16] G. Caire, G. Taricco, and E. Biglieri, "Bit-interleaved coded modulation," **IEEE Transactions on Information Theory**, vol. 44, no. 3, pp. 927–946, May 1998. Cited page 9

[17] A. Charnes and W. W. Cooper, "Programming with linear fractional functionals," **Naval Research logistics quarterly**, vol. 9, no. 3-4, pp. 181–186, 1962. Cited page 93

[18] A. Chelli, E. Zedini, M. S. Alouini, J. R. Barry, and M. Pätzold, "Performance and delay analysis of hybrid ARQ with incremental redundancy over double rayleigh fading channels," **IEEE Transactions on Wireless Communications**, vol. 13, no. 11, pp. 6245–6258, Nov. 2014. Cited page 57

[19] Y. Chen and N. Beaulieu, "Estimation of ricean K parameter and local average SNR from noisy correlated channel samples," **IEEE Transactions on Wireless Communications**, vol. 6, no. 2, pp. 640–648, Feb. 2007. Cited pages 27 and 28

[20] ——, "Estimation of ricean and nakagami distribution parameters using noisy samples," in **IEEE International Conference on Communications**, Jun. 2004, pp. 562–566 Vol.1. Cited pages 27, 28, 32, and 39

[21] ——, "Estimators using noisy channel samples for fading distribution parameters," **IEEE Transactions on Communications**, vol. 53, no. 8, pp. 1274–1277, Aug. 2005. Cited pages 27 and 28

[22] ——, "Maximum likelihood estimation of the K factor in ricean fading channels," **IEEE Communications Letters**, vol. 9, no. 12, pp. 1040–1042, Dec. 2005. Cited pages 27, 28, 32, and 35

[23] M. Chiang, "Geometric programming for communication systems," **Foundations and Trends® in Communications and Information Theory**, vol. 2, no. 1–2, pp. 1–154, 2005. Cited page 59

[24] M. Chiang, C. W. Tan, D. P. Palomar, O. Daniel, D. Julian **et al.**, "Power control by geometric programming," **IEEE Transactions on Wireless Communications**, vol. 6, no. 7, pp. 2640–2651, Jul. 2007. Cited pages 89 and 90

[25] J. Choi, J. Ha, and H. Jeon, "On the energy delay tradeoff of HARQ-IR in wireless multiuser systems," **IEEE Transactions on Communications**, vol. 61, no. 8, pp. 3518–3529, August 2013. Cited pages 58 and 59

[26] M. Conti and S. Giordano, "Mobile ad hoc networking: milestones, challenges, and new research directions," **IEEE Communications Magazine**, vol. 52, no. 1, pp. 85–96, Jan. 2014. Cited page 1

[27] S. L. Cotton, "Human body shadowing in cellular device-to-device communications: Channel modeling using the shadowed $\kappa - \mu$ fading model," **IEEE Journal on Selected Areas in Communications**, vol. 33, no. 1, pp. 111–119, Jan. 2015. Cited page 10

[28] J. Crouzeix, J. Ferland, and S. Schaible, "An algorithm for generalized fractional programs," **Journal of Optimization Theory and Applications**, vol. 47, no. 1, pp. 35–49, 1985. Cited pages 64, 66, 114, 120, and 146

[29] P. de Kerret, D. Gesbert, and M. Filippone, "Team deep neural networks for interference channels," in **IEEE International Conference on Communications Workshops (ICC Workshops)**, May 2018, pp. 1–6. Cited page 133

[30] A. P. Dempster, N. M. Laird, and D. B. Rubin, "Maximum likelihood from incomplete data via the em algorithm," **Journal of the royal statistical society. Series B (methodological)**, pp. 1–38, 1977. Cited pages 45 and 46

[31] J. Denis, M. Pischella, and D. L. Ruyet, "Resource allocation for asynchronous cognitive radio networks with FBMC/OFDM under statistical CSI," in **IEEE International Conference on Acoustics, Speech and Signal Processing (ICASSP)**, Mar. 2016, pp. 3656–3660. Cited page 69

[32] ——, "Energy-efficiency-based resource allocation framework for cognitive radio networks with FBMC/OFDM," **IEEE Transactions on Vehicular Technology**, vol. 66, no. 6, pp. 4997–5013, Jun. 2017. Cited pages 58 and 59

[33] J. Denis, S. Smirani, B. Diomande, T. Ghariani, and B. Jouaber, "Energy-efficient coordinated beamforming for multi-cell multicast networks under statistical CSI," in **IEEE International Workshop on Signal Processing Advances in Wireless Communications (SPAWC)**, Jul. 2017. Cited pages 58 and 59

[34] W. Dinkelbach, "On nonlinear fractional programming," **Management science**, vol. 13, no. 7, pp. 492–498, 1967. Cited pages 65, 114, and 123

[35] A. Dogandzic and J. Jin, "Maximum likelihood estimation of statistical properties of composite gamma-lognormal fading channels," **IEEE Transactions on Signal Processing**, vol. 52, no. 10, pp. 2940–2945, Oct. 2004. Cited page 45

[36] B. Du, C. Pan, W. Zhang, and M. Chen, "Distributed energy-efficient power optimization for CoMP systems with max-min fairness," **IEEE Communications Letters**, vol. 18, no. 6, pp. 999–1002, Jun. 2014. Cited pages 58 and 59

[37] E. Eraslan and B. Daneshrad, "Low-complexity link adaptation for energy efficiency maximization in MIMO-OFDM systems," **IEEE Transactions Wireless Communications**, vol. 16, no. 8, pp. 5102–5114, Aug. 2017. Cited page 57

[38] E. Eraslan, C. Y. Wang, and B. Daneshrad, "Practical energy-aware link adaptation for MIMO-OFDM systems," **IEEE Transactions on Wireless Communications**, vol. 13, no. 1, pp. 246–258, Jan. 2014. Cited page 108

[39] J. J. Escudero-Garzás, B. Devillers, and A. García-Armada, "Fairness-adaptive goodput-based resource allocation in ofdma downlink with arq," **IEEE Transactions on Vehicular Technology**, vol. 63, no. 3, pp. 1178–1192, March 2014. Cited page 16

[40] D. Falconer, S. L. Ariyavisitakul, A. Benyamin-Seeyar, and B. Eidson, "Frequency domain equalization for single-carrier broadband wireless systems," **IEEE Communications Magazine**, vol. 40, no. 4, pp. 58–66, Apr. 2002. Cited page 74

[41] D. Feng, C. Jiang, G. Lim, L. J. Cimini, G. Feng, and G. Y. Li, "A survey of energy-efficient wireless communications," **IEEE Communications Surveys Tutorials**, vol. 15, no. 1, pp. 167–178, Feb. 2013. Cited page 17

[42] P. Frenger, S. Parkvall, and E. Dahlman, "Performance comparison of HARQ with chase combining and incremental redundancy for HSDPA," in **IEEE Vehicular Technology Conference (VTC) Fall**, Oct. 2001. Cited page 13

[43] P. K. Frenger, P. Orten, T. Ottosson, and A. B. Svensson, “Rate-compatible convolutional codes for multirate DS-CDMA systems,” **IEEE Transactions Communications**, vol. 47, no. 6, pp. 828–836, Jun. 1999. Cited pages 15 and 96

[44] J. Gaveau, C. J. Le Martret, and M. Assaad, “Grouping of subcarriers and effective snr statistics in wideband ofdm systems using eesm,” in **IEEE International Conference on Wireless and Mobile Computing, Networking and Communications (WiMob)**, Oct. 2017, pp. 1–7. Cited page 30

[45] S. Ge, Y. Xi, H. Zhao, S. Huang, and J. Wei, “Energy efficient optimization for CC-HARQ over block Rayleigh fading channels,” **IEEE Communications Letters**, vol. 19, no. 10, pp. 1854–1857, Oct. 2015. Cited page 57

[46] A. Z. Ghanavati and D. Lee, “Optimizing the bit transmission power for link layer energy efficiency under imperfect CSI,” **IEEE Transactions Wireless Communications**, vol. 17, no. 1, pp. 29–40, Jan. 2018. Cited page 57

[47] G. Giunta, C. Hao, and D. Orlando, “Estimation of rician K-factor in the presence of nakagami-m shadowing for the los component,” **IEEE Wireless Communications Letters**, pp. 1–1, 2018. Cited pages 27, 28, 31, 44, 45, 51, and 52

[48] A. Goldsmith, **Wireless communications**. Cambridge university press, 2005. Cited page 109

[49] I. S. Gradshteyn and I. M. Ryzhik, **Table of integrals, series, and products**. Academic press, 2014. Cited pages 33, 45, and 139

[50] L. Greenstein, D. Michelson, and V. Erceg, “Moment-method estimation of the ricean K-factor,” **IEEE Communications Letters**, vol. 3, no. 6, pp. 175–176, Jun. 1999. Cited pages 27 and 28

[51] J. A. Gubner, “A new formula for lognormal characteristic functions,” **IEEE Transactions on Vehicular Technology**, vol. 55, no. 5, pp. 1668–1671, Sep. 2006. Cited page 36

[52] A. Hadjtaieb, A. Chelli, and M. S. Alouini, “Maximizing the spectral and energy efficiency of ARQ with a fixed outage probability,” in **International Wireless Communications and Mobile Computing Conference (IWCMC)**, Aug. 2015. Cited page 57

[53] J. Hagenauer, “Rate-compatible punctured convolutional codes (RCPC codes) and their applications,” **IEEE Transactions on Communications**, vol. 36, no. 4, pp. 389–400, Apr. 1988. Cited page 14

[54] Z. K. Ho, V. K. Lau, and R. S. Cheng, “Cross-layer design of FDD-OFDM systems based on ACK/NACK feedbacks,” **IEEE Transactions on Information Theory**, vol. 55, no. 10, pp. 4568–4584, Oct. 2009. Cited page 94

[55] P. G. Hoel **et al.**, “Introduction to mathematical statistics.” **Introduction to mathematical statistics.**, no. 2nd Ed, 1954. Cited page 135

[56] M. Jabi, L. Szczecinski, M. Benjillali, and F. Labeau, “Outage minimization via power adaptation and allocation in truncated hybrid arq,” **IEEE Transactions on Communications**, vol. 63, no. 3, pp. 711–723, Mar. 2015. Cited page 134

[57] M. Jabi, M. Benjillali, L. Szczecinski, and F. Labeau, “Energy efficiency of adaptive HARQ,” **IEEE Transactions on Communications**, vol. 64, no. 2, pp. 818–831, Feb. 2016. Cited page 57

[58] R. Jain, D.-M. Chiu, and W. R. Hawe, **A quantitative measure of fairness and discrimination for resource allocation in shared computer system**, 1984, vol. 38. Cited page 98

[59] F. Jemni, W. Bchimi, I. Bousnina, and A. Samet, "Closed-form cramer-rao lower bounds of the ricean K-factor estimates from I/Q data," in **IEEE International Workshop on Signal Processing Advances in Wireless Communications (SPAWC)**, Jun. 2010, pp. 1–5. Cited pages 28 and 38

[60] N. L. Johnson and S. Kotz, **Distributions in Statistics: Continuous Univariate Distributions: Vol.: 2**. Houghton Mifflin, 1970. Cited page 135

[61] Y. Jong, "An efficient global optimization algorithm for nonlinear sum-of-ratios problem," **[Online], Available: http://www.optimization-online.org/DB_HTML/2012/08/3586.html**, 2012. Cited pages 64, 67, 81, 114, and 115

[62] S. M. Kay, **Fundamentals of statistical signal processing: estimation theory**. Prentice-Hall, Inc., 1993. Cited pages 28, 32, 36, 37, and 38

[63] S. Kim and H. Yu, "Energy-efficient HARQ-IR for massive MIMO systems," **IEEE Transactions on Communications**, pp. 1–1, 2018. Cited page 57

[64] S. Kim, B. G. Lee, and D. Park, "Energy-per-bit minimized radio resource allocation in heterogeneous networks," **IEEE Transactions on Wireless Communications**, vol. 13, no. 4, pp. 1862–1873, Apr. 2014. Cited page 65

[65] N. Ksairi, P. Ciblat, and C. J. Le Martret, "Near-Optimal Resource Allocation for Type-II HARQ Based OFDMA Networks Under Rate and Power Constraints," **IEEE Transactions on Wireless Communications**, vol. 13, no. 10, pp. 5621–5634, 2014. Cited pages 11, 23, 73, 74, 78, 81, and 97

[66] L. Lauwers, K. Barbe, W. V. Moer, and R. Pintelon, "Estimating the parameters of a rice distribution: A bayesian approach," in **IEEE Instrumentation and Measurement Technology Conference**, May 2009, pp. 114–117. Cited pages 27 and 28

[67] A. Le Duc, "Performance closed-form derivations and analysis of Hybrid-ARQ retransmission schemes in a cross-layer context," Ph.D. dissertation, Télécom ParisTech, Paris, France, 2009. Cited page 14

[68] W. Lee, M. Kim, and D. Cho, "Deep power control: Transmit power control scheme based on convolutional neural network," **IEEE Communications Letters**, vol. 22, no. 6, pp. 1276–1279, Jun. 2018. Cited page 133

[69] C. Lemoine, E. Amador, and P. Besnier, "On the K -factor estimation for rician channel simulated in reverberation chamber," **IEEE Transactions on Antennas and Propagation**, vol. 59, no. 3, pp. 1003–1012, Mar. 2011. Cited pages 27 and 28

[70] Y. Li, M. Sheng, C. W. Tan, Y. Zhang, Y. Sun, X. Wang, Y. Shi, and J. Li, "Energy-efficient subcarrier assignment and power allocation in OFDMA systems with max-min fairness guarantees," **IEEE Transactions on Communications**, vol. 63, no. 9, pp. 3183–3195, Sep. 2015. Cited pages 58, 59, and 66

[71] Y. Li, G. Ozcan, M. C. Gursoy, and S. Velipasalar, "Energy efficiency of hybrid-ARQ under statistical queuing constraints," **IEEE Transactions on Communications**, vol. 64, no. 10, pp. 4253–4267, Oct. 2016. Cited page 57

[72] C. Loo, "A statistical model for a land mobile satellite link," **IEEE Transactions on Vehicular Technology**, vol. 34, no. 3, pp. 122–127, Aug. 1985. Cited page 10

[73] P. Loskot and N. C. Beaulieu, "Prony and polynomial approximations for evaluation of the average probability of error over slow-fading channels," **IEEE Transactions on Vehicular Technology**, vol. 58, no. 3, pp. 1269–1280, Mar. 2009. Cited page 109

[74] C. Y. Lou and B. Daneshrad, "PER prediction for convolutionally coded MIMO OFDM systems - an analytical approach," in **IEEE Military Communications Conference (MILCOM)**, Oct. 2012, pp. 1–6. Cited page 109

[75] M. Maaz, P. Mary, and M. Hélard, "Energy minimization in HARQ-I relay-assisted networks with delay-limited users," **IEEE Transactions Vehicular Technology**, vol. 66, no. 8, pp. 6887–6898, Aug. 2017. Cited pages 58, 59, and 125

[76] M. Maaz, J. Lorandel, P. Mary, J.-C. Prévotet, and M. Hélard, "Energy efficiency analysis of hybrid-ARQ relay-assisted schemes in LTE-based systems," **EURASIP Journal on Wireless Communications and Networking**, vol. 2016, no. 1, pp. 1–13, 2016. Cited page 57

[77] S. Marcille, "Allocation de ressources pour les réseaux ad hoc mobiles basés sur les protocoles HARQ," Ph.D. dissertation, Télécom ParisTech, Paris, France, 2013. Cited pages 2, 11, 15, and 126

[78] B. R. Marks and G. P. Wright, "A general inner approximation algorithm for nonconvex mathematical programs," **Operations research**, vol. 26, no. 4, pp. 681–683, 1978. Cited pages 69 and 70

[79] S. Medawar, P. Handel, and P. Zetterberg, "Approximate maximum likelihood estimation of rician K-factor and investigation of urban wireless measurements," **IEEE Transactions on Wireless Communications**, vol. 12, no. 6, pp. 2545–2555, Jun. 2013. Cited pages 27 and 28

[80] N. I. Miridakis, D. D. Vergados, and A. Michalas, "Dual-hop communication over a satellite relay and shadowed rician channels," **IEEE Transactions on Vehicular Technology**, vol. 64, no. 9, pp. 4031–4040, Sep. 2015. Cited page 10

[81] R. Mochaourab, P. Cao, and E. Jorswieck, "Alternating rate profile optimization in single stream mimo interference channels," **IEEE Signal Processing Letters**, vol. 21, no. 2, pp. 221–224, Feb. 2014. Cited page 69

[82] A. Mutapcic, K. Koh, S. Kim, and S. Boyd, "Ggplab version 1.00: a matlab toolbox for geometric programming," 2006. Cited pages 85 and 119

[83] A. Naimi and G. Azemi, "K-factor estimation in shadowed ricean mobile communication channels," **Wireless Communications and Mobile Computing**, vol. 9, no. 10, pp. 1379–1386, 2009. Cited pages 27, 28, 31, 44, 49, and 51

[84] D. T. Ngo, S. Khakurel, and T. Le-Ngoc, "Joint subchannel assignment and power allocation for OFDMA femtocell networks," **IEEE Transactions on Wireless Communications**, vol. 13, no. 1, pp. 342–355, Jan. 2014. Cited page 16

[85] K. G. Nguyen, L. N. Tran, O. Tervo, Q. D. Vu, and M. Juntti, "Achieving energy efficiency fairness in multicell MISO downlink," **IEEE Communications Letters**, vol. 19, no. 8, pp. 1426–1429, Aug. 2015. Cited pages 58 and 59

[86] M. Nissila and S. Pasupathy, "Joint estimation of carrier frequency offset and statistical parameters of the multipath fading channel," **IEEE Transactions on Communications**, vol. 54, no. 6, pp. 1038–1048, Jun. 2006. Cited page 45

[87] D. P. Palomar and J. R. Fonollosa, "Practical algorithms for a family of waterfilling solutions," **IEEE Transactions on Signal Processing**, vol. 53, no. 2, pp. 686–695, Feb. 2005. Cited page 121

[88] F. Peng, J. Zhang, and W. E. Ryan, "Adaptive modulation and coding for IEEE 802.11n," in **2007 IEEE Wireless Communications and Networking Conference**, Mar. 2007, pp. 656–661. Cited page 108

[89] J. G. Proakis, **Digital Communications**, 2nd ed. Mc Graw - Hill Companies, 1989. Cited pages 10, 34, 109, 137, and 138

[90] Y. Qi, R. Hoshyar, M. A. Imran, and R. Tafazolli, "H2-ARQ-relaying: Spectrum and energy efficiency perspectives," **IEEE Journal on Selected Areas in Communications**, vol. 29, no. 8, pp. 1547–1558, Sep. 2011. Cited page 57

[91] R. Ramamonjison and V. K. Bhargava, "Energy efficiency maximization framework in cognitive downlink two-tier networks," **IEEE Transactions on Wireless Communications**, vol. 14, no. 3, pp. 1468–1479, Mar. 2015. Cited page 67

[92] J. Ren and R. Vaughan, "Rice factor estimation from the channel phase," **IEEE Transactions on Wireless Communications**, vol. 11, no. 6, pp. 1976–1980, Jun. 2012. Cited pages 27 and 28

[93] W. J. J. Roberts and S. Furui, "Maximum likelihood estimation of k-distribution parameters via the expectation-maximization algorithm," **IEEE Transactions on Signal Processing**, vol. 48, no. 12, pp. 3303–3306, Dec. 2000. Cited pages 45 and 139

[94] F. Rosas, R. D. Souza, M. E. Pellenz, C. Oberli, G. Brante, M. Verhelst, and S. Pollin, "Optimizing the code rate of energy-constrained wireless communications with HARQ," **IEEE Transactions on Wireless Communications**, vol. 15, no. 1, pp. 191–205, Jan. 2016. Cited page 57

[95] M. K. Samimi and T. S. Rappaport, "3-D millimeter-wave statistical channel model for 5G wireless system design," **IEEE Transactions on Microwave Theory and Techniques**, vol. 64, no. 7, pp. 2207–2225, Jul. 2016. Cited page 9

[96] R. Sassioui, M. Jabi, L. Szczecinski, L. B. Le, M. Benjillali, and B. Pelletier, "HARQ and AMC: Friends or foes?" **IEEE Transactions on Communications**, vol. 65, no. 2, pp. 635–650, Feb. 2017. Cited pages 74 and 101

[97] S. Sesia, I. Toufik, and M. Baker, **LTE: the Long Term Evolution - From theory to practice**. Wiley, 2009. Cited pages 13 and 94

[98] T. Shafique, O. Amin, and M. S. Alouini, "Energy and spectral efficiency analysis for selective ARQ multi-channel systems," in **IEEE International Conference on Communications (ICC)**, May 2017, pp. 1–6. Cited page 57

[99] Z. Shi, S. Ma, G. Yang, and M. Alouini, "Energy-efficient optimization for HARQ schemes over time-correlated fading channels," **IEEE Transactions on Vehicular Technology**, vol. 67, no. 6, pp. 4939–4953, Jun. 2018. Cited page 57

[100] B. T. Sieskul and T. Kaiser, "On parameter estimation of ricean fading MIMO channel: Correlated signals and spatial scattering," in **IEEE International Symposium on Personal, Indoor and Mobile Radio Communications (PIMRC)**, 2005, pp. 522–526. Cited page 28

[101] I. Stanojev, O. Simeone, Y. Bar-Ness, and D. H. Kim, "Energy efficiency of non-collaborative and collaborative hybrid-ARQ protocols," **IEEE Transactions on Wireless Communications**, vol. 8, no. 1, pp. 326–335, Jan. 2009. Cited page 57

[102] X. Sun, N. Yang, S. Yan, Z. Ding, D. W. K. Ng, C. Shen, and Z. Zhong, "Joint beamforming and power allocation in downlink NOMA multiuser MIMO networks," **IEEE Transactions on Wireless Communications**, pp. 1–1, 2018. Cited page 69

[103] L. Szczecinski, S. R. Khosravirad, P. Duhamel, and M. Rahman, "Rate allocation and adaptation for incremental redundancy truncated harq," **IEEE Transactions on Communications**, vol. 61, no. 6, pp. 2580–2590, Jun. 2013. Cited page 134

[104] K. K. Talukdar and W. D. Lawing, "Estimation of the parameters of the rice distribution," **the Journal of the Acoustical Society of America**, vol. 89, no. 3, pp. 1193–1197, 1991. Cited pages 27 and 28

[105] M. N. Tehrani, M. Uysal, and H. Yanikomeroglu, "Device-to-device communication in 5G cellular networks: challenges, solutions, and future directions," **IEEE Communications Magazine**, vol. 52, no. 5, pp. 86–92, May 2014. Cited pages 1 and 7

[106] C. Tepedelenlioglu, A. Abdi, and G. Giannakis, "The ricean K factor: estimation and performance analysis," **IEEE Transactions on Wireless Communications**, vol. 2, no. 4, pp. 799–810, Jul. 2003. Cited pages 27 and 28

[107] D. N. Tse and P. Viswanath, **Fundamentals of Wireless Communications**. Cambridge University Press, 2005. Cited pages 9 and 20

[108] M. Uysal, "Pairwise error probability of space-time codes in rician-nakagami channels," **IEEE Communications Letters**, vol. 8, no. 3, pp. 132–134, Mar. 2004. Cited page 10

[109] L. Venturino, A. Zappone, C. Risi, and S. Buzzi, "Energy-efficient scheduling and power allocation in downlink ofdma networks with base station coordination," **IEEE Transactions on Wireless Communications**, vol. 14, no. 1, pp. 1–14, Jan 2015. Cited pages 58 and 59

[110] E. Vinogradov, W. Joseph, and C. Oestges, "Measurement-based modeling of time-variant fading statistics in indoor peer-to-peer scenarios," **IEEE Transactions on Antennas and Propagation**, vol. 63, no. 5, pp. 2252–2263, May 2015. Cited page 9

[111] G. Wang, J. Wu, and Y. R. Zheng, "Optimum energy and spectral-efficient transmissions for delay-constrained hybrid ARQ systems," **IEEE Transactions on Vehicular Technology**, vol. 65, no. 7, pp. 5212–5221, Jul. 2016. Cited page 57

[112] Y. Wang, J. Zhang, and P. Zhang, "Energy-efficient power and subcarrier allocation in multiuser OFDMA networks," in **IEEE International Conference on Communications (ICC)**, Jun. 2014, pp. 5492–5496. Cited page 65

[113] V. Witkovskỳ, "Computing the distribution of a linear combination of inverted gamma variables," 2001. Cited page 136

[114] C. Y. Wong, R. S. Cheng, K. B. Letaief, and R. D. Murch, "Multiuser OFDM with adaptive subcarrier, bit, and power allocation," **IEEE Journal on Selected Areas in Communications**, vol. 17, no. 10, pp. 1747–1758, Oct. 1999. Cited page 16

[115] J. Wu, G. Wang, and Y. R. Zheng, "Energy efficiency and spectral efficiency tradeoff in type-I ARQ systems," **IEEE Journal on Selected Areas in Communications**, vol. 32, no. 2, pp. 356–366, Feb. 2014. Cited page 57

[116] Y. Wu and S. Xu, "Energy-efficient multi-user resource management with IR-HARQ," in **IEEE Vehicular Technology Conference (VTC Spring)**, May 2012. Cited pages 58 and 59

[117] L. Xu, G. Yu, and Y. Jiang, "Energy-efficient resource allocation in single-cell OFDMA systems: Multi-objective approach," **IEEE Transactions on Wireless Communications**, vol. 14, no. 10, pp. 5848–5858, Oct. 2015. Cited pages 58 and 59

[118] L. Yang, J. Cheng, and J. F. Holzman, “Maximum likelihood estimation of the lognormal-rician fso channel model,” **IEEE Photonics Technology Letters**, vol. 27, no. 15, pp. 1656–1659, Aug. 2015. Cited page 45

[119] G. Yu, Q. Chen, R. Yin, H. Zhang, and G. Y. Li, “Joint downlink and uplink resource allocation for energy-efficient carrier aggregation,” **IEEE Transactions on Wireless Communications**, vol. 14, no. 6, pp. 3207–3218, Jun. 2015. Cited pages 58, 59, and 67

[120] A. Zappone and E. Jorswieck, “Energy efficiency in wireless networks via fractional programming theory,” **Foundations and Trends in Communications and Information Theory**, vol. 11, no. 3-4, pp. 185–396, 2015. Cited pages 17, 59, 64, 77, 83, 91, and 119

[121] A. Zappone, P. Cao, and E. A. Jorswieck, “Energy efficiency optimization in relay-assisted MIMO systems with perfect and statistical CSI,” **IEEE Transactions on Signal Processing**, vol. 62, no. 2, pp. 443–457, Jan. 2014. Cited pages 58 and 59

[122] A. Zappone, M. Debbah, and Z. Altman, “Online energy-efficient power control in wireless networks by deep neural networks,” in **IEEE International Workshop on Signal Processing Advances in Wireless Communications (SPAWC)**, Jun. 2018. Cited page 133

[123] S. Zhu, T. S. Ghazaany, S. M. R. Jones, R. A. Abd-Alhameed, J. M. Noras, T. V. Buren, J. Wilson, T. Suggett, and S. Marker, “Probability distribution of rician K -factor in urban, suburban and rural areas using real-world captured data,” **IEEE Transactions on Antennas and Propagation**, vol. 62, no. 7, pp. 3835–3839, Jul. 2014. Cited page 35

[124] M. Zorzi and R. R. Rao, “Energy-constrained error control for wireless channels,” **IEEE Personal Communications**, vol. 4, no. 6, pp. 27–33, Dec. 1997. Cited pages 16 and 17

[125] ——, “On the use of renewal theory in the analysis of ARQ protocols,” **IEEE Transactions on Communications**, vol. 44, no. 9, pp. 1077–1081, Sep. 1996. Cited page 15

ÉCOLE DOCTORALE

Sciences et technologies de l'information et de la communication (STIC)

Titre : Allocation de ressources pour les HARQ dans les réseaux ad hoc mobiles

Mots clés : HARQ, allocation de ressources, optimisation, efficacité énergétique, canal de Rice

Résumé : Cette thèse traite le problème de l'allocation des ressources physiques dans les réseaux ad hoc mobiles en contexte multi-utilisateurs. Nous considérons qu'un noeud du réseau, appelé gestionnaire des ressources (GR) a pour tache d'effectuer cette allocation de ressources, et que pour ce faire, les autres noeuds lui communiquent des informations relatives aux canaux de propagations de leurs liens de communications. Ce modèle de réseaux induit un délai entre le moment où les noeuds envoient leurs informations au GR et le moment où le GR leur envoie leur allocation de ressource, ce qui rend impossible l'utilisation d'informations de canal instantanées pour effectuer l'allocation. Ainsi, nous considérons que le GR ne disposent que d'informations statistiques relatives aux canaux des différents liens de communications. De plus, nous supposons que chaque lien utilise le mécanisme de l'ARQ Hybride (HARQ). Dans ce contexte, la thèse comporte deux objectifs principaux : *i)* proposer des procédures d'estimation de la statistique du canal de propagation, et plus particulièrement du facteur K du canal de Rice avec et sans effet de masquage. *ii)* Proposer et étudier des algorithmes d'allocation de ressources basés sur les statistiques du canal et prenant en compte l'utilisation de l'HARQ ainsi que de schéma de modulation et de codage pratique. En particulier, on cherche à maximiser des grandeurs relatives à l'efficacité énergétique du système. Les ressources à allouer à chaque lien sont une énergie de transmission et une proportion de la bande de fréquence.

Title : Resource Allocation for HARQ in Mobile Ad Hoc Networks

Keywords : HARQ, resource allocation, optimization, energy efficiency, Rician channel

Abstract : This thesis addresses the Resource Allocation (RA) problem in multiuser mobile ad hoc networks. We assume that there is a node in the network, called the resource manager (RM), whose task is to allocate the resource and thus the other nodes send him there channel state information (CSI). This network model induces a delay between the time the nodes send the RM their CSI and the time the RM sends them their RA, which renders impossible the use of instantaneous CSI. Thus, we assume that only statistical CSI is available to perform the RA. Moreover, we assume that an Hybrid ARQ (HARQ) mechanism is used on all the links. In this context, the objective of the thesis is twofold: *i)* propose procedures to estimate the statistical CSI, and more precisely to estimate the Rician K factor with and without shadowing. *ii)* Propose and analyse new RA algorithms using statistical CSI and taking into account the use of HARQ and practical modulation and coding schemes. We aim to maximize energy efficiency related metrics. The resource to allocate are per-link transmit energy and bandwidth proportion.

Université Paris-Saclay
Espace Technologique / Immeuble Discovery
Route de l'Orme aux Merisiers RD 128 / 91190 Saint-Aubin, France